

Investigation of the role of xylosyltransferases I and II and of the kinase Fam20B in the regulation of proteoglycan synthesis

Irfan Shaukat

▶ **To cite this version:**

Irfan Shaukat. Investigation of the role of xylosyltransferases I and II and of the kinase Fam20B in the regulation of proteoglycan synthesis. Biochemistry, Molecular Biology. Université de Lorraine, 2015. English. NNT : 2015LORR0267 . tel-01754553

HAL Id: tel-01754553
https://hal.univ-lorraine.fr/tel-01754553

Submitted on 9 Jan 2019

HAL is a multi-disciplinary open access archive for the deposit and dissemination of scientific research documents, whether they are published or not. The documents may come from teaching and research institutions in France or abroad, or from public or private research centers.

L'archive ouverte pluridisciplinaire **HAL**, est destinée au dépôt et à la diffusion de documents scientifiques de niveau recherche, publiés ou non, émanant des établissements d'enseignement et de recherche français ou étrangers, des laboratoires publics ou privés.

AVERTISSEMENT

Ce document est le fruit d'un long travail approuvé par le jury de soutenance et mis à disposition de l'ensemble de la communauté universitaire élargie.

Il est soumis à la propriété intellectuelle de l'auteur. Ceci implique une obligation de citation et de référencement lors de l'utilisation de ce document.

D'autre part, toute contrefaçon, plagiat, reproduction illicite encourt une poursuite pénale.

Contact : ddoc-theses-contact@univ-lorraine.fr

LIENS

Code de la Propriété Intellectuelle. articles L 122. 4
Code de la Propriété Intellectuelle. articles L 335.2- L 335.10
http://www.cfcopies.com/V2/leg/leg_droi.php
http://www.culture.gouv.fr/culture/infos-pratiques/droits/protection.htm

UNIVERSITÉ DE LORRAINE

Ecole Doctorale BioSE (Biologie-Santé-Environement)

Thèse

Présenté et soutenu publiquement pour l'obtention du titre de

DOCTEUR DE L'UNIVERSITE DE LORRAINE
Mention : 《Science de la Vie et de la Santé》

Par Irfan SHAUKAT

Etude du rôle des xylosyltransférases I et II et de la kinase Fam20B dans la régulation de la biosynthèse des protéoglycanes

Investigation of the role of xylosyltransferases I and II and of the kinase Fam20B in the regulation of proteoglycan synthesis.

Soutenue publiquement le 18 Novembre 2015

Membres de jury :

Rapporteur:	M. Abderrahman MAFTAH	PR, Université de Limoges
	M. Yanusz WEGROWSKI	CR, Université de Reims
Examinateur:	M. Marc DIEDERICH	PR, LBMCC, Luxemburg
	M. Mohamed OUZZINE	DR, Université de Lorraine Directeur de thèse

---

UMR 7365 CNRS, INGENIERIE MOLECULAIRE ET PHYSIOPATHOLOGIE ARTICULAIRE (IMoPA)
9, Avenue de la Foret de Haye, Biopôle de l'Université de Lorraine, 54500 Vandoeuvre lès Nancy

Acknowledgement

I would like to express my deepest gratitude to my thesis director Mohamed OUZZINE, Directeur de Recherche, a l'INSERM for accepting me under his kind supervision and his patience and encouragement throughout my research. It was impossible to complete this thesis without his guidance.

I am grateful to Pr Abderrahman MAFTAH and Dr. Yanusz WEGROWSKI for accepting the request to be Rapporteur of my thesis and Pr Marc DIEDERICH for accepting to be part of my thesis Jury.

I would like to thank Li Dong and Lydia Barré for their help in experiments. I will not forget the nice company of Xavier especially during late hours and weekends.

This research work was conducted in the UMR-6375 IMoPA (Ingénierie Moléculaire et Physiopathologie Articulaire), Biopole, Faculty of medicine, University de Lorraine. Therefore, I am grateful to Pr. Jouzeau, Director, UMR-6375 and Pr. Magdalou the previous director of UMR-7561 for welcoming me in the Lab.

I am grateful to all the members of équipe 2, Ingénierie Moléculaire, Cellulaire, Thérapeutique & Glycosyltransférases (MolCelTEG) of UMR-7365 IMoPA, especially Sylvie Fournel-Gigleux, Sandrine Gulberti, Nick Ramalanjaona and Jean-Baptiste Vincourt.

I am highly grateful to all my office mates Ann, Caroline, Dima, Mathieu, Mahdia, Mineem, Isabelle, Xiaomeng and Xu for their nice company, humor, friendliness, and valuable suggestions.

I would like to like to acknowledge previous PhD students Emilie, Hassan, Jun, Lina, Mustafa, Reine and Suzanne. I would like to thanks all other members of the UMR-6375 IMoPA.

Last but not least, I would like to thank my family for their support despite the geographical distance.

Irfan SHAUKAT

Table of Contents

Acknowledgement 1

Table of Contents 2

List of Figures 5

List of tables 7

List of abbreviations 8

Chapter 1 10

1. Proteoglycans 11

1.1 Glycosaminoglycans (GAGs) chains 11

1.2 Classification of the PGs 13

1.3 Heparan sulfate proteoglycans (HSPG) 15

1.3.1 HS synthesis 15

1.3.2 Syndecans 18

1.3.3 Glypicans 22

1.3.4 Perlecan 25

1.3.5 Betaglycan/TGFβ type III receptor 26

1.4 Chondroitin sulfate proteoglycans (CSPG) 28

1.4.1 Decorin 28

1.4.2 Biglycan 32

1.4.3 CSPG4/NG2 34

1.4.4 Aggrecan 35

1.4.5 Versican 36

Chapter 2 38

2. Biosynthesis of GAG chains 39

2.2 Synthesis of the tetrasaccharide linker 39

2.3 Elongation of the CS chains 40
2.4 Elongation of the HS Chains 41
2.4 Regulation of PG synthesis 44
Chapter 3 47
3 Xylosyltransferase 48
3.1 Specificity of the xylosyltransferase 48
3.2 Structure of the XT-I and XT-II 49
3.4 Structural/Functional relationship 50
3.4 Purification of the XT from tissue source 52
3.5 Purification of the XT from cellular source as cDNA cloning 52
3.6 Intracellular localization 53
3.7 XT activity analysis 54
3.8 XT in health and disease 55
3.9 XT-I and XT-II genetic variants 55
3.10 Regulation of Xylosyltransferase 61
Chapter 4 63
4. Fam20B 64
4.1 Structure of Fam20B 64
4.4 Interaction of phosphoxylose with GalT-I, GalT-II, GlcAT-I, EXTL2 and ChGn-I 66
Chapter 5 71
5. Xylosides 72
5.1 GAG priming xylosides 73
5.2 GAG inhibiting xylosides 73
Aims and objectives 76
Publication No 1 79

Publications No 2 118

Publication No 3 166

General discussion 190

Conclusions and perspectives 197

Bibliography 200

Résumé En Français 223

List of Figures

Figure 1:- Classification of proteoglycans.. 14

Figure 2:- Distribution of HSPGs during embryogenesis at E 5.5. 15

Figure 3:- HSPG perform diverse cellular functions inside and outside the cells.. 16

Figure 4: Heparan sulfate (HS) structure. 17

Figure 5 :- Structure of human syndecans 1-4. 19

Figure 6:- The shedding of the syndecans 2 and 4. 21

Figure 7:- Role of syndecans in cancer.. 22

Figure 8:- Glypican structure. 23

Figure 9:- Role of glypican in Hh signaling pathways. 25

Figure 10:- The molecular structure of perlecan. 26

Figure 11:- Structure of betaglycan.. 27

Figure 12:- Molecular structure of decorin. 28

Figure 13:- Interaction of decorin with collagen fibers. 29

Figure 14:- Role of decorin in autophagy. 30

Figure 15:- The decorin acts as matrix guardian. 31

Figure 16:- The biological functions and regulating targets of decorin in tumor 32

Figure 17:- Structure of Biglycan. 33

Figure 18:- Biglycan signaling in the osteoprogenitor cells.. 33

Figure 19:- Structure of CSPG4 34

Figure 20:- Structure, function, synthesis and degradation of the aggrecan.. 35

Figure 21:- The structure of four versican isoforms.. 37

Figure 22:- The enzymes involved in the synthesis of the CS-, DS- and HSPGs 40

Figure 23:- The Biosynthesis of the CS and HS (Hacker et al., 2005). 41

Figure 24:- Strategies to improve the nervous tissue repair. 46

Figure 25:- Structure of XT-I and XT-II..... 49

Figure 26:- Structure of XT-I and XT-II genes. 51

Figure 27:- The methods for the determination of Xylosyltransferase activity..... 54

Figure 28:- Clinical features of patients with XT-I mutation R481W..... 56

Figure 29:- Clinic features of desbuquois dysplasia type 2 patients with XT-I mutation R598C. 57

Figure 30:- A patient with XT-II mutation at 14 years of age. 59

Figure 31:- Regulation of XT-I promoter by AP-I, SP1, and SP3..... 61

Figure 32:- GAG synthesis on biglycan by XT-I and XT-II. 62

Figure 33:- Structure of Fam 20 family. 65

Figure 34:- The crystal structure of the *C. elegans* Fam20.. 66

Figure 35:- Crystal structure of GlcAT-I.. 67

Figure 36:- Regulation of GAG synthesis by Fam20B is dependent on the EXTL2 68

Figure 37:- Regulation of CS biosynthesis by phosphorylation of xylose.. 69

Figure 38:- Xylose phosphorylation by Fam20B and regulation of GAG synthesis. 70

Figure 39:- Xyloside are used for GAG priming or inhibition. 72

Figure 40:- The effect of 4-MU4-deoxy-xyloside on TGF-β1 induced fibrotic markers in primary lung fibroblast.. 199

List of tables

Table 1:- Repeating disaccharide units of glycosaminoglycans with their characteristics..... 12

Table 2: The molecular mass of human syndecans and GAG attachment sites. 18

Table 3:- The enzymes involved in synthesis of tetrasaccharide linkage region..... 39

Table 4:- The enzymes involved in synthesis of repeating disaccharide units of CS chains..... 42

Table 5:- The enzymes involved in synthesis of repeating disaccharide units of HS chains 43

Table 6:- XT-I variants along with their location and pathological conditions. 60

Table 7:- XT-II variants along with their location and pathological conditions..... 60

List of abbreviations

ATP	Adenosine Triphosphate
BMP	Bone morphogenetic protein
cDNA	complementary deoxyribonucleic acid
CFSE	Carboxyfluorescein succinimidyl ester
ChABC	Chondroitinase ABC
CS	Chondroitin sulfate
CSPG	Chondroitin sulphate proteoglycans
DMEM	Dulbecco's modified Eagle's medium
DS	Dermatan sulfate
ECM	Extracellular Matrix
EGFR	Epidermal growth factor receptor
ER	Endoplasmic reticulum
ERK	Extracellular signal-regulated kinase
EXT1	Exostosin-1
EXT2	Exostosin-2
FACS	Flow cytometry
Fam20B	Family of sequence similarity 20 member B
FBS/FCS	Fetal bovine/calf serum
FGF	Fibroblast growth factor
FITC	Fluorescein isothiocyanate
GAG	Glycosaminoglycan
Gal	Galactose
Gal T	Galactosyltransferase
GalNAc	N- Acetylgalactosamine
GalNAcT	N-acetylgalactosaminyltransferase
GFP	Green fluorescent protein
GlcA	Glucuronic Acid
GlcN	Glucosamine
GlcNAc	N-acetyl-D-glucosamine
GlcNS	N-sulfated-D-glucosamine
GnT I/II	N-acetylglucosaminyltransferase I/II
GPI	Glycosylphosphatidylinositol
HA	Hyaluronic Acid
HEK	Human Embryonic Kidney 293 Cells
HS	Heparin sulphate
HSPGs	Heparan sulfate proteoglycans

IdoA	Iduronic acid
IF	Immunofluorescence
IGF	Insulin like growth factor
IL-β	Interleukin-β
IPF	Idiopathic pulmonary fibrosis
kDa	KiloDalton
KO	Knockout
KS	Keratan sulfate
MAPK	Mitogen-activated protein kinase
MMPs	Metalloproteinases
NDST	N-deacetylase-N-sulfotransferase
NRE	Non-reducing end
PAGE	Polyacrylamide gel electrophoresis
PAPS	3'-phosphoadenosine-5'-phosphosulfate
PBS	Phosphate-buffered saline
PG	Proteoglycan
RE	Reducing end
RNA	Ribonucleic acid
RT	Room temperature
RT-PCR	Reverse transcriptase polymerase chain reaction
SD	Standard deviation
SDS	Sodium dodecyl sulfate
Ser	Serine
ShRNA	Small hairpin RNA
siRNA	Small interfering RNA; silencing RNA
TCA	Trichloroacetic acid
TGF-β	Transforming growth factor β
Thr	Threonine
TNF-α	Tumor necrosis factor-α
UDP	Uridine diphosphate
VEGF	Vascular endothelial growth factor
WB	Western blot
WT	Wild type
XT	Xylosyltransferase
Xyl	Xylose
α-SMA	α-Smooth Muscle Actin

Chapter 1
Proteoglycans

1. Proteoglycans

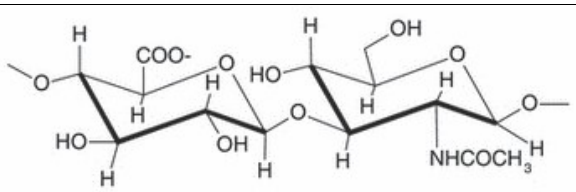
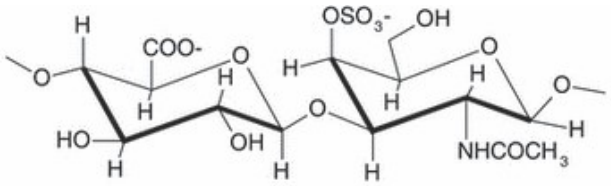
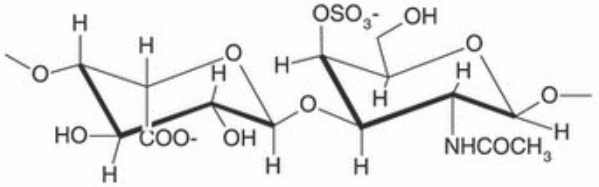
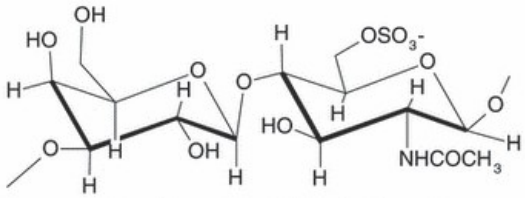
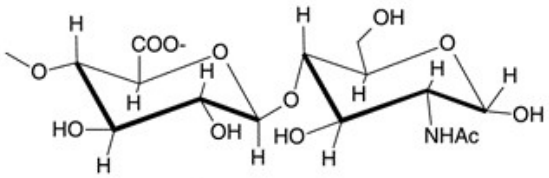
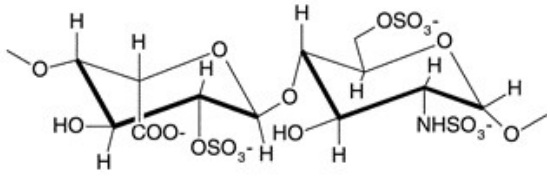
Proteoglycans (PGs) are important bio-macromolecules composed of core protein and glycosaminoglycan (GAGs) chains. PGs are major components of extracellular matrix and perform various biological processes such as extracellular matrix deposition, cell differentiation, adhesion and migration, normal as well as tumor cell proliferation. PGs interact with a variety of cytokines, growth factors and various protein ligands to mediate their effect inside the cells (Couchman, 2010; Iozzo and Schaefer, 2015; Prydz and Dalen, 2000).

1.1 Glycosaminoglycans (GAGs) chains

The GAGs are covalently linked on the specific serine residues of the core protein. The GAGs are polyanionic, long, unbranched formed by repeating disaccharide units. The disaccharides are an amino sugar (N-acetyl-D-glucosamine (GlcNAc) or N-acetyl-D-galactosamine (GalNAc)) and an uronic acid (D-glucuronic acid (GlcA) or L-iduronic acid (IdoA)). These residues are sulphated at various positions. The GAGs are classified into the non-sulphated containing only hyaluronic acid (HA also called hyaluronan) and sulphated which are further subdivided into the chondroitin sulphate (CS), dermatan sulphate (DS), keratan sulphate (KS), heparin and heparan sulphate (HS).

The hyaluronan is not attached to the core protein and it contains a long polysaccharide with a single disaccharide-repeating unit. It differs from the other GAG in molecular size and by the biosynthetic pathway (Cowman et al., 2015). The CS contains GlcA while in DS the GlcA is epimerized to IdoA and is linked to core protein by *O*-glycosylation. The KS do not contain uronic acid residues instead it contains Gal residues and is linked to core protein by both O- and N-glycosylation. HS and heparin are most complex and highly sulphated GAGs and linked to core protein by O-glycosylation. The repeating units are listed in the table 1.

Table 1:- Repeating disaccharide units of glycosaminoglycans with their characteristics (Gandhi and Mancera, 2008)

Glycosaminoglycans	Disaccharide units	Characteristics
Hyaluronic acid	 D-GlcA- β(1→ 4)-D-GlcNAc-α(1→ 4)	✚ Molecular mass 4–8 000 kDa ✚ Non-sulphated non-covalently attached to proteins in the ECM ✚ Usually found in synovial fluid, vitreous humour and ECM of loose connective tissue ✚ Lubricators and shock absorber
Chondroitin sulfate	 D-GlcA-β(1→ 3)-D-GalNAc4S-β(1→ 4)	✚ Molecular mass 5–50 kDa ✚ Most abundant GAG in the body ✚ Found in cartilage, tendon, ligament and aorta ✚ Bind to proteins (like collagen) to form proteoglycan aggregates
Dermatan sulfate	 L-IdoA-α(1→ 3)-D-GalNAc4S-β(1→ 4)	✚ Molecular mass 15–40 kDa ✚ Found in skin, blood vessels and heart valves
Keratan sulfate I and II	 D-Gal-β(1→ 4)-D-GalNAc6S-β(1→ 3)	✚ Molecular mass 4–19 kDa ✚ Most heterogeneous GAG ✚ KS I is found in the cornea ✚ KS II is found in cartilage aggregated with CS
Heparan sulfate	 D-GlcA-β(1→4)-D-GlcNAc-α(1-4)	✚ Molecular mass 10–70 kDa ✚ Extracellular component found in the basement membrane and as an ubiquitous component of cell surfaces
Heparin	 L-IdoA2S-α(1→4)-D-GlcNS6S-α(1→4)	✚ Molecular mass 10–12 kDa ✚ Intracellular component of mast cells, especially in the liver, intestine, lungs and skin

The negative charge on the GAGs is due to acidic sugar residues and presence of sulphate groups. Therefore GAGs adsorb water and act as hydrogel and lubricant in the joints and they also interact with growth factors and modulate their signalling pathways. The core protein is attached to one or several GAG chains. The GAG chains are synthesized by the stepwise addition of UDP-sugars by specific glycosyltransferases (GTs) (Prydz and Dalen, 2000). Further, these residues are modified by addition of sulphate groups by specific sulfotransferases. The residues are also epimerized by specific enzymes. The synthesis of the GAG chains occurs in the endoplasmic reticulum (ER) and Golgi lumen. The GAGs are more complex macromolecules due to the sulphation at various positions. Hence octasaccharide form one billion (10^5) different sulphation sequences (Gandhi and Mancera, 2008).

1.2 Classification of the PGs

The PGs are classified into four major classes based on their cellular and subcellular localization (Figure 1). The first class corresponds to intracellular PGs and contains only one member called serglycin which is packed into granules inside cells and released from the granules inside or outside cells (Kolset and Pejler, 2011). The second class corresponds to cell surface PGs and contains the syndecans (1-4), chondroitin sulfate proteoglycan 4 (CSPG4/NG2), betaglycan and phosphacan which are attached to the cell membrane through transmembrane domain and glypicans (1-6), which are attached to cell membrane by glycosyl-phosphatidyl-inositol (GPI) anchor. The third class are the pericellular and basement membrane PGs. They are attached to the cell surface by integrins and are also present on basement membranes, and these PGs include perlecan, agrin, collagens XVIII and XV. The fourth class are the extracellular proteoglycans which are subdivided into hyalectans including aggrecan, versican, neurocan and brevican and non hyalectans containing SLRPs such as decorin and biglycan, and SPOCK containing testicans (1-3) (Iozzo and Schaefer, 2015).

PGs are also classified into heparan-sulfate PGs (HSPGs), dermatan-sulfate PGs (DSPG), chondroitin-sulfate PGs (CSPG) and keratan-sulfate PGs (KSPGs) based on the GAG chains (Iozzo and Schaefer, 2015; Prydz and Dalen, 2000).

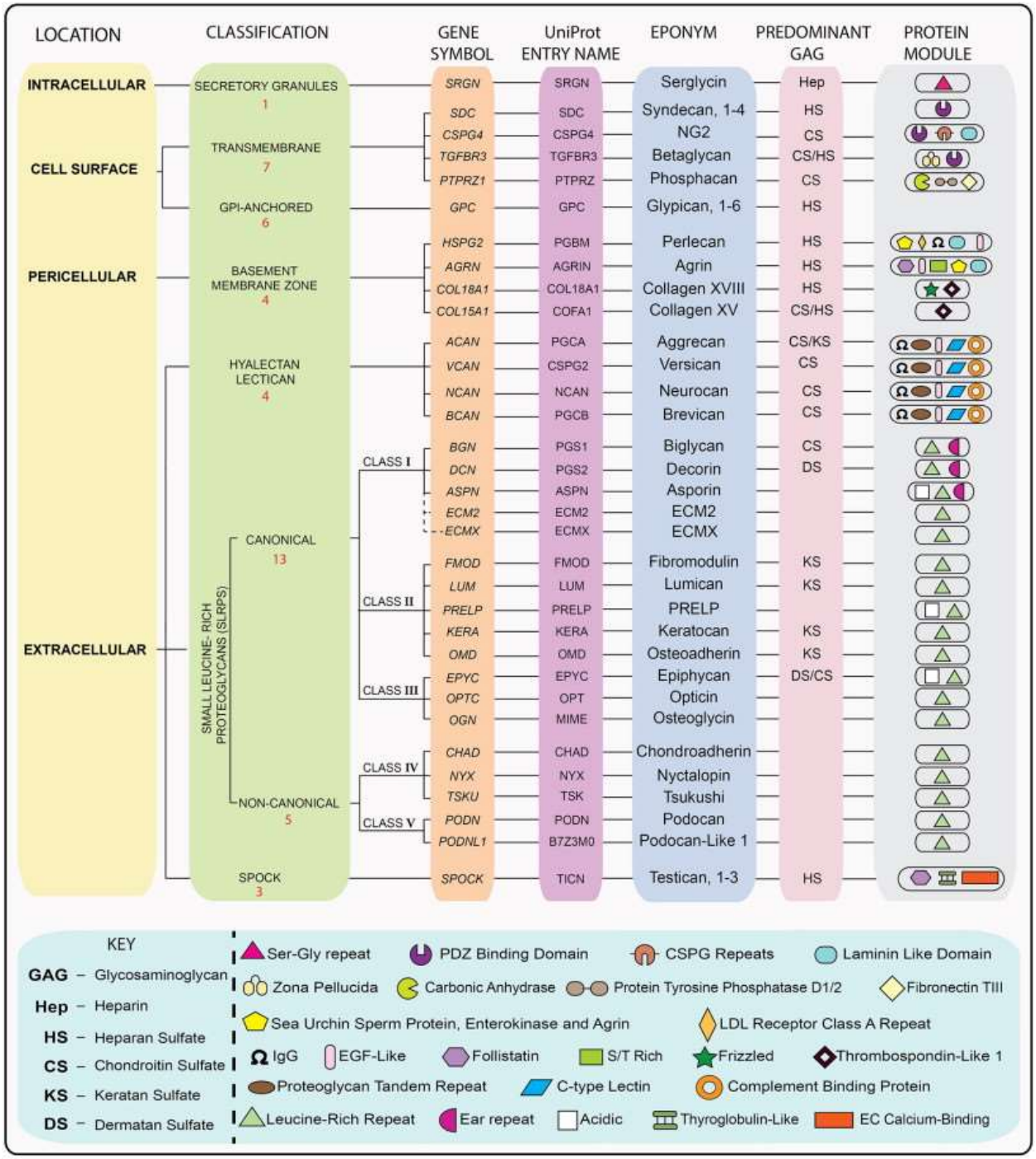


Figure 1:- Classification of proteoglycans. PGs are classified based on cellular and subcellular localization and homology at the protein and genomic levels. The key modules are present in the bottom panel (Iozzo and Schaefer, 2015).

1.3 Heparan sulfate proteoglycans (HSPG)

The HSPGs are important for tissue homeostasis and play a crucial role in cell survival, division, migration, differentiation and cancer development. HSPGs binds and regulate the activity of various signaling pathways such as Wnt, Fibroblast growth factor (FGF), Hedgehog (Hh), and bone morphogenetic protein (BMP). They also regulate and maintain morphogen gradients during the early stages of embryogenesis (Figure 2). The loss of HSPGs during embryogenesis leads to defects in neural tube, axon sorting convergent extension and gastrulation (Matsuo and Kimura-Yoshida, 2013).

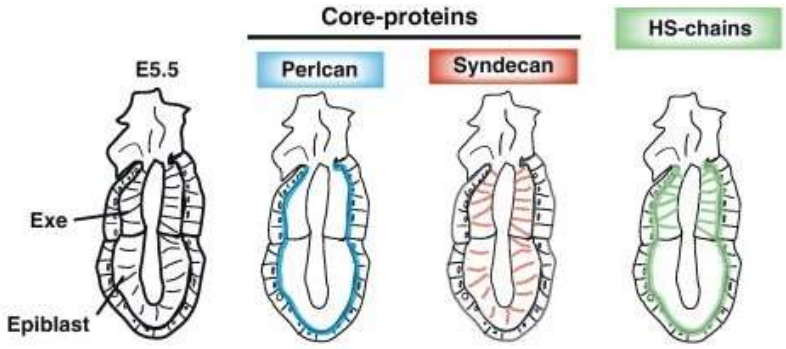


Figure 2:- Distribution of HSPGs during embryogenesis at E 5.5. The perlecan core protein (blue) and HS-GAG chains (green) are present on basement membranes. The syndecan core protein (red) and HS-GAG chains (green) are localized on cell surface of extraembryonic ectoderm. (Matsuo and Kimura-Yoshida, 2013).

The interaction of the HSPGs with different receptors is mediated mainly through their GAG chains (Sarrazin et al., 2011). The shedding of transmembrane HSPGs by specific matrix metalloproteinases (MMPs) produce soluble form, and is secreted into the ECM (Figure 3). Therefore shedding of PGs influence the signaling pathways because the GAG chains are not available for interaction with receptors and ligands (Giráldez et al., 2002; Manon-Jensen et al., 2010; Manon-Jensen et al., 2013).

1.3.1 HS synthesis

HSPGs are synthesized on the tetrasaccharide linkage region and HS backbone is mediated by glycosyltransferases of the exostosin family (EXTs) containing five membranes Ext1, Ext2, Extl1, Extl2, and Extl3. The first residue N-acetyl-D-glucosamine (GlcNAc) residue

is attached by the Extl3 and after GlcA and GlcNAc are attached stepwise on the non-reducing end of the chain by the Ext1 and Ext2 complex. Mutations in human EXT genes cause inherited autosomal disease called multiple hereditary osteochondroma (previously called hereditary multiple exostoses) which is characterized by the presence of multiple benign cartilage-capped tumors (Bishop et al., 2007; Busse-Wicher et al., 2014).

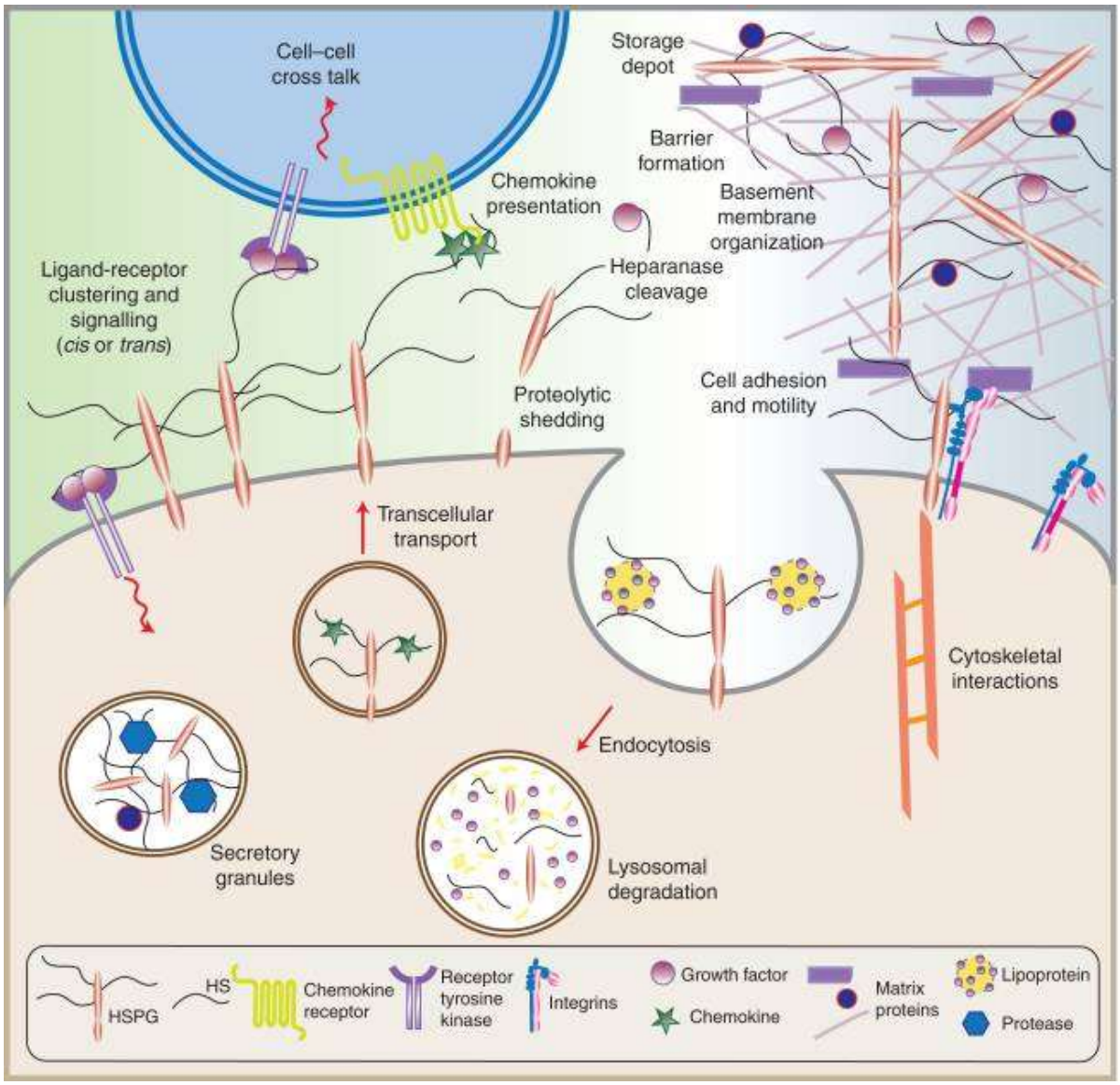


Figure 3:- HSPG perform diverse cellular functions inside and outside the cells. They act as co-receptors for growth factors and tyrosine kinases either of same cell or nearby cells. The shedding of the syndecans and glypicans into the ECM is produced by proteases and their HS chains are degraded by heparanase (Bishop et al., 2007; Sarrazin et al., 2011).

Several modifications occur on the HS chain like removal of the acetyl groups from clusters of GlcNAc residues and substitution of the free amino groups with sulfate, catalyzed by one or more N-deacetylase-N-sulfotransferases (Ndst). The C5 epimerase epimerizes D-glucuronic acids to L-iduronic acid (IdoA) and several sulfotransferases transfer the sulfate at various positions of the different residues: 2-O-sulfotransferase (Hs2st) adds sulfate at C2 of iduronic acids, 6-O-sulfotransferases (Hs6st1-3) transfer sulfate at C6 to the N-sulfoglucosamine units and 3-O-sulfotransferases (Hs3st1-6) add sulfate at C3 of glucosamine units (N-sulfated or N-unsubstituted). These modifications result in cluster formation of variable length of modified domain (N-sulfated or NS domains) and unmodified domains (N-acetylated or NA domains). The regions between these domains are called NA/NS domains (Bishop et al., 2007; Sarrazin et al., 2011). These regions are important for the ligand binding with HS chains. FGF and anti-thrombin bind to the region when IdoA is sulphated at 2nd position (Figure 4).

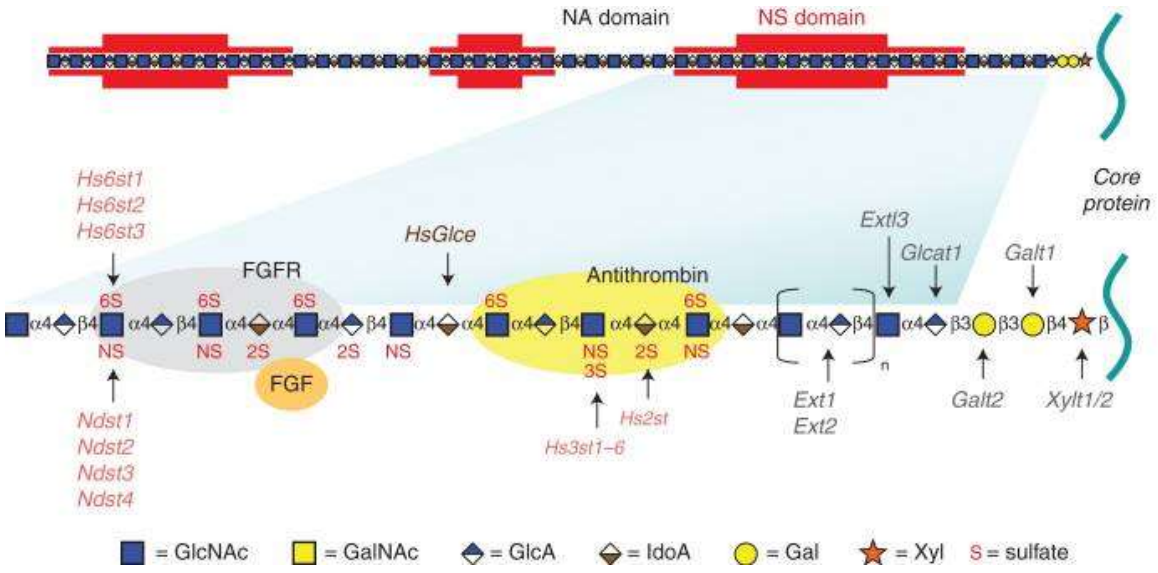


Figure 4: Heparan sulfate (HS) structure. HS biosynthesis is initiates on the tetrasaccharide primer by the attachment of the GlcNAc by Extl3 and chain elongates by the Ext1 and Ext2 complex. The sulphation and epimerization occur to form different domains. (Sarrazin et al., 2011)

Recently, it has been shown that a mutation in HS elongation enzymes EXT2 and EXTL3 reduced cell migration and inhibition of sulphation of HS chains by sodium chlorate showed similar results. Analysis of the mechanism involved showed that the loss of GAG chains or defective sulphation

results in impairment of the FGF signaling. This led to activation of Wnt/ β-catenin signaling and inhibition of chemokine receptor cxcr7b which results in delayed collective cell migration (Venero Galanternik et al., 2015). Moreover, reduced expression of EXTL2 in HEK-293 cells produced HS chains with longer size however overexpression of this protein has no effect on the size of GAG chains (Katta et al., 2015)

1.3.2 Syndecans

Syndecans (SDCs) are the major class of HSPGs mainly present on the cell surface and as soluble form in the ECM. Four types of SDCs are present in humans and other vertebrates whereas invertebrates possess only one type.

1.3.2.1 Expression and Structure

Different types of SDCs are expressed in various cells and tissues. Briefly, syndecan-1 (SDC-1) is mainly expressed in epithelial cells as well as in some leukocytes. Syndecan-2 (SDC-2) is expressed in mesenchymal cell fibroblasts, liver, and developing neural tissue. Syndecan-3 (SDC-3) is present in the neuronal tissue and developing musculoskeletal system. Syndecan-4 (SDC-4) is ubiquitously expressed in most cell types (Leonova and Galzitskaya, 2013). The SDC-2 and SDC-4 contains only HS-GAG chains whereas the SDC-1 and SDC-3 also contains the CS-GAG chains. The CS chains are mostly close to transmembrane domain, however CS is also attached near N-terminal (at Serine 37) in SDC-1. The human SDCs amino acid length, molecular mass and GAG attachment sites are given in Table 2.

Table 2: The molecular mass of human syndecans and GAG attachment sites.

	Amino acids	Molecular Mass (kDa)	HS attachment site	CS attachment site	Uniprot No
Syndecan-1	310	32	45, 47	37, 206, 216	P18827
Syndecan-2	201	22	41, 55, 57		P34741
Syndecan-3	442	45	80, 82, 84, 91	314, 367	O75056
Syndecan-4	198	22	39, 61, 63		P31431

The SDCs core proteins range from 20 kDa to 45 kDa and have the transmembrane topology containing three distinct structural domains, such as a C-terminal cytoplasmic domain,

transmembrane domain and N-terminal extracellular domain or ectodomain (Figure 5). The cytoplasmic domain contains two conserved regions C1 and C2 separated by the variable sequence (V). The C2 region (EFYA motif) interacts with PDZ domains of cytoplasmic proteins and this interaction is important for cell adhesion, migration and many signaling pathways.

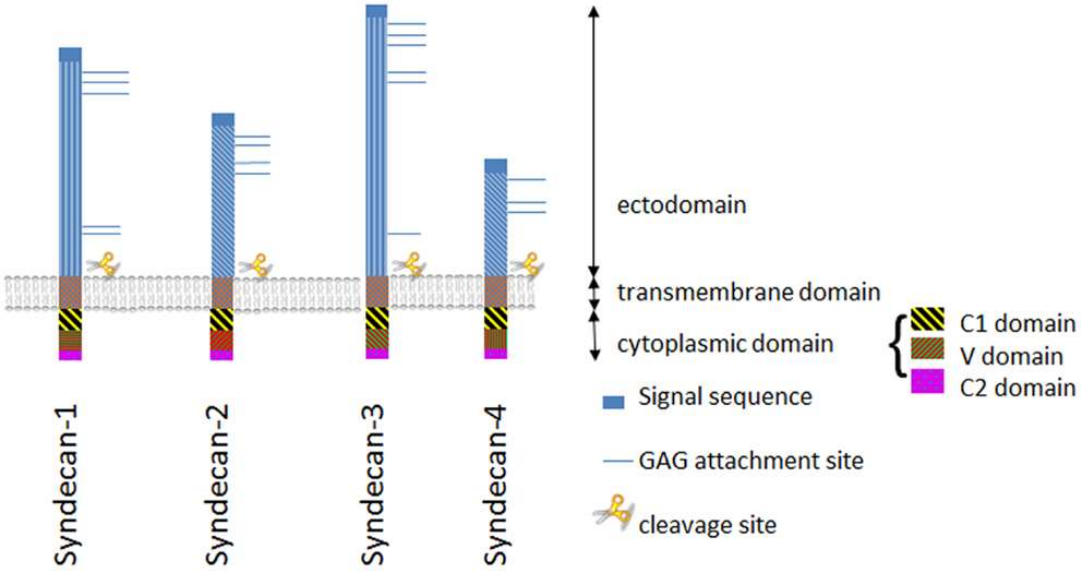


Figure 5 :- Structure of human syndecans 1-4. The GAG chains are attached on the conserved serine residues of extracellular domain. The C1 and C2 are the conserved and V is the variable motif in cytoplasmic domain (Szatmári and Dobra, 2013).

The transmembrane domain is highly conserved and contains a GxxxG motif. This motif is important for the dimerization of SDCs and for membrane retention (Choi et al., 2011; Leonova and Galzitskaya, 2015). The amino acid residues are highly conserved in the cytoplasmic domain and transmembrane region and have about 60–70% homology. The extracellular domain is variable and has only 10-20% amino acid sequence homology but contains conserved motifs for GAG attachment, cell interaction and proteolytic cleavage. The extracellular domain of SDCs is cleaved near transmembrane domain, the process is called shedding. The zinc-dependent endopeptidases and MMPs are responsible for shedding of SDCs and shedding occurs under normal physiological conditions but it is increased in the presence of a stimuli such as chemokines, growth factors, heparanase, insulin, cellular stress and virulent components of bacteria.

1.3.2.2 Functions

All the SDC subtypes play a crucial role in various body functions. SDC-1 contains two HS chains and three CS-GAG chains. It is important for leukocyte migration, wound healing and also reduces the risk of atherosclerosis (Gharbaran, 2015; Savery et al., 2013). The increased shedding of SDC-1 is associated with multiple myeloma, gastric, hepatocellular and colorectal carcinomas, pancreatic, ovarian and breast cancer (Szatmári and Dobra, 2013). SDC-2 contains only three HS-GAG chains and it is mainly expressed in kidney, lungs, stomach, cartilage and bones. It plays an important role in cell adhesion by activation of integrin β1 and is important for the nervous system development and angiogenesis during embryonic stage (Sarrazin et al., 2011). The higher level of secreted SDC-2 was described in melanoma, Lewis lung carcinoma, esophageal squamous carcinoma, colon and prostate cancer (Lee et al., 2011; Leonova and Galzitskaya, 2015).

The SDC-3 has large extracellular domain containing three HS near N-terminal domain and two CS chains close to cell membrane. SDC-3 is mainly expressed in nerve tissue and skeletal muscle cells and is important for neurological functions such as normal functioning of brain and memory strengthening. It modulates synaptic plasticity and hence influences hippocampus-dependent memory. It also regulate appetite and knockout mice ($SDC3^{-/-}$) are viable however their feeding behaviors is change and are not prone to obesity (Sarrazin et al., 2011)

SDC-4 is also believed to be involved in various malignancies including melanoma, breast cancer, urinary bladder carcinoma, osteosarcoma, hematopoietic malignancy, colon and testicular germ cell tumors (Barbouri et al., 2014; Kusano et al., 2004; Labropoulou et al., 2013). The knockout mice for $SDC\text{-}4^{-/-}$ are also viable and have delayed angiogenesis and wound healing and disturb various signaling pathways.

SDCs might be less essential during the development process because SDC-1, -3, and -4 deficient mice are viable and fertile. However SDC-2 mice have not been reported yet. Rather, they are important regulators for homeostasis, regeneration, synaptic plasticity and tumorigenesis (Leonova and Galzitskaya, 2013; Sarrazin et al., 2011)

The shedding of the SDCs (Figure 6) is enhanced under various pathological conditions like inflammation, wound and also in many cancers. Therefore, the shedding of the SDCs is important

for prognosis of the cancer. The tumor microenvironment consists of the vascular network, various ECM molecules, fibroblasts, immune cells, under the influence of the cytokines and growth factors. Therefore, healthy cells close to the tumorous microenvironment initiate the remodeling of the ECM in order to facilitate tumor cell growth, migration, and invasion. The PGs especially the SDCs play an important role in this regard and are key regulators of tumorigenesis and tumor progression and are biomarkers for cancer detection and severity (Figure 7). Interestingly SDCs play a dual role in tumor progression as they either enhance or inhibit tumor progression (Barbouri et al., 2014).

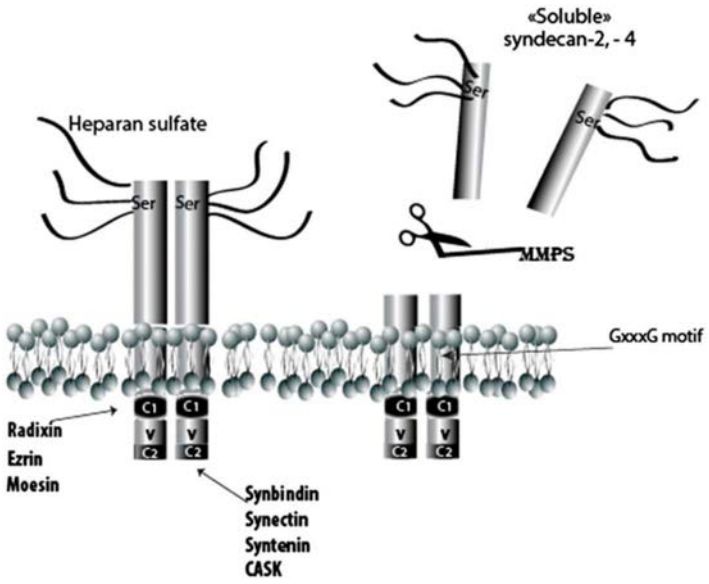


Figure 6:- The shedding of the syndecans 2 and 4. The extracellular domain is cleaved by MMPs to release the soluble form. The transmembrane domain contains a GxxxG motif for membrane retention (Leonova and Galzitskaya, 2015).

It is well documented that SDCs interact with several ECM macromolecules including collagens, elastin, fibronectin (FN), laminins, tenascin, thrombospondin through their GAG chains, therefore the length of the GAG chains is critical for these interactions. Cell surface SDCs act as co-receptors for growth factors, integrins, and other signaling molecules. Growth factors like fibroblast growth factor (FGF), epidermal growth factor (EGF), vascular endothelial growth factor (VEGF), insulin growth factor (IGF), and platelet-derived growth factor (PDGF) are key players in several malignancies. SDC-1 and SDC-4 regulate the formation of FGF-2/HSPG/FGFR-1 complex in breast carcinoma cells, and the altered sulphated HS chains are present in the malignant conditions.

Moreover, heparanase expression is increased in cancer which results in increased degradation of HS-GAG chains in the tumor microenvironment to promote tumor growth, angiogenesis and metastasis (Figure 7) (Barbouri et al., 2014; Leonova and Galzitskaya, 2013; Leonova and Galzitskaya, 2015).

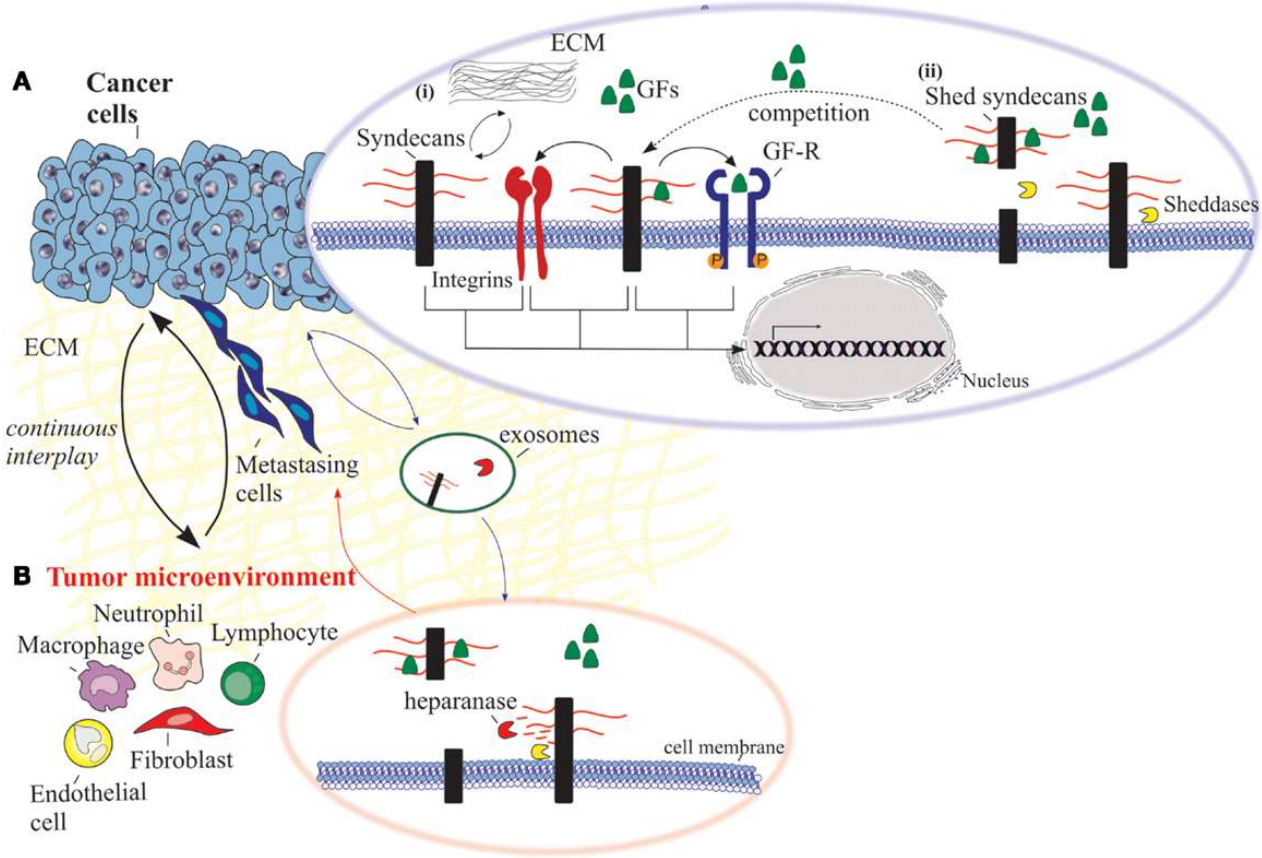


Figure 7:- Role of syndecans in cancer. In cancer cells SDCs interact with integrins to control cell proliferation, adhesion, migration, and invasion. It also modulates the activity of various growth factors and shedding of syndecan contributes to cancer progression (A). In the tumor microenvironment the degradation of the HS chains by heparanase promotes tumor growth, angiogenesis and metastasis (B) (Barbouri et al., 2014).

1.3.3 Glypicans

Glypicans are also cell-surface heparan sulfate proteoglycans (HSPG) but unlike syndecans, they are attached to the cell membrane by a glycosylphosphatidylinositol (GPI) anchor. In human and other higher mammals six glypicans types (GPC1 to GPC6) have been described, while *Drosophila melanogaster* has only two glypican subtypes called Dally and Dally-like protein

(Dally and Dlp) and the *C. elegans* also express two subtypes called Gpn-1 and Lon-2 (Fico et al., 2011; Filmus et al., 2008).

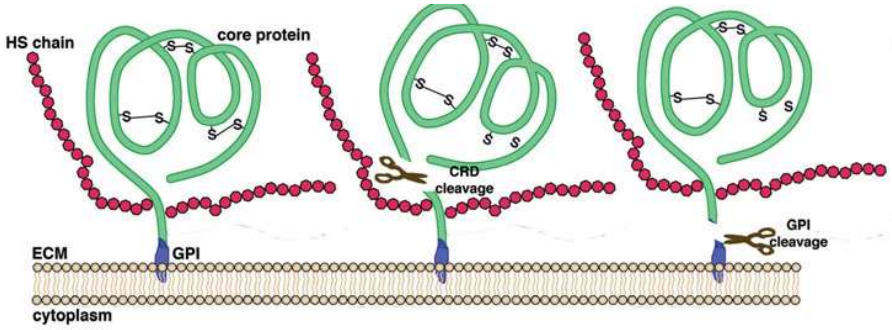


Figure 8:- Glypican structure. The core protein is linked to the plasma membrane with GPI anchor. The GAG chains are attached to the core protein. The core protein is cleaved at either CRD or GPI cleavage sites (Fico et al., 2011).

1.3.3.1 Structure

The glypican core proteins are much more similar than SDCs and they contain about 555 to 580 amino acids with a molecular mass of 60 to 70 kDa. The structure of glypican is conserved among all subtypes, the N-terminal domain contains a secretory signal peptide and 14 evolutionarily conserved cysteine residues. The HS attachment domain is present at the C-terminal region, and a hydrophobic domain for addition of the GPI anchor at the C-terminus (Figure 8). The glypicans are coiled randomly and contain approximately 1–5 heparan sulfate attachment sites. The photolytic cleavage of glypican occurs either at the GPI anchor by an extracellular lipase or at a cysteine rich domain (CRD) to produce the soluble form (Fico et al., 2011). Based on the sequence similarity, the glypicans have two broad subfamilies, glypicans 1/2/4/6 and glypicans 3/5. Moreover the human glypican 3/4 gene is localized on X chromosome while glypican 5/6 and glypican 1 and 2 genes are present on the chromosome 2 and 7, respectively (Filmus et al., 2008). In drosophila, the knockdown of Dally results in defects in brain, antennae, eye and wings (Tsuda et al., 1999).

1.3.3.2 Functions

Mutations in the glypican-3 gene are associated with the Simpson-Golabi-Behmel Syndrome (SGBS), which is an X-linked disorder characterized by pre- and post-natal overgrowth, visceral

and skeletal abnormalities and prone for development of embryonic tumors (Li et al., 2001). The deficiency of glypican-6 has recently been shown to cause omodysplasia, a genetic disorder characterized by cardiac defects, mental retardation, skeletal abnormalities and short stature (Campos-Xavier et al., 2009).

The glypicans, HS-GAG chains are attached on the C-terminal near the cell membrane. This suggests that the HS chain interacts with the other proteins and receptors on the cell surface. Therefore, glypicans play a crucial role in various signaling pathways especially Wnts, Hhs, FGFs, BMPs and morphogen gradients during development. The binding of the Hh with the glypican core protein suppress the downstream signaling, whereas binding of the Hh with GAG chains enhanced the downstream signaling. Indeed, glypican 3 core protein without GAG chains strongly suppress the Hh signaling (Figure 9). The glypican 5, contains five GAG chains and acts as positive regulator, while glypican 3 and 1 act as negative regulators of Hh signaling (Filmus and Capurro, 2014).

The glypican 3 is upregulated in the hepatocellular carcinoma (HCC) and is the purposed biomarker for the diagnosis of HCC. However, the overexpression of soluble glypican 3 (lacking GPI anchor) inhibits the Wnt signaling, reduce the cell proliferation and activation of Erk-1/2 and AKT signaling in the hepatic cell lines. Soluble form of glypican 3 suppress HCC cell proliferation and migration and also in vivo in the mice xenograft model (Zittermann et al., 2010).

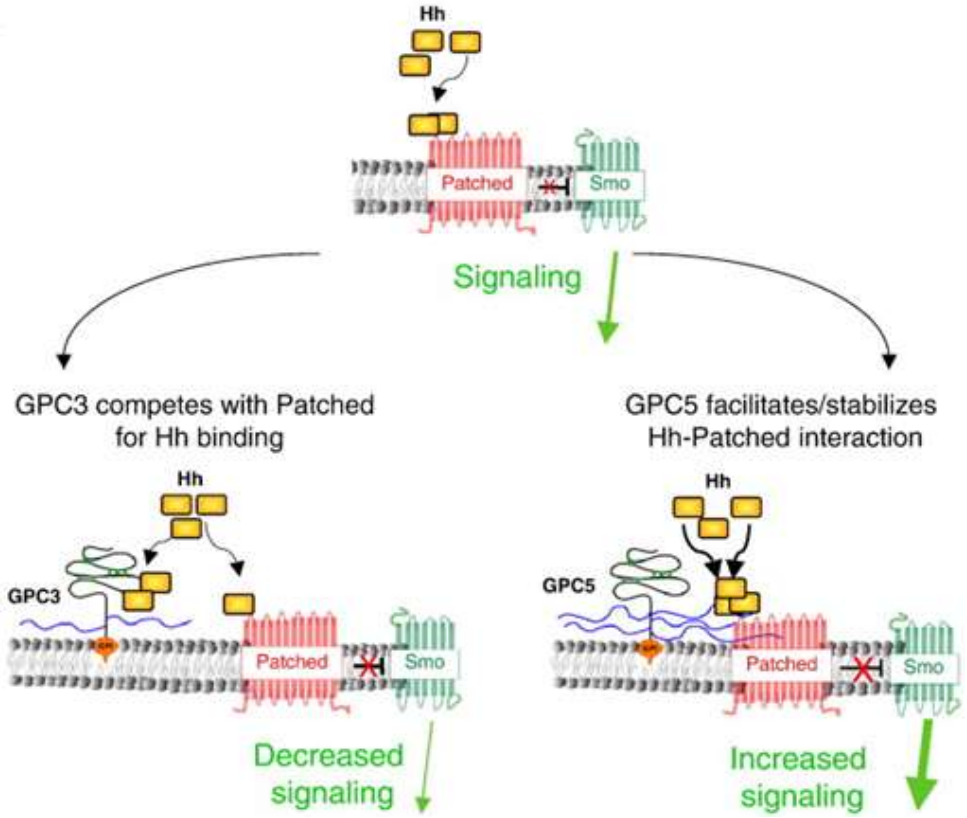


Figure 9:- Role of glypican in Hh signaling pathways. Glypican 3 core protein binds with Hh and suppress the Hh signaling. The glypican 5 has more GAG chains and binding of Hh with GAG chains increase the Hh signaling by stabilizing Hh-Patched interaction (Filmus and Capurro, 2014).

1.3.4 Perlecan

Perlecan belongs to the HSPG with a core protein of about 400 kDa. The core protein has five domains (Figure 10). It has three GAG attachment sites at its N-terminus. It is mainly present in the basement membranes and plays a key role in vascular homeostasis. It interacts with various biological molecules and growth factors to mediate cell signaling, migration, proliferation, and differentiation. Its has dual role in cancer either favors the angiogenesis and tumor progression by activation of FGF-FGFR and VEGFR2-Akt pathways or reduced angiogenesis and tumor growth through endorepellin and LG3 and interaction with integrin (Roberts et al., 2012; Whitelock et al., 2008). It has crucial role during the development therefore prelecan-deficient mice are embryonic lethal and showed severe chondrodysplasia, disturbed cardiac functions (Ford-Perriss et al., 2003; Whitelock et al., 2008).

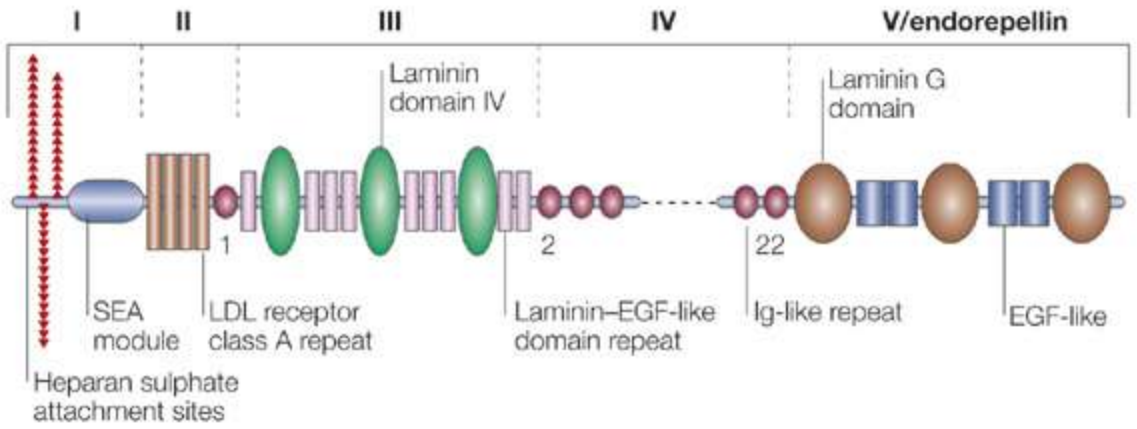


Figure 10:- The molecular structure of perlecan. It contains five domains and GAG attachment site is on N-terminal. (Iozzo, 2005)

1.3.5 Betaglycan/TGFβ type III receptor

The betaglycan belongs to the HSPG and contains two sites for the attachment of GAG chains and have a molecular mass of about 93 kDa. Betaglycan is member of TGF-β superfamily of co-receptors also known as TGF-β type III receptor (TGFB3). It has a single-pass transmembrane topology (Figure 11). The extracellular domain contains site for GAG attachment at 534 and 545 position and protease-sensitive sequences near the transmembrane domain (Figure 11). The GAG chains are important for its proper function and the TGFβ downstream signaling. The GAG chains of betaglycan regulate the cell migration by interaction with other co-receptors in the ECM (Mythreye and Blobe, 2009b). However, the mechanism by which betaglycan GAG modifications regulate cell migration is still unknown. The extracellular domain also contains a cleavage site for proteases which release the soluble form of betaglycan. The soluble form downregulate TGFβ signaling and suppress the migration of the breast cancer cell lines (Elderbroom et al., 2014). The short intracellular domain contains many serine and threonine residues which are phosphorylated by PKC (López-Casillas et al., 1991). The intracellular domain also contains PDZ-binding domain. The betaglycan regulate cell migration by interaction with β-arrestin2 via the PDZ domain and mediate activation of Cdc42 (Mythreye and Blobe, 2009b). The betaglycan knockout (*Tgfbr3*$^{-/-}$) mice showed embryonic lethality (Sarraj et al., 2013).

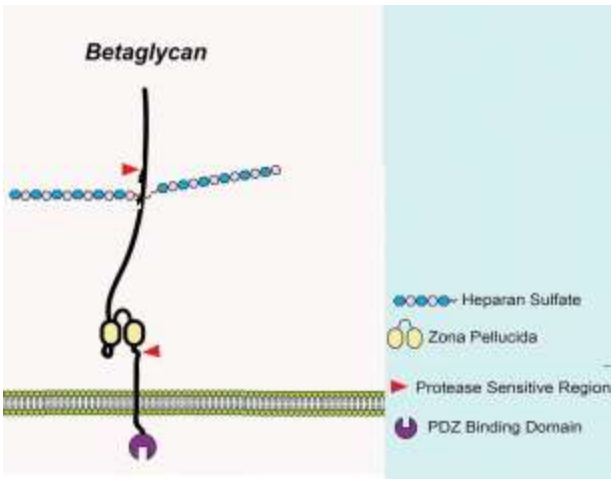


Figure 11:- Structure of betaglycan. It has transmembrane topology and contain two GAG chains on the extracellular domain. The PDZ binding domain is present in intracellular domain (Iozzo and Schaefer, 2015).

1.4 Chondroitin sulfate proteoglycans (CSPG)

1.4.1 Decorin

1.4.1.1 Structure

Decorin belongs to a multifunctional family of PGs collectively designated as small leucine-rich PGs (SLRPs). Decorin core protein molecular mass is around 40 kDa. It contains only one GAG chain either CS or DS. The CS-type GAG chains are mostly present in cartilage, while DS-type GAG chains present in other tissues.

The core protein contains four domains. The first domain or N-terminal domain consists of a signal peptide (14-amino acids) and a propeptide (16-amino acids) and this part is cleaved before secretion of the protein. The second domain contains several cysteine residues and DEASGIG motif (Ser34) for attachment of GAG chain. The third domain contains leucine-rich repeats consisting of 10 repeats of 24 amino acids rich in leucine and three sites for the N-linked glycosylation (Asn211, Asn262 and Asn303). The fourth domain or C-terminal domain contains two cysteine residues and a conserved disulfide loop (Figure 12).

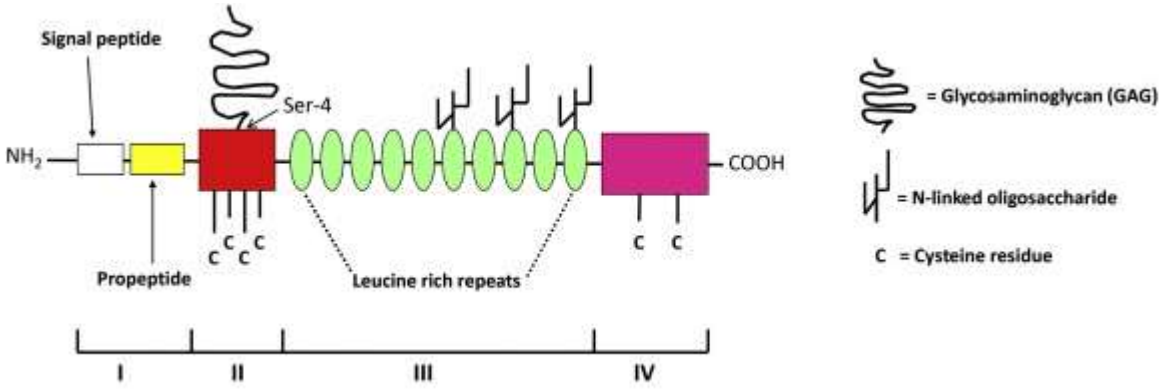


Figure 12:- Molecular structure of decorin. The decorin has four domains containing leucine rich repeats and one GAG attachment site. It also contains three N-linked glycosylation sites (Järveläinen et al., 2015).

1.4.1.2 Functions

The core protein interacts with type I and type II collagens and also with various growth factors (Figure 13). The soluble decorin is present in the normal human plasma and its secretion is increased in patients with diabetes and septicemia (Bolton et al., 2008). However, the secretion of

decorin is reduced in various disease conditions such as in patients suffering acute ischemic stroke and esophageal squamous cell carcinomas (Wu et al., 2010).

Fibroblasts and myofibroblasts produce a large amount of decorin which is secrete into the ECM as soluble form. Decorin is important in collagen fibers assembly and it decorate the collagen fibers. It is involved in various physiological and pathological conditions associated with dysfunctions of the ECM. If decorin is not secreted as in decorin KO mice, collagen fibers become thinner however in the presence of decorin without GAG chains, collagen fibers become thicker (Seidler, 2012). It is produced by human dermal fibroblasts and is major PGs expressed in dermal ECM. The young skin contains longer decorin-GAG chains compared to the aged groups. This shows the variation of the structure of decorin with age (Li et al., 2013).

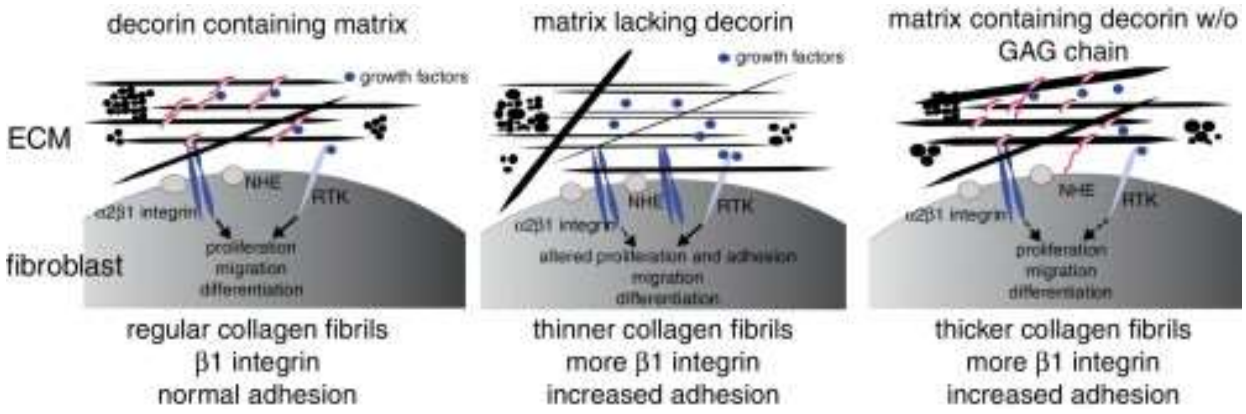


Figure 13:- Interaction of decorin with collagen fibers. The decorin stabilizes the collagen fibers and in its absence the collagen fibers become thin, while the lack of GAG chain on decorin led to thicker collagen fibers (Seidler, 2012).

The soluble form of decorin acts as endogenous pan-receptor tyrosine kinase (RTK) inhibitor. It downregulate tumor development, migration, and angiogenesis. The decorin core protein interacts with RTK members and influences their downstream signaling. Treatment with decorin inhibits the metastatic spreading and growth of breast carcinoma xenografts in mice. The transcriptome profiling of tumor after the treatment with decorin revealed upregulation of paternally expressed gene 3 (PEG3) which is not originally expressed in tumors. The treatment of decorin showed higher PEG3 expression leading to upregulation of the autophagic proteins like Beclin 1 (BECN1) and light chain 3 (LC3) in the vascular endothelial cells. The PEG3, BECN1 and LC3 form

complex and induce the autophagy (Buraschi et al., 2013). Hence, it is suggested that decorin acts as an appetite for autophagy of vascular endothelial cells (Figure 14) (Neill et al., 2013).

Decorin interacts with kinase death receptor (KDR) to stimulate PIK3 dependent activation of LC3, BECN1 and PEG3 complex. This complex activate autophagy directly or enhance the transcription of BECN1 and LC3 to initiate autophagy. However, the siRNA against KDR and PEG3 blocks decorin dependent autophagy (Figure 13). Decorin attenuates the EGFR and suppresses downstream anti-autophagic effectors (Akt, mTOR, p70S6K), hence, stimulate autophagy markers like Bcl-2, BECN1, and LC3. The decorin also enhance the mitophagy by activating the Met receptor (Neill et al., 2014).

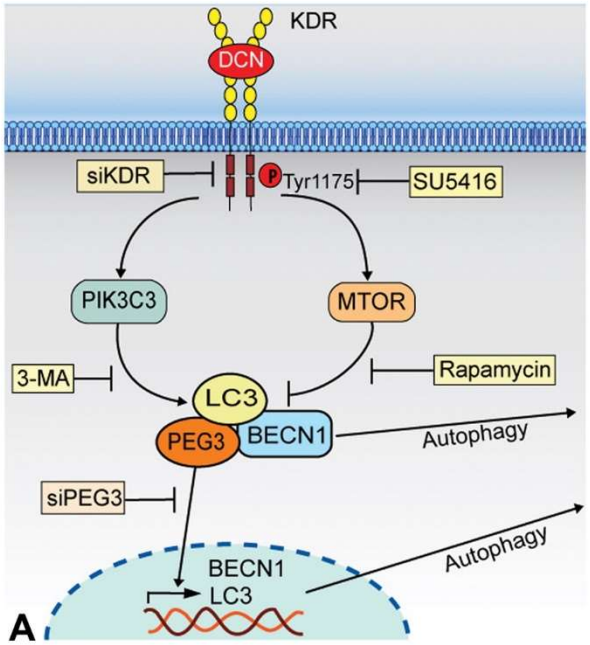


Figure 14:- Role of decorin in autophagy. The soluble decorin binds to KDR ectodomain and induce the expression of the PEG3, LC3 and BECN1for autophagic induction. The siRNA against KDR and PEG3 inhibits the decorin induced autophagy (Neill et al., 2013).

The overexpression of decorin in the human alveolar adenocarcinoma (A549) cells has antiproliferative effect. It produces accumulation of cells at G1 phase and counteract the TGF-β1 effects and phosphorylation of EGFR. It increases the expression of the P53 and P21 (Liang et al., 2013). Recently, it has been shown that the expression of decorin is reduced in the Non-small cell lung cancer (NSCLC) tissues and the reduction is proportional to the size, stage and metastasis of

tumor. Decorin inhibits tumor metastasis by downregulation the E-cadherin in NSCLC cells (Shi et al., 2014).

The soluble form of decorin interacts with various growth factors and cytokines receptors. This includes transforming growth factor (TGF-β1) receptor, epidermal growth factor receptor (EGFR), the insulin-like growth factor receptor I (IGF-IR), and the hepatocyte growth factor receptor (Met). Therefore, decorin influence their intracellular signaling pathways. Both the decorin core protein and GAG chain are important in decorin mediated signaling, but some interactions are mediated by either decorin core protein or decorin GAG chain. Hence, it is suggested that decorin acts as guardian for the matrix (Figure 15).

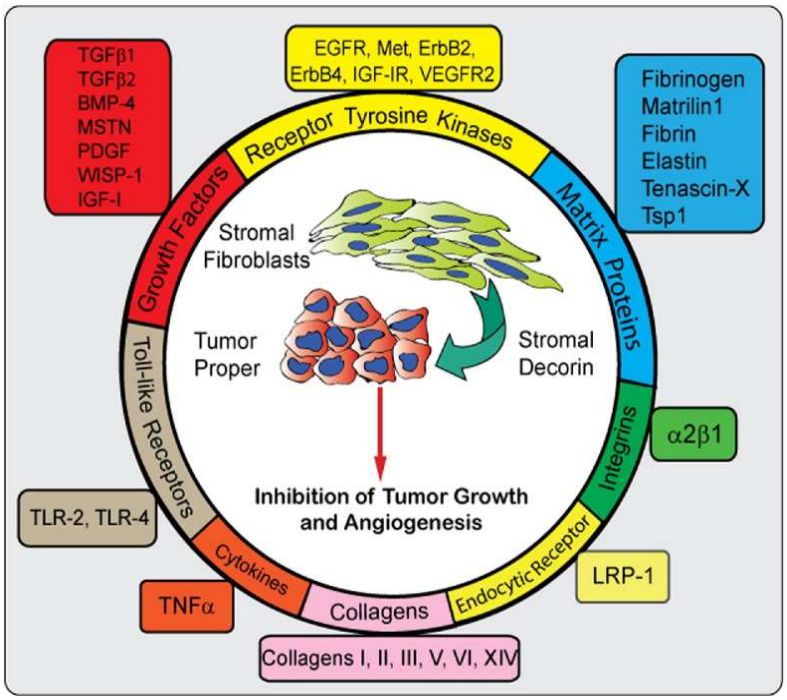


Figure 15:- The decorin acts as matrix guardian. It interacts with growth factors, receptors, cytokines, collagen fibers and various ECM proteins (Neill et al., 2012).

Decorin also plays an important role in the mineralization of the human smooth muscle cells (VSMC). Indeed, it has been reported that the oxidized low density lipoprotein (Ox-LDL) induced mineralization of VSMC is dependent on the decorin core protein and the CS/DS GAG chain. Treatment of VSMC with Ox-LDL results in upregulation of XT-I (the enzyme that initiate the GAG synthesis) and Msx2 (marker of mineralization). It is also responsible for the activation of

TGF-β dependent Smad signaling pathway to enhance the mineralization. The inhibition of XT-I suppressed decorin induced mineralization (Yan et al., 2011).

Decorin GAG chain interact with collagen fibrils and play a crucial role in matrix assembly and in the pathophysiology of angiogenesis. Decorin has an important role in angiogenesis and tumorogensis. It either promote or inhibit angiogenesis. But, it is interesting that it has inhibitory effect on tumor associated angiogenesis. Therefore, decorin based therapies have positional role in controlling tumor growth, metastasis and angiogenesis (Bi and Yang, 2013). Taken together, decorin emerged as potential therapeutic target for various tumors (Figure 16).

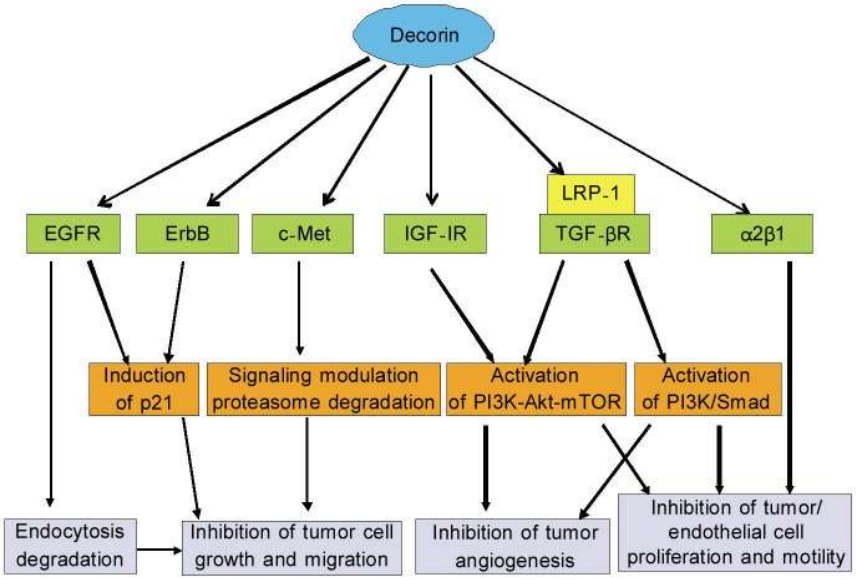


Figure 16:- The biological functions and regulating targets of decorin in tumor (Bi and Yang, 2013).

1.4.2 Biglycan

1.4.2.1 Structure

The biglycan belongs to the CSPG, SLRP class 1, with core protein of about 42 kDa and contains two GAG chains (Figure 17). The chondroitin or dermatan sulfate GAG chains are attached on the N-terminal. It is synthesized as precursor and BMP-I cleaves the N-terminal propeptide to release the active form. Biglycan interacts with many ECM components such as decorin, it also interacts with various growth factors and cytokines like TGF, BMP and TNF-α.

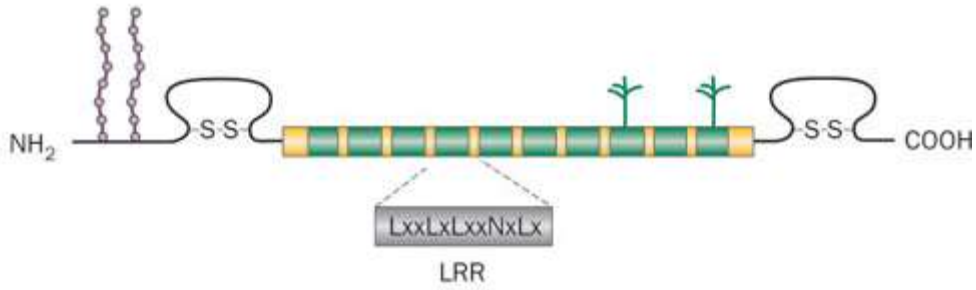


Figure 17:- Structure of Biglycan. It contains two GAG chains at N-terminal and the core protein has several leucine rich repeats (Edwards, 2012).

1.4.2.2 Functions

Biglycan has an important role in the signaling pathways because it act as ligand for Toll-like receptors (TLRs)-2 and -4 (Schaefer et al., 2005), P2X7/P2X4 receptors, low-density lipoprotein receptor-related protein 6 (LRP6) and receptor tyrosine kinase (MuSK) (Amenta et al., 2012; Nastase et al., 2012). Biglycan also has an important role in the innate immunity and inflammation. Its expression is upregulated in the pulmonary inflammation and asthma. It stimulates the canonical Wnt/β-catenin signaling (Berendsen et al., 2011; Wang et al., 2015), BMP and TGFβ signaling pathways in osteoprogenitor cells to enhance the bone formation (Figure 18) (Nastase et al., 2012).

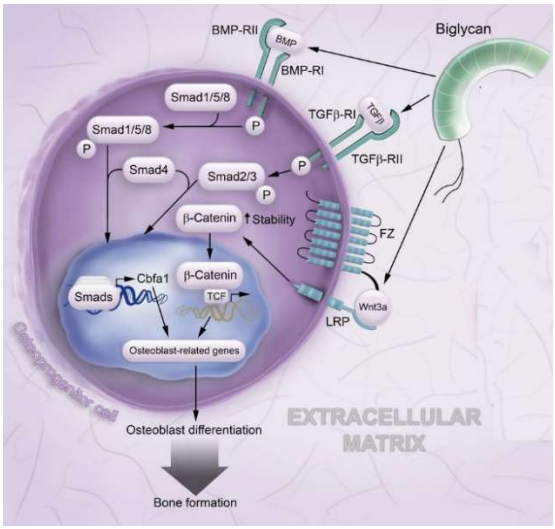


Figure 18:- Biglycan signaling in the osteoprogenitor cells. The biglycan mediate the BMP, TGFβ and Wnt conical signaling pathways to stimulate the osteoblast differentiation to form bone (Nastase et al., 2012).

1.4.3 CSPG4/NG2

CSPG4/NG2 is a CSPG containing one CS/DS chain. The core protein of CSPG4/NG2 is about 250 kDa with a type I transmembrane topology (Figure 19). The large extracellular domain is subdivided into three subdomains, the N-terminal domain (D1 subdomain) contains two laminin-like globular (LG) repeats, the central domain (D2 subdomain) contains 15 tandem repeats and have site for the CS attached GAG chains and the juxtamembrane domain (D3 subdomain) have several sites for the protease cleavage. The LG repeats in the D1 region interact with integrins and RTKs to mediate the cell–matrix, cell–cell and cell-ligand interactions. The CS GAG chain in the D2 region is also important for cell-matrix interaction and interacts with collagen fibres. The D3 binds with integrins and galectin (Price et al., 2011). A small transmembrane domain followed by the intracellular domain. The intracellular domain contains the PDZ domain for the binding of the PDZ family of proteins. Intracellular domain is important for the phosphorylation by PKCα and ERK1/2 kinases (Iozzo and Schaefer, 2015; Price et al., 2011).

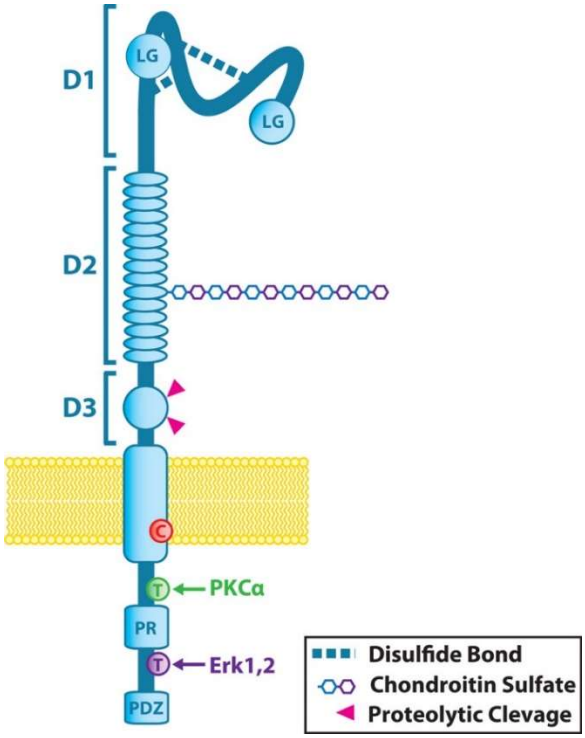


Figure 19:- Structure of CSPG4. The extracellular domain is subdivided into three domains and have one GAG chain site. The transmembrane domain contains one cysteine residue. The intracellular domain contains sites for phosphorylation and for PDZ binding proteins (Price et al., 2011).

The CSPG4/NG2 promotes tumor vascularization and survival of brain tumors but interestingly it reduce the tumor angiogenesis (You et al., 2014). Moreover the combined therapies with CSPG4/NG2 and activated natural killer cells showed great potential for the treatment of glioblastoma in mouse models (Poli et al., 2013; Wang et al., 2011).

1.4.4 Aggrecan

Aggrecan belongs to the CSPG group called hyalectans. Its molecular size is more than 200 kDa. It contains three (G1, G2, G3) domains (Figure 20A). The N-terminal domain (G1) contains IgG fold and the link protein to form stable complex with HA. The G2 is next to G1 domain and it contains conserved sites for the attachments of the keratin sulphate. The C-terminal domain (G3) contains complementary regulatory protein, C-type lectin and two EGF like repeats. The central region between G2 and G3 contain several GAG attachment sites. This region is encoded by large single exon with 120 ser-gly repeats for the attachment of the GAG chains. It has CS1 and CS2 region (Iozzo and Schaefer, 2015).

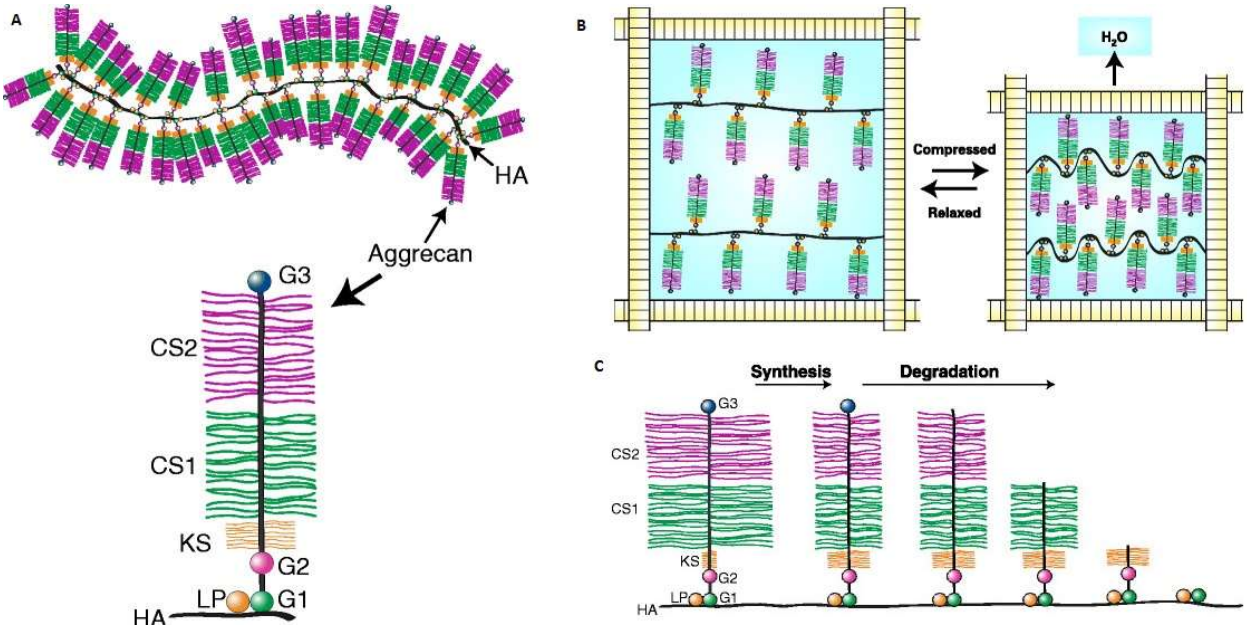


Figure 20:- Structure, function, synthesis and degradation of the aggrecan. Several aggrecans are linked to the HA by G1 domain and central region contains the GAG attachment site (A). The aggrecan adsorb water in the relax form expel water in the compression of cartilage (B). The GAG chains degrade with aging (C) (Roughley and Mort, 2014).

It is mainly present in the cartilage and it forms densely-packed aggregates and attracts water and maintains collagen fibers assembly and is responsible for the load bearing capability of the cartilage and also acts as lubricant. The aggrecan GAG chains are important for its water holding capacity (Roughley and Mort, 2014).

In osteoarthritis (OA) cartilage, the catabolism of the aggrecan increased due the presence of various cytokines such as interleukin-1 (IL-1) and tumor necrosis factor α (TNFα). These cytokines downregulate aggrecan synthesis and upregulate the proteinases that degrade aggrecan (Roughley and Mort, 2014; Troeberg and Nagase, 2012). The aggrecan is also present in the nervous tissue (Domowicz et al., 2008; Dyck and Karimi-Abdolrezaee, 2015).

1.4.5 Versican

Versican also belongs to the CSPG family, with a core protein of about 400 kDa (V0). The core protein contains two conserved domains (G1 and G3) at both ends and the central region has several GAG attachment sites. The N-terminal domain (G1) have IgG fold and interacts with link protein for attachment of the HA (Figure 21). The C-terminal domain (G3) contains two EGF like repeats, complementary regulatory domain and C-type lectin domain. The versican gene is located at 5q14.3 in human (Wight et al., 2014). However, the alternative splicing of the versican gene produces four isoform with different GAG attachment sites. The three isoforms (V0, V1, V2) contains the GAG chains but one isoform (V3) has no GAG chains. In the full versican (V0), the central GAG attachment domain is divided into a short α and a relatively big β region. The versican (V1) has only β region and versican (V2) contains only α region. The versican (V3) contains only core protein having G1 and G3 domain but did not have GAG attachment domain. Recently, Kischel et al reported a new versican isoform (V4) that is upregulated in the breast cancer. The versican (V4) has the G1 domain, the first 398 amino acids of the β-GAG region and the G3 domain (Kischel et al., 2010; Wight et al., 2014).

Versican plays crucial role in the regulation of cell migration, adhesion, inflammation and it interacts with other components of the ECM. In the inflammation, it facilitate the leukocytes migration and interaction with receptors such as CD44, P-selectin glycoprotein 1 (PSGL-1) and Toll-like receptor 2 (TLR2) (Wight et al., 2014).

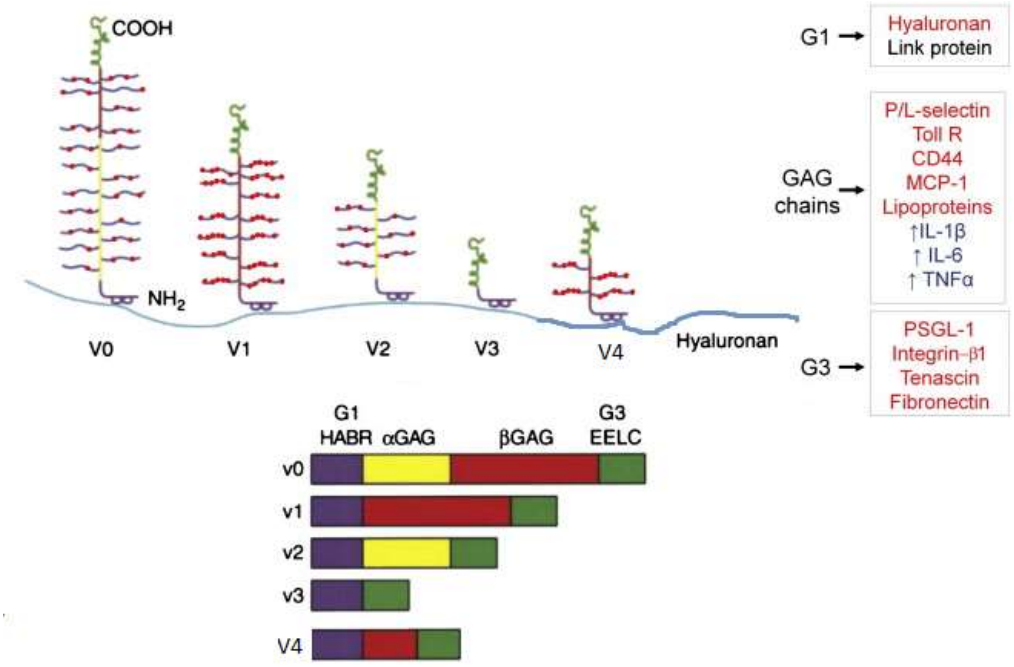


Figure 21:- The structure of four versican isoforms. All isoforms are attached to the HA on N-terminal via G1 domain. The C-terminal G3 domain interacts with fibronectin and integrin. The central region contains two α and β GAG attachment region (Wight et al., 2014).

Chapter 2

Biosynthesis and Regulation of Glycosaminoglycan and Proteoglycans

2. Biosynthesis of GAG chains

The GAG chains are synthesized on the core protein by stepwise addition of individual sugar residues. The first step in GAG synthesis pathway is the formation of tetrasaccharide linker region. This linker region acts as primer for the synthesis of both CSPG and HSPG.

2.2 Synthesis of the tetrasaccharide linker

The HS and CS/DS synthesis is primed on the common tetrasaccharide linker and is formed by the stepwise addition of sugar residues. The first step in the tetrasaccharide linker formation is the xylosylation of the core protein on specific serine residues by xylosyltransferase (EC 2.4.2.26), XT. The XT has two isoforms (XT-I and XT-II) and both are able to initiate the GAG synthesis. After xylosylation, two galactose residues are added by GalT-I (β1,4-galactosyltransferase 7) and GalT-II (β1,3-galactosyltransferase 6). The fourth reside, glucuronic acid, is transferred by GlcAT-I (β1,3-glucuronyltransferase I). The mutation in the GTs involved in the tetrasaccharide linker region results in various diseases (Figure 22) and impact of these mutations on the GAG synthesis is described in XT mutation chapter.

Table 3:- The enzymes involved in synthesis of tetrasaccharide linkage region

Enzymes (activity)	Genes	Chromosomal location	mRNA accession number
Xylosyltransferase	XT-I	16p12.3	NM_022166
	XT-II	17q21.33	NM_022167
β1,4-Galactosyltransferase-I	GalT-I	5q35.2–q35.3	NM_007255
β1,3-Galactosyltransferase-II	GalT-II	1p36.33	NM_080605
β1,3-Glucuronyltransferase-I	GlcAT-I	11q12.3	NM_012200
Xylose 2-O-kinase	FAM20B	1p25	NM_014864
Xylose 2-O-phosphatase	ACPL2 (XYLP)	3q23	NM_152282

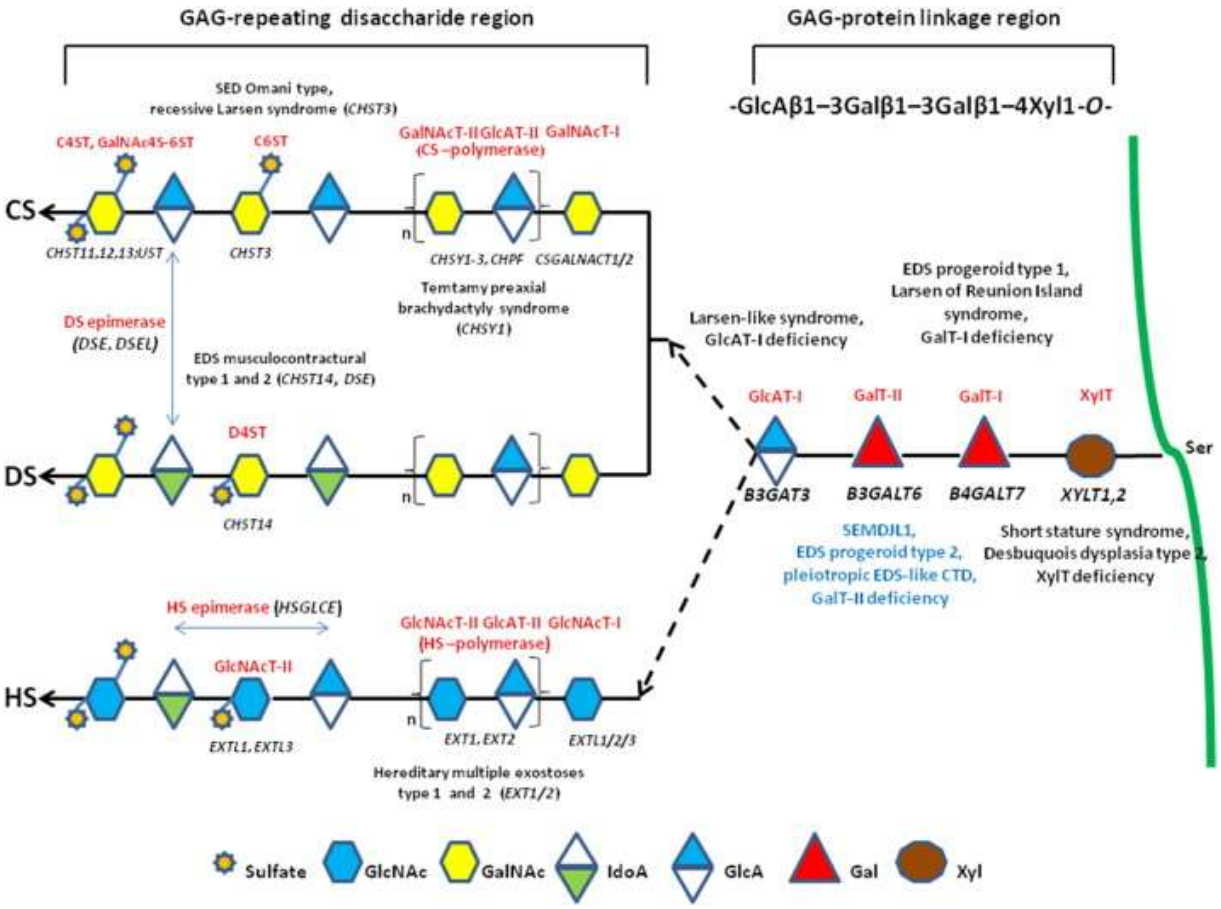


Figure 22:- The enzymes involved in the synthesis of the CS-, DS- and HSPGs (Ritelli et al., 2015). The PGs are attached to core protein through a common tetrasaccharide linker region which after differentiate into either CS/DSPGs or HSPGs. The mutation in enzymes involved in synthesis are linked with various syndromes.

2.3 Elongation of the CS chains

Chondroitin sulfate contain the repeating disaccharide units [(–4GlcAβ1–3GalNAcβ1–)n] linked to core protein via a common linker region. The GTs involved in the CS synthesis are chondroitin synthase-1 and 3 (ChSy-1, ChSy-3), chondroitin polymerizing factor (ChPF), and chondroitin N-acetylgalactosaminyltransferases 1 and 2 (ChGn-1 and ChGn-2) (Izumikawa et al., 2015; Mikami and Kitagawa, 2013).

The CS polymerization requires the co-expression of any two of the three enzymes ChSy-1, ChSy-3 and ChPF for addition of the GalNAc and GlcUA residues. ChGn-1 and ChGn-2 are also involved in chain initiation and elongation (Mikami and Kitagawa, 2013).

The CS chains are modified by sulphation at 2nd, 4th and 6th position of residues by seven sulfotransferases. The 2-OST transfer the sulphate at 2nd position of the iduronic acid. The 4-OST transfer the sulphate at 4th position of the GalNAc are referred as C4ST-1, -2, and -3. The 6-OST transfer the sulphate at 6th position of GalNac (Mikami and Kitagawa, 2013).

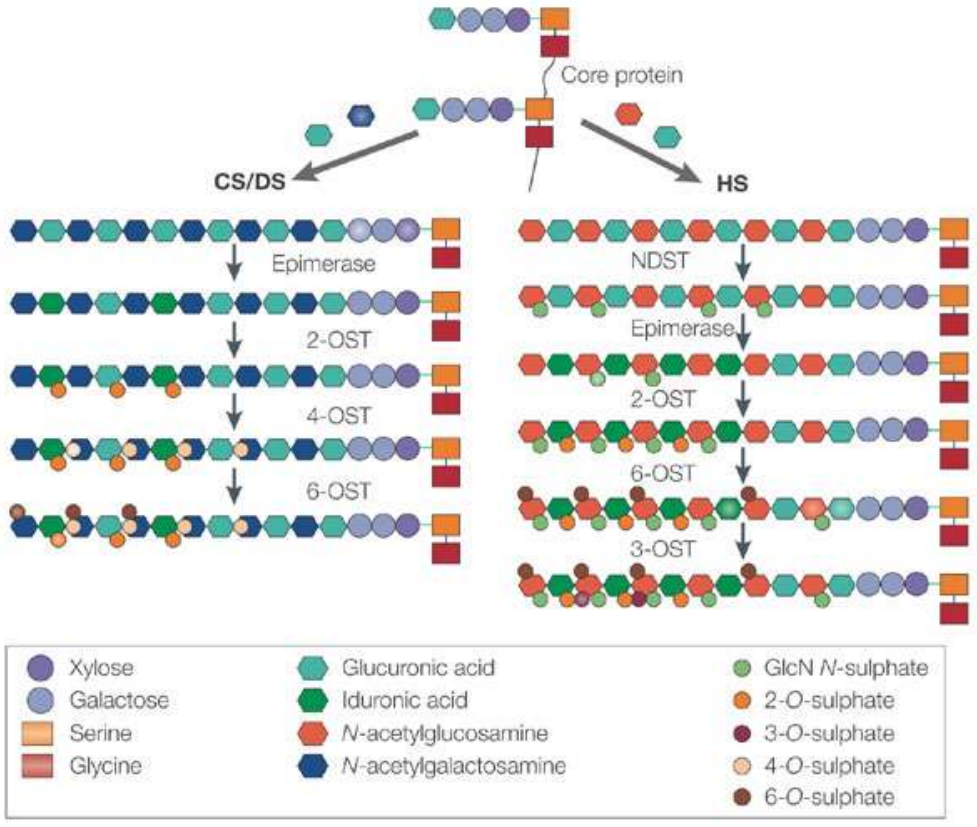


Figure 23:- The Biosynthesis of the CS and HS (Hacker et al., 2005).

2.4 Elongation of the HS Chains

The attachment of the N-acetylglucosamine (GlcNAc) residue to the non-reducing end of tetrasaccharide linkage region by EXTL family initiate the synthesis of HS chains. The HS chain synthesis is initiation by the EXTL1-3 and all are able to transfer the α-GlcNAc for the HS synthesis (Kim et al. 2001) .However, EXTL3 is major enzyme to start HS synthesis. The EXTL2

transfer GlcNAc or GalNAc to common linker region, the HS synthesis in initiated by the transfer of GlcNAc while addition of α-GalNAc blocks GAG synthesis (Nadanaka and Kitagawa, 2014). After initiation of the HS synthesis by the EXTL1-3, the chains polymerization is catalyzed by the EXT1 and EXT2.

Like CS, several modifications occur on the HS chain. The GlcNAc is deacetylated and sulphated by deacetylase-N-sulfotransferases (Ndst). The D-glucuronic acids are epimerized to L-iduronic acid (IdoA) by C5 epimerase. The HS chains are formed by modified domain (N-sulfated or NS domains) and unmodified domains (N-acetylated or NA domains). The region between these domains are called NA/NS domains. Sulfotransferases transfer sulfate at various position of the disaccharide unites. The 2-O-sulfotransferase (Hs2st) adds sulfate at C2 of the iduronic acids, 6-O-sulfotransferases (Hs6st1-3) transfer sulfate at C6 to the N-sulfoglucosamine units and 3-O-sulfotransferases (Hs3st1, 2, 3a,3b, 4, 5, 6) add sulfate at C3 of glucosamine units.

Table 4:- The enzymes involved in synthesis of repeating disaccharide units of CS chains

Enzymes (activity)	Abbreviation	Chromosomal location	mRNA accession number
Chondroitin synthase	ChSy-1	15q26.3	NM_014918
(GalNAcT-II, GlcAT-II)			
	ChSy-3	7q36.1	NM_019015
Chondroitin polymerizing factor	ChPF	2q35	NM_024536
Chondroitin GalNAc transferase (GalNAcT-I, GalNAcT-II)	ChGn-1	8p21.3	NM_018371
	ChGn-2	10q11.21	NM_018590
Sulfotransferases and epimerases			
Chondroitin 4-O-sulfotransferase	C4ST-1	12q	NM_018413
	C4ST-2	7p22	NM_018641
	C4ST-3	3q21.3	NM_152889
Dermatan 4-O-sulfotransferase	D4ST-1	15q15.1	NM_130468
Chondroitin 6-O-sulfotransferase	C6ST-1	10q22.1	NM_004273
Uronyl 2-O-sulfotransferase	UST	6q25.1	NM_005715
GalNAc 4-sulfate 6-O-sulfotransferase	GalNAc4S-6ST	10q26	NM_015892
Glucuronyl C-5 epimerase	DS-epi1	6q22	NM_013352
	DS-epi2	18q22.1	NM_032160

Table 5:- The enzymes involved in synthesis of repeating disaccharide units of HS chains

Enzymes (activity)	Abbreviation	Chromosomal location	mRNA accession number
Exostosin (GlcA and GlcNAc transferases)	EXT1	8q24.11	NM_000127
	EXT2	11p12-p11	NM_000401
Exostosin-like 2 (GlcNAc transferase-I)	EXTL2	1p21	NM_001439
(GlcNAc transferase-I and -II)			
GlcNAc N-deacetylase and N-sulfotransferase	NDST1	5q33.1	NM_001543
	NDST2	10q22	NM_003635
	NDST3	4q26	NM_004784
	NDST4	4q26	NM_022569
Sulfotransferases and epimerases			
HS GlcUA C5-epimerase	GLCE	15q23	NM_015554
HS 2-O-sulfotransferase	HS2ST1	1p22.3	NM_012262
HS 6-O-sulfotransferase	HS6ST1	2q21	NM_004807
	HS6ST2	Xq26.2	NM_147174
	HS6ST-3	13q32.1	NM_153456
HS 3-O-sulfotransferase	HS3ST1	4p16	NM_005114
	HS3ST2	16p12	NM_006043
	HS3ST3A1		NM_006042
	HS3ST3B1	17p12	NM_006042
	HS3ST3B1		NM_006041
	HS3ST4	16p11.2	NM_006040
	HS3ST5	6q22.31	NM_153612
	HS3ST6	16p13.3	NM_001009606
HS 6-O-endosulfatase	SULF1	8q13.2-q13.3	NM_015170
	SULF2	20q12–q13.2	NM_198596

2.4 Regulation of PG synthesis

The PG-GAG synthesis is regulated by cytokines and growth factors. The major cytokines involved in the PG regulation is the IL-β1 which suppress GAG synthesis. Whereas growth factors such as TGF-β and PGDF enhance GAG synthesis. The most important GT that regulates the GAG biosynthesis is the XT which catalyzes the first and rate limiting step in the GAG synthesis pathways.

TGF-β induces the synthesis of chondroitin sulphate GAGs in the rat dental pulp cells. Treatment with TGF increases the synthesis of 4 and 6 sulphated CS-GAGs (Nishikawa et al., 2000). TGF-β also enhances the GAG synthesis in the mesenchymal cells derived from the murine embryonic palate (MEPM). The cells treated with TGFβ produce more GAGs compare to untreated cells (D'Angelo and Greene, 1991).

The accumulation of CSPG after nervous tissue injury plays an inhibitory effect on the repair process. The CSPG in the nervous tissue is also regulated by the TGF-β. It induces the expression of CSPG core protein like neurocan, phosphacan, brevican and of the glycosyltransferase, XT-I (Susarla et al., 2011).

The PG-GAGs are important component of the articular cartilage and regulated by the TGF-β and IL-β (Pujol et al., 2008). TGF-β upregulate the expression of XT-I and enhance the GAG synthesis whereas treatment with IL-β1 suppress GAG synthesis by downregulation of XT-I expression (Venkatesan et al., 2012; Venkatesan et al., 2009b). It has recently been shown that the GAG accumulation in the pulmonary fibrosis is mediated by TGF-β1 through upregulation XT-I (Venkatesan et al., 2014).

The PG-GAG synthesis is decreased in osteoarthritis (OA) and rheumatoid arthritis (RA) in human and animal models. The decrease in the GAG synthesis is due the down regulation of XT-I. In antigen-induced arthritis (AIA) OA model showed that XT-I is reduced significantly at day 7 and IL-β1, a proinflammatory cytokine, is responsible for this down-regulation of XT-I expression and reduce the PG synthesis. Further the same study elaborates the role of XT-I in cartilage repair in rat model, the papain injection in rat knees increased the PG synthesis up to 70% at 4 day. The increase in the PG synthesis is due to up-regulate XT-I gene expression and silencing of XT-I

expression by XT-I shRNA prevent cartilage repair and reduce the PG synthesis (Venkatesan et al., 2009b). The increase in the XT-I expression in papain induced cartilage repair is governed by TGF-β signaling and blocking the TGF-β signaling during cartilage repair decrease the XT-I expression and PG-GAG synthesis (Venkatesan et al., 2009b). Recently, it has been showed that XT-I gene expression is upregulated in the early and downregulated at late phase in human OA cartilage. Similarly, the GAG synthesis is increased in the early stage OA and decreased in the late phase of OA (Venkatesan et al., 2012).

The CSPGs expression is increased after nervous tissue injury which led to delay in repair process. Therefore strategies are designed either to reduce the CSPG synthesis or increase their degradation to enhance the nervous tissue repair (Figure 24). The deoxyribozyme to XT-1 enhanced nervous tissue repair process. This technique has been successfully used to repair spinal card injury. The use of XT-I deoxyribozyme showed promising results in the repair of the nervous tissue (Grimpe, 2011; Grimpe et al., 2005; Grimpe and Silver, 2004).

The other strategy is to use the synthetic xyloside to inhibit the GAG synthesis. Xyloside analogues are used to inhibit GAG synthesis to repair nervous tissue injury. They suppress the CSPG synthesis and enhance the nervous tissue repair process (Hashemian et al., 2014; Lau et al., 2012; Swarup et al., 2013).

The phosphorylation of xylose by Fam20B plays a crucial role in the regulation of the PG-GAG synthesis. The phosphorylation of the xylose occurs transiently after the attachment of the xylose (Moses et al., 1997) and addition of the glucuronic acid results in the rapid dephosphorylation. However, we have previously shown that phosphorylated xylose analog could not be used as substrate by GalT-I for chain elongation. (Gulberti et al., 2005b). Moreover it is recently shown that phosphorylated xylose is an important regulator of both CS (Izumikawa et al., 2015) and HS (Nadanaka et al., 2013) biosynthesis pathways. The phosphorylation of eth xylose is catalyzed by Fam20B, therefore GAG synthesis (Wen et al., 2014).

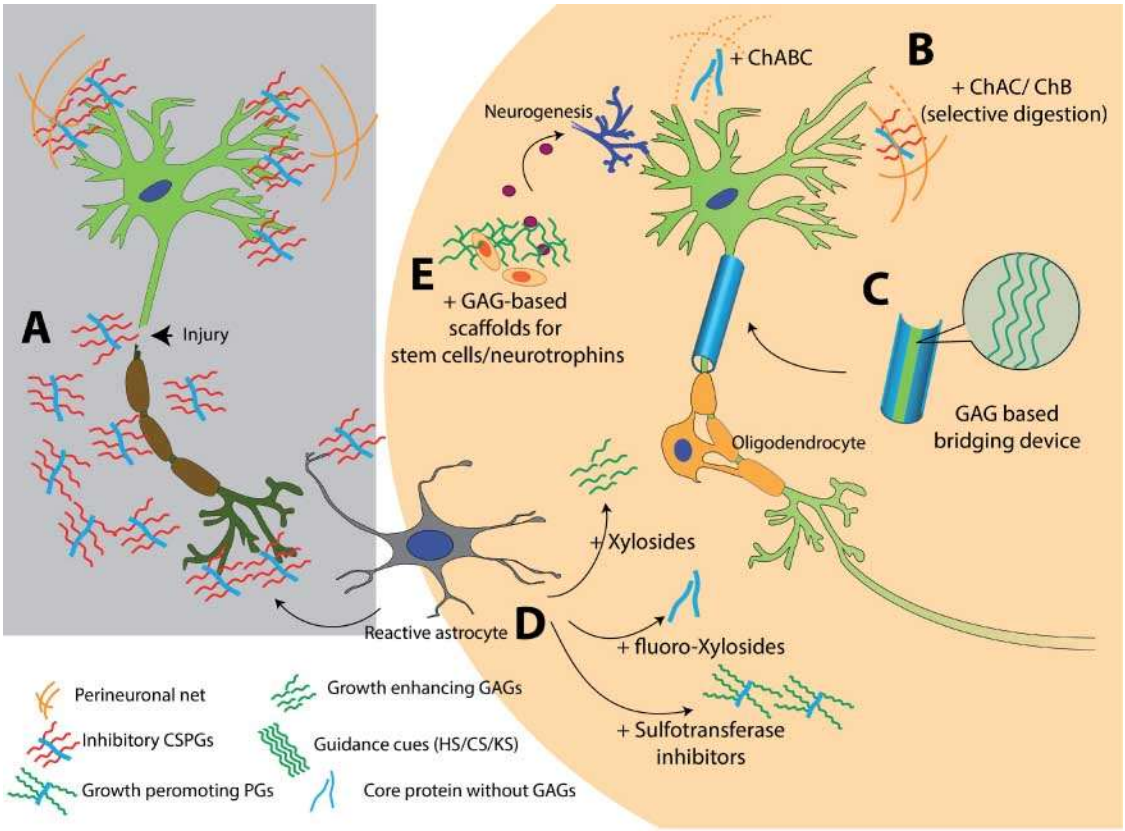


Figure 24:- Strategies to improve the nervous tissue repair. After the neuronal CSPGs are overexpressed and this inhibits the tissue repair (A). The chondroitinase ABC is mostly used to eliminate the inhibitory CSPGs but selective digestion with chondroitinase A and B might give better results. BC can be done using ChAC and ChB enzymes (B). The use of GAG bridge facilitate guide regenerating axons (C). The xyloside and sulphotransferase inhibitors also improve nerve tissue repair by inhibiting GAG synthesis and sulphation on GAG chains (D). The GAG basted scaffolds can be designed to deliver stem cells or neurotropic factors at the scar site (E). These therapies might be used as single or in combination to cure the neurological disorders (Swarup et al., 2013).

Chapter 3
Xylosyltransferase I and II

3 Xylosyltransferase

The XT transfer the xylose from UDP-xylose to the specific serine residues of the core protein to initiate the common tetrasaccharide linker region for CS- and HS-GAG Chains. XT is the rate limiting enzyme in the biosynthesis of GAG chains and has two isoforms XT-I and XT-II.

3.1 Specificity of the xylosyltransferase

Muir et al reported for the first time in 1958 that the serine residues of PGs are involved in the synthesis of chodroitin sulphate (Muir, 1958). Further, Gregory et al in 1964, showed the incorporation of radiolabeled UDP-xylose to the serine residues of the core protein by XT (Gregory et al., 1964). Afterwards, the radiolabeled xylose incorporation is confirmed by using various tissue sources such as hen oviduct, murine mastocytoma and embryonic chicken cartilage (Grebner et al., 1966a; Grebner et al., 1966b). Various acceptors have been used for the xylosylation and GAG synthesis (Baker et al., 1972; Campbell et al., 1990). The silk fibroin containing the Ser-Gly-Ala-Gly-Ala-Gly repeats and short peptides Ser-Gly-Gly, Gly-Ser-Gly and Gln-Ser-Gly were also used as acceptors for xylosylation (Brinkmann et al., 1997; Campbell et al., 1984).

The replacement of the serine with threonine has also been tested for the XT activity. The bikunin type peptide, (QEEEGSGGQGG) containing threonine instead of serine has more xylosylation potential (Pfeil and Wenzel, 2000). However, site directed mutagenesis of serine in the decorin GAG attachment motif (Asp-Glu-Ala-Ser-Gly-Ile-Gly) with threonine showed only 10% glycosylation (Mann et al., 1990).

The shortest motif for the XT is the Ser-Gly motif and this GAG attachment motif is present in many natural tissues like bovine tracheal cartilage, Bikunin and other peptides (Wilson, 2004a). Moreover the presence of acidic residues at -2 position of the serine also has a role in the substrate recognition of XT (Huber et al., 1988). The XT from different species use same acceptor substrate and therefore is not specie specific. For example, bikunin like peptide served as acceptor substrate for the XT from human, C. elegans and Drosophila (Wilson, 2004a).

3.2 Structure of the XT-I and XT-II

The XT-I isoform is encoded by *XYLT-1* gene located on chromosomes 16p13.1 and contains 12 exons with a total length of about 300kb. This encodes for a protein of 959-amino acid residues with molecular weight of about 100 kDa.

Like other GTs, XT-I exhibits a transmembrane topology (Figure 25) with a short cytoplasmic domain, transmembrane domain and intraluminal domain containing the catalytic site and a stem region. The cytoplasmic and transmembrane domains are encoded by the exons 1 and 2, while the extracellular domain is encoded by the exons 3 to 12. The soluble form of the enzyme, lacking cytoplasmic and transmembrane domain, showed catalytic activity (Götting et al., 2007).

XT-II is encoded by *XTLT-II* gene present on the chromosomes 17q21.3 containing 11 exons with a size of 15kb. The XT-II contains 865 amino acid and has the molecular weight of 97 kDa. The XT-II also has transmembrane topology containing short cytoplasmic domain, an intraluminal domain containing the catalytic site and short stem region (Figure 25). The cleavage at stem region release the soluble form of XT which is catalytic active (Götting et al., 2007).

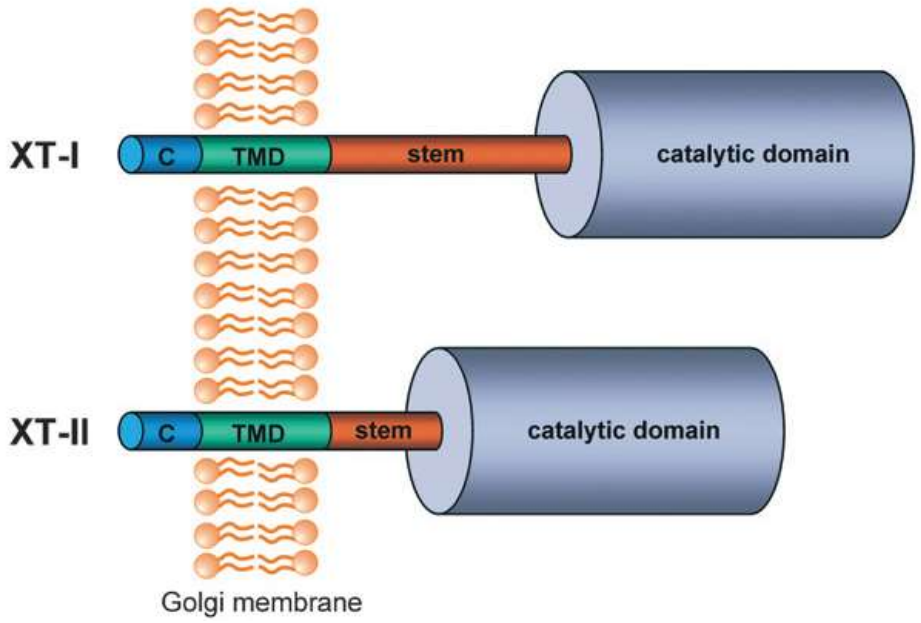


Figure 25:- Structure of XT-I and XT-II. XT-I and XT-II present a transmembrane topology with short cytoplasmic domain (C), transmembrane domain (TMD) and a large intraluminal domain containing stem region and catalytic domain (Götting et al., 2007).

The second isoform of the XT was discovered in 2000 (Götting et al., 2000a) and its catalytic activity of XT-II has been assigned in 2007 (Cuellar et al., 2007; Pönighaus et al., 2007; Voglmeir et al., 2007). Both, XT-I and XT-II have similar activity for the bikunin peptide (QEEEEGSGGQKK). However, human XT-I showed higher specificity for amyloid protein precursor protein (TENEGSGTLNIK) compare to XT-II (Casanova et al., 2008; Götting et al., 1998). Interestingly, the recombinant mouse XT-I and XT-II showed equivalent activity for amyloid protein precursor protein (Condac et al., 2009).

Site directed mutagenesis was used to replace the surrounding glycine residues of the Bikunin Gly-Ser-Gly motif to study the difference in the acceptor specificity of the XT-I and XT-II. The mutated peptides were used to measure the activity of both XT isoforms and most of these mutants was utilized by XT-I but not for XT-II. This indicated that XT-I has flexible acceptor acceptance compare to XT-II (Roch et al., 2010). Moreover, XT-I and XT-II are also differentiated by the donor xylose modifications. XT-I is able to transfer the UDP-4-azido-4-deoxyxylose (UDP-XylAz) to the bikunin peptide, whereas XT-II is unable to use this compound (Kuhn et al., 2015).

3.4 Structural/Functional relationship

Although, the XT has been purified, the 3D crystal structure has not been resolved yet, therefore the structure-function information is gained from the site directed mutagenesis of specific amino acid residues, deletion and truncation of specific regions. Most families of GTs contains DXD motif which is important for their catalytic activity (Breton et al., 1998; Wiggins and Munro, 1998). Similarly, XTs contain two DXD motifs present in the N- and C-terminal of the protein (Figure 26). The XT-I DXD motif is present in the exon 4 and 11, whereas the XT-II DXD motif is located in the exon 5 and 10. In XT-I, the mutations in N-terminal DXD motif (^{314}DED^{316}) did not alter the catalytic activity of enzyme indicating that this motif might not be crucial. However, the C-terminal DXD motif (^{745}DWD^{747}) plays an important role in the catalytic activity. Indeed, mutation of aspartic acid 745 to glycine results in the 95% decrease in catalytic activity. However, mutation of conservative aspartic acid residue 745 to glutamic acid does not alter the XT-I activity. Therefore, negative charge of the DXD motif is importance (Götting et al., 2004).

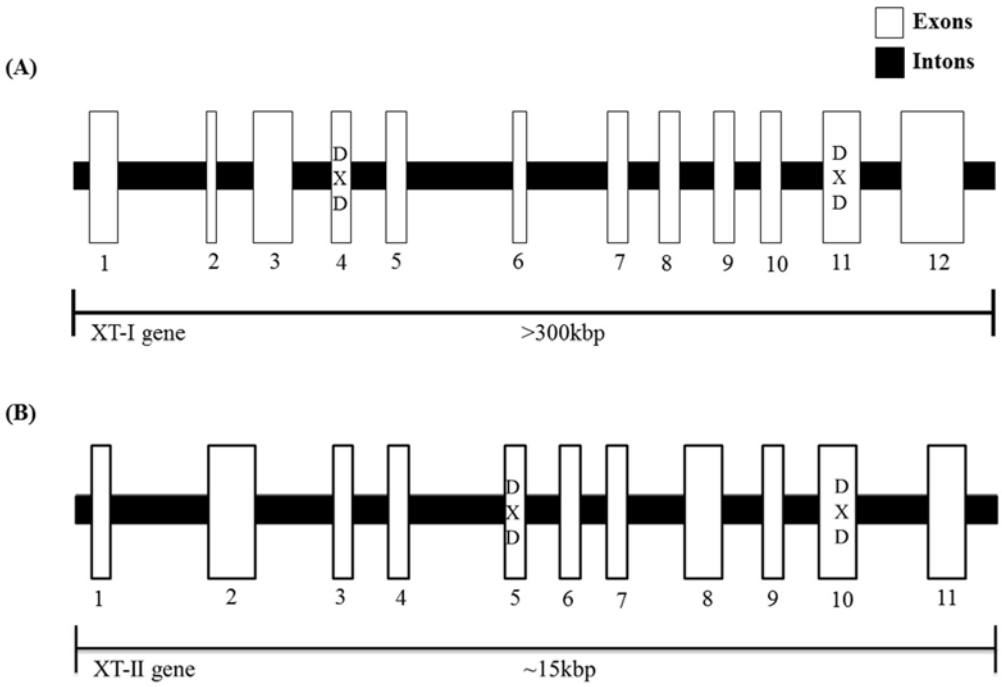


Figure 26:- Structure of XT-I and XT-II genes. XT-I gene contains 12 exons and DXD motif is located in the exon 4 and 11, while the XT-II gene have 11 exons and the DXD motif is present on exon 5 and 10 (Götting et al., 2004).

It is interesting to note that deletion of twelve amino acid residues from 261-272 reduced by 98% the enzymatic activity, indicating that the motif (^{261}GKEAISALSRAK^{272}) is important for the catalytic activity of XT-I. The truncation of these amino acid led to a loss-of-function without significantly altering the substrate binding (Muller et al., 2006).

The disulphide bonds are important for the stability and folding of the protein and hence are important to maintain the 3D structure and catalytic activity. Like other enzymes, GTs also contain several conserved cysteine residues (Holmes et al., 2000; Wang et al., 1994). The multiple sequence analysis of XT-I from different species revealed that XT-I contains 14 highly conserved cysteine residues. These cysteine residues were analyzed by site directed mutation to explore their importance for the function of the enzyme. Each of these residues was mutated to alanine. The cysteine residues at 471 and 574 are most important for catalytic activity of the enzyme and their mutation to alanine blocks the catalytic activity of the enzyme (Muller et al., 2005).

3.4 Purification of the XT from tissue source

Since the discovery of XT in 1958, various attempts have been made to purify the enzyme from different tissue sources. Thus XT was purified from the embryonic chick epiphyseal cartilage using ammonium sulphate fractionation and density gradient centrifugation (Stoolmiller et al., 1972). Afterwards, XT has also been purified from the rat chondrosarcoma and embryonic cartilage using differential centrifugation, Sephadex gel chromatography and affinity chromatography. XT from all sources has molecular weight of about 95-100 kDa (Schwartz and Dorfman, 1975; Schwartz and Rodén, 1974). XT was also purified from crude extract with affinity chromatography using the dodeca peptide Q-E-E-E-G-S-G-G-G-Q-G-G as ligand for xylosylation yielding highly purified enzyme. The purified XT is a monomer with molecular weight of 78 kDa (Pfeil and Wenzel, 2000).

3.5 Purification of the XT from cellular source as cDNA cloning

It has been reported that XT is secreted into the ECM in CHO cells expressing XT, only 2% activity was determined in the cell lysate whereas 98% is secreted into the medium (Götting et al., 2000b). XT has been purified from medium of cultured JAR choriocarcinoma cell (Kuhn et al., 2001). The human JAR choriocarcinoma cells were grown in a hollow-fiber bioreactor in serum free medium. The XT was purified from 18.5 liters of enriched cell culture supernatant. The purification process includes the plethora of chromatography techniques including the ammonium sulphate precipitation, heparin affinity chromatography, ion exchange chromatography and protamine affinity chromatography. The purified enzyme is a monomer with molecular weight of about 120 kDa on SDS-PAGE. The Edman degradation of this purified enzyme gives eleven peptide fragments which are characterized by the matrix-assisted laser desorption / ionization mass spectrometry-time of flight (MALDI-TOF). The amino acid sequences of 11 peptides were determined and used to design the specific primers for the cloning of the XT-cDNA and to design the specific antibodies for XT detection (Kuhn et al., 2001). The further characterization of these peptides revealed that there are two isoform of the XT in the human and rat (Götting et al., 2000b). Afterwards, it has been shown by three different research groups that the XT-II is catalytically active enzyme can initiate the GAG synthesis (Cuellar et al., 2007; Pönighaus et al., 2007; Voglmeir et al., 2007).

The recombinant XT-I was produced from stable transfection of the XT expressing plasmid into High Five insect cell line (Kuhn et al., 2003). These transfected cells were grown in roller flask and XT was purified with heparin affinity chromatography and nickel chelate affinity chromatography to yield the highly purified and catalytically active XT-I (Kuhn et al., 2003).

The XT-II was overexpressed in *P. pastoris* strain X-33 with XT-II expressing plasmid and purified from 40 litres of the culture medium. The medium was concentrated and XT-II was purified by ammonium sulphate precipitated, heparin affinity and ion exchange chromatography yielding pure enzyme with molecular weight of 95.8 kDa on SDS-PAGE. The catalytic activity was measured using bikunin as acceptor substrate, the purified XT-II exhibited 2.4-fold higher catalytic efficiency compare to XT-I.

3.6 Intracellular localization

The GTs which initiate the N-glycosylation were localized in endoplasmic reticulum (ER) (Aebi, 2013), but most of the GTs involved in GAG synthesis are localized in the Golgi (Dick et al., 2012). The localization of the XT is still contradictory some studies indicate that the XT is localized in the ER and some studies also suggest a Golgi localization (Wilson, 2004a)

Nuwayhid et al showed that the xylosylation occurs in a Golgi rich compartment in liver, tissue suggesting the Golgi localization of the XT (Nuwayhid et al., 1986), another study using core protein extracted from rat chondrosarcoma also suggest that xylosylation occurs mainly in a Golgi compartment (Lohmander et al., 1989).

The embryonic chick cartilage subculture fractions showed that the CS chains initiate in the rough endoscopic reticulum (RER) (Horwitz and Dorfman, 1968). Hofmman et al also suggested that xylosylation occurs in the RER and hence XT is localized in the RER (Hoffmann et al., 1984). Latter, Vertal et al used electron microscopy to visualized the xylosylation process and showed that XT is localized in the ER (Vertel et al., 1993). The same group showed that after xylosylation in the ER the elongation of GAG chains take place in the Golgi compartment (Kearns et al., 1993).

Latter a report by Schon et al showed that XT-I and XT-II were localized in the Golgi. They transected the HEK-293 cells with GFP tagged XT-I and XT-II plasmid and used

immunofluorescence microscopy to detect the localization. According to their results both XT-I and XT-II are localized in the cis-Golgi (Schön et al., 2006b) .

The XT isozymes are deferentially expressed in various tissues and cell lines. The liver tissue and cells are enriched in XT-II while cartilage contains the XT-I (Condac et al., 2007; Götting et al., 2000a; Roch et al., 2010). Similarly the xylosylation from the liver tissue showed the Golgi localization (Nuwayhid et al., 1986)and the cartilage tissue showed that xylosylation occurs in ER (Horwitz and Dorfman, 1968). This indicates that both isoforms (XT-I and XT-II) might have different localization.

3.7 XT activity analysis

The XT activity is measured by the incorporation of the radiolabeled UDP-xylose into the acceptor bikunin peptide and analyzed by liquid scintillation counting (Figure 27).

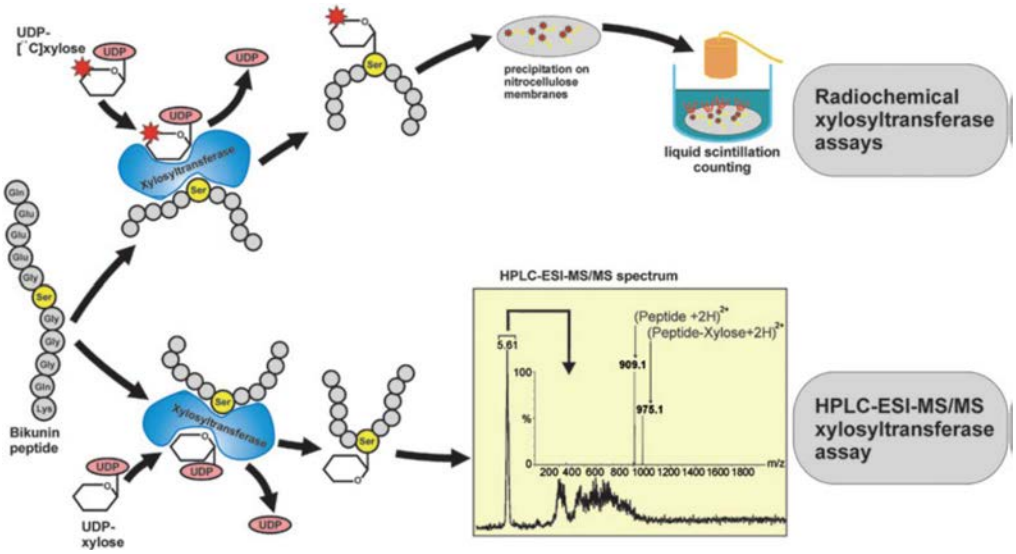


Figure 27:- The methods for the determination of Xylosyltransferase activity. The activity is measured by radiolabeled UDP-xylose incorporation and detected by liquid scintillation. The activity is also measured by HPLC-ESI-MS/MS using non-radiolabeled UDP-xylose (Götting et al., 2007).

Non-radiolabeled, methods have also been developed for detection of XT activity using MALDI-TOF (Wilson, 2002). The XT activity has been measured by xylosylation of synthetic peptide biotin-NH-Gln-Glu-Glu-Glu-Gly-Ser-Gly-Gly-Gly-Gln-Lys-Ly (5-fluorescein)-CONH2 as acceptor substrate and analyzed by the liquid chromatography-tandem mass spectrometry (LC-

MS/MS) (Kuhn et al., 2006). However, these analytical methods were unable to differentiate between the two isoforms. Recently, Khun et al showed that UDP-XylAz is selectively used by XT-I (Kuhn et al., 2015).

3.8 XT in health and disease

PGs are secreted in to the ECM and play an important role in patho-physiology of several biological processes. The XT is secreted into the ECM along with newly synthesized PGs but the function of this secreted XT is still unknown. Therefore XT in serum is used as potential biomarker for PG-GAG associated pathological conditions (Götting et al., 2007). Recently, it has been shown that XT-II is the main XT present in the serum and is derived from the platelets (Condac et al., 2009; Kuhn et al., 2015).

High XT activity has been found in serum of patient with systemic sclerosis (SSc), skin fibrosis, liver fibrosis, PXE, dilated cardiomyopathy, OA, RA, bone development, disturbed blood brain barrier and lung fibrosis (Götting et al., 2007).

3.9 XT-I and XT-II genetic variants

Various diseases are caused by defective glycosylation of proteoglycans caused by mutations in glycosyltransferase encoding genes. Mutations in the β4GalT7 leads to development of Ehlers–Danlos syndrome (EDS) type 1 and Larsen of Reunion Island syndrome (LRS). EDS is heterogeneous group of diseases characterized by aged appearance, short stature, generalized osteopenia, joint hyperlaxity, hypotonic muscles, and elastic skin. The mutation reported in the EDS patients are p.Ala186Asp, p.Leu206Pro and p.Arg270Cys. These mutants results in reduced enzymatic activity and therefore decorin and biglycan were not glycosylated (Faiyaz-Ul-Haque et al., 2011; Götte et al., 2008; Okajima et al., 1999; Seidler et al., 2006b). The LRS is characterized by large joints with ligamentous hyperlaxity, dwarfism, round flat face, prominent forehead and prominent bulging eyes (Laville et al., 1994). Recently, p.Arg270Cys mutation in the β4GalT7 is reported in LRS patients (Cartault et al., 2015).

Mutation of the XT-I and XT-II has also been reported in several proteoglycan-associated diseases and are risk factor for the severity of the disease. Recently a homozygous missense mutation (c.1441C>T [p.Arg481Trp]) in XT-I has been reported and causes an autosomal recessive short stature syndrome characterized by distinct facial features, alterations of fat distribution, mild

skeletal changes and moderate intellectual disability (Figure 28). Fibroblasts from their patients showed decorin without GAG chains and reduced XT expression. The in vitro enzymatic activity was measured using bikunin as acceptor peptide and is similar in patients and control (Schreml et al., 2014).



Figure 28:- Clinical features of patients with XT-I mutation R481W. Both patients III-1 and III-2 have distinctive facial features, short stature and moderate intellectual disability (Schreml et al., 2014).

Five mutations of the XT-I has been reported in the desbuquois dysplasia type 2 patients. These mutations include one missense mutation (c.1792C>T [p.Arg598Cys]) located in the catalytic domain of XT-I. Two nonsense mutations resulted in the premature stop codon (c.276dupG [p.Pro93Alafs*69], c.439C>T [p.Arg147*]) and leading to the truncated form enzyme. The other two were splice site mutations (c.1290-2A>C, c.1588-3C>T) located in exons 6 and 8 respectively. These mutants led to decreased GAG synthesis (Bui et al., 2014). The patients exhibit short limbs, flat face, narrow thorax and intellectual disability (Figure 29).

In mice, XT-I mutation W932R produced by N-ethyl-N-nitrosourea (ENU) treatment called pug mutation led to reduce body length (dwarfism). The pug mutant display reduced (15–20%) skeletal length at embryonic stage E14.5. The difference in skeletal length increase with age and at E16.5 the pug mutant has 40% reduction compare to wild-type. At the adult age, the pug mutants also

show reduction in body size, a smaller ribcage and broadening of the ribs, small skull, limbs and tail compare to wild-type mice. Analysis of the molecular mechanisms indicates that chondrocytes from the pug mutants mature more rapidly because they express more collagen X and have increased Ihh signaling. The pug mutants have less XT activity and therefore have reduced GAG synthesis (Mis et al., 2014).

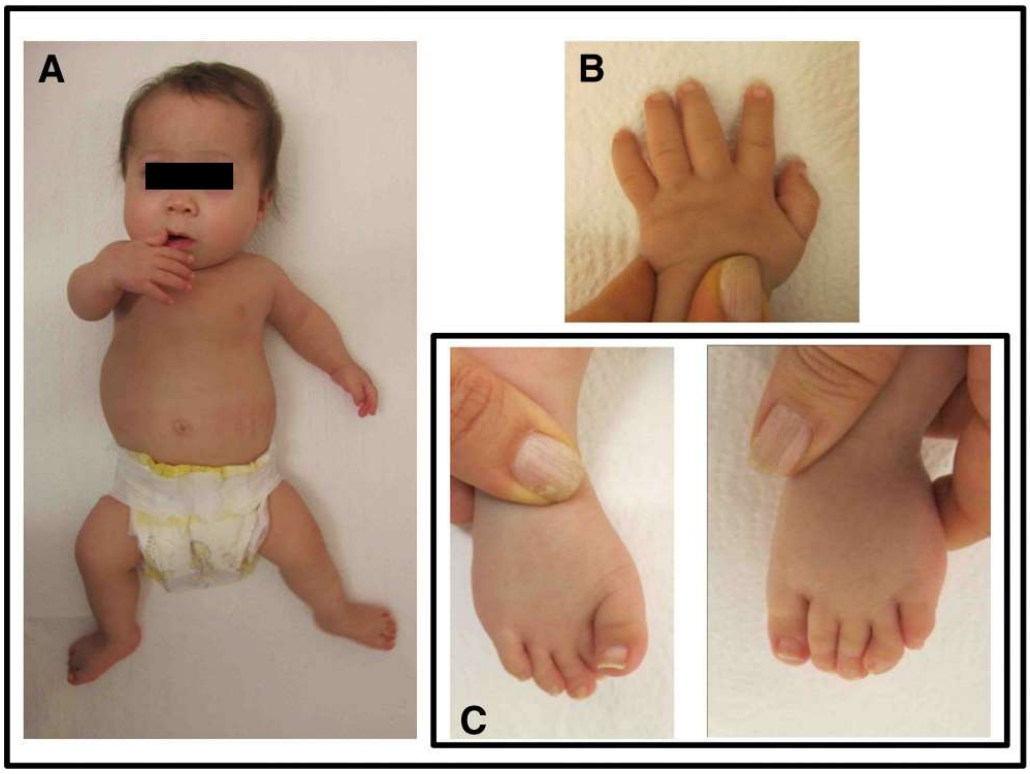


Figure 29:- Clinic features of desbuquois dysplasia type 2 patients with XT-I mutation R598C. The child of 12 month age has flat face, narrow thorax, short limbs (A) with hip dislocation, hyperlaxity of fingers (B), and deviation of toes (C) (Bui et al., 2014).

Polymorphisms in *XYLT1* and *XYLT2* have been associated with several diseases such as Type I diabetes, diabetic nephropathy, pseudoxanthoma elasticum (PXE), and osteoarthritis (Götting et al., 2007). These variants have been described in the table 6 for XT-I and table 7 for XT-II. The XT-II mutation D56N, P418L and T801R are associated with severity of the disease in PXE patients (Schön et al., 2006d).

PG metabolism is disturbed in diabetic patients and decreased HSPG content are found in the basement membranes. In diabetes both type I and type II, the XT activity is decreased leading to reduced GAG contents in various tissues especially in arteries (Vogl-Willis and Edwards, 2004) and kidney (Vernier et al., 1992). The SNP (c.343G>T, p.A115S) in XT-I is associated with risk factor for diabetic nephropathy (Schön et al., 2006c; Schön et al., 2005) whereas XT-II SNP are not significantly linked for the development of diabetic nephropathy. In fact, one XT-II haplotype SNP (c.1569C>T) is less frequently occurred in type 1 diabetic patients with nephropathy compared to patients without renal impairment. Therefore this variant is a protective genetic factor against renal complications in diabetes (Hendig et al., 2008). However, this SNP in XT-II is linked to severity in the PXE disease and early onset of osteoarthritis.

XT-II is mainly expressed in liver and XT-II knockout mice have significantly reduced liver PG expression especially the HSPGs which are reduced by 87%. The XT-II KO mice develop hepatic cysts compare to normal mice. Moreover, the liver from the KO mice is bigger in size and weight, but interestingly liver functions are normal (Condac et al., 2007). The XT-II deficient mice also develop the renal complications and showed GAG-deficient decorin and versican. The loss of XT-II might be compensated with XT-I expression therefore renal complications are not very severe.

Recently, Munns et al showed that homozygous frameshift mutation (p.Ala174Profs*35) in XT-II with premature codon results in truncated form of XT-II. This leads to sensorineural hearing loss, eye and heart defects and vertebral compression fractures like spondylo-ocular syndrome of unknown cause (Figure 30). They hypothesized that PG-GAG expression in the lens, retina, heart muscle, inner ear, and bone are dependent on XT-II. The XT activity is also lower in the serum and plasma of patients and they also have less PG synthesis rate (Munns et al., 2015). However the XT-I expression is similar to control but the XT-II expression is significantly lower as compare to control. But these findings are contradictory with the XT-II deficient mice because these mice develop normal and did not show these symptoms. This might be possible that these symptoms are due the involvement of some other genes, such as UDP-xylose synthase1 (uxs1). The UXS1 is involved in the production of UDP-xylose required for the PG-GAG synthesis. The Knockdown of UXS1 in mice produces severe effect compare to the XT-I and Fam20B mutation (Eames et al., 2011). It has been shown that the Uxs1 activity is essential for the PG production and organization

of skeletal extracellular matrix and its deficiency decrease the cartilage synthesis and bone morphogenesis in zabrafish (Eames et al., 2010). Recently, the XT-II promoter has also been analyzed for the presence of SNPs. Seven SNP s were but these have no significant effect on the promoter activity and on XT-II.



Figure 30:- A patient with XT-II mutation at 14 years of age (Munns et al., 2015).

Table 6:- XT-I variants along with their location and pathological conditions.

XYLT-1 mutations in human			
p.A115S	exon 1	Type I diabetes, diabetic nephropathy , PXE, healthy blood donors, osteoarthritis	(Bahr et al., 2006a; Schön et al., 2006a; Schön et al., 2005; Schön et al., 2006d)
P385L	exon 5	diabetes, osteoarthritis	(Schön et al., 2006a; Schön et al., 2005)
R406W	exon 5	PXE, osteoarthritis	(Schön et al., 2006a; Schön et al., 2006d)
R481W		short stature syndrome	(Schreml et al., 2014)
I552S	exon 8	osteoarthritis	(Schön et al., 2006a)
R586C	exon 8	diabetic nephropathy	(Bahr et al., 2006a)
R598C	exon 9	Desbuquois Dysplasia Type 2	(Bui et al., 2014)
R628H	exon 9	Type I diabetes	(Schön et al., 2005)
G640S	exon 9	diabetic nephropathy	(Bahr et al., 2006a)
T665M	exon 9	diabetic nephropathy , PXE,	(Bahr et al., 2006a; Schön et al., 2006d)
R892Q	exon 12	Type I diabetes, PXE, osteoarthritis	(Schön et al., 2006a; Schön et al., 2005; Schön et al., 2006d)
XYLT-1 mutations in mice			
W932R		Pug Mutation results in dwarfism	(Mis et al., 2014)
XYLT-1 mutations in zebrafish			
S534A		Skeletal defect and early chondrocyte maturation	(Eames et al., 2011)

Table 7:- XT-II variants along with their location and pathological conditions.

XYLT-2 mutations in human			
D56N	Exon2	Type I diabetes, PXE, osteoarthritis, healthy blood donors	(Schön et al., 2006a; Schön et al., 2005; Schön et al., 2006d)
P115L	Exon2	PXE	(Schön et al., 2006d)
R120H	Exon2	Type I diabetes	(Schön et al., 2005)
A186T	Exon2	Type I diabetes	(Schön et al., 2005)
T305R	Exon 4	Type I diabetes, PXE, osteoarthritis	(Schön et al., 2006a; Schön et al., 2005; Schön et al., 2006d)
R406C	Exon 6	osteoarthritis	(Schön et al., 2006a)
P418L	Exon 6	Type I diabetes, PXE, osteoarthritis, healthy blood donors	(Schön et al., 2006a; Schön et al., 2005; Schön et al., 2006d)
T801R	Exon 11	Type I diabetes, PXE, osteoarthritis, risk factor for diabetic nephropathy	(Bahr et al., 2006a; Schön et al., 2006a; Schön et al., 2005; Schön et al., 2006d)

3.10 Regulation of Xylosyltransferase

Recently it has been showed that IL-1β induced activation of the XT-I gene promoter by the recruitment of AP-1 transcription factor to the AP-1 response elements site in the promoter. The activation of the XT-I expression is mediated by JNK and p38 MAPK signaling pathways. The JNK and p38 inhibitors suppressed the activation of the XT-I promoter induced by IL-1. Down regulation of PG synthesis in late phase of OA is also mediated by IL-1β is dependent on the recruitment of Sp3 transcription factor to proximal Sp1 binding site leading to suppression of XT-I promoter activity (Figure 31) (Khair et al., 2012). XT-I promoter does not contain a TATA box, instead this region contains more GC residues and form many GC boxes. The XT-I promoter is inducible with TGF-β (Müller et al., 2009).

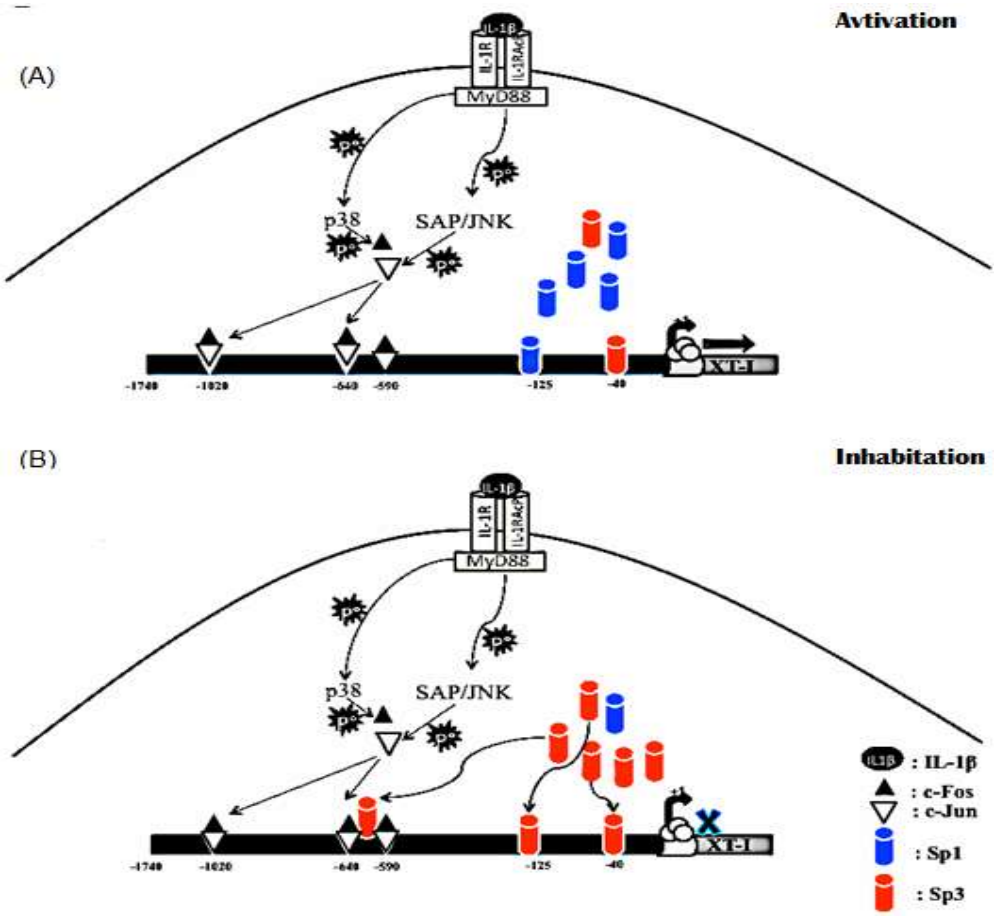


Figure 31:- Regulation of XT-I promoter by AP-I, SP1, and SP3. The activation of XT-I gene expression is induced by binding of the AP-I to API binding site (A). The inhibition is achieved by binding of SP3 on SP1 and AP1 binding sites (B) (Khair et al., 2012)

The XT-II promoter has been studied in hepatoma cell line HepG2. The XT-II promoter is also rich in GC and do not contain the TATA and CAAT box. The -177 proximal promoter element is sufficient for basal expression of XT-II in HepG2 cells. XT-II premotor has several sites for the Sp1 and Sp3 transcription factors. The XT-II promoter do not have putative AP-1 binding site (Müller et al., 2013). Moreover, no cytokines reported to regulate the XT-II promoter.

Both biglycan core protein and glycosylated form are decreased by UV exposure. The UV exposure also reduce the expression of XT-I but that of XT-II is less effected. Interestingly, silencing of XT-I resulted in decrease of high molecular weight GAGs, whereas XT-II silencing has no such effects. Therefore, the chains primed by XT-I are longer compare to those primed by XT-II. This study also suggest that XT-I inhibits GAG chains on serine 42 and 47 of biglycan, whereas XT-II only initiate the GAG chain on serine 42 (Figure 32) (Jin et al., 2015). However mutation of serine 42 still gave rise to GAG attached biglycan by XT-II. Therefore, this needs further investigations.

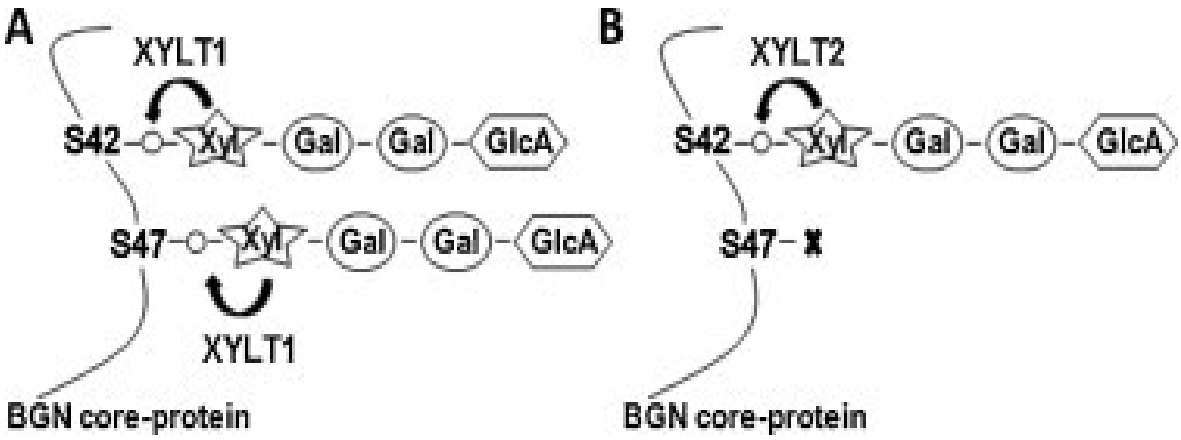


Figure 32:- GAG synthesis on biglycan by XT-I and XT-II. The XT-I initiate the GAG synthesis on both serine 42 and 47, whereas XT-II only initiate the GAG synthesis on serine 42 (Jin et al., 2015).

Chapter 4
Fam20B

4. Fam20B

PG-GAGs are synthesized on the common tetrasaccharide linker region. This linker region undergoes various modifications including phosphorylation of the xylose and sulphation of galactose residues (Gulberti et al., 2005a, b). Phosphorylation of the xylose occurs at 2-O-position and sulphation of the galactose occurs at 4^{th} and 6^{th} position. The phosphorylation of xylose in the GAG synthesis is purposed several years ago, however the kinase responsible for the phosphorylation is identified only recently as Fam20B (Koike et al., 2009). The phosphorylation of xylose is found in both CSPG and HSPG whereas sulphation of galactose residues are reported only in CS and DS chains but not in HS or Heparin. Therefore the sulphate groups on galactose residues might be involved in selective CS/DS synthesis (Mikami and Kitagawa, 2013; Prydz and Dalen, 2000).

4.1 Structure of Fam20B

It has been reported that the phosphorylation of xylose is transient phenomena during the biosynthesis of the decorin. The phosphorylation starts after xylosylation and continues until the attachment of glucuronic acid which results in rapid dephosphorylation. The phosphorylation rate is 96% after xylosylation and only 19% remains after attachment of glucuronic acid residues (Moses et al., 1997). Fam20B was discovered ten years ago by Nalbant et al and its phosphorylation activity towards xylose is established by Koike et al (Koike et al., 2009; Nalbant et al., 2005).

Fam20B belongs to family of sequence similarity 20 called Fam20 (family of sequence similarity 20) containing 3 members Fam20A, Fam20B, Fam20C. They are expresses in various tissues. The Fam20 family have sequence similarity with Four-jointed family (Ishikawa et al., 2008; Sreelatha et al., 2015). Both family have a short sequence of hydrophobic amino acids at N-terminal, the signal peptide/signal anchor and the conserved C-terminal domain with kinase activity (Figure 33) (Sreelatha et al., 2015; Tagliabracci et al., 2013a).

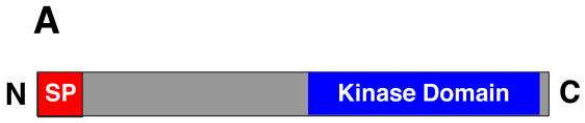


Figure 33:- Structure of Fam 20 family. The secreted protein kinase consists of an N-terminal SP, a C-terminal kinase domain (Tagliabracci et al., 2012b).

Fam20A is differentially expressed in hematopoietic tissue is associated with their differentiation and regulation (Nalbant et al., 2005). Fam20A is also expressed in teeth cells such as ameloblasts and odontoblasts. It has crucial role in enamel biomineralization and deficiency of Fam20A leads to tooth eruption in mice and humans (Cho et al., 2012; Vogel et al., 2012). Mutations in Fam20A cause amelogenesis imperfect (AI) and gingival hyperplasia syndrome (Kantaputra et al., 2014; O'Sullivan et al., 2011).

However, Fam20C is a Golgi casein kinase and is located on chromosome 7p22.3. Fam20C is considered as mother of kinases because it phosphorylate majority of the phosphoproteins present in the blood, CSF and serum/plasma (Cozza et al., 2015; Tagliabracci et al., 2015; Wrighton, 2015). Fam20C is mainly expressed in the biomineralized tissues especially in teeth and bones. The mutations in Fam20C are associated with Raine syndrome, characterized by a lethal osteosclerotic bone dysplasia. Most of Raine syndrome mutations are lethal (Tagliabracci et al., 2012a; Tagliabracci et al., 2013a) but some non-lethal mutations in the Fam20C has also been reported (Simpson et al., 2009).

Mutations in the XT-I and Fam20B are associated with less cartilage matrix production which leads to abnormal skeletal development in zebrafish (Eames et al., 2011). The crystal structure of Fam20C from *C. elegans* contains protein kinase-like fold containing five disulfide and two asparagine residues for N-linked glycosylation (Figure 34). It contains Asp-Phe-Gly (DFG) motif starts from Asp387 and this DFG motif is important for binding of metal ions. The Asp366 is present in the catalytic domain.

Both Asp387and Asp366 are important for catalytic activity of ceFam20C and their mutation with Alanine abolishes enzymatic activity. Moreover these aspartic acid residues are conserved in all Fam20 family (Xiao et al., 2013a)

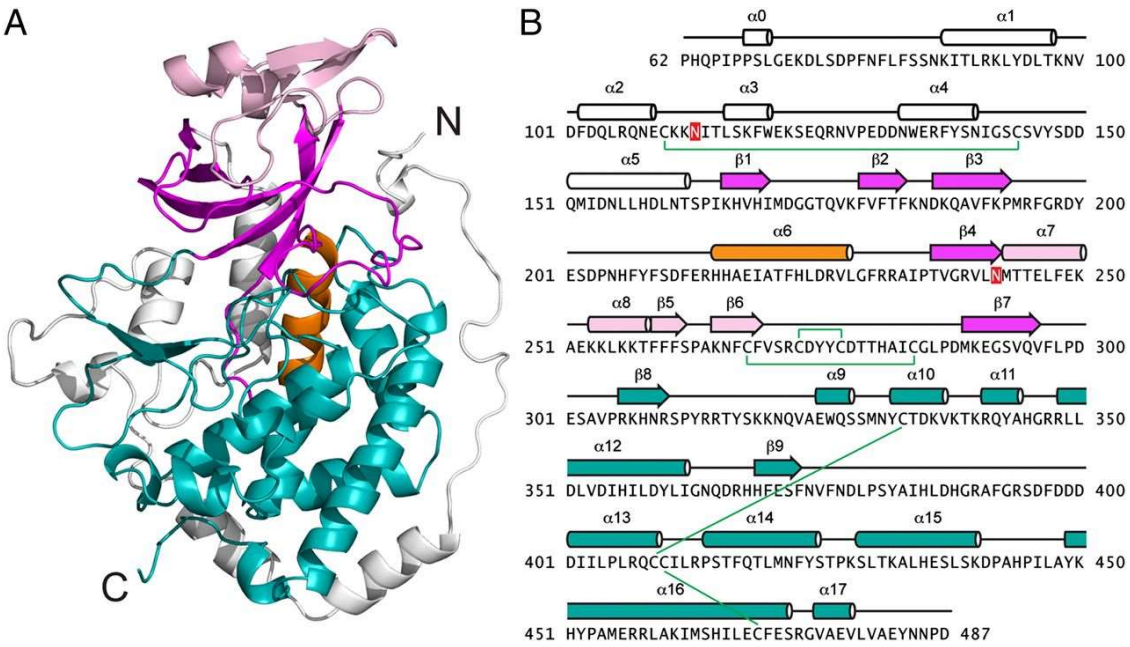


Figure 34:- The crystal structure of the *C. elegans* Fam20. It has a protein kinase-like fold and the ribbon structure with N-terminal lobe (magenta), C-terminal lobe (teal), the α6 helix (orange) and the the N-terminal insertion domain (white and pink) (A). The primary amino acids sequence with disulphide bonds and amino acid domains which forms the tertiary structure as in A with same color coding (B) (Xiao et al., 2013a).

4.4 Interaction of phosphoxylose with GalT-I, GalT-II, GlcAT-I, EXTL2 and ChGn-I

Our group has previously showed that GalT-I efficiently transfer the galactose to unmodified xylose. However, phosphorylated xylose inhibits the activity of GalT-I (Gulberti et al., 2005b). This suggests that xylose is phosphorylated after the attachment of galactose residues or a rapid phosphorylation and dephosphorylation may occur before the attachment of the galactose or that the phosphate is added on certain chains which are not processed. Hence, phosphorylation of xylose, might regulate the rate of GAG chains synthesis.

Recently, it has been shown, phosphorylation of xylose by Fam20B upregulates the expression of GalT-II and hence influence the rate of GAG synthesis (Wen et al., 2014). The knowdown of Fam20B suppress GalT-II expression and reduce the GAG synthesis. It has been also reported that GalT-II exhibits higher activity towards phosphorylated disaccharide linked with a benzyl group (Ben) on its reducing end (Gal-Xyl(P)-Ben), whereas it is unable to transfer the galactose onto the unphosphorylated disaccharide (Gal-Xyl-Ben). Instead, the sialic acid is added on the disaccharide (Gal-Xyl-Ben) (Wen et al., 2014).

Tone et al reported that phosphorylated trisaccharide is better acceptor for glucuronyltransferase-I (GlcAT-I) compare to the non-phosphorylated form. The modified trisaccharide with either phosphate [Gal-Gal-Xyl(2-O-phosphate)-Ser] and sulphate [Gal-Gal(6-O-sulfate)-Xyl-Ser] or with both [Gal-Gal(6-O-sulfate)-Xyl(2-O-phosphate)-Ser] are better acceptors for GlcAT-I compare to the non-modified tetrasaccharide [Gal-Gal-Xyl-Ser]. Whereas, the sulphation of the second galactose [Gal(6-O-sulfate)-Gal-Xyl(2-O-phosphate)-Ser] inhibits the activity of GlcAT-I. Moreover, the crystal structure of GlcAT-I (Figure 35) also revealed that second galactose could not fit into the catalytic pocket of the enzyme. However, it is not clear why the modified substrates (with phosphate and sulphate) are better substrate for the enzyme (Tone et al., 2008).

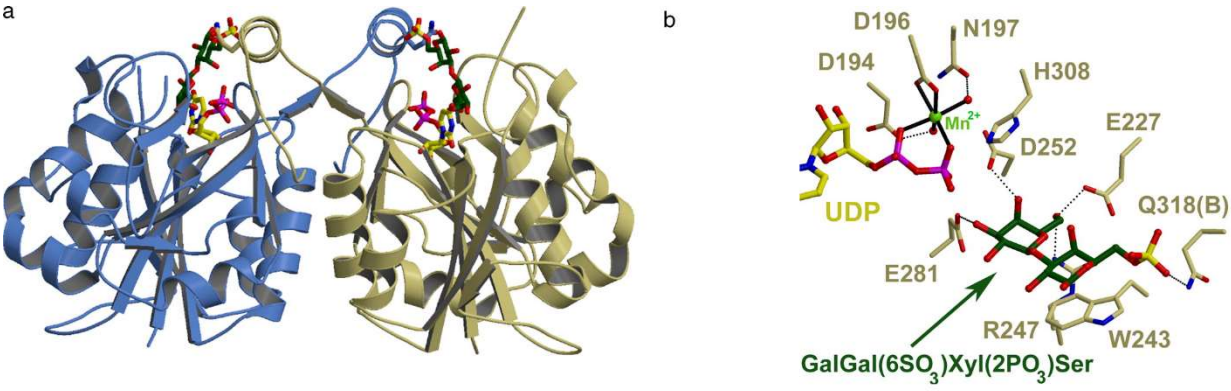


Figure 35:- Crystal structure of GlcAT-I. (A)The GlcAT-I form complex with Galβ1-3Gal(6-O-sulfate)β1-4Xyl(2-O-phosphate)β1-O-Ser, UDP and Mn^{2+} ions. The enzyme forms dimer and Gln318 interfere with second galactose at position 6^{th} of trisaccharide shown in green and UDP in yellow. (B)The active site of GlcAT-I with donor analog UDP (yellow) and acceptor trisaccharide (green) and Mn^{2+} ion (light green). (Tone et al., 2008).

Moreover, it has been recently reported that EXTL2 (an enzyme that transfer the N-acetylglucosamine residue to the tetrasaccharide linkage region for the heparan sulfate biosynthesis) could not initiate the GAG synthesis if the tetrasaccharide contains phosphorylated xylose. In addition, EXTL2 knockout mice produce more GAGs compared to wild type mice (Nadanaka et al., 2013).

Recently the phosphatase responsible for the dephosphorylation of the xylose has been identified as 2-phosphoxylose phosphatase (XYLP). The overexpression of the xylose phosphatase increased GAG synthesis and knockdown decreased the GAG synthesis for both CS and HS (Koike et al., 2014). This suggested that the Fam20B regulates the GAG synthesis by controlling the phosphorylation of the xylose residue (Figure 36).

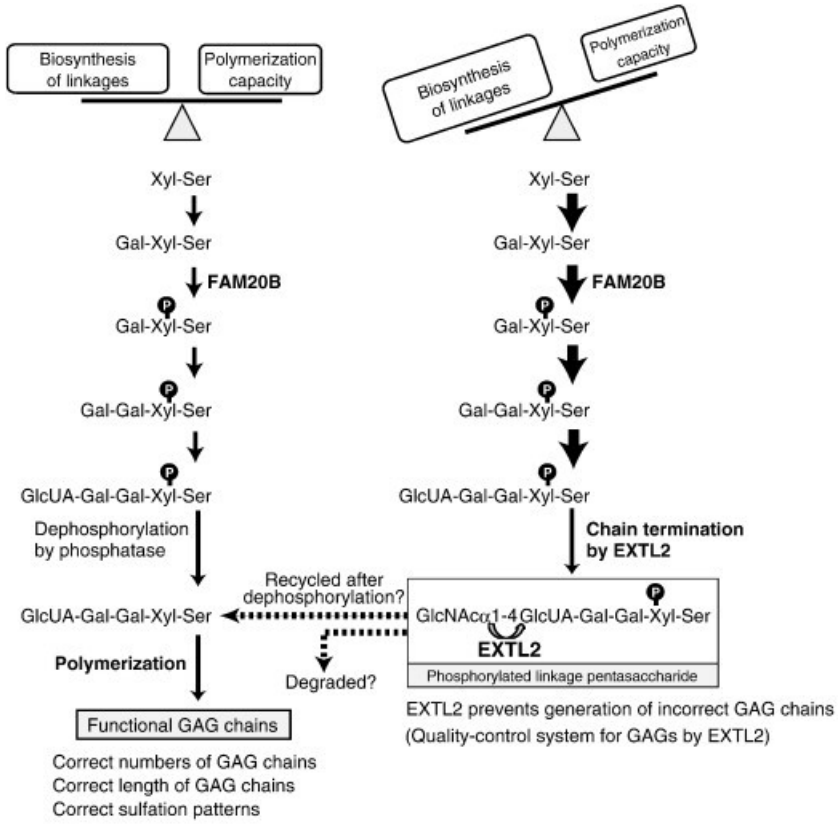


Figure 36:- Regulation of GAG synthesis by Fam20B is dependent on the EXTL2. It is purposed that the addition of GlcA residues led to dephosphorylation of xylose allowing HS chain synthesis. If the xylose remains phosphorylated the EXTL2 adds GlcNA and GAG chain synthesis is blocked and might be degraded (Nadanaka and Kitagawa, 2014).

It has been shown that phosphorylated tetrasaccharide is the preferred substrate for the GhGn-1. The GalNAcT-I activity of ChGn-1 is 100 time higher for phosphorylated tetrasaccharide linked to thrombomodulin (TM) [GlcA-Gal-Gal-Xyl (P)-TM] compare to unmodified form (GlcA-Gal-Gal-Xyl-TM). Interaction of ChGn-1 with XYLP is observed by pulldown. The transfer of GalNAc by ChGn-I results in rapid dephosphorylation of xylose by XYLP.

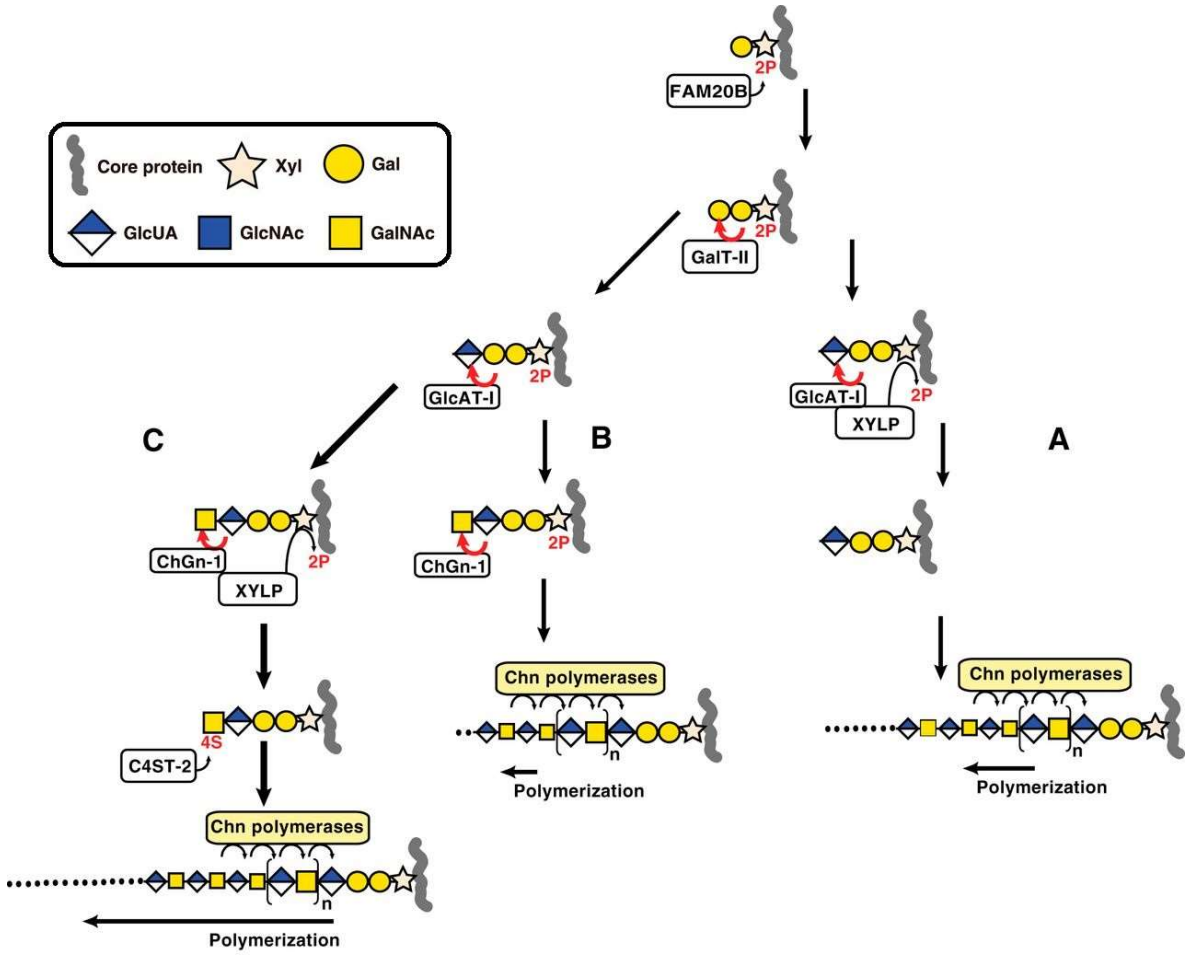


Figure 37:- Regulation of CS biosynthesis by phosphorylation of xylose. The addition of the GlcA by GlcAT-I rapidly dephosphorylate xylose and ChGn-1 polymerize linkage region for CS synthesis (A). The ChGn-1 catalyzes the transfer of a single GalNAc residue to the phosphorylated tetrasaccharide linkage region which is less efficiently used for CS biosynthesis (B). The 4-*O*-sulfation of the non-reducing terminal GalNAc residue by C4ST-2. This is used for the CS chain elongation efficiently (C) (Izumikawa et al., 2015).

The pentasaccharide is 4-O- sulphated by C4ST2 at non reducing end of GalNAc to enhance the CS chain formation. ChGn-I knockout mice do not produce the GalNAc (4-O-sulfate) and showed less CS synthesis. In the growth plate cartilage and chondrocyte from ChGn-1$^{-/-}$ mice showed accumulation of phosphorylated tetrasaccharide linker region (GlcA-Gal-Gal-Xyl(P)) and pentasaccharide linker region (GlcNAc-GlcA-Gal-Gal-Xyl(P)) capped with GlcNAc (Izumikawa et al., 2015) and is used less efficiently for the CS polymerization (Figure 37). Similar pentasaccharide structure (GlcNAc-GlcA-Gal-Gal-Xyl(P)) is found in the EXTL2 overexpressing cells as immature GAG chain.

All these reports showed that phosphoxylose is not found in the mature CS and HS chains and if the xylose remains phosphorylated it could not be used for GAG synthesis. To conclude the first xylose and its modifications are important for the regulation of the PG-GAG synthesis (Figure 38).

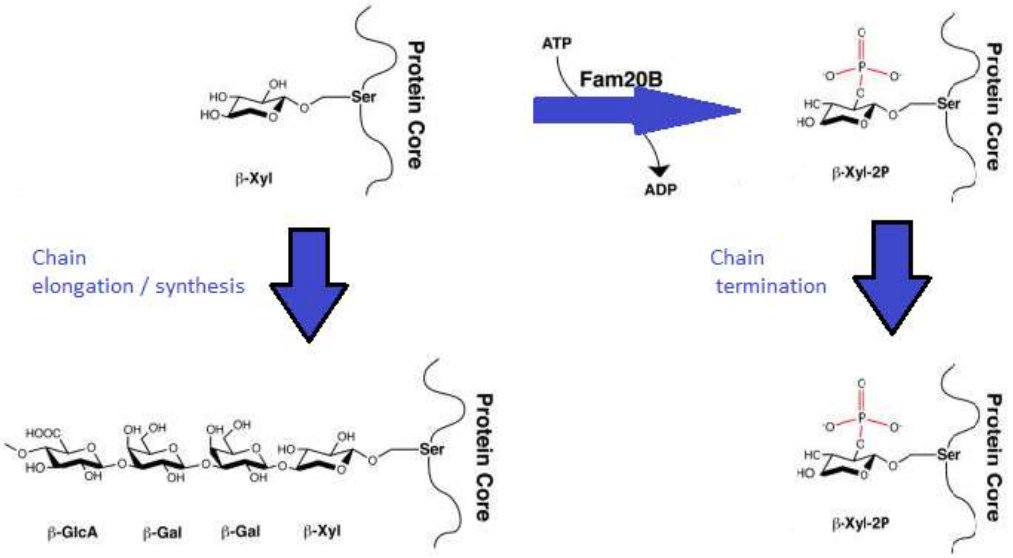


Figure 38:- Xylose phosphorylation by Fam20B and regulation of GAG synthesis. The unmodified xylose is used for the chain elongation whereas phosphorylation of xylose by Fam20B inhibits GalT-I and blocks GAG chain synthesis.

Chapter 5
Xylosides

5. Xylosides

PGs play an important role in various physiological processes like cell proliferation differentiation and growth factor signaling. They also promote various pathological processes like cancer cell proliferation, migration, invasion and metastases. PGs synthesis is increased in fibrotic diseases like skin and pulmonary fibrosis. PGs, especially CSPGs are increased in nervous tissue injury and inflammation. Excessive PG production plays an inhibitory effect on the nervous tissue repair. As most of PGs functions are governed by their GAG chains, therefore selective inhibition of GAG chain synthesis may provide promising treatment for these pathologies.

Xylosides with hydrophobic aglycones are used to prime GAG chain synthesis and these synthetic xyloside has been already used (Figure 39) (Fukunaga et al., 1975; Helting and Rodén, 1968; Johnsson et al., 2007; Victor et al., 2009). Recently, GAG suppressing xyloside has also been synthesized in which the acceptor OH group at C-4 position for the attachment of the galactose is replaced with deoxy or flouro group (Garud et al., 2008; Raman et al., 2011; Tsuzuki et al., 2010). These GAG inhibiting xyloside are important for the selective and reversible inhibition of GAG chain biosynthesis (Figure 39).

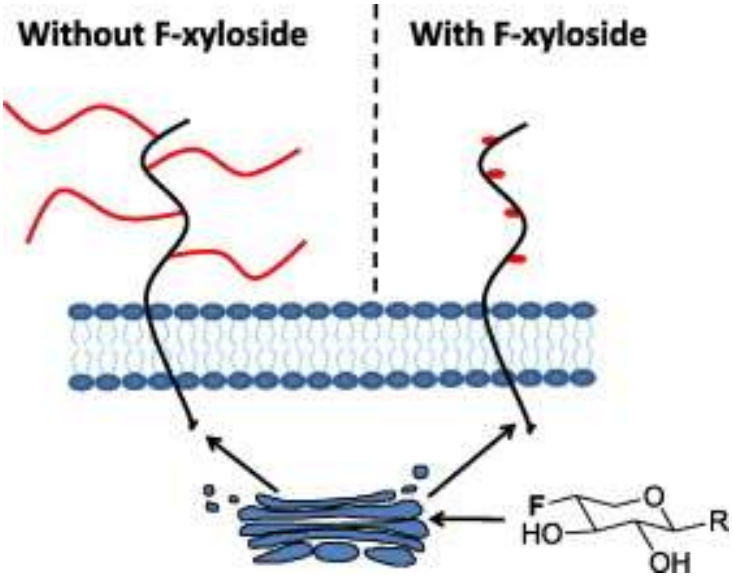


Figure 39:- Xyloside are used for GAG priming or inhibition. The exogenous xyloside with aglycon moiety cross the cell membrane and prime the GAG synthesis in the Golgi. If the hydroxyl group at 4th position is absent or substituted. It inhibits GAG synthesis by competing with PG core protein (Raman et al., 2011)**.**

5.1 GAG priming xylosides

Helting and Rodén showed for the first time that GAG could be primed on exogenous xyloside linked to serine (Helting and Rodén, 1968). Okayama and co-workers synthesized for the forst time a xyloside linked to p-nitrophenol and a series of xylosides linked to alkyl ethers of different length. They also prepare the xyloside coupled with thiophenol (Okayama et al., 1973). The 4-methyl-umbelliferyl β-D-xylopyranoside which prime the GAG chains mainly CS was prepared by Fukunaga et al (Fukunaga et al., 1975).

The first naphthol based xylosides (XylNapOH) are developed by the Mani et al in 1998. These xyloside inhibits the cell growth in different cell lines (Mani et al., 1998). This compound also inhibits tumor growth in mice (Mani et al., 2004a). They also prepare the bis-xyloside (the aglycon aromatic ring is linked to two xylosides) but these xyloside showed less antiproliferative activity (Johnsson et al., 2007). Afterwards, they modified the xyloside with the acetyl groups. The peracetylated mono- and bis-xylosylated dihydroxynaphthalenes prime the GAG synthesis. This peracetylated analog of XylNapOH was more efficient compare to the parent compound. The antiproliferative effect of the peracetylated mono- and bis-xylosylated dihydroxynaphthalenes is tested in the bladder cancer cell line (T24) and Human fetal lung fibroblast (HFL-1). Both peracetylated mono and bis-xyloside efficiently inhibits the proliferation compare to no acetylated xylosides (Nilsson et al., 2009). The administration of the bi and tri-xylosides into the zabrafish embryo cause the elongation of the embryo trough enhanced FGF signaling pathway. The mono-xylosides could not elongate the embryo (Nguyen et al., 2013). Recently, a library of xylosides have been synthesized including mono, di, tri and tetra xyloside linked to one aglycon moiety. They showed that with tetra xyloside higher GAG priming ability is obtained (Tran et al., 2013).

5.2 GAG inhibiting xylosides

Garud et al showed that the 4-deoxy-4-fluoroxylosides inhibits the GAG synthesis because of absence of the acceptor hydroxyl group at C-4 position for the attachment of galactose residues. They synthesized a library of 4-deoxy-4-fluoroxylosides with various aglycones using click chemistry and showed that these xylosides inhibit the synthesis of the heparan sulfate and chondroitin sulfate in CHO cells at different extent. They concluded that aglycon moiety is important for GAG inhibiting xyloside because among nine GAG inhibiting xyloside only two xyloside anlages efficiently inhibits the GAG synthesis to about 80% compare to control. This

shows that aglycon moiety plays an essential role not only for the GAG initiating xylosides but also for the GAG inhibiting xylosides (Garud et al., 2008).

The same group synthesized a series of 4-deoxy-4-fluoroxyloside derivatives using click chemistry with different aglycon moiety as reported before and the GAG inhibition is examined in the bovine lung microvascular endothelial cells (BLMVEC) using radiolabeled ^{35}S sulphate incorporation and HPLC analysis. All the seven inhibitors are non-toxic and inhibit the GAG synthesis, whereas two derivatives are best inhibitors of the GAG synthesis (80% inhibition) (Tsuzuki et al., 2010).

The fluoro-xylosides with different aglycon derivatives has been used to study their effect on the angiogenesis. Interestingly, two xylosides out of seven are potent inhibitors of endothelial tube formation in vitro (Raman et al., 2011). Recently, Saliba et al showed that 4-Methylumbelliferyl-4-deoxy-D-xylopyranoside and 4-methylumbelliferyl-4-fluoro-D-xylopyranoside inhibits GAG synthesis efficiently whereas Naphthyl-4-deoxy-D-xylopyranoside is a weak inhibitor (Saliba et al., 2015). The crystal structure of the Drosophila melanogaster and human β4GalT7 are quite similar (Ramakrishnan and Qasba, 2010; Tsutsui et al., 2013b). The binding of the UDP-Gal and manganese ion in the catalytic pocket of the β4GalT7 initiate the conformational reorganization from an open form to a closed conformation.

Modification of aglycon moiety has been studied using a panel of various aglycon side chains. The modifications on 2-O-position of the xyloside analog are less prone to galactosylation compare to parent XylNap (2-naphthyl β-d-xylopyranoside). The 2-deoxy analog strongly inhibits the galactosylation to about 64% and the 2-fluoro, 2-methoxy analogs inhibit the galactosylation but to less extent (Siegbahn et al., 2014b). Similarly, the xyloside with phosphate at 2-O-position could not be used as acceptor substrate for β4GalT7 (Gulberti et al., 2005b). According to the 3D structure the hydroxyl group in position 2 might interacts with the Aspartic acid residues at position 212 of the β4GalT7. The modifications at 3 and 5-O-position such as deoxy, fluoro or methoxy groups result in the inactivation of the acceptor xyloside and could not be processed by β4GalT7. Similarly the modification at 4-O position 4-Methyl, 4-deoxy, 4-floudo strongly inhibits the activity of the enzyme by interfering with aspartic acid 212 within binding pocket of β4GalT7 (Siegbahn et al., 2014b). Therefore, the modifications of xylose moiety are important in design of effective inhibitors of GAG synthesis. The detailed substitution/modification of xyloside at all

position (2, 3, 4 and 5) showed that the position 4 of xylose is the most interesting for the design of the perspective of inhibitor of β4GalT7.

Aims and objectives

Aims and objective of the study

PGs have central role in various biological functions and their functions are governed by GAG chains. Hence, PG-GAGs play a crucial role in physiology and pathophysiology of various diseases. CSPG and HSPG are synthesized on a common tetrasaccharide linker region. The initial and rate limiting step in tetrasaccharide is xylosylation of core protein which is catalyzed XT. XT has two isoforms XT-I and XT-II, both isoforms differentially expressed in various tissues and cell lines and are able to initiate GAG synthesis. However, the difference between GAG chains primed by XT-I and XT-II is unknown. It is also interesting that their localization is still contradictory because some groups reported that XT is localized in ER while others showed Golgi localization for the enzyme. XT-I is regulated by cytokines (IL-β1) and growth factors (TGF-β1), however, XT-II regulation is still unknown. Moreover, mutations in XT-I and XT-II are associated with various diseases and the impact of these mutants on the PG-GAG synthesis is still unknown.

The objective of first part is to determine the structure/function relationship between XT-I and XT-II. The difference in the GAG chains primed by XT-I and XT-II and their localization using specific markers. We also studied the effect of genetic variants of XT-I and XT-II on GAG synthesis.

The tetrasaccharide linker region is modified by sulphation of galactose residues and phosphorylation of xylose residues. This phosphorylation plays an important role in regulation of PG-GAG biosynthesis. The phosphorylation of xylose is reported in both CSPG and HSPG. The kinase for phosphorylation of xylose is Fam20B which belongs to the family of sequence similarity 20 (Fam20). The Fam20 have three members, Fam20A and Fam20C are responsible for phosphorylation of biomineralized tissue and Fam20B is xylosylkinase. The phosphoxylose could not be used as acceptor substrate for GalT-I, hence, block GAG chain synthesis. Recently, the enzyme responsible for dephosphorylation of xylose has been discovered.

The second part, we studied the effect of Fam20B on regulation of biosynthesis of GAG chains using gain and loss of function of Fam20B. We have also studied the effect of conserved residues crucial for the catalytic activity of Fam20B.

The GAG synthesis is primed on the exogenous xylosides (synthetic analogs). The xyloside with aglycon moiety penetrate cell membrane and compete with endogenous xylose for GAG priming. The xyloside with deoxy group at 4^{th} position prevent elongation of GAG chains hence these xylosides could be used for GAG inhibition. In some disease like fibrosis results in overproduction of GAG chains. Therefore, GAG inhibiting xylosides could be used as potential therapeutics for treatment of these diseases.

In the third part, we studied the effect of 4-MU4-deoxy-β-D-xylopyranoside on GAG synthesis in rat lung fibroblasts. This xyloside acts as competitive inhibitor of GalT-I. Since, TGF-β is upregulated in fibrosis to enhance GAG synthesis therefore we also studied the effect of this xyloside analog on TGF-β induced GAG synthesis and smad signaling. Effect of 4-MU4-deoxy-β-D-xylopyranoside on transdifferention of fibroblast to myofibroblast was also studies.

Publication No 1

Structure/Function relationship of xylosyltransferase isoforms (XT-I and XT-II) and the role of their genetic variants in GAG synthesis.

Dong Li, Irfan Shaukat, Lydia Barré and Mohamed Ouzzine*

*Corresponding author.

Correspondence: Mohamed Ouzzine.

UMR 7365 CNRS-Université de Lorraine, Biopôle-Faculté de Médecine, CS 50184, 54505 Vandoeuvre-lès-Nancy Cedex, France

Tel: +33 383 685 427; Fax: +33 383 685 409

E-mail address: Mohamed.ouzzine@univ-lorraine.fr

Abstract

Heparan- and chondroitin-sulfate proteoglycans (PGs) are essential regulators of many biological processes including cell differentiation, signalization, proliferation and morphogenesis. Synthesis of PGs is initiated by the addition of xylose on specific serine residues of the PG core protein. This initial and rate limiting step is catalyzed by xylosyltransferase I and II (XT-I and XT-II). However, nothing is known of the specific roles of XT-I and XT-II, if any, and of the impact of XT-I and XT-II mutations on the chondroitin-sulfate (CS) and heparin-sulfate (HS) PG synthesis. Here, we bring evidence that XT-I and XT-II exhibited different subcellular localization with XT-I being in the ER and XT-II in the cis-Golgi compartment. In addition, we showed that CS- and HS glycosaminoglycan (GAG) chains primed by XT-I exhibits a large size compare to that initiated by XT-II. Interestingly, we showed that delocalizing of XT-II in the ER led to increased size of PG-GAG chains. We further demonstrated that PGs primed by XT-I exhibited a delayed secretion compare to those primed by XT-II and bring evidence that sulfation regulates the polymerization of GAG chains initiated by XT-I but not of those initiated by XT-II. Moreover, we showed that XT-II was secreted in the medium following cleavage by γ-secretase, whereas XT-I was not detected in the extracellular milieu. Finally, we showed that XT-I genetic variants produced less PG-GAGs compare to wild-type enzyme and found that two XT-II genetic variants were mislocalized into the ER and were not able to initiate the synthesis of PG-GAG chains of either CS or HS type.

Keywords: Proteoglycan synthesis, xylosyltransferase I and II, genetic variants,

Significance Statement

Proteoglycans (PGs) have diverse role and regulate several biological process such as extracellular matrix deposition, cell differentiation, adhesion and migration, normal as well as tumour cell proliferation. PGs mediate intracellular signalling of various growth factors and cytokines mainly through glycosaminoglycan (GAG) chains. The initial and rate limiting step in PG-GAGs synthesis is the xylosylation of core protein, catalysed by xylosyltransferase (XT-I and XT-II). However the structure/function difference between two isoform is unknown.

We provide evidence that XT-I is localized in the ER and prime longer GAG chains compare to XT-II which is present in the cis-Golgi compartment. The mutations of XT-I and XT-II has been reported in various diseases such PXE, osteoarthritis, diabetes, short stature syndrome, desbuquois dysplasia type 2. Our study indicated that mutants of XT-I and XT-II produce less PGs and might have altered cellular functions.

Introduction

Heparan-sulfate (HS) and chondroitin-sulfate (CS) proteoglycans (PGs) are essential regulators of many biological processes including cell differentiation, signalization, proliferation and morphogenesis (1-3). PGs act as receptors for growth factors, enzymes and cell adhesion proteins, thereby modulating their concentration, gradient formation and biological activity (4). Evidences for the involvement of PGs in the pathogenesis of many diseases including arthropathies (1), atherosclerosis (5), Alzheimer's disease (6) lung diseases (7, 8) liver fibrosis (9) and cancer (10) have been reported. Altered PG synthesis and deposition was observed in pathological processes that are accompanied by accumulation of extracellular matrix components and connective tissue remodeling. These observations have stimulated much interest in the understanding of the glycosyltransferases (GTs) involved in the biosynthesis pathway of PGs, which may represent promising pharmacological targets.

The assembly of glycosaminoglycan (GAG) side chains of PGs is a non-template-driven and a complex process, relying on multiples enzyme activities. The initial steps of both CS and HS synthesis share a common tetrasaccharide linkage region (GlcAβ1,4Galβ1,3Galβ1,4Xyl-O-Ser)

attached on specific serine residues of the core protein. This process begins with the transfer of xylose from UDP-xylose to the hydroxyl group of specific serine residues of PG core proteins (11, 12) catalyzed by xylosyltransferase I (XT-I) and xylosyltransferase II (XT-II). After xylosylation, two galactose residues are attached to xylose by β1,4-galactosyltransferase 7 (β4GalT7) and β1,3-galactosyltransferase 6 (β3GalT6). The next step is the attachment of a glucuronic acid by β1,3-glucuronosyltransferase I (GlcAT-I). After the synthesis of the tetrasaccharide primer, it will differentiate into either CSPG or HSPG. The tetrasaccharide primer undergo various modification including phosphorylation of the xylose and sulfation of galactose residues (13).

Several studies indicated that XT enzymes may act as regulators for PG synthesis. Indeed, increase in PG synthesis was associated with high XT activity in human heart biopsies from patients with dilated cardiomyopathy (14) and in lung from rat model of lung fibrosis (7, 8). Upregulation of XT-I gene expression was associated with increase PG synthesis in cartilage, whereas reduced PG synthesis was associated with down regulation of XT-I gene expression (15), suggesting that quantitative changes in the expression of XT-I would dictate variations in PG synthesis. Interestingly, XT activity is present in the serum following shedding and secretion of the protein probably after proteolytic cleavage at the stem region. Although the biological significance of the soluble form in the extracellular milieu remains elusive altered serum XT activity has been proposed as a biomarker of altered PG metabolism in various diseases (12). Thus, increased XT activity in the serum was reported in patients with systemic sclerosis, a chronic inflammatory disease of connective tissues (16) and in patients with pseudoxanthoma elasticum (PXE) (17), a disease characterized by progressive calcification and fragmentation of elastic fibers in the connective tissues. However, the identity of the isoenzyme (XT-I or/and XT-II) responsible for the increase in serum XT activity was not established, although it was attributed to XT-I (18). Recently, studies based on the measurement of XT activity in mouse serum using synthetic acceptor peptide bikunin showed a high reduction in XT activity in serum of XT-II knock-out mice (xylt-II$^{-/-}$) mice, compared to that of wild-type mice, suggesting a predominance of XT-II enzyme activity in mouse serum (19).

A number of mutations in GAG biosynthetic enzyme genes have been reported and have revealed the crucial role of PG-GAG chains in key physiological processes. Thus, mutations in β4GalT7, the enzyme that catalyzes the transfer of the first galactose to the xylose residue in the linkage

region of PGs, have been linked to the pathology of the progeroid form of the Ehlers-Danlos syndrome (20). Clinically, these mutations can lead to an aged appearance, developmental delay and dwarfism (21, 22). Biochemically, these mutations result in an inefficient substitution of the PG decorin and biglycan with CS/DS GAG chains (23) which might be responsible for defects in collagen fibrogenesis and wound repair observed in β4GalT7-deficient patients (24). Mutations in EXT1 or EXT2 genes, encoding EXT1 and EXT2 that catalyze the polymerisation of HS-GAG chains, have been linked to the hereditary multiple exostoses, an autosomal dominant hereditary disorder characterized by reduced skeletal size and multiple cartilage-capped tumors that arise from the growth plate of endochondral bones, known as osteochondromas or exostoses (25, 26). The molecular mechanism leading to the development of exostoses is poorly understood, however reduced level of HS resulting from mutation of either EXT1 or EXT2 has been shown detrimental for chondrocyte proliferation and differentiation (27, 28).

Several mutations that may act as a risk factor in PG-associated pathologies have been described for human *xylt-I* and *xylt-II* genes. Among these, mutation of the XT-I residue A115S has been linked to increased risk for diabetic nephropathy (29) and mutation of the XT-II residue D56N was associated with a severe Pseudoxanthoma elasticum (PXE) disease course, (17). Several other mutations in *xylt-I* and *xyl-II* genes have been reported in various PG-associated pathogenesis such as osteoarthritis (30), diabetes (29, 31, 32), essential hypertension (33), aortic aneurysms (12), the autosomal short stature syndrome (34) and desbuquois dysplasia type 2 (35). However, nothing is known of the specific roles of XT-I and XT-II, if any, and of the impact of XT-I and XT-II mutations on the CS- and HS-PG synthesis. These are critical for the understanding the relationship between XT mutations and the risk to develop PG-associated pathologies. Here, we bring evidence that XT-I and XT-II exhibited different subcellular localization with XT-I being in the ER and XT-II in cis-Golgi compartment. Interestingly, we showed that XT-I initiated longer CS- and HS-GAG chains compared to XT-II and demonstrated that this was linked to their respective subcellular localisation. Further we demonstrated that PGs primed by XT-I exhibited delayed secretion compared to those initiated by XT-II and bring evidence that sulfation regulates the polymerization of GAG chains initiated by XT-I but not of those initiated by XT-II. Moreover, we showed that XT-II was secreted in the medium following cleavage by γ-secretase, whereas XT-I was not detected in the extracellular milieu, suggesting that it was not a secreted protein. Finally, we have

addressed the question of whether genetic mutations of XT-I and XT-II impact CS- and HS-PG synthesis. We found that, genetic mutations of XT-I strongly reduced the capacity of the enzyme to initiate the synthesis of CS- and HS-attached PGs. In addition, we found that XT-II variants R406C or P418L lack the capacity to initiate PG-GAG chain synthesis and were mislocalisation to the ER compartment.

Results:

XT-I exhibited an ER subcellular localization whereas XT-II is resident in cis-Golgi, and both initiate PG-GAG chain synthesis

It has been previously shown that both XT-I and XT-II are able to catalyze the transfer of xylose residue to specific serine of PGs *in vitro* using PG-homologous peptides as acceptor substrates. In addition, both XT-I and XT-II were able to restore GAG-attached PG synthesis in XT-I/XT-II-deficient CHO cells, pgsA-745, therefore suggesting that they are functionally redundant. To investigate whether XT-I and XT-II function redundantly in the synthesis of PGs, we first set to determine whether XT-I and XT-II are present in the same subcellular localization. We first analyzed whether XT-I and XT-II were efficiently expressed in CHO pgsA-745 cells. As shown in Figure 1A, Western blot analysis showed that transfection of CHO pgsA-745 cells with pCMV-XT-I vector resulted in the synthesis of a polypeptide of a molecular mass of about 110 kDa (Fig. 1A) and transfection with pCMV-XT-II vector resulted in a production of a polypeptide of a molecular mass of about 97 kDa (Fig. 1B), whereas no polypeptide was produced in CHO pgsA-745 cells transfected with empty pCMV vector (control). These results indicated that both XT-I and XT-II were efficiently expressed in CHO pgsA-745 cells. Next, we analyzed the subcellular expression of XT-I and XT-II by immunofluorescence using specific antibodies. Interestingly, immunofluorescence staining clearly indicated that XT-I and XT-II exhibited different subcellular localizations. XT-I displayed a staining pattern that is restricted to a perinuclear ER-like distribution (Fig. 1C and 1D), whereas XT-II displayed a paranuclear Golgi staining pattern (Fig. 1E and 1F). Co-localization with the ER resident protein

marker calnexin and the cis-Golgi marker GM130 clearly showed that XT-I staining completely co-localized with the ER protein calnexin (Fig. 1C merge) but not with the cis-Golgi GM130 (Fig. 1D, merge). In contrast, XT-II completely co-localized with cis-Golgi GM130 (Fig. 1F, merge) and not with the ER protein calnexin (Fig. 1E, merge), indicating that XT-I is an ER resident protein, whereas XT-II is a cis-Golgi protein. To further demonstrate that XT-I and XT-II exhibit different localization, we co-expressed XT-I and XT-II in CHO pgsA-745 cells (Fig. 1G). Immunofluorescence analysis clearly showed that XT-I staining pattern (Red) did not overlap with that of XT-II (Green), thus confirming that XT-I and XT-II are not present in the same subcellular compartment. We next examined whether XT-I and XT-II were able to restore PG synthesis in CHO pgsA-745 cells by analysing the expression of endogenous HS-attached PG present on the cell surface using 10E4 anti-HS monoclonal antibody, which is commonly used to detect HS chains of PGs (38-40). Prominent staining of the cell membrane was observed in CHO pgsA-745 cells transfected with XT-I expression vector (Fig. 2A) and with XT-II expression vector (Fig. 2B), whereas no signal could be observed in cells transfected with empty vector (Fig. 2C). When transfected cells were probed with anti-XT-I antibodies, efficient expression of XT-I was revealed in cell expressing cell surface HSPGs (Fig. 2A, merge). Similar results were observed for XT-II (Fig. 2B, merge), indicating that despite their different subcellular localization, XT-I and XT-II are able to restore the synthesis of endogenous HSPGs in CHO pgsA-745 cells and therefore to efficiently initiate HS-GAG chain synthesis.

XT-I initiates the synthesis of CSPGs and HSPGs with large GAG chain length

Having shown that XT-I and XT-II exhibited different subcellular localizations, we next asked whether PGs initiated by XT-I are structurally similar to those initiated by XT-II. For this purposes, we used decorin (DCN) which contains a single CS/DS-attached site and syndecan 4 (SDC4) containing three HS-attached sites as reporter PG core proteins for the synthesis of CS and HS, respectively. pCMV-DCN-EGFP vector expressing human decorin core protein fused at the C-terminus with EGFP and pCMV- SDC4$^{(\Delta CT)}$-EGFP vector expressing human syndecan 4 core protein, in which the transmembrane domain and the C-terminus were deleted and

replaced by EGFP leading to the secretion in the cell culture medium of SDC4$^{(\Delta CT)}$-EGFP protein were designed and used to transfect CHO pgsA-745 cells stably expressing XT-I and XT-II (CHO/XT-I and CHO/XT-II). DCN-EGFP and SDC4$^{(\Delta CT)}$-EGFP produced in cell culture supernatants were analyzed by western blot after immunoisolation with anti-EGFP-coupled affinity column chromatography. Unexpectedly, DCN-EGFP produced by CHO/XT-I was of a large size compared to that produced by CHO/XT-II (Fig. 3A), suggesting the presence of longest CS chains in decorin produced by CHO/XT-I cells. Similar results were observed for the HS-attached PG syndecan 4 which showed predominance of higher sized SDC4$^{(\Delta CT)}$-EGFP produced in CHO/XT-I compared to that produced in CHO/XT-II (Fig. 3A). As expected, only protein-free GAG chains were produced in CHO pgsA-745 cells (control).

To determine whether the increase in size represents an increase in GAG chains size, CHO/XT-I and CHO/XT-II cells were transfected with pCMV-DCN-EGFP vector and GAG chains were metabolically labeled with ^{35}S-sulfate. DCN-EGFP was immunopurified from cell culture supernatant. SDS-PAGE analysis of radiolabeled DCN-EGFP produced in CHO/XT-I showed an increased size compared to that produced in CHO/XT-II (Fig. 3B). Interestingly, SDS-PAGE analysis of radiolabeled CS chains obtained following treatment of radiolabeled DCN-EGFP with proteinase K to release ^{35}S-labeled CS chains from decorin core protein clearly showed high size CS chains in decorin produced in CHO/XT-I compared to that expressed in CHO/XT-II cells (Fig. 3B). Of note, a strong reduction in the amount of shorter CS chains (14 to 37 kDa) was observed in decorin produced in CHO/XT-I cells compared to that produced in CHO/XT-II (Fig. 3B). These results indicated that XT-I initiates PGs with longer GAG chains compared to XT-II.

Targeting XT-II to the ER initiates the synthesis of PGs with GAG chains of larger size

Differential localization of XT-I and XT-II raised the possibility that the mechanism by which they initiate PG with GAG chains of different size may be related to their respective subcellular localizations. To test this hypothesize, XT-II was delocalized from the cis-Golgi to the ER compartment by addition of a C-terminal *KDEL* ER-retrieval motif. We first analyzed whether XT-II/KDEL was efficiently expressed in CHO pgsA-745 cells as it was for XT-II.

Western blot analysis showed that transfection of CHO pgsA-745 cells with pCMV-XT-II/KDEL vector resulted in a synthesis of a polypeptide at similar level and molecular mass to those observed for XT-II (Fig. 4A), indicating that XT-II/KDEL is efficiently expressed in CHO pgsA-745 cells. Investigation of the subcellular localization of XT-II/KDEL by immunofluorescence showed that XT-II/KDEL displayed a perinuclear ER-like pattern (Fig. 4B) and co-localize with the ER resident protein marker calnexin (Fig. 4B, merge) but not with the cis-Golgi marker GM130 (Fig. 4C, merge), indicating that the enzyme is retained in the ER. To determine whether delocalization of XT-II to the ER impaired its activity, the ability of the enzyme to restore PG synthesis in CHO pgsA-745 cells was investigated. As shown in figure 4D, XT-II/KDEL was able to restore the expression of cell surface HSPGs as demonstrated by immunofluorescence using anti-HS monoclonal antibody, indicating that delocalizing XT-II from cis-Golgi to the ER is not detrimental to its enzyme activity. Next, we investigated whether the subcellular localization of XT-II has an impact on the size of the initiated GAG chains. DCN-EGFP was produced in CHO pgsA-745 cells expressing XT-II or XT-II/KDEL and analyzed by SDS-PAGE. Interestingly, DCN-EGFP from cells expressing XT-II/KDEL was of a large size compared to that produced in cells expressing XT-II (Fig. 3E), indicating that delocalisation of XT-II to the ER led to initiation of PG with large size GAG chains. Of note, as observed for XT-I, there was a strong reduction in DCN-EGFP with shorter GAG chains produced in CHO pgsA-745 cells expressing XT-II/KDEL compared to that produced in CHO pgsA-745 cells expressing XT-II (Fig. 4E).

Expression of XT-I increased the size of PG-GAG chains produced in cells XT-II-expressing cells

To further demonstrate that XT-I initiates large size GAG chains compared to XT-II, we analyzed the effect of the expression of XT-I on the size of GAG chain produced in XT-II expressing cells. CHO pgsA-745 cells stably expressing XT-II were co-transfected with pCMV-DCN-EGFP or pCMV-SDC4$^{(\Delta CT)}$-EGFP along with various concentration of pCMV-XT-I vector. GAG-attached DCN-EGFP and SDC4$^{(\Delta CT)}$-EGFP were immunopurified from cell culture supernatants and analyzed by Western blot using anti-EGFP antibodies. Interestingly, expression of XT-I in cells

expressing XT-II increased the size of DCN-EGFP in a dose dependent manner (Fig. 4A). The size of DCN-EGFP increased following transfection with 0.2 μg of XT-I expression vector to 1 μg. These results confirmed that XT-I produce larger size GAG chains compare to XT-II. Similar results were obtained for HS-attached SDC4$^{(\Delta CT)}$-EGFP. High amount of SDC4$^{(\Delta CT)}$-EGFP with HS chains of large size was observed at 0.5 μg of pCMV-XT-I vector (Fig. 5B).

PGs with GAG chains primed by XT-II are secreted earlier to those primed by XT-I

To analyses the mechanism by which XT-I produces large size GAG chains, we hypothesized that this may be due to different maturation process of the GAG chains initiated by XT-I and XT-II. For this purposes, we performed pulse-chase experiments to study the kinetics of DCN-GFP transport in CHO/XT-I, CHO/XT-II and CHO/XT-II/KDEL cells stably expressing XT-I, XT-II and XT-II/KDEL. Cells were transfected with DCN-GFP and pulsed with 30 μCi of ^{35}S-sulfate for 2 h then chased with DMEM-F12 complete media for different time points. ^{35}S-labeled DCN-GFP was immunopurified and loaded onto the SDS-PAGE. The autoradiography showed that most of ^{35}S-radiolabeled GAG-attached DCN-GFP was secreted into the medium of CHO/XT-II at 2 h of chase, whereas no radiolabeled DCN-GFP was observed after 6 h of chase (Fig. 6). However, in the case of CHO/XT-I most of ^{35}S-radiolabeled GAG-attached DCN-GFP was secreted into the medium at 6 h of chase (Fig. 6). Similar results were observed for CHO/XT-II/KDEL (Fig. 6), indicating a delay in GAG-attached DCN-GFP secretion in XT-I and XT-II/KDEL cells compared to XT-II cells. These results suggested that DCN-GFP is may be processed and secreted through distinct pathways in CHO/XT-I and CHO/XT-II.

Sulfation regulates the length of GAG chains initiated by XT-I but not of GAG chains initiated by XT-II

It has been reported that inhibition of GAG sulfation by chlorate, a competitive inhibitor of the formation of 3'-phosphoadenosine 5'-phosphosulfate (PAPS), the high energy sulfate donor in cellular sulfation reactions, increased GAG chain length in cultured adipocytes (36) and in MDCK cells (37) but did not affect the degree of GAG chain polymerization in skin fibroblasts (38). To determine whether sulfation regulates the length of GAG chains initiated by XT-I and XT-II,

CHO/XT-I and CHO/XT-II cells were transfected with pCMV-DCN-EGFP vector, respectively and cultured in medium containing or not 25 mM of chlorate. We used a concentration of 25 mM, to assure an almost complete sulfation blockage of CS-GAGs (39). To monitor the effectiveness of chlorate, we metabolically labeled GAG chains by ^{35}S-sulfate incorporation, and observed an almost complete absence of ^{35}S-sulfated DCN-EGFP after chlorate treatment, whereas in absence of chlorate (solvent) high amount of ^{35}S-sulfated GAG-attached DCN-EGFP was observed in both CHO/XT-I and CHO/XT-II cells (Fig. 7A). Interestingly, Western blot analysis of DCN-EGFP produced in CHO/XT-I cells clearly showed that treatment with chlorate strongly increased the size of GAG-attached DCN-EGFP compared to control (solvent) (Fig. 7B). Whereas, chlorate treatment did not produce any significant effect on the size of GAG-attached DCN-EGFP produced in CHO/XT-II cells (Fig 7B). These results indicated that chlorate treatment increased GAG chain polymerization in CHO/XT-I cells but not in CHO/XT-II cells and therefore that sulfation regulates the polymerization of GAG chains initiated by XT-I but not of those initiated by XT-II. Of note, chlorate treatment increased the size of GAG-attached DCN-EGFP produced in CHO/XT-II/KDEL (Fig 7C), indicating that delocalization of XT-II from the cis-Golgi to the ER compartment induced sulfate-dependent regulation of GAG chain polymerization. Altogether, these results suggest that GAG chains initiated in the ER are probably processed differently from those initiated in cis-Golgi (XT-II).

Genetic variants of XT-I and XT-II exhibit deficient initiation of PG-GAG chains

Genetic variations in the *xylt-I* and *xylt-II* genes have been described as risk factors in PG-associated pathologies, however the consequences of these mutations were not investigated. To study the impact of the mutations of XT-I and XT-II on PG synthesis, we designed and stably expressed five XT-I variants Al15S, R406W, R481W, R598C and T665M and five XT-II variants D56N, P115L, R305T, R406C and P418L in addition to wild-type XT-I and XT-II in CHO pgsA-745 cells. Analysis of the expression of recombinant proteins by Western blot showed that wild-type XT-I and mutants (Fig. 8A) were efficiently expressed and in similar amount. Similar results were obtained for wild-type and XT-II mutants (Fig. 8B).

To determine the impact of genetic variations of XT-I and XT-II on biosynthesis of PGs,

pgsA-745 cell lines stably expressing wild-type and XT-I mutants as well as wild-type and XT-II mutants, respectively were challenged for the biosynthesis of CSPGs and HSPGs using decorin (DCN-EGFP) and syndecan4 (SDC4$^{(\Delta CT)}$-EGFP) as reporter PG core proteins, respectively. For these purposes, cells were transfected with pCMV-DCN-EGFP and pCMV- SDC4$^{(\Delta CT)}$-EGFP and at 48 h posttransfection DCN-EGFP and SDC4$^{(\Delta CT)}$-EGFP produced in cell culture supernatants were analyzed by Western blot after immunopurification with anti-EGFP-coupled affinity column chromatography. The results indicated that wild-type XT-I initiates the synthesis of GAG-attached decorin and syndecan-4, therefore producing GAG-attached DCN-EGFP and SDC4$^{(\Delta CT)}$-EGFP (Fig. 8 C and D). However, the XT-I mutants Al15S, R406W and R598C produced only few amount of GAG-attached DCN-EGFP and SDC4$^{(\Delta CT)}$-EGFP (Fig. 8 C and D), indicating that these mutations alter but not abolish XT-I activity. In contrast, the XT-I mutants R481W and T665M were not able to initiate the synthesis of GAG chains of either CS or HS type, indicating that these mutations were detrimental to the XT-I activity.

Similarly, Western blot analysis showed that wild-type XT-II and XT-II mutant R305T efficiently initiated the synthesis of GAG-attached both decorin and syndecan-4, therefore producing GAG-attached DCN-EGFP and SDC4$^{(\Delta CT)}$-EGFP (Fig. 8 E and F). However, the XT-II mutant P115L produced less amount of GAG-attached DCN-EGFP and SDC4$^{(\Delta CT)}$-EGFP compared to wild-type, indicating that this mutation alters to some extent the capacity of XT-I to initiate GAG synthesis. In contrast, the XT-II mutants D56N, R406C and P418L were not able to initiate the synthesis of GAG chains of either CS or HS type (Fig. 8 E and F), indicating that these mutations severely alter XT-I activity.

The XT-II genetic mutations R406C and P4I8L induced mislocalization of the enzyme to the ER compartment

To determine whether lack of the ability of XT-I and XT-II variants to assemble GAG chains on the core proteins was caused by alteration of the enzyme localization, we examined their subcellular localization. Immunofluorescence analysis showed that XT-II staining completely co-localize with the cis-Golgi marker GM 130 and did not

overlap with the ER marker calnexin revealing that it is localized in a cis-Golgi compartment (Fig. 9A). However, the XT-II variants R406C or P418L displayed an immunofluorescence pattern that is more restricted to a perinuclear ER-like distribution (Fig. 9B). Indeed, these cells showed a co-localisation with the ER resident protein calnexin, indicating that R406C and P418L mutants were retained in the ER compartment (Fig. 9). These data strongly suggest that R406C and P418L genetic variations induced a mislocalization of the XT-II protein from the cis-Golgi to the ER compartment.

XT-II but not XT-I is secreted in the culture medium

Xylosyltransferase (XT) activity has been detected in serum and proposed as biomarker of various diseases involving alterations in PG metabolism (12). To determine whether XT-I and XT-II were secreted, culture supernatants of cells stably expressing XT-I and XT-II were collected and analyzed by Western blot. As shown in figure 10, XT-II was secreted in culture medium and as expected exhibited a lower molecular size compared to the intracellular enzyme (Fig. 10A). However the XT-I is not secreted into the medium or might be below the detection limit of the anti-XT-I antibody (Fig. 10B). Interestingly, inhibition of the γ-secretase by a specific inhibitor strongly reduced the secretion of XT-II (Fig. 10C). Analysis of the secretion of XT-II genetic variants showed that D56N, P115L and R305T variants were secreted, whereas R406C and P418L were not (Fig. 10D).

Discussion

PGs are complex biomacromolecules present on the cell surface and extracellular matrix that regulate various biological processes. PGs are formed by the covalent attachment of the GAG chains onto the core protein. It is now an established fact that GAG chains are responsible for most

of the PGs functions (2, 40, 41). Both CS- and HS-GAG chains are linked to the core protein with a common tetrasaccharide linker region formed by stepwise addition of individual sugar residues. The first step in the synthesis of the common tetrasaccharide linker is the transfer of xylose from UDP-xylose to the specific serine residues of core protein. This initial and rate limiting step is catalyzed by xylosyltransferase (11, 12). Human xylosyltransferase has two isoforms, XT-I and XT-II encoded by *xylt-I* and *xylt-II* genes. Both XT-I and XT-II were able to restore GAG-attached PG synthesis in XT-I/XT-II-deficient CHO cells, pgsA-745, therefore suggesting that they are functionally redundant. To investigate whether XT-I and XT-II function redundantly in the synthesis of PGs, we analyzed the subcellular localization of the two XT isoforms. The localization of XT-I and XT-II is still unclear, some groups suggest that XT-I and XT-II are present in Golgi compartment (42), while other showed that xylosylation take place in the ER compartment (43-46). Our study showed that XT-I is localized in the ER, whereas XT-II is resident in cis-Golgi compartment, which may explain the presence of XT activity in both ER and Golgi as previously reported.

Unexpectedly, we observed that PGs primed by XT-I displayed larger size compare to those primed by XT-II. Size increases of PGs are due to elongation of the GAG as demonstrated by the chemical cleavage of the chains from the core proteins and GAG size analysis by SDS-PAGE. We further demonstrated this process is XT-I-driven as overexpression of XT-I in CHO/XT-II increased the size of GAG-attached decorin. Interestingly, delocalization of XT-II to the ER, using KDEL retrieval motif, resulted in the synthesis of PGs with larger size GAG chains, indicating that the subcellular localization of XT-II dictates the size of the GAG chain. PG interaction with various legends is mediated through GAG chains, therefore the length of the GAG chains may play a crucial role in these interactions and likely to influence the biological activity of these molecules. It has been reported that long PG-GAG chains were produced in cartilage during early stages of osteoarthritis (47) probably to counteract the loss of PGs and cartilage homeostasis induced by proinflammatory cytokines. Interestingly, we have previously showed that XT-I is regulated by interleukin 1β in human cartilage early stage (48). Long GAG chains were also observed in aggrecan produced by bone marrow stromal cells a process associated with superior biomechanical proprieties (49), and are prevalent in aggrecan from immature cartilage (50, 51), growth plate (27) and newly synthesized aggrecan after injury (52). We have analyzed the

expression of XT-I and XT-II in these cells and observed high expression of XT-I compared to XT-II (unpublished data). PGs with long GAG chains are present in advanced atherosclerotic lesions and exhibit high affinity for low density lipoproteins, therefore playing an important role in atherosclerosis pathogenesis (53).

Of note, it has been shown that the expression of XT-I is regulated by cytokines and growth factors (14, 48), whereas no such regulation was reported for XT-II, suggesting that XT-I expression is modulated in physiological and pathophysiological conditions as observed during osteogenic differentiation of mesenchymal stem cells (54) and in cartilage (48).

In an attempt to determine the molecular mechanism involved in the synthesis of PGs with long GAG chains when initiated by XT-I, we hypothesized they may undergo maturation process and/or undertake secretory pathway different from those initiated by XT-II. We showed using pulse and chasse experiment that PGs with GAG chains primed by XT-II were secreted earlier compared to those initiated by XT-I, suggesting that they may be processed and secreted through distinct pathways. In polarized cells such in Madin-Darby canine kidney (MDCK) cells, it has been shown that CS-GAG chains of serglycin-GFP (serglycin with a GFP tag) secreted apically are longer than CS-GAG chains attached to basolaterally secreted serglycin-GFP, supporting the view that separate pathways exist for GAG synthesis (55). The authors suggested that serglycin molecules destined for apical and basolateral surfaces domains are segregated early during synthesis indicating that information concerning sorting into different secretory routes may be localized to GAG chains and added in the very first evenets of modification. GAG chains and the linker tetrasaccharide sugars undergo modifications such as sulfation during synthesis. Whether, GAG chains were differently modified by sulfation when initiated by XT-I and XT-II will be investigated in a future study. However, we showed here that inhibition of sulfation by chlorate resulted in extended elongation of GAG chains initiated by XT-I, whereas it did not produce any significant effect on the length of the GAG chains initiated by XT-II, suggesting that sulfation regulates the polymerization of GAG chain initiated by XT-I but not of those initiated by XT-II. Interestingly, we showed that delocalization of XT-II from the cis-Golgi to the ER compartment induced sulfate-dependent regulation of the elongation of GAG chain, suggesting that the required information for the regulation of GAG chain polymerization by sulfation is likely added in the ER following the attachment of xylose residue on a PG core protein.

XT-I plays an important role in skeletal and brain development. Recently, two homozygous XT-I mutations, R481W and R598C have been reported in patients with short stature syndrome and intellectual disability (56) and in the Desbuquois dysplasia type 2 patients, respectively. These patients have short limbs, flat face, narrow thorax and intellectual disability (21). Polymorphism in the *xylt-I* and *xylt-II* genes have been reported and was shown to be associated with increased risk factor for various PG-associated pathogenesis (30). However, the impact of these genetic variations on the synthesis of PGs and their GAG chains is unknown. We showed here that, the two mutants R406C and P418L were retained in ER and did not show any enzyme activity. The Fam20C is a Golgi Kinase and phosphorylates the proteins important for biomineralization and mutations in Fam20C are associated with Raine syndrome. The mutations in the Fam20C that results in misslocalized of the enzyme from the Golgi to the ER compartment were catalytically inactive(57)

Material and Methods

Cell lines and culture conditions

CHO pgsA-745 cells (ATCC, CRL-2242) were cultured in DMEM F12 (Dulbecco's modified Eagle's medium) supplemented with 10% fetal bovine serum (FBS, GIBCO-Invitrogen, Cergy-Pontoise, France), penicillin (100 IU/m1), streptomycin (100 µg/m1) and 2 mM glutamine. Cells were maintained at 37°C with humidified atmosphere in a 5% CO_2.

Vector constructions

Human XT-I and XT-II cDNAs were isolated by PCR from human placenta Quick-Clone cDNA (Clontech, Mountain View, CA, USA) and ligated into the unique XbaI-HindIII sites of mammalian expression vector pCMV (Clontech, Mountain View, CA, USA) to generate pCMV-XT-I and pCMV-XT-II, respectively. To generate pCMV-XT-II/KDEL, XT-II/KDEL sequence was obtained following PCR amplification of XT-II cDNA using 5' primer containing XbaI site, the sequence encoding the first eight N-terminal residues of the

protein and a 3' primer containing a HindIII site and the sequence encoding for the last eight C-terminal amino acids of the XT-II protein in addition to the sequence encoding for KDEL motif. The amplified fragment was ligated into the unique XbaI-HindIII sites of mammalian expression vector pCMV to generate pCMV-XT-II/KDEL. Each vector was checked by DNA sequencing.

The vectors pCMV-DCN-EGFP and pCMV-SDC4$^{(\Delta CT)}$-EGFP expressing decorin and syndecan-4 (deleted from the forty C-terminus residues) PG core proteins in fusion with EGFP were obtained following PCR amplification of DCN and SDC4 cDNAs from placenta Quick-Clone cDNA using 5' primer containing XhoI site, the sequence encoding the first eight N-terminal residues of the protein and a 3' primer containing a BamHI site and the sequence encoding for the last eight C-terminal amino acids. The amplified fragments were inserted into XhoI-BamHI sites in frame with the sequence encoding EGFP protein in the pEGFP-C2 (Clontech). The vectors were checked by DNA sequencing

Stable expression of XT-I, XT-II and XT-II/KDEL

pCMV-XT-I, pCMV-XT-II, pCMV-XT-II/KDEL and empty pCMV vectors were stably transfected into CHO-psgA-745 cells, as previously described (58). Briefly, CHO-psgA-74 cells were grown in 6-well culture plate until 80% confluency and transfected with 1 µg of pCMV-XT-I, pCMV-XT-II, pCMV-XT-II/KDEL and empty pCMV (control), respectively along with 200 ng of pSVneo using ExGen500 reagent (Euromedex, Souffelweyersheim, France). At 24 h post-transfection, cells were trypsinized and cultured in F12-DMEM containing 1 mg/ml G418 in 10 cm culture dish. For each transfection, twenty clones were isolated and analyzed for the expression of recombinant XT-I, XT-II and XT-II/KDEL, respectively by Western blot. Clones that express high level of recombinant proteins were selected for further studies.

Cell transfection

Cells were seeded in 6-well culture plate until 80% confluency and transfected with 1 µg of either pCMV-DCN-EGFP or pCMV-SDC4$^{(\Delta CT)}$-EGFP using Exgen 500 reagent

(Euromedex, Souffelweihersheim, France) according to the manufacturer's instructions. Expression and secretion of DCN-EGFP and SDC4$^{(\Delta CT)}$-EGFP in culture medium was analyzed at 48 h post-transfection by Western blotting using monoclonal anti-EGFP antibodies (Cell Signalling Technology, MA, USA). For transient expression of XT-I, XT-II and XT-II/KDEL, respectively cells were transfected as above and the expression of recombinant proteins were analysed from cell lysates by Western Blot using specific antibodies.

Site-directed mutagenesis

Site directed mutagenesis of XT-I and XT-II residues was performed using the QuickChange site-directed mutagenesis kit (Stratagene) according to the recommendations of the manufacturer. pCMV-XT-I and pCMV-XT-II expression vectors were used as template. Sense and antisense oligonucleotides introducing the desired mutations were given in table 1. Full length mutated cDNAs were systematically checked by DNA sequencing.

Protein expression analysis

Cells were grown at confluency in the 6-well culture plate, then washed with PBS and suspended in sucrose Hepes buffer (0.25 M sucrose, 5 mM Hepes, pH 7.4) containing Complete Mini™ protease inhibitors (Roche Molecular Biochemicals). Cells were lysed by three 5 s sonication (Vibra Cell, Bioblock Scientific) and were centrifuged at 12,000 x *g* for 20 min. Protein concentration of the cell lysate was evaluated by the Bradford method (1976) (59).

Secretion of XT-I and XT-II

For analysis of the secretion of XT-I, XT-II and mutants proteins in culture medium, cells were grown in 6-well culture plate until 80% confluency then medium was replaced by serum-free medium and culture was carried out for an additional 24 h. Then 1 ml of conditioned medium was collected and centrifuged at 12,000 x *g* for 10 min at 4°C. Proteins from conditioned medium were precipitated by addition of 200 µl of 60% (w/v) trichloroacetic acid solution followed by incubation for 30 min on ice and centrifugation at 12,000 x *g* for 15

min. The pellet was washed with 200 µl acetone and dissolved in 30 µl of Laemmli buffer. Proteins were separated by SDS-PAGE and analysed by Western Blot using anti-XT-I and anti-XT-II specific antibodies.

Immunopurification of DCN-EGFP and SDC4$^{(\Delta CT)}$-EGFP

Conditioned media from recombinant cells were collected at 48 h post-transfection and DCN-EGFP and SDC4$^{(\Delta CT)}$-EGFP PGs were immunopurified with anti-EGFP-coupled affinity column chromatography using GFP purification kit (µMACS, Miltenyi Biotec). Briefly, conditioned medium was mixed with 50 µl of anti-GFP magnetic beads and incubated for 30 min on ice. The mixture was applied onto the column and washed four times with 200 µl of buffer A (150 mM NaCl, 1% NP-40, 0.5% sodium deoxycholate, 0.1% SDS, 50 mM Tris HC1, pH 8.0) and once with 100 µl of buffer B (20 mM Tris HC1, pH 7.5) then eluted with 50 µl of elution buffer (50 mM DTT, 1% SDS, 1 mM EDTA, 0.005% bromophenol blue, 10% glycerol, 50 mM Tris HC1, pH 6.8), pre-heated at 95°C and analyzed by western blot.

Western blot analysis

Proteins from cell lysate and conditioned medium were subjected to SDS-PAGE and transferred onto the PVDF membrane (Millipore). The membrane was blocked with 5% skimmed milk in Tris-bufferd saline (TBS) and incubation with primary antibodies: anti-XT-I (1:500, Sigma), anti-XT-II (1:250, Santa Cruz Bitechnology) and anti-GFP antibodies (1:1000, Cell Signalling Technology) overnight at 4°C followed by incubation with horseradish-peroxidase-conjugated secondary antibodies. The reactive bands were detected by chemiluminescence using clarity^{TM} western ECL substrate (BioRad).

Pulse-chase experiments

CHO pgsA-745 cells expressing XT-I, XT-II and XT-II-KDEL, respectively and CHO pgsA-745 cells (control) were grown in 6 well culture plates until 80% confluency and transfected with

pCMV-DCN-EGFP vector. At 36 h post-transfection, cells were labeled with 30 μCi of ^{35}S-sulfate in sulfate free medium for 2 h. Cells were then washed twice with PBS and incubated for various chase times in non-radioactive DMEM-F12 compete medium. At the end of the chase intervals, conditioned medium was collected and ^{35}S-labeled DCN-EGFP was immunopurified with anti-EGFP-coupled affinity column chromatography then loaded onto the SDS-PAGE. The gel was dried and subjected to autoradiography.

Indirect immunofluorescence staining

The cells were grown on glass coverslips and fixed with 3% (w/v) paraformaldehyde in PBS for 20 min. Cells were permeabilized by treatment with 0.1% (w/v) Triton X-100/PBS solution for 4 min. After extensive washing in 0.2% (w/v) fish skin gelatin in PBS, cells were incubated with 0.2 % gelatin for 20 min. Cell were then incubated with primary antibodies anti-XT-I (1:100, Sigma), anti XT-II (1:100, Santa Cruz), anti-GM130 (1:200, cis-Golgi marker, BD), anti-calnexin (1:200, ER marker, Sigma), and anti-HS antibodies (1:100, 10E4 monoclonal, US Biological), respectively for 20 min. Cover slips were then washed several times with PBS and incubated with secondary antibodies coupled with Alexa Fluor 488 and Alexa Fluor 555 (Molecular Probes) for 20 min. After washing with PBS nuclei were stained with Hoechst/PBS solutions and coverslips were mounted with Moviol (National Diagnostics, U.K.) containing 1% propylgallate (Sigma). Digital images were captured with an inverted microscope Lieca DMI3000 B (Leica Microsystems, Germany).

Acknowledgements

This work was supported by the Région Lorraine research grant.

Reference

1. Schwartz NB & Domowicz M (2002) Chondrodysplasias due to proteoglycan defects. *Glycobiology* 12(4):57-68.
2. Gesslbauer B, Theuer M, Schweiger D, Adage T, & Kungl AJ (2013) New targets for glycosaminoglycans and glycosaminoglycans as novel targets. *Expert Review of Proteomics* 10(1):77-95.
3. Chen S & Birk DE (2013) The regulatory roles of small leucine-rich proteoglycans in extracellular assembly. *FEBS Journal* 280(10): 2120-2137.
4. Esko JD & Selleck SB (2002) Order Out of Chaos: Assembly of Ligand Binding Sites in Heparan Sulfate 1. *Annual Review of Biochemistry* 71(1):435-471.
5. Shriver Z, Liu D, & Sasisekharan R (2002) Emerging views of heparan sulfate glycosaminoglycan structure/activity relationships modulating dynamic biological functions. *Trends in cardiovascular medicine* 12(2):71-77.
6. van Horssen J, Wesseling P, van den Heuvel LP, de Waal RM, & Verbeek MM (2003) Heparan sulphate proteoglycans in Alzheimer's disease and amyloid-related disorders. *The Lancet Neurology* 2(8):482-492.
7. Koslowski R*, et al.* (2001) Changes in xylosyltransferase activity and in proteoglycan deposition in bleomycin-induced lung injury in rat. *European Respiratory Journal* 18(2):347-356.
8. Venkatesan N*, et al.* (2013) Glycosyltransferases and Glycosaminoglycans in Bleomycin and Transforming Growth Factor-β1-Induced Pulmonary Fibrosis. *American Journal of Respiratory Cell and Molecular Biology*.
9. Kuhn J, Gressner OA, Götting C, Gressner AM, & Kleesiek K (2009) Increased serum xylosyltransferase activity in patients with liver fibrosis. *Clinica Chimica Acta* 409(1–2):123-126.
10. Wegrowski Y & Maquart F-X (2004) Involvement of stromal proteoglycans in tumour progression. *Critical reviews in oncology/hematology* 49(3):259-268.
11. Wilson IBH (2004) The never-ending story of peptide O-xylosyltransferase. *CMLS, Cell. Mol. Life Sci.* 61(7-8):794-809.

12. Götting C, Kuhn J, & Kleesiek K (2007) Human xylosyltransferases in health and disease. *Cell. Mol. Life Sci.* 64(12):1498-1517.
13. Gulberti S*, et al.* (2005) Phosphorylation and sulfation of oligosaccharide substrates critically influence the activity of human β1,4-galactosyltransferase 7 (GalT-I) and β1,3-glucuronosyltransferase I (GlcAT-I) involved in the biosynthesis of the glycosaminoglycan-protein linkage region of proteoglycans. *Journal of Biological Chemistry* 280(2):1417-1425.
14. Prante C*, et al.* (2007) Transforming growth factor β1-regulated xylosyltransferase I activity in human cardiac fibroblasts and its impact for myocardial remodeling. *Journal of Biological Chemistry* 282(36):26441-26449.
15. Venkatesan N*, et al.* (2009) Modulation of xylosyltransferase i expression provides a mechanism regulating glycosaminoglycan chain synthesis during cartilage destruction and repair. *FASEB Journal* 23(3):813-822.
16. Götting C*, et al.* (1999) Serum xylosyltransferase: a new biochemical marker of the sclerotic process in systemic sclerosis. *Journal of investigative dermatology* 112(6):919-924.
17. Schön S*, et al.* (2006) Polymorphisms in the xylosyltransferase genes cause higher serum XT-I activity in patients with pseudoxanthoma elasticum (PXE) and are involved in a severe disease course. *Journal of Medical Genetics* 43(9):745-749.
18. Götting C*, et al.* (2005) Elevated xylosyltransferase I activities in pseudoxanthoma elasticum (PXE) patients as a marker of stimulated proteoglycan biosynthesis. *Journal of Molecular Medicine* 83(12):984-992.
19. Condac E*, et al.* (2009) Xylosyltransferase II is a significant contributor of circulating xylosyltransferase levels and platelets constitute an important source of xylosyltransferase in serum. *Glycobiology* 19(8):829-833.
20. Almeida R*, et al.* (1999) Cloning and Expression of a Proteoglycan UDP-Galactose: β-Xylose β1, 4-Galactosyltransferase IA SEVENTH MEMBER OF THE HUMAN β4-GALACTOSYLTRANSFERASE GENE FAMILY. *Journal of Biological Chemistry* 274(37):26165-26171.

21. Bui C*, et al.* (2010) Molecular characterization of β1, 4-galactosyltransferase 7 genetic mutations linked to the progeroid form of Ehlers–Danlos syndrome (EDS). *FEBS Letters* 584(18):3962-3968.
22. Faiyaz-Ul-Haque M*, et al.* (2004) A novel missense mutation in the galactosyltransferase-I (B4GALT7) gene in a family exhibiting facioskeletal anomalies and Ehlers–Danlos syndrome resembling the progeroid type. *American Journal of Medical Genetics Part A* 128(1):39-45.
23. Götte M & Kresse H (2005) Defective Glycosaminoglycan Substitution of Decorin in a Patient With Progeroid Syndrome Is a Direct Consequence of Two Point Mutations in the Galactosyltransferase I (ß4galT-7) Gene. *Biochemical genetics* 43(1-2):65-77.
24. Seidler D*, et al.* (2006) Defective glycosylation of decorin and biglycan, altered collagen structure, and abnormal phenotype of the skin fibroblasts of an Ehlers–Danlos syndrome patient carrying the novel Arg270Cys substitution in galactosyltransferase I (β4GalT-7). *Journal of Molecular Medicine* 84(7):583-594.
25. McCormick C, Duncan G, Goutsos KT, & Tufaro F (2000) The putative tumor suppressors EXT1 and EXT2 form a stable complex that accumulates in the Golgi apparatus and catalyzes the synthesis of heparan sulfate. *Proceedings of the National Academy of Sciences* 97(2):668-673.
26. Wu Y*, et al.* (2013) Novel and recurrent mutations in the EXT1 and EXT2 genes in Chinese kindreds with multiple osteochondromas. *Journal of Orthopaedic Research*.
27. Deutsch AJ, Midura RJ, & Plaas AH (1995) Structure of chondroitin sulfate on aggrecan isolated from bovine tibial and costochondral growth plates. *Journal of Orthopaedic Research* 13(2):230-239.
28. Koziel L, Kunath M, Kelly OG, & Vortkamp A (2004) Ext1-dependent heparan sulfate regulates the range of Ihh signaling during endochondral ossification. *Developmental cell* 6(6):801-813.
29. Schön S*, et al.* (2005) Impact of polymorphisms in the genes encoding xylosyltransferase I and a homologue in type 1 diabetic patients with and without nephropathy. *Kidney International* 68(4):1483-1490.

30. Schön S*, et al.* (2006) Mutational and functional analyses of xylosyltransferases and their implication in osteoarthritis. *Osteoarthritis and Cartilage* 14(5):442-448.
31. Schön S*, et al.* (2006) The xylosyltransferase I gene polymorphism c.343G>t (p.A125S) is a risk factor for diabetic nephropathy in type 1 diabetes. *Diabetes Care* 29(10):2295-2299.
32. Götting C, Kuhn J, & Kleesiek K (2008) Serum Xylosyltransferase Activity in Diabetic Patients as a Possible Marker of Reduced Proteoglycan Biosynthesis. *Diabetes Care* 31(10):2018-2019.
33. Pönighaus C*, et al.* (2009) Xylosyltransferase gene variants and their role in essential hypertension. *American Journal of Hypertension* 22(4):432-436.
34. Schreml J*, et al.* (2013) The missing "link": an autosomal recessive short stature syndrome caused by a hypofunctional XYLT1 mutation. *Human genetics*:1-11.
35. Bui C*, et al.* (2014) XYLT1 mutations in Desbuquois dysplasia type 2. *The American Journal of Human Genetics* 94(3):405-414.
36. Hoogewerf AJ, Cisar L, Evans D, & Bensadoun A (1991) Effect of chlorate on the sulfation of lipoprotein lipase and heparan sulfate proteoglycans. Sulfation of heparan sulfate proteoglycans affects lipoprotein lipase degradation. *Journal of Biological Chemistry* 266(25):16564-16571.
37. Safaiyan F*, et al.* (1999) Selective effects of sodium chlorate treatment on the sulfation of heparan sulfate. *Journal of Biological Chemistry* 274(51):36267-36273.
38. Greve H, Cully Z, Blumberg P, & Kresse H (1988) Influence of chlorate on proteoglycan biosynthesis by cultured human fibroblasts. *Journal of Biological Chemistry* 263(26):12886-12892.
39. Fjeldstad K*, et al.* (2002) Sulfation in the Golgi lumen of Madin-Darby canine kidney cells is inhibited by brefeldin A and depends on a factor present in the cytoplasm and on Golgi membranes. *Journal of Biological Chemistry* 277(39):36272-36279.
40. Couchman JR (2010) Transmembrane Signaling Proteoglycans. *Annual Review of Cell and Developmental Biology* 26(1):89-114.
41. Manon-Jensen T, Itoh Y, & Couchman JR (2010) Proteoglycans in health and disease: The multiple roles of syndecan shedding. *FEBS Journal* 277(19):3876-3889.

42. Schön S*, et al.* (2006) Cloning and Recombinant Expression of Active Full-length Xylosyltransferase I (XT-I) and Characterization of Subcellular Localization of XT-I and XT-II. *Journal of Biological Chemistry* 281(20):14224-14231.
43. Horwitz AL & Dorfman A (1968) SUBCELLUAR SITES FOR SYNTHESIS OF CHONDROMUCOPROTEIN OF CARTILAGE. *The Journal of Cell Biology* 38(2):358-368.
44. Vertel BM, Walters LM, Flay N, Kearns AE, & Schwartz NB (1993) Xylosylation is an endoplasmic reticulum to Golgi event. *Journal of Biological Chemistry* 268(15):11105-11112.
45. Hoffmann H-P, Schwartz NB, Rodén L, & Prockop DJ (1984) Location of xylosyltransferase in the cisternae of the rough endoplasmic reticulum of embryonic cartilage cells. *Connective Tissue Research* 12(2):151-163.
46. Kearns AE, Vertel BM, & Schwartz NB (1993) Topography of glycosylation and UDP-xylose production. *Journal of Biological Chemistry* 268(15):11097-11104.
47. Carney SL, Billingham ME, Muir H, & Sandy JD (1985) Structure of newly synthesised (35S)-proteoglycans and (35s)-proteoglycan turnover products of cartilage explant cultures from dogs with experimental osteoarthritis. *Journal of Orthopaedic Research* 3(2):140-147.
48. Khair M*, et al.* (2012) Regulation of Xylosyltransferase I gene expression by interleukin 1β in human primary chondrocyte cells: mechanism and impact on proteoglycan synthesis. *Journal of Biological Chemistry*.
49. Lee HY*, et al.* (2010) Adult bone marrow stromal cell-based tissue-engineered aggrecan exhibits ultrastructure and nanomechanical properties superior to native cartilage. *Osteoarthritis and Cartilage* 18(11):1477-1486.
50. Inerot S, Heinegård D, Audell L, & Olsson S (1978) Articular-cartilage proteoglycans in aging and osteoarthritis. *Biochemical Journal* 169(1):143-156.
51. Plaas AH, Wong-Palms S, Roughley PJ, Midura RJ, & Hascall VC (1997) Chemical and immunological assay of the nonreducing terminal residues of chondroitin sulfate from human aggrecan. *Journal of Biological Chemistry* 272(33):20603-20610.

52. Brown M*, et al.* (2007) Exercise and injury increase chondroitin sulfate chain length and decrease hyaluronan chain length in synovial fluid. *Osteoarthritis and Cartilage* 15(11):1318-1325.
53. Gutierrez P*, et al.* (1997) Differences in the Distribution of Versican, Decorin, and Biglycan in Atherosclerotic Human Coronary Arteries. *Cardiovascular Pathology* 6(5):271-278.
54. Müller B*, et al.* (2008) Increased levels of xylosyltransferase I correlate with the mineralization of the extracellular matrix during osteogenic differentiation of mesenchymal stem cells. *Matrix Biology* 27(2):139-149.
55. Vuong TT, Prydz K, & Tveit H (2006) Differences in the apical and basolateral pathways for glycosaminoglycan biosynthesis in Madin–Darby canine kidney cells. *Glycobiology* 16(4):326-332.
56. Schreml J*, et al.* (2014) The missing "link": an autosomal recessive short stature syndrome caused by a hypofunctional XYLT1 mutation. *Human genetics* 133(1):29-39.
57. Ishikawa HO, Xu A, Ogura E, Manning G, & Irvine KD (2012) The Raine Syndrome Protein FAM20C Is a Golgi Kinase That Phosphorylates Bio-Mineralization Proteins. *PLoS ONE* 7(8):e42988.
58. Ouzzine M, Barré L, Netter P, Magdalou J, & Fournel-Gigleux S (2006) Role of the carboxyl terminal stop transfer sequence of UGT1A6 membrane protein in ER targeting and translocation of upstream lumenal domain. *FEBS Letters* 580(8):1953-1958.
59. Bradford MM (1976) A rapid and sensitive method for the quantitation of microgram quantities of protein utilizing the principle of protein-dye binding. *Analytical biochemistry* 72(1):248-254.

Figure legends

Fig. 1. Expression and localization of XT-I and XT-II. The pgsA-745 cells were transfected with pCMV-XT-I, pCMV-XT-II and pCMV (control) vectors and expression was analyzed by western blot using specific antibodies against XT-I (A) and XT-II (B). Immunofluorescence analysis of

cells transfected with pCMV-XT-I and pCMV-XT-II vectors with antibodies specific to XT-I, XT-II as showed in green whereas calnexin and GM130 as ER and Golgi marker, respectively as seen in red. The pgsA-745 cells stable expressing XT-II were transfected with pCMV-XT-I vector and immunofluorescence was used to determine the co-localization of XT-I (red) and XT-II (green) using specific antibodies (F). Nuclei were stained (blue) using Hoechst.

Fig. 2. Immunofluorescence analysis of cell surface heparin sulphate proteoglycans. The pgsA-745 cells were transfected with pCMV-XT-I (A), pCMV-XT-II (B) and pCMV (C) vectors and expression of cell surface HSPGs was examined by immunofluorescence using anti-heparan sulphate 10E4 antibody (red). The XT-I and XT-II expression was analyzed using specific antibodies (green). Nuclei were stained with Hoechst/PBS solution (blue).

Fig. 3. Both XT-I and XT-II initiate PG-GAGs synthesis**.** (A) The pgsA-745 cells stably expressing pCMV-XT-I, pCMV-XT-II and pCMV (control) were transfected with DCN-EGFP expression vector and medium containing secreted CSPGs attached to decorin were immunopurified and analyzed by Western blot using anti-GFP antibody. (B) The pgsA-745 cells stably expressing pCMV-XT-I, pCMV-XT-II and pCMV (control) were transfected with SDC4-EGFP expression vector and secreted HSPGs were immunopurified from the medium and analyzed by Western blot using anti-GFP specific antibody. (C) The pgsA-745 cells stably expressing pCMV-XT-I and pCMV-XT-II were transfected with DCN-EGFP expression vector and medium labelled with 10μCi ^{35}S-sulphate and immunopurified with and without digestion of core protein with proteinase-K and analyzed by SDS-PAGE.

Fig. 4. The expression, localization and GAG synthesis of XT-II with KDEL motif. The pgsA-745 cells were transfected with pCMV-XT-II-KDEL and pCMV (control) vectors and expression was analyzed by western blot using specific antibodies against XT-II (A). Immunofluorescence analysis of cells transfected with pCMV-XT- II-KDEL vector with XT-II specific antibody (green) with calnexin and GM130 as, ER and Golgi marker (red) respectively (B and C). The cell surface HSPGs was analysed by immunofluorescence analysis with anti-heparan sulphate 10E4 antibody (red) and XTII-KDEL was probed with XT-II antibody (green) (D). Nuclei were stained with Hoechst/PBS solution (blue). The pgsA-745 cells stably expressing pCMV-XT-I, pCMV-XT-II, pCMV-XT-II KDEL and pCMV (control) were transfected with DCN-EGFP expression vector

and medium containing secreted CSPGs attached to decorin were immunopurified and analyzed by Western blot using anti-GFP antibody (E).

Fig. 5. Effect of overexpression of XT-I in cells stably expressing XT-II on GAG synthesis. The pgsA-745 cells stably expressing pCMV-XT-II were co-transfected with DCN-EGFP expression vector and various concentration (0.2, 0.5 and 1 μg) of pCMV-XT-I expression vector. The conditioned medium was collected secreted PGs were precipitated with CPC and analyzed by Western blot using anti-GFP specific antibody (A). The pgsA-745 cells stably expressing pCMV-XT-II were co-transfected with SDC4-EGFP expression vector and different concentrations (0.2 and 0.5 μg) of pCMV-XT-I expression vector. The conditioned medium was collected secreted HSPGs were precipitated with CPC and analyzed by Western blot using anti-GFP specific antibody.

Fig. 6. Analysis of the secretion of PGs by pulse and chase method. The pgsA-745 cells stably expressing pCMV-XT-I, pCMV-XT-II, pCMV-XT-II-KDEL and pCMV (control) were transfected with DCN-EGFP expression vector and 24 after the transfection pulsed with 30 μCi of ^{35}S-sulfate for 2h and then chased with DMEM-F12 complete media for different time points(1, 2 and 6h). The secretion of ^{35}S-labeled DCN-GFP was immunopurified and analyzed by SDS-PAGE.

Fig. 7. The effect of sodium chlorate on GAG chains. The pgsA-745 cells stably expressing pCMV-XT-I and pCMV-XT-II were transfected with DCN-EGFP expression vector and treated with or without 25μM sodium chlorate in medium containing 10 μCi of 35S-sulfate for 24h and 35S-labeled DCN-GFP was immunopurified and analyzed by SDS-PAGE (A). The pgsA-745 cells stably expressing pCMV-XT-I, pCMV-XT-II and pCMV-XT-II-KDEL were transfected with DCN-EGFP expression vector and treated with or without 25μM sodium chlorate in DMEM-F12 medium for 24h and secreted DCN-GFP was immunopurified and analyzed by Western blot using anti-GFP specific antibody (B).

Fig. 8. The expression and GAG synthesis analysis of XT-I and XT-II mutants. The pgsA-745 cells were transfected with wild type XT-I and mutants (pCMV-XT-I, pCMV-XT-I^{A115S}, pCMV-XT-I^{W481R}, pCMV-XT-I^{R406W}, pCMV-XT-I^{R598C}, pCMV-XT-I^{T665M}) expression vector and their expression was analyzed by western blot using specific antibodies against XT-I (A). The pgsA-745 cells were transfected with wild type XT-II and mutants (pCMV-XT-II, pCMV-XT-II ^{D56N}, pCMV-XT-II^{P115L}, pCMV-XT-II^{R305L}, pCMV-XT-II^{R406C}, pCMV-XT-II^{P418L}) vectors and expression was analyzed by western blot using specific antibodies against XT-II (B). The pgsA-745 cells expressing wild type XT-I and mutants were transfected with DCN-EGFP expression vector and medium containing secreted DCN-EGFP in the medium were immunopurified and analyzed by Western blot using anti-GFP antibody (C). The cells expressing wild type XT-I and mutants were transfected with SDC4-EGFP expression vector and medium containing secreted SDC4-EGFP in the medium were immunopurified and analyzed by Western blot using anti-GFP antibody (D). The pgsA-745 cells expressing wild type XT-II and mutants were transfected with DCN-EGFP expression vector and medium containing secreted DCN-EGFP in the medium were immunopurified and analyzed by Western blot using anti-GFP antibody (E). The cells expressing wild type XT-II and five XT-II mutants were transfected with SDC4-EGFP expression vector and medium containing secreted SDC4-EGFP in the medium were immunopurified and analyzed by Western blot using anti-GFP antibody (F)

Fig. 9. Analysis of the subcellular localization of XT-II mutants. Immunofluorescence analysis of pgsA-745 cells transfected with pCMV-XT-II ^{D56N}(A), pCMV-XT-II^{R406C}(B), and pCMV-XT-II^{P418L}(C) expression vectors with antibodies specific to XT-II as showed in green whereas calnexin and GM130 as ER and Golgi marker, respectively as seen in red. Nuclei were stained (blue) using Hoechst.

Fig. 10. Analysis of the secretion of XT-I, XT-II and XT-II mutants in medium. The pgsA-745 cells were transfected with pCMV-XT-II expression vector and the conditioned media was collected after 48h and expression in cells and medium was analyzed by western blot using specific antibodies against XT-II (A). The conditioned media was collected after 48h from the cells expressing pCMV-XT-I vector and analyzed by western blot using specific antibodies against XT-

I (B). The pgsA-745 cells stably expressing pCMV-XT-II were treated with or without (0, 50, 100, 150 μM) of γ-secretase and the conditioned medium was analyzed by western blot using specific antibodies against XT-II (C). The pgsA-745 cells were transfected with wild type XT-II and mutants (pCMV-XT-II, pCMV-XT-II ^{D56N}, pCMV-XT-II^{P115L}, pCMV-XT-II^{R305L}, pCMV-XT-II^{R406C}, pCMV-XT-II^{P418L}) vectors, the conditioned media was collected after 48h and expression in cells and medium was analyzed by western blot using specific antibodies against XT-II (D)

Table 1: Primers used for site directed mutagenesis of XT-I and XT-II

XT-I	A115S	Forward primer	CAG CCC GCC AGC AGA GGC ***TCC*** CTG CCC GCC AGA GCC CTG
		Reverse primer	CAG GGC TCT GGC GGG CAG GGA GCC TCT GCT GGC GGG CTG
	W481R	Forward primer	ATG TGG CGC CTG GGA GAT ***TGC*** CGG ATC CCA GAG GGC ATT
		Reverse primer	AAT GCC CTC TGG GAT CCG GCA ATC TCC CAG GCG CCA CAT
	R406W	Forward primer	CGG CCT ACC TTC TTT GCC ***TGC*** AAG TTT GAA GCC GTG GTG AAT
		Reverse primer	ATT CAC CAC GGC TTC AAA CTT GCA GGC AAA GAA GGT AGG CCG
	R598C	Forward primer	TCC ACC TAC CTG CAG ATG ***TGG*** GAC CTC CTC GAG ATG ACC
		Reverse primer	GGT CAT CTC GAG GAG GTC CCA CAT CTG CAG GTA GGT GGA
	T665M	Forward primer	GGT CTT CGA CGG GCC GAG ***ATG*** TCC CTG CAC ACG GAT GGG
		Reverse primer	CCC ATC CGT GTG CAG GGA CAT CTC GGC CCG TCG AAG ACC
XT-II	D56N P418L	Forward primer	CAG AGG AAG CCA CGA CTG ***AAC*** CCT GGC GAA GGT TCC AAG
		Reverse primer	CTT GGA ACC TTC GCC AGG GTT CAG TCG TGG CTT CCT CTG
	P115L	Forward primer	CTC CCA CCT GCC CCA CCT **CAG** GAA GCC CCA GGC CGC CAG
		Reverse primer	CTG GCG GCC TGG GGC TTC CTG AGG TGG GGC AGG TGG GAG
	R305L	Forward primer	GGC GGG GCC AGC CTC CTG ***AGG*** ATG TAC CTG CGG AGC ATG
		Reverse primer	CAT GCT CCG CAG GTA CAT CCT CAG GAG GCT GGC CCC GCC
	R406C	Forward primer	GAC TGG TTC GTG CTG ACA T***GC*** AGE TTT GTG GAG TAT GTG
		Reverse primer	CAC ATA CTC CAC AAA ECT GCA TGT CAG CAC GAA CCA GTC
	P418L	Forward primer	GTG GTG TAC ACA GAT AAC ***CTG*** CTT GTG GCC CAG CTG CGC
		Reverse primer	GCG CAG CTG GGC CAC AAG CAG GTT ATC TGT GTA CAC CAC

Figure 1

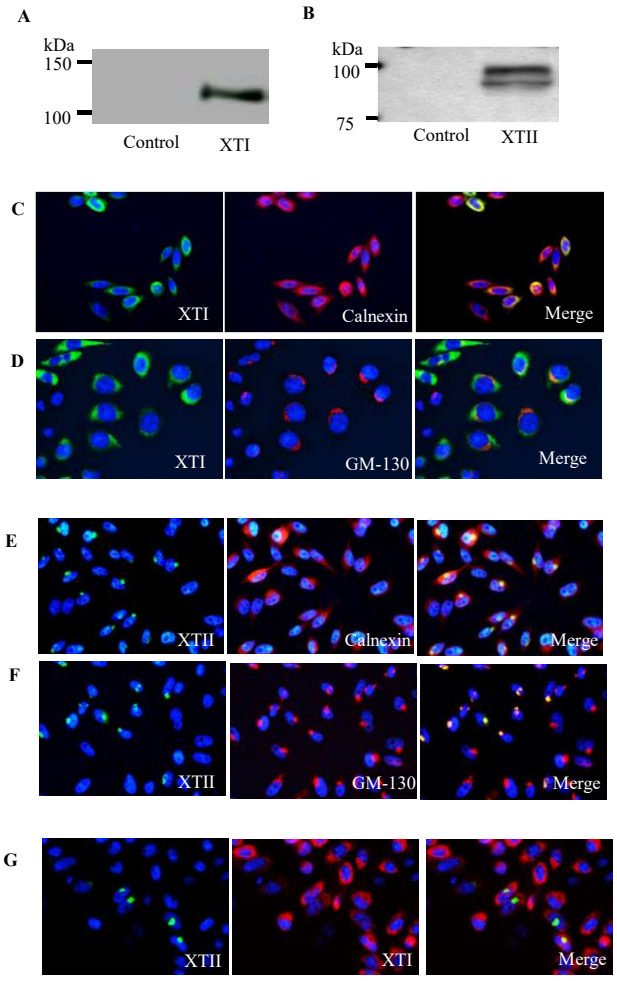

A
kDa
150
100
Control
XTI
B
kDa
100
75
Control
XTII
C
XTI
Calnexin
Merge
D
XTI
GM-130
Merge
E
XTII
Calnexin
Merge
F
XTII
GM-130
Merge
G
XTII
XTI
Merge

Figure 2

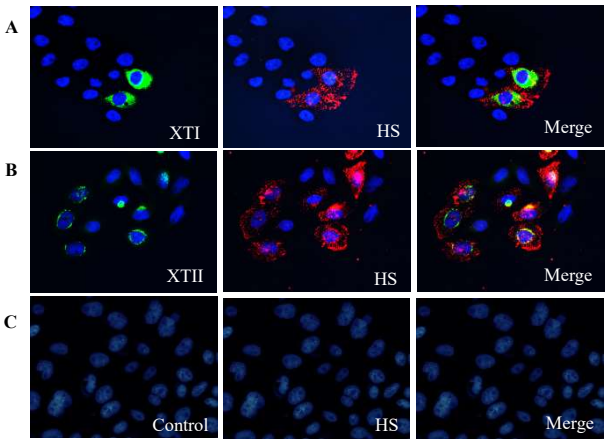


Figure 3

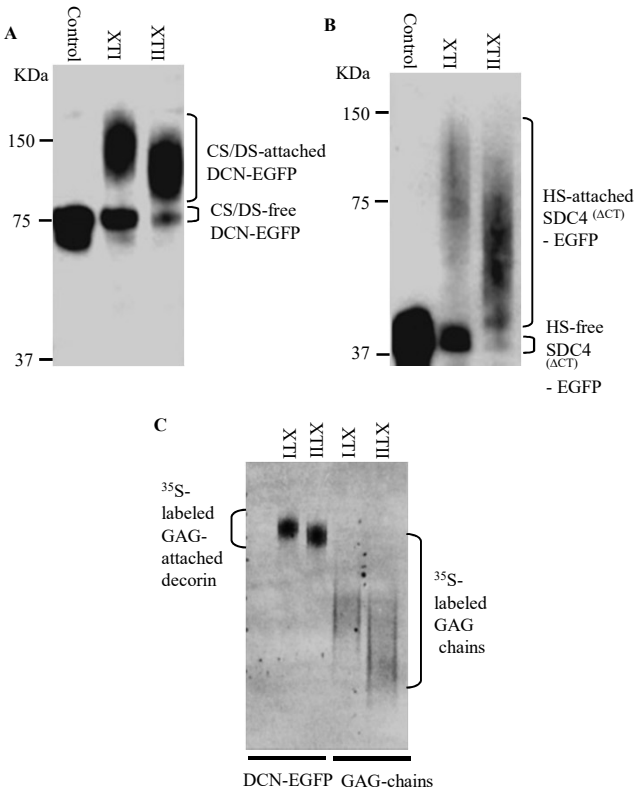

A
Control
XTI
XTII
KDa
150
75
37
CS/DS-attached
DCN-EGFP
CS/DS-free
DCN-EGFP
B
Control
XTI
XTII
KDa
150
75
37
HS-attached
SDC4 (ΔCT)
- EGFP
HS-free
SDC4
(ΔCT)
- EGFP
C
XTI
XTII
XTI
XTII
35S-
labeled
GAG-
attached
decorin
35S-
labeled
GAG
chains
DCN-EGFP
GAG-chains

Figure 4

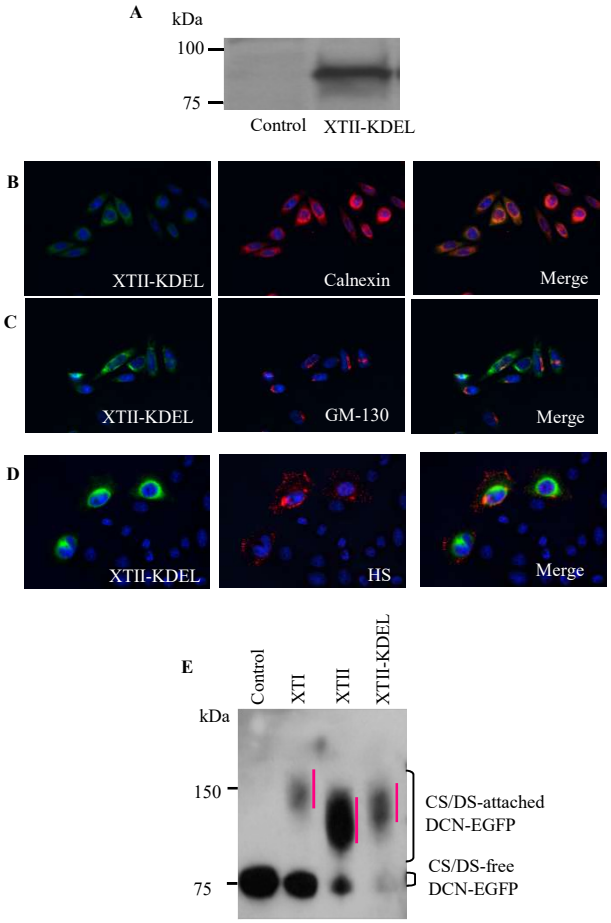

A
kDa
100
75
Control
XTII-KDEL
B
XTII-KDEL
Calnexin
Merge
C
XTII-KDEL
GM-130
Merge
D
XTII-KDEL
HS
Merge
E
Control
XTI
XTII
XTII-KDEL
kDa
150
75
CS/DS-attached
DCN-EGFP
CS/DS-free
DCN-EGFP

Figure 5

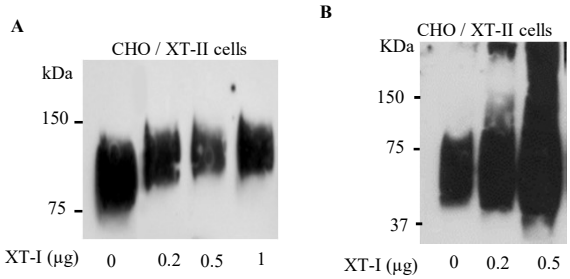

A
CHO / XT-II cells
kDa
150
75
XT-I (µg) 0 0.2 0.5 1
B
CHO / XT-II cells
KDa
150
75
37
XT-I (µg) 0 0.2 0.5

Figure 6

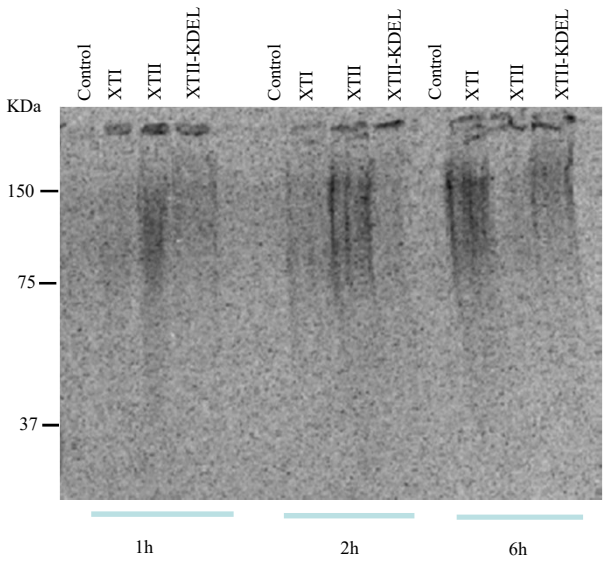

Control
XTI
XTII
XTII-KDEL
Control
XTI
XTII
XTII-KDEL
Control
XTI
XTII
XTII-KDEL
KDa
150
75
37
1h
2h
6h

Figure 7

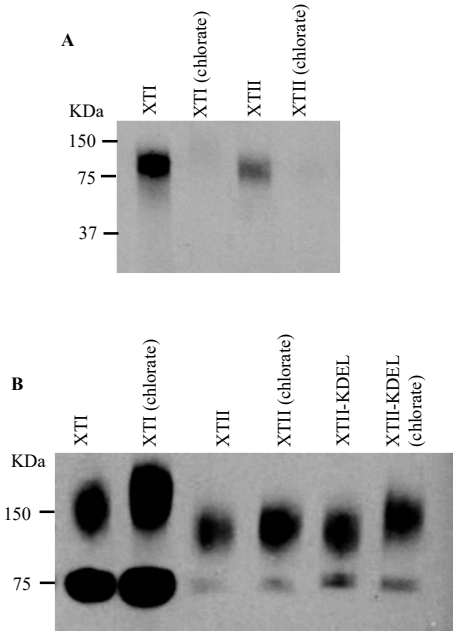

A
KDa
XTI
XTI (chlorate)
XTII
XTII (chlorate)
150
75
37
B
XTI
XTI (chlorate)
XTII
XTII (chlorate)
XTII-KDEL
XTII-KDEL (chlorate)
KDa
150
75

Figure 8

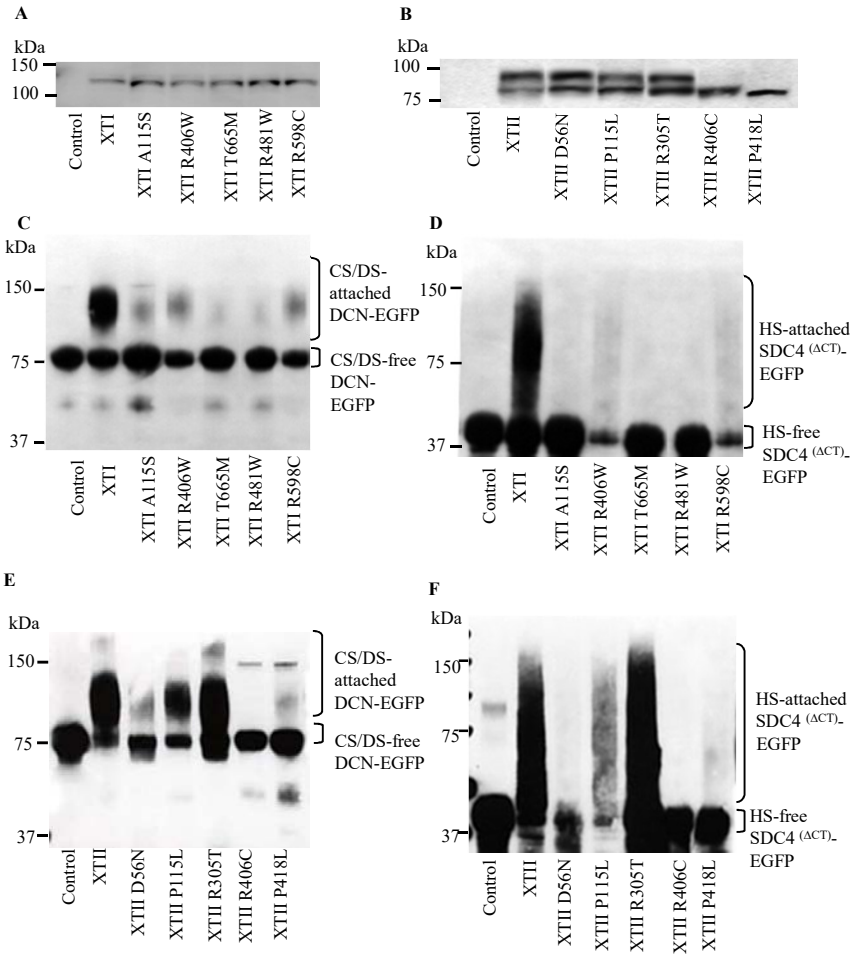

A
kDa
150
100
Control
XTI
XTI A115S
XTI R406W
XTI T665M
XTI R481W
XTI R598C
B
kDa
100
75
Control
XTII
XTII D56N
XTII P115L
XTII R305T
XTII R406C
XTII P418L
C
kDa
150
75
37
CS/DS-attached DCN-EGFP
CS/DS-free DCN-EGFP
Control
XTI
XTI A115S
XTI R406W
XTI T665M
XTI R481W
XTI R598C
D
kDa
150
75
37
HS-attached SDC4 (ΔCT)-EGFP
HS-free SDC4 (ΔCT)-EGFP
Control
XTI
XTI A115S
XTI R406W
XTI T665M
XTI R481W
XTI R598C
E
kDa
150
75
37
CS/DS-attached DCN-EGFP
CS/DS-free DCN-EGFP
Control
XTII
XTII D56N
XTII P115L
XTII R305T
XTII R406C
XTII P418L
F
kDa
150
75
37
HS-attached SDC4 (ΔCT)-EGFP
HS-free SDC4 (ΔCT)-EGFP
Control
XTII
XTII D56N
XTII P115L
XTII R305T
XTII R406C
XTII P418L

Figure 9

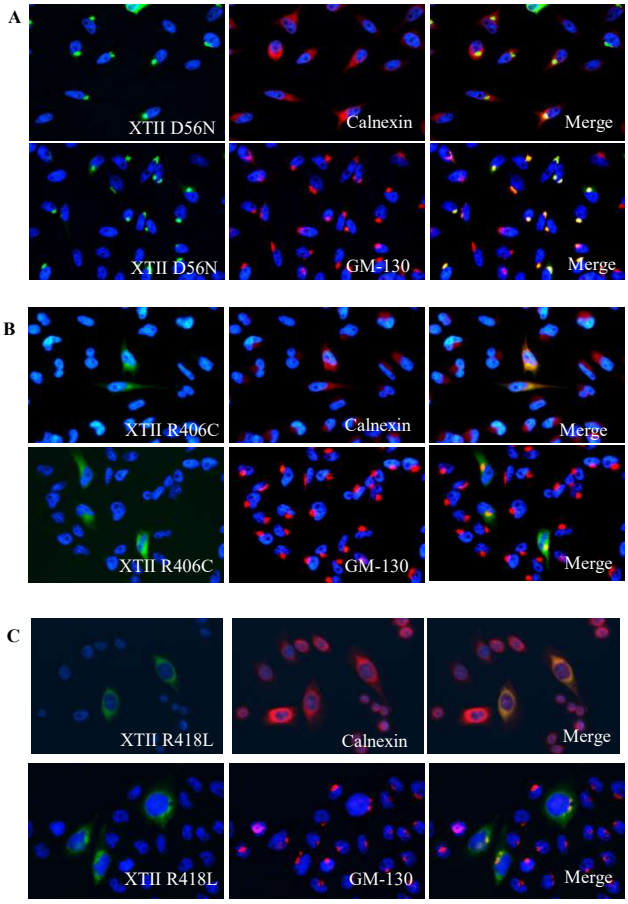
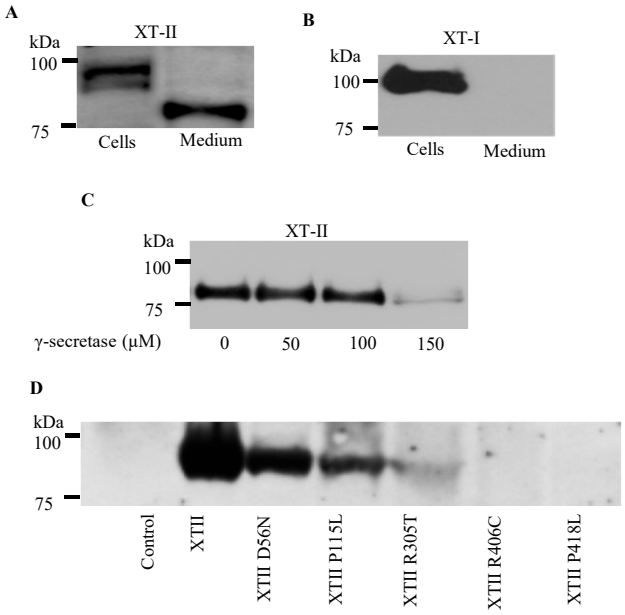

A
XTII D56N
Calnexin
Merge
XTII D56N
GM-130
Merge
B
XTII R406C
Calnexin
Merge
XTII R406C
GM-130
Merge
C
XTII R418L
Calnexin
Merge
XTII R418L
GM-130
Merge

Figure 10


A
XT-II
kDa
100
75
Cells
Medium
B
XT-I
kDa
100
75
Cells
Medium
C
XT-II
kDa
100
75
γ-secretase (μM)
0
50
100
150
D
kDa
100
75
Control
XTII
XTII D56N
XTII P115L
XTII R305T
XTII R406C
XTII P418L

Publications No 2

Fam20B negatively regulates proteoglycan synthesis by suppressing glycosaminoglycan chain formation

Irfan Shaukat, Lydia Barré, Sylvie-Fournel-Gigleux and Mohamed Ouzzine*

UMR7365 CNRS-Université de Lorraine, Biopôle, Faculté de Médecine, CS 50184, 54505 Vandoeuvre-lès-Nancy Cedex, France

*Corresponding author:

E-mail address: Mohamed.ouzzine@univ-lorraine.fr

Tel.: +33 383 685 427; fax: +33 383 685 409

ABSTRACT

Heparan-sulfate (HS) and chondroitin-sulfate (CS) proteoglycans (PGs) are essential regulators of many biological processes including cell differentiation, signalisation and proliferation. PGs interact, mainly via their glycosaminoglycan (GAG) chains, with a large number of ligands including growth factors, enzymes and extracellular matrix components, thereby modulating their biological activities. HSPGs and CSPGs share a common tetrasaccharide linker region, which undergoes modifications particularly phosphorylation of the xylose residue by the kinase Fam20B. Here, we demonstrated that Fam20B gain-of-function suppressed the synthesis of both CS- and HS-attached PGs and that mutation of Fam20B aspartic residues D289 and D309 abolished its ability to suppress PG-GAG chain synthesis. In contrast, knockdown of Fam20B stimulated the synthesis process. Noteworthy, Fam20B is able to supress GAG chain synthesis primed by the xyloside analog 4-Methylumbelliferyl-β-D-xylopyranoside, suggesting that the presence of PG core protein is not required for its function. Furthermore, our results suggested that Fam20B acts following xylose attachment to the PG core protein before the addition of galactose residue by the β4GalT7 enzyme. Finally, we showed that Fam20B significantly decreased the proliferation of glioblastoma and chondrosarcoma cells and reduced their ability to migrate, suggesting that Fam20B may constitute a new target for cancer therapy.

Introduction

Proteoglycans (PGs) are complex macromolecules that are found on cell surface and in the extracellular matrix[1]. They are formed by the covalent attachment of one or more glycosaminoglycan (GAG) chains onto the core protein. PG-GAG chains interact with a large number of ligands including growth factors and morphogens and their receptors, and extracellular matrix structural molecules where they regulate activity, as well as ligand stability. PGs regulate several biological process including cell-cell and cell-matrix interactions, development, signaling, proliferation, differentiation and various pathological conditions such as inflammation, tumor progression and viral and bacterial infection[2-5].

Most commonly occurring PGs are chondroitin-sulphate PGs (CSPGs) and Heparan-sulphate PGs (HSPGs). These PGs share a common tetrasaccharide linker region (GlcAβ1-3Galβ1-3Galβ1-4Xyl-O-Ser) for the attachment of the GAG chain onto the PG core protein. The first step in the synthesis of the tetrasaccharide primer is the addition of xylose on specific serine residues of the core protein. This initial and limiting step in GAG synthesis is catalyzed by xylosyltransferase I and II[6-8]. Subsequently, two galactose residues are attached to xylose by β1,4-Galactosyltransferase 7 and β1,3-Galactosyltransferase 6 (β4GalT7 and β3GalT6), and one glucuronic acid by β1,3-Glucuronosyltransferase (GlcAT-I), therefore completing the synthesis of the terasaccharide primer. HS- and CS-GAG chains of PGs are built up on this linkage tetrasaccharide region by the alternate addition of *N*-acetylhexosamine and glucuronic acid residues[9]. The specificity of interaction between ligands and GAG chains is influenced by the fine structure of the GAG chain,

primarily its sulfation pattern[10]. The tetrasaccharide primer also undergoes various modifications including sulfation of galactose residues and phosphorylation of xylose[11,12].

Fam20 (family of sequence similarity 20) contains three members Fam20A, Fam20B and Fam20C[13]. Their function has recently been established[13,14]. The substrates for Fam20A are unknown; however, Fam20A is important for the enamel biomineralization and tooth eruption[15,16]. Mutations in Fam20A are associated with various tooth disorders named human amelogenesis imperfecta and gingival hyperplasia syndrome[17], and in some cases the renal calcification are also involved along with tooth disorders such as in Enamel Renal Syndrome[15,18]. Fam20C is a Golgi casein kinase and is mainly expressed in the biomineralized tissues. The mutations in Fam20C are associated with Raine syndrome, characterized by a lethal osteosclerotic bone dysplasia[19,20]. Recently, Fam20C from the *C. Elegans* (ceFam20C) have been crystallized [21]. The 3D structure revealed the presence of protein kinase-like fold with five disulfide and two Asparagine residues for N-linked glycosylation. The ceFam20C also contains a DFG (Asp-Phe-Gly) variant motif, in which the aspartate residue Asp^{387} co-ordinates the divalent cation required for catalysis and a catalytic segment that includes the putative catalytic aspartate residue, Asp^{366}. The Asp^{387} and Asp^{366} residues are conserved in all the Fam20 family[21].

Fam20B is a kinase that phosphorylates the xylose in the tetrasaccharide linkage region of PGs[22,23]. Recently, studies in HeLa cells suggested that Fam20B is a positive regulator of HS and CS synthesis[22,23]. In contrast, it has been shown that loss-of-function of XYLP, the 2-phosphoxylose phosphatase that de-phosphorylates xylose of PG linker region, decreased

HS and CS synthesis and inversely, gain-of-function increased their synthesis[24]. Therefore, suggesting that Fam20B decreases HS and CS synthesis process.

In line with this, we have shown in a previous study that β4Gal7 which catalyses the addition of galactose residue on xylose was unable to use phosphorylated xylose analog as substrate[11]. This, suggested that phosphorylation of xylose may prevent the attachment of galactose to the xylose residue of the core protein leading to premature termination of the synthesis of the tetrasaccharide primer and subsequent elongation of the GAG chain.

Here, we bring evidence that Fam20B negatively regulates PG synthesis by suppressing the synthesis of their GAG chains. We demonstrated by using CS and HS reporter PG core proteins and by analyzing the synthesis of endogenous PGs that Fam20B suppressed the synthesis of both CS- and HS-attached PGs. In addition, based on the crystal structure of ceFam20C, we showed that aspartic acid residues D289 and D309 are essentials for Fam20B suppression of the synthesis of CS and HS-attached PGs. Furthermore, we showed that Fam20B blocks the synthesis of PGs following xylose attachment to the PG core protein. Moreover, we found that Fam20B expression decreased proliferation and reduced migration of glioblastoma and chondrosarcoma cells.

Results

Fam20B suppresses the synthesis of GAG-attached PGs. Fam20B is a newly identified kinase that catalyses the 2-O-phosphorylation of xylose in the tetrasaccharide linkage region of PGs[22]. To analyze the effect of Fam20B on the synthesis of PGs, gain-of-function experiment were conducted in HEK293 cells. For this purposes, pCMV-Fam20B vector expressing human Fam20B

with a C-terminal Flag epitope tag was designed and used to transfect HEK293 cells. Western-blot analysis showed that cells transfected with pCMV-Fam20B efficiently expressed a polypeptide of about 46 kDa corresponding to Fam20B protein, which was absent in cells transfected with pCMV empty vector (Fig. 1a). Fam20B contains potential *N*-glycosylation sites. To test whether Fam20B is N-glycosylated, proteins from HEK293 cells expressing recombinant Fam20B were treated with the enzyme N-glycosidase F (PNGase) and analyzed by Western blot. Treatment with PNGase produced a decrease of about 2 kDa in the apparent molecular mass of Fam20B polypeptide (Fig. 1b), indicating that Fam20B is sensitive to PNGase and therefore is N-glycosylated.

Next, we analyzed the effect of Fam20B on PG synthesis. As determined by ^{35}S-sulfate incorporation, the level of PG synthesis was decreased by 75% in cells expressing Fam20B compared to control (Fig. 2a). This was confirmed by SDS-PAGE analysis of radiollabeled GAG chains of PGs which shows strong reduction (90%) in overall GAG chains produced in Fam20B expressing cells compared to control (Fig. 2b and 2c). These results indicated that Fam20B negatively regulates the synthesis of PGs.

Fam20B suppresses the synthesis of both CS- and HS-attached PGs. Given the fact that Fam20B modifies the xylose residue of the tetrasaccharide linker common to both CS and HS, we hypothesized that Fam20B may impact the synthesis of both HSPGs and CSPGs. To examine this hypothesis, we used decorin (DCN) which contains a single CS-attached site and syndecan 4 (SDC4) containing three HS-attached sites as reporter PG core proteins for the synthesis of CS and HS, respectively. pCMV-DCN-EGFP vector expressing human decorin core protein fused at the C-terminus with EGFP and pCMV- SDC4$^{(\Delta CT)}$-EGFP vector expressing human syndecan 4 core

protein, in which the transmembrane domain and the C-terminus were deleted and replaced by EGFP leading to the secretion in the cell culture medium of SDC4$^{(\Delta CT)}$-EGFP protein were designed and used to transfect HEK293 and CHO-K1 cells. Expression of DCN-EGFP and SDC4$^{(\Delta CT)}$-EGFP was analyzed by immunobloting in cell conditioned medium following immunoisolation with anti-EGFP column. Transfection of CHO-K1 cells with pCMV-DCN-EGFP resulted in the secretion in the medium of high amount of CS/DS-attached DCN-EGFP (Fig. 3a). However, when DCN-EGFP was co-expressed with Fam20B, the amount of GAG-containing DCN-EGFP in the medium was considerably reduced but not that of CS/DS-free DCN-EGFP (Fig. 3a). Similar results were observed when CPC method, which selectively precipitates GAG-attached PGs was used (Fig. 3b). To examine whether this process is cell type specific, similar experiments were conducted in HEK293 cells. As observed for CHO-K1 cells, transfection of HEK293 cells with pCMV-DCN-EGFP led to the secretion of CS/DS-attached DCN-EGFP (Fig. 3c), whereas coexpression of DCN-EGFP with Fam20B dramatically decreased the amount of CS/DS-processed DCN-EGFP secreted in the medium (Fig. 3c). These results indicated that Fam20B blocks the synthesis of CS/DS-attached decorin.

We next tested whether Fam20B produced similar inhibitory effect on the synthesis of HS-attached PGs, as we observed for CSPGs. For these purposes, we used SDC4$^{(\Delta CT)}$-EGFP, a secreted form of SDC4 fused to EGFP as HSPG reporter core protein. Expression of SDC4$^{(\Delta CT)}$-EGFP was carried out in both CHO-K1 and HEK293 cells. SDC4$^{(\Delta CT)}$-EGFP was immunoisolated from CHO-K1 cells conditioned medium using anti-EGFP column and analyzed by immunoblot. Expression of SDC4$^{(\Delta CT)}$-EGFP resulted in the secretion in the medium of high amount of HS-attached SDC4$^{(\Delta CT)}$-EGFP (Fig. 4a). However, co-expression with Fam20B suppressed the production of HS-attached SDC4$^{(\Delta CT)}$-EGFP, but not that of HS-free SDC4$^{(\Delta CT)}$-EGFP (Fig. 4a). Similar results

were observed when HS-attached SDC4$^{(\Delta CT)}$-EGFP was selectively isolated by CPC precipitation method (Fig. 4b). These results were further confirmed in HEK293 cells. Expression of SDC4$^{(\Delta CT)}$-EGFP in HEK293 cells produced high amount of HS-attached SDC4$^{(\Delta CT)}$-EGFP in the medium (Fig. 4c), while co-expression of SDC4$^{(\Delta CT)}$-EGFP with Fam20B dramatically reduced the amount of HS-attached SDC4$^{(\Delta CT)}$-EGFP in the medium (Fig. 4c), indicating that Fam20B suppresses the synthesis of HS-attached SDC4$^{(\Delta CT)}$-EGFP. Altogether, these results demonstrated that Fam20B blocks the synthesis of PGs of both type, CS and HS.

To further confirm these results, we studied the effect of Fam20B expression on the synthesis of endogenous decorin in human primary skin fibroblasts and lung fibroblast cell line A549 which produce and secrete high amount of CS/DS-attached decorin in the medium. As expected, CPC precipitation of PGs from conditioned medium of human primary skin fibroblasts and lung fibroblast cells A549 showed high amount of CS/DS-attached decorin, as revealed by immunobloting using anti-decorin antibodies (Fig. 5a and 5c, respectively). However, transfection with Fam20B expression vector led to a decrease of about 90% and 80% of CS/DS-attached decorin in the medium of human primary skin fibroblasts (Fig. 5a and 5b) and lung fibroblast cells A549 (Fig. 5c and 5d), respectively compared to control. These results clearly showed that Fam20B suppresses the synthesis of CS/DS-attached decorin.

Cell surface HSPGs are important for many vital cell-signaling processes[3-5]. To further examine the effect of Fam20B on the expression of cell surface HSPG, we carried out indirect immunofluorescence analysis of the CHO-K1 cells, using anti-HS monoclonal antibody 10E4, which is commonly used to detect HS chains of PGs[25-27]. Prominent staining of the cell membrane was observed in CHO-K1 cells (Fig. 6a), whereas no or very low signal could be observed in cells transfected with Fam20B expression vector (Fig. 6b). When recombinant cells were probed with

anti-Flag antibodies, efficient expression of Fam20B-Flag was revealed (Fig. 6b), whereas cells transfected with pCMV (control) showed no staining (Fig. 6a). Noteworthy, when cells express Fam20B, no staining for cell surface HSPG was observed (Fig 6b, Merge). These data indicated that Fam20B blocks the synthesis of endogenous cell surface HSPGs.

Fam20B knockdown increased PG synthesis. We showed above that Fam20B gain-of-function suppresses the synthesis of PGs, we then hypothesized that the knockdown of Fam20B may lead to increased PG synthesis. We therefore generated a HEK293 cell line stably expressing a shRNA to Fam20B, shRNA-Fam20B. As determined by RT-qPCR, the expression level of Fam20B was reduced by about 90% in Fam20B knockdown HEK293 cells, compared to control HEK293 cells that stably express an shRNA-control (Fig. 7a), indicating that Fam20B was efficiently knockdown in shRNA-Fam20B expressing cells. We then measured the level of PG synthesis using ^{35}S-sulfate incorporation. The results showed an increase of about 44% in Fam20B knockdown cells compared to control cells (Fig. 7b). This was confirmed by SDS-PAGE analysis of radiollabeled PG-GAG chains which showed a significant increase in overall PG-GAG chains produced in shRNA-Fam20B expressing cells, compared to control (Fig. 7c and 7d). Next, we investigated whether Fam20B knockdown affected the synthesis of CS- and HS-attached PGs, using DCN-EGFP and SDC4$^{(\Delta CT)}$-EGFP as CS and HS reporter PG core proteins. Analysis of GAG-attached DCN-EGFP showed that Fam20B knockdown cells produced a significant increase (2-fold) of CS/DS-containing DCN-EGFP, compared to control (Fig. 7e and 7f). Similarly, the knockdown of Fam20B led to an increase of about 2-fold in the synthesis of HS-attached SDC4$^{(\Delta CT)}$-EGFP (Fig. 7g and 7h), indicating that Fam20B negatively regulates the synthesis of both CS- and HS-attached PGs. Altogether, gain- and loss-of-function experiments indicated that

Fam20B is a negative regulator of PG synthesis.

Fam20B is able to suppress GAG chain synthesis primed in the absence of PG core protein. The GAG chain synthesis process is initiated by the attachment of xylose to specific serine residues of the core protein. However, it is well known that xyloside analogs can function as GAG chain initiators without the presence of PG core protein provided that xylosides carry a hydrophobic group[28-30]. To determine whether Fam20B is able to block GAG chain synthesis in the absence of PG core protein, we analyzed its effect on the synthesis of GAG chains primed with the xyloside analog 4-Methylumbelliferyl-β-D-xylopyranoside in HEK293 and CHO-K1 cell lines. Primed GAGs were metabolically labelled with ^{35}S-sulfate incorporation and isolated by CPC precipitation then analyzed by SDS-PAGE. As shown in figure 8, HEK293 cells (Fig. 8a) as well as CHO-K1 cells (Fig. 8b) produced high amount of primed GAGs in the medium. Interestingly, expression of Fam20B strongly impaired this process. Indeed, the amount of primed GAG chains produced in the medium was reduced by about 80% in HEK293 (Fig. 8a and 8c) and by about 85% in CHO-K1 cells expressing Fam20B ((Fig. 8b and 8c), indicating that Fam20B is able to block the synthesis of GAG chains primed with the xyloside analog 4-Methylumbelliferyl-β-D-xylopyranoside. These results indicate that the presence of PG core protein is not required for Fam20B function.

Aspartic acid residues in catalytic domain and DFG motif are essential for Fam20B activity. Based on the structure/function studies and 3D structure analysis of *C. Elegans* Fam20C (ceFam20C), it has been shown that the aspartic residue of the ^{387}DHG^{389} sequence, a variant of the DFG motif present in canonical protein kinases which co-ordinates Mn^{2+} cation and the

putative catalytic aspartic residue present in the catalytic segment ^{366}DRHHYE^{371} are essential for ceFam20C activity[21]. The corresponding aspartic residues are present in the human Fam20B and are Asp^{309} and Asp^{289}, respectively. We therefore analyzed the effect of the mutation of these residues on human Fam20B activity. To this end, Asp^{309} to alanine (D309A) and Asp^{289} to Alanine (D289A) mutants of Fam20B were engineered and expressed in CHO-K1 cells. Western blot analysis showed that Fam20B^{D309A} and Fam20B^{D289A} mutants were expressed in a similar amount as wild-type Fam20B protein (Fig. 9a). To determine whether the D309A and D289A mutations impair Fam20B activity, DCN-EGFP and SDC4(CT$^{\Delta}$)-EGFP were co-expressed with either wild-type Fam20B or with the mutants Fam20B^{D309A} and Fam20B^{D289A}, respectively and GAG-attached DCN-EGFP and SDC4$^{(\Delta CT)}$-EGFP produced in the medium were analyzed by immunoblot (Fig. 9b and 9c). In contrast to wild-type Fam20B, co-expression with the mutants Fam20B^{D309A} and Fam20B^{D289A} did not suppress the synthesis of either CS/DS-attached DCN-EGFP (Fig. 9b) nor that of HS-attached SDC4(CT$^{\Delta}$)-EGFP (Fig. 9c). Indeed, high amount of CS/DS-containing DCN and HS-attached SDC4 was produced in the presence of Fam20B^{D309A} and Fam20B^{D289A}, respectively indicating that mutation of Asp^{309} and Asp^{289} to alanine abolished the ability of Fam20B to suppress PG-GAG synthesis and therefore impair the activity of Fam20B. To further confirm this finding, the mutants Fam20B^{D289A}, pCMV-Fam20B^{D309A} were transfected along with wild-type Fam20B into HEK293 cells and neosynthesized PG-GAG chains were radilolabeled using ^{35}S-sulfate incorporation. SDS-PAGE analysis of radiolabeled PG-GAG chains produced by Fam20B^{D289A} and pCMV-Fam20B^{D309A} expressing cells showed similar pattern as in the control (Fig. 9d), whereas cell expressing wild-type Fam20B presented strong

reduction (90%) in overall GAG chains produced (Fig. 9d and 9e). We next analyzed the effect of Fam20B mutations on the synthesis of decorin in human lung cancer cell line A549 which abundantly produced this PG in the medium. Immunoblot analysis of decorin from culture supernatants of lung fibroblast cells expressing Fam20B^{D289A} and pCMV-Fam20B^{D309A} mutants showed high amount of CS/DS-attached decorin (Fig. 9f), as in control cells. However, the amount of CS/DS-attached decorin produced by cells expressing wild-type Fam20B was decreased by about 80% (Fig. 9f and 9g). These results showed that Fam20B^{D289A}, pCMV-Fam20B^{D309A} mutants did not suppress the synthesis of endogenous CS/DS-attached decorin in lung fibroblasts as wild-type Fam20B does. Thus, these results clearly demonstrated that expression of an altered form of Fam20B did not alter the synthesis of GAG-attached PGs, therefore confirming that Fam20B is a negative regulator of PG synthesis.

Fam20B suppresses PG synthesis following xylose attachment to PG core protein. To determine at which step of the GAG biosynthesis pathway Fam20B suppressed PG synthesis, we took advantage of CHO pgsB618 cells deficient for β4GalT7 enzyme. These cells initiates GAG synthesis by catalyzing the transfer of xylose residues on the PG core protein, but they are not able to catalyse the second step which consist in the addition of galactose on the xylose residue, therefore precluding the formation of completed tetrasaccharide primer and subsequent elongation of PG-GAG chain. Expression of DCN-EGFP and SDC4$^{(\Delta CT)}$-EGFP in CHO pgsB618 cells resulted in the synthesis in the culture medium of high amount of GAG chain-free DCN-EGFP (Fig. 10a) and SDC4$^{(\Delta CT)}$-EGFP (Fig. 10c), indicating that xylose-modified PGs are produced in the medium. Interestingly, when Fam20B is co-expressed the synthesis in the medium of GAG chain-free DCN-EGFP was reduced by about 90% (Fig. 10c and 10b). Similar results were

observed for and GAG chain-free SDC4$^{(\Delta CT)}$-EGFP (Fig. 10c and 10d), suggesting that phosphorylation of xylose strongly reduced the expression of PGs in the medium. To further demonstrate that this is linked to Fam20B activity, DCN-EGFP was co-expressed with Fam20B in the presence and absence of β4GalT7 in CHO pgsB618 cells. As shown in figure 10e, co-expression with Fam20B led to strong reduction in the amount of GAG chain-free DCN-EGFP produced in the medium, whereas co-expression with β4GalT7 restored the synthesis of GAG-attached decorin in the medium. Interestingly, co-expression of DCN-EGFP with both β4GalT7 and Fam20B supressed the synthesis of GAG-attached DCN-EGFP (Fig. 10e). This also produced significant reduction in the amount of GAG chain-free DCN-EGFP present in the medium (Fig. 10e). Altogether, these results suggest that phosphorylation of the xylose residue occurs following its attachment to the PG core protein and probably before the addition of galactose residue by the β4GalT7 enzyme. This impairs the secretion of the modified PG in the medium probably because of its degradation inside the cell.

Fam20B inhibits proliferation and migration of chondrosarcoma cells. Because PGs play an important role in cell migration and proliferation, we hypothesized that Fam20B-dependent inhibition of PG-GAG synthesis may affect these processes. To test this hypothesis, Fam20B was expressed in chondrosarcoma cells SW1353, a cartilage cancer cell line and in glioblastoma cell line T98G. Cell proliferation was measured using CyQUANT NF Cell Proliferation Assay Kit at 24 h and 48 h after transfection. As shown in figure 11a, glioblastoma cells transfected with Fam20B presented a significant reduction in cell proliferation and reached about 14% at 24 h and 28% at 48 h, compared to control. Similar results were observed for chondrosarcoma cells. Expression of Fam20B in chondrosarcoma

produced a reduction in cell proliferation of about 24% at 24 h and 25% at 48 h, compared to control (Fig. 11a). We next analyzed the ability of Fam20B-transfected cells to migrate using scratch wound-healing experiments and demonstrated that Fam20B expressing cells were impaired in their ability to migrate when compared to control cells (Fig. 11 b and c). The migration assays reveal a slower rate of cell migration by the Fam20B-transfected cells compared with control cells. Indeed, expression of Fam20B in glioblastoma cells reduced the number of cells that migrate in scratch area by about 36% at 6h and 53% at 24 h, compared to control (Fig. 11 b and c). Similarly, expression of Fam20B in chondrosarcoma cells resulted in a reduction in the number of cells that migrate in scratch area by about 46% at 6 h and 57% at 24 h, compared to control cells (Fig. 11 d and e). Therefore, the wound closure was delayed in Fam20B-transfected cells. The control cells had closed the wound by 24 h, whereas the Fam20B-transfected cells had not (Fig. 11c). These results support that Fam20B-dependant inhibition of PG-GAG synthesis impairs cell proliferation and migration, therefore confirming a role for GAGs in the wound repair process.

Discussion

In this study we have demonstrated that Fam20B negatively regulates PG synthesis. Gain-of-function experiments showed that Fam20B induced a strong reduction in overall PG-GAG chains produced in the cell culture medium, whereas loss-of-function increased the level of PG-GAGs produced. We further bring evidence that Fam20B negatively regulates the synthesis of both CS- and HS-attached PGs by using decorin and syndecan 4 as reporter proteins for CS and HS-attached PGs, respectively. We showed that Fam20B suppressed the synthesis in the medium

of both CS/DS-attached DCN-EGFP and HS-attached SDC4$^{(\Delta CT)}$-EGFP in CHO-K1 and HEK293 cells, whereas the knockdown of Fam20 led to an increase in the level of these PGs in the medium. This has been further confirmed using human skin and lung fibroblasts expressing high amount of endogenous decorin in the medium. Again, expression of Fam20B blocks the synthesis of decorin in both skin and lung fibroblast cells. Similar results were obtained for endogenous HSPGs. Indeed, by using anti-HS 10E antibody which is commonly used to detect HS chains of PGs [25-27], we showed that expression of Fam20B strongly attenuates the amount of cell surface HSPGs. Altogether, these data clearly demonstrate that Fam20B negatively regulates the synthesis of PGs of both types CS and HS. As the synthesis of CS and HS GAGs share a common tetrasaccharide primer, blocking of any step in the synthesis of this primer will obviously impact the synthesis of both CS and HS. Our results are in agreement with the recent study in which overexpression of the xylose phosphatase, XYLP that dephosphotylates xylose increased PG synthesis for both CSPG and HSPG in Hela cells, whereas the knockdown of the XYLP reduced the synthesis of both types of PGs[24]. In contrast to this, it has been previously reported that stable expression of Fam20B in Hela cells enhanced PG-GAG synthesis[22]. This raises the question whether Fam20B function in cell type specific manner. However, in this study we have used several cell lines as well as primary fibroblast cells and found that Fam20B blocks CSPG and HSPG synthesis in all the cells tested.

In agreement with this, in a previous study we have reported using synthetic xyloside analogs that β4GalT7 efficiently catalyzes the transfer of galactose residue onto the nonphosphorylated xyloside analogs, whereas the phosphorylated analog at position 2-O was not substrate, suggesting that the 2-O phosphorylation precludes the transfer of the galactose on xylose[11]. In line with this, Siegbahn et al., showed recently that most modifications of position 2 in xylose, rendered analogs

less prone to galactosylation by β4GalT7 [31]. The same authors have shown previously that xylose analogs carrying modification on the 2-O position were not able to prime GAG synthesis in human cell lines[32]. These data indicate that the hydroxyl in position 2 might act as a hydrogen bond acceptor. The crystal structure of the β4GalT7 has been published recently and revealed that the Tyr^{177}, Tyr^{179}, Trp^{207}, and Leu^{209} are important for the hydrophobic binding of the xylose and that the Asp^{211} forms a strong hydrogen bond with the OH present in the 4^{th} position of the acceptor xylose. Whereas, the Asp^{212} interacts via a hydrogen bond with the OH present at 2^{nd} position of the xylose [33]. We therefore can speculate that phosphorylation of the xylose at 2-O position may alter this interaction or impair other essential interactions.

All the members of the Fam20 contain a conserved C-terminal domain including the catalytic domain DRHHYE and a DFG motif which is crucial for the metal ion binding. It has been shown that mutation of the aspartic acid residues present in the catalytic segment and in the DFG motif of Fam20C abolished the enzyme activity[20]. These aspartic acid residues are conserved in all members of the Fam20 family and correspond to Asp^{289} and Asp^{309} of the human Fam20B. Mutation of either of the two aspartic residues to alanine abolished the ability of Fam20B to block the synthesis of both CS- and HS-attached PGs, suggesting that mutation of Asp^{289} and Asp^{309} impaired Fam20B activity, consistent with the putative role of theses residues in catalysis and in the binding of the divalent cation Mn^{2+}, respectively. These results also confirm that Fam20B negatively regulates PG synthesis.

It is well known that the biosynthesis of GAG chains can also be initiated in the absence of a core protein by xyloside analogs carrying a hydrophobic aglycon, such as 4-

Methylumbelliferyl-β-D-xylopyranoside. The xyloside can, when exogenously supplied to cells, act as acceptor substrate for β4GalT7, then elongated by other glycosyltransferases leading to the production in the medium of xyloside-primed GAG chains. We used this model system for GAG synthesis and showed that Fam20B was able to block the synthesis of GAG chains primed with Methylumbelliferyl-β-D-xylopyranoside, indicating that Fam20B does not require the presence of PG core protein. In a similar manner β4GalT7 enzyme does not require the presence of PG core protein to catalyse the transfer of the galacose residue on the xylose analogs such as 4Methylumbelliferyl-β-D-xylopyranoside, suggesting that the substrate for both enzymes is probably restricted to the xylose residue or that the hydrophobic aglycon may play some role but this needs further investigation.

On the other hand, it has been reported that, *in vitro*, EXTL2 transfer the GlcNAc residue on the tetrasaccharide when phosphorylated by Fam20B and this phosphorylated pentasaccharide is not used for HS chain elongation by HS polymerase and therefore terminates GAG elongation[24]. However, Katta et al., reported that overexpression of EXTL2 in HEK293 cells did not affect the synthesis of PG-GAGs and showed that this is not due to lack of Fam20B in the cell line[34]. In addition, our study strongly suggested that Fam20B acts immediately following the addition of xylose residue to block the synthesis of PG-GAG chains. This was supported by the facts that in CHO pgsB618 cells deficient for β4GalT7, xyloside-modified decorin and syndecan 4 were produced in the medium, whereas in the presence of Fam20B their level was strongly reduced, suggesting that following Fam20B modification they are degraded inside the cells. We showed that this process was dependent on an active Fam20B enzyme. In addition, given that pgsB618 cells add only a xylose residue on PG core proteins, these results indicate that addition of only xylose on the core protein is sufficient for Fam20B to achieve

its activity and strongly suggest that Fam20B acts immediately following the addition of xylose residue to block the synthesis of PG-GAG chains and not after the formation of the tetrasaccharide linker.

Furthermore, we found that expression of Fam20B was not accompanied by an accumulation of a PG core protein in the medium, therefore strongly suggesting that phosphorylation of xylose residue by Fam20B led to the degradation of the phospho-xylose-modified PG. Indeed, expression of DEC-EGFP and SDC4$^{(\Delta CT)}$-EGFP resulted in the synthesis of both GAG-attached and GAG-free PGs (Fig. 3a and Fig. 4a). Synthesis of GAG-free PGs in the medium, which is due to the overexpression of the PG core protein leading to saturation of GAG synthesis pathway, was not impaired by Fam20B, indicating that the kinase acts only when the GAG chain synthesis is initiated on a PG core protein.

On the other hand, analysis of biological process including cell proliferation and migration indicated that both cell proliferation and migration were impaired in Fam20B-transfected cells. Expression of Fam20B in glioblastoma and chondrosarcoma cells led to a significant reduction in proliferation and in the ability of cells to migrate in scratch-wound healing assays. The importance of PGs and their GAG chains in cell proliferation and migration is well established[35] and numerous PGs have been implicated in tumor growth and metastasis[36]. Therefore, Fam20B-dependent inhibition of PG-GAG synthesis could contribute to the cell proliferation and migration defects in Fam20B-transfected chondrosarcoma cells.

Material and Methods

Cell lines and culture conditions. The Chinese hamster ovary cells (CHO-K1), CHO galactosyltransferase I deficient cell line (pgsB-618), human embryonic kidney cells (HEK293), human chondrosarcoma cells (SW1353), human glioblastoma cells (T98G), human lung adenocarcinoma cells (A549) and human primary skin fibroblasts were cultured in DMEM (4.5 mg/ml glucose) or DMEM-F12 medium supplemented with 2 mM glutamin, 100 IU/ml penicillin, 100 µg/ml streptomycin and 10% fetal bovine serum (FBS, GIBCO-Invitrogen, Cergy-Pontoise, France) at 37°C with humidified atmosphere in a 5% CO_2.

Vector constructions. Fam20B was amplified from human placenta cDNA library (Clontech) by PCR using 5'GAATTCCACCATGAAGCTAAAGCAGCGAGTCGTG3' (forward) including *EcoRI* site and 5'GGATCCTTACAAGTGTGAGAGAGCCATCCT3' (reverse) primers including *BamHI* site, using Advantage GC 2 Polymerase Mix (Clontech). The amplified product was ligated into pCR2.1-TOPO vector (Invitrogen). The coding region for Fam20B was excised and ligated into the pCMV vector (Stratagene) by double digestion with *EcoRI* and *BamHI* to generate pCMV-Fam20B.

The vectors pCMV-SDC4$^{(\Delta CT)}$-EGFP expressing syndecan-4 (deleted from the forty C-terminus residues) and pCMV-DCN-EGFP expressing decorin in fusion with EGFP were obtained following PCR amplification of DCN and SDC4 cDNAs from placenta Quick-Clone cDNA using 5' primer containing *XhoI* site, the sequence encoding the first eight N-terminal residues of the protein and a 3' primer containing a *BamHI* site and the sequence encoding for the last eight C-terminal amino acids. The amplified fragments were inserted into *XhoI-BamHI* sites in frame with the sequence encoding EGFP protein

in the pEGFP-C2 (Clontech).

The shRNA to Fam20B was generated using 5'TCTCCCTTTCACTTGGACAGGATTCT TCTTGTCAAATCGTGTCCA3' (forward) and 5'CTGCAGGCCTTTCACTTGGACAGG ATTTGACAGGAAGAATCCTGT3' (reverse) primers cloned into the pGeneClip™ Vector using GeneClip™ U1 Hairpin Cloning Systems (Promega), according to manufacturer instructions. Briefly, the primers were annealed by heating at 90°C for 3 min and incubation at 37°C for 15 min. The annealed hairpin oligonucleotides were then ligated into the pGeneClip™ vector to generate pGeneClip™-shRNA-Fam20B. The vector was verified by sequencing. pGeneClip™-shRNA-control vector was used to generate cells stably expressing shRNA-control.

Stable expression of shRNA-Fam20B. HEK293 cells were transfected with pGeneClip™-shRNA-Fam20B vector and cultured in medium containing G418 (Geneticin) to select clones that stably express the shRNA-Fam20B. The inhibition of Fam20B in selected clones was confirmed by qPCR. The clones that exhibited more than 90% inhibition in the expression of Fam20B were selected for further experiments.

Site-directed mutagenesis. Site directed mutagenesis of the residues Asp289 to Ala289 and Asp309 to Ala309 in Fam20B were performed using the QuickChange site-directed mutagenesis kit (Stratagene) according to the recommendations of the manufacturer. pCMV-Fam20B expression vector was used as template. Sense and antisense oligonucleotides introducing the desired mutations were for D289A: 5'CTGATTGGCAA TGCTGCCCGCATCACTATGAG3' (forward) and 5'CTCATAGTGATGGCGGGC AGC

ATTGCCAATCAG3' (reverse) and for D309A: 5'TGCTCATCCTTCTTGCTAATGCCAA AAGCTTT GG3' (forward) and 5'CCAAAGCTTTTGGCATTAGCAAGAAGGATGAGC A3' (reverse). Full length mutated cDNA Fam20B^{D289A} and Fam20B^{D309A} were checked by DNA sequencing.

Cell transfection. Cells were seeded in 6-well culture plates and transfected at 80% confluency with 1 µg of either pCMV-DCN-EGFP or pCMV-SDC4$^{(\Delta CT)}$-EGFP in combination with 1 µg pCMV-Fam20B, pCMV-Fam20B^{D289A}, pCMV-Fam20B^{D309A} or native pCMV (control) using Exgen 500 reagent (Euromedex, Souffelweihersheim, France) according to the manufacturer's instructions.

Immunopurification of DCN-EGFP and SDC4$^{(\Delta CT)}$-EGFP. Conditioned media from recombinant cells were collected at 48 h post-transfection and DCN-EGFP and SDC4$^{(\Delta CT)}$-EGFP PGs were immunopurified using GFP purification kit (µMACS, Miltenyi Biotec). Briefly, conditioned medium was mixed with 50 µl of anti-GFP magnetic beads and incubated for 30 min on ice. The mixture was applied onto the column and washed four times with 200 µl of buffer A (150 mM NaCl, 1% NP-40, 0.5% sodium deoxycholate, 0.1% SDS, 50 mM Tris HC1, pH 8.0) and once with 100 µl of buffer B (20 mM Tris HC1, pH 7.5) then eluted with 50 µl of elution buffer (50 mM DTT, 1% SDS, 1 mM EDTA, 0.005% bromophenol blue, 10% glycerol, 50 mM Tris HC1, pH 6.8), pre-heated at 95°C and analyzed by western blot.

N-glycosylation analysis. Cells were grown in 6-well culture plate at 80% confluency

then transfected with Flag-tagged Fam20B. At 24 h post-transfection the cells were lysed in the HEPES buffer and protein concentration was measured by the Bradford method[37]. Twenty µg of protein was digested with PNGase F (New England Biolabs), which cleaves asparagine-linked (N-linked) oligosaccharides, according the manufacturer's instructions.

Western blot analysis. Proteins (30µg) from cell lysates and from cell culture supernatants were separated by SDS-PAGE and transferred onto the PVDF membrane (Millipore). The membrane was blocked with 5 % skimmed milk for 1 h and incubated with primary antibodies anti-GFP antibody (1:1000) (Cell Signaling), anti-decorin antibody (1:1000) (R&D) or anti-FLAG M2 antibody (1:1000) (Sigma) overnight at 4°C followed by incubation with horseradish-peroxidase-conjugated secondary antibodies. The reactive bands were detected by chemiluminescence using clarity™ western ECL substrate (BioRad)

Metabolic labelling of GAG chains. Metabolic labelling of PG-GAG chains was carried out using ^{35}S-sulfate incorporation method as described by De Vries et al, [38]. Briefly, cells were grown in 6-well culture plate and transfected with pCMV-Fam20B, pCMV-Fam20B^{D289A}, pCMV-Fam20B^{D309A}, pCMV, pGeneClip™-shRNA-Fam20B or pGeneClip™-shRNA-control. Cells were then radiolabeled with 10 µCi/ml of ^{35}S-sulfate (Perkin Elmer) in sulfate free media containing 2% dialyzed FBS. In the case of GAG chains primed by the xyloside analog 4-methylumbelliferyl-β-D-xylopyranoside, cells were incubated with 100 µM of the 4-methylumbelliferyl-β-D-xylopyranoside in the presence of 10 µCi/ml of ^{35}S-sulfate. After 24 h, the culture medium was collected,

digested with papain (1 mg/ml) and ^{35}S-labeled GAGs were precipitated by cetylpyridinium chloride (CPC) as described by Bronson et al[39]. The CPC precipitated radiolabeled GAGs were separated by SDS-PAGE on a 4-12% Nu-PAGE gel. The gel was dried and exposed to autoradiography film. For CPC precipitation of DCN-EGFP and SDC4$^{(\Delta CT)}$-EGFP from culture medium, the culture supernatants were not digested by papain.

Immunofluorescence. Briefly, cells were grown on glass coverslips and fixed with 3% (w/v) paraformaldehyde in PBS for 20 min. Cells were permeabilized by treatment with 0.1% (w/v) Triton X-100/PBS solution for 4 min. After saturation in 0.2% (w/v) fish skin gelatin in PBS. Cells were then incubated with 10E4 monoclonal anti-HS antibodies (AMSBIO) diluted 1:100 in PBS/0.2% gelatin) for 20 min. Cover slips were washed several times and incubated with secondary antibody (anti-mouse IgG coupled with Alexa Fluor 488, Molecular Probes) diluted 1:200 in PBS/0.2% gelatin for 20 min. Nuclei were stained with Hoechst/PBS solutions and coverslips were mounted with Moviol (National Diagnostics, U.K.) containing 1% propylgallate (Sigma). Digital images were captured with an inverted microscope Lieca DMI3000 B (Leica Microsystems, Germany).

Cell migration assay. Cell migration was measured using scratch wound healing assay (ibidi) according to manufacture instructions. Briefly, cells were seeded at 2.5x10^4 cells by side on both sides of the chamber then transfected with pCMV or pCMV-Fam20B. At 24 h post-transfection the scratch was removed and cell migration in scratch area was monitored by microscope. Cells migrated in the scratch area for a given time were counted

and shown in the bar graph.

Cell proliferation assay. Cell proliferation was measured using CyQUANT NF Cell Proliferation Assay Kit (Thermo Scientific) according to manufacture instructions. Briefly, cells were seeded in 96 well plates at $2x10^4$ cells/well and transfected with pCMV or pCMV-Fam20B vector. At 24 h and 48 h post-transfection cells were labelled with DNA binding dye for 1 h at 37°C and fluorescence of each sample was measured using the microplate reader Varioskan Flash Multimode reader (Fisher Scientific) with excitation at 485 nm and emission detection at 530 nm.

Statistical analysis. The results are presented as mean ± SD of three independent experiments. Statistical differences between control and treated groups were evaluated using Student's test. A two-sided P-value <0.05 was considered statistically significant for all analysis.

References

1 Perrimon, N. & Bernfield, M. Specificities of heparan sulphate proteoglycans in developmental processes. *Nature* **404**, 725-728 (2000).

2 Gesslbauer, B., Theuer, M., Schweiger, D., Adage, T. & Kungl, A. J. New targets for glycosaminoglycans and glycosaminoglycans as novel targets. *Expert Review of Proteomics* **10**, 77-95 (2013).

3 Couchman, J. R. Transmembrane Signaling Proteoglycans. *Annual Review of Cell and Developmental Biology* **26**, 89-114, doi:doi:10.1146/annurev-cellbio-100109-104126 (2010).

4 Manon-Jensen, T., Itoh, Y. & Couchman, J. R. Proteoglycans in health and disease: The multiple roles of syndecan shedding. *FEBS Journal* **277**, 3876-3889 (2010).

5 Li, L., Ly, M. & Linhardt, R. J. Proteoglycan sequence. *Molecular BioSystems* **8**, 1613-1625, doi:10.1039/c2mb25021g (2012).

6 Venkatesan, N. *et al.* Modulation of xylosyltransferase i expression provides a mechanism regulating glycosaminoglycan chain synthesis during cartilage destruction and repair. *FASEB Journal* **23**, 813-822 (2009).

7 Venkatesan, N. *et al.* Xylosyltransferase-I Regulates Glycosaminoglycan Synthesis during the Pathogenic Process of Human Osteoarthritis. *PLoS ONE* **7**, e34020 (2012).

8 Khair, M. *et al.* Regulation of Xylosyltransferase I Gene Expression by Interleukin 1β in Human Primary Chondrocyte Cells MECHANISM AND IMPACT ON PROTEOGLYCAN SYNTHESIS. *Journal of Biological Chemistry* **288**, 1774-1784 (2013).

9 Breton, C., Fournel-Gigleux, S. & Palcic, M. M. Recent structures, evolution and mechanisms of glycosyltransferases. *Current Opinion in Structural Biology* **22**, 540-549 (2012).

10 Habuchi, H., Habuchi, O. & Kimata, K. Sulfation pattern in glycosaminoglycan: does it have a code? *Glycoconjugate journal* **21**, 47-52 (2004).

11 Gulberti, S. *et al.* Phosphorylation and sulfation of oligosaccharide substrates critically influence the activity of human β1,4-galactosyltransferase 7 (GalT-I) and β1,3-glucuronosyltransferase I (GlcAT-I) involved in the biosynthesis of the glycosaminoglycan-protein linkage region of proteoglycans. *Journal of Biological Chemistry* **280**, 1417-1425 (2005).

12 Gulberti, S. *et al.* Modifications of the glycosaminoglycan-linkage region of proteoglycans: phosphorylation and sulfation determine the activity of the human beta1,4-galactosyltransferase 7 and beta1,3-glucuronosyltransferase I. *TheScientificWorldJournal [electronic resource]*. **5**, 510-514 (2005).

13 Nalbant, D. *et al.* FAM20: an evolutionarily conserved family of secreted proteins expressed in hematopoietic cells. *BMC genomics* **6**, 11 (2005).

14 Tagliabracci, V. S., Xiao, J. & Dixon, J. E. Phosphorylation of substrates destined for secretion by the Fam20 kinases. *Biochemical Society Transactions* **41**, 1061-1065 (2013).

15 Cho, S. H. *et al.* Novel FAM20A mutations in hypoplastic amelogenesis imperfecta. *Human mutation* **33**, 91-94 (2012).

16 Vogel, P. *et al.* Amelogenesis imperfecta and other biomineralization defects in Fam20a and Fam20c null mice. *Veterinary Pathology Online* **49**, 998-1017 (2012).

17 O'Sullivan, J. *et al.* Whole-Exome Sequencing Identifies FAM20A Mutations as a Cause of Amelogenesis Imperfecta and Gingival Hyperplasia Syndrome. *The American Journal of Human Genetics* **88**, 616-620 (2011).

18 Jaureguiberry, G. *et al.* Nephrocalcinosis (Enamel Renal Syndrome) Caused by Autosomal Recessive FAM20A Mutations. *Nephron Physiology* **122**, 1-6 (2013).

19 Tagliabracci, V. S., Pinna, L. A. & Dixon, J. E. Secreted protein kinases. *Trends in biochemical sciences* **38**, 121-130 (2013).

20 Tagliabracci, V. S. *et al.* Secreted Kinase Phosphorylates Extracellular Proteins That Regulate Biomineralization. *Science* **336**, 1150-1153, doi:10.1126/science.1217817 (2012).

21 Xiao, J., Tagliabracci, V. S., Wen, J., Kim, S.-A. & Dixon, J. E. Crystal structure of the Golgi casein kinase. *Proceedings of the National Academy of Sciences* **110**, 10574-10579 (2013).

22 Koike, T., Izumikawa, T., Tamura, J. I. & Kitagawa, H. FAM20B is a kinase that phosphorylates xylose in the glycosaminoglycan–protein linkage region. *Biochemical Journal* **421**, 157-162, doi:10.1042/bj20090474 (2009).

23 Wen, J. *et al.* Xylose phosphorylation functions as a molecular switch to regulate proteoglycan biosynthesis. *Proceedings of the National Academy of Sciences* **111**, 15723-15728, doi:10.1073/pnas.1417993111 (2014).

24 Koike, T., Izumikawa, T., Sato, B. & Kitagawa, H. Identification of Phosphatase That Dephosphorylates Xylose in the Glycosaminoglycan-Protein Linkage Region of Proteoglycans. *Journal of Biological Chemistry* **289**, 6695-6708, doi:10.1074/jbc.M113.520536 (2014).

25 Mani, K. *et al.* The heparan sulfate–specific epitope 10E4 is NO-sensitive and partly inaccessible in glypican-1. *Glycobiology* **14**, 599-607 (2004).

26 David, G., Bai, X. M., Van Der Schueren, B., Cassiman, J.-J. & Van Den Berghe, H. Developmental changes in heparan sulfate expression: in situ detection with mAbs. *The Journal of Cell Biology* **119**, 961-975 (1992).

27 Leteux, C. *et al.* 10E4 antigen of scrapie lesions contains an unusual nonsulfated heparan motif. *Journal of Biological Chemistry* **276**, 12539-12545 (2001).

28 Lugemwa, F. N. & Esko, J. Estradiol beta-D-xyloside, an efficient primer for heparan sulfate biosynthesis. *Journal of Biological Chemistry* **266**, 6674-6677 (1991).

29 Mani, K. *et al.* Tumor attenuation by 2(6-hydroxynaphthyl)-β-d-xylopyranoside requires priming of heparan sulfate and nuclear targeting of the products. *Glycobiology* **14**, 387-397 (2004).

30 Galligani, L., Hopwood, J., Schwartz, N. B. & Dorfman, A. Stimulation of synthesis of free chondroitin sulfate chains by beta-D-xylosides in cultured cells. *Journal of Biological Chemistry* **250**, 5400-5406 (1975).

31 Siegbahn, A. *et al.* Rules for priming and inhibition of glycosaminoglycan biosynthesis; probing the β4GalT7 active site. *Chemical Science* **5**, 3501-3508 (2014).

32 Siegbahn, A. *et al.* Synthesis, conformation and biology of naphthoxylosides. *Bioorganic & Medicinal Chemistry* **19**, 4114-4126 (2011).

33 Tsutsui, Y., Ramakrishnan, B. & Qasba, P. K. Crystal Structures of β-1,4-Galactosyltransferase 7 Enzyme Reveal Conformational Changes and Substrate Binding. *Journal of Biological Chemistry* **288**, 31963-31970, doi:10.1074/jbc.M113.509984 (2013).

34 Katta, K. *et al.* Reduced expression of EXTL2, a member of the EXT family of glycosyltransferases, in human embryonic kidney 293 cells results in longer heparan sulfate chains. *Journal of Biological Chemistry* **282**, 32802-32810, doi:10.1074/jbc.M114.631754 (2015).

35 Mythreye, K. & Blobe, G. C. Proteoglycan signaling co-receptors: roles in cell adhesion, migration and invasion. *Cell. Signal.* **21**, 1548-1558 (2009).

36 Afratis, N. *et al.* Glycosaminoglycans: key players in cancer cell biology and treatment. *FEBS Journal* **279**, 1177-1197 (2012).

37 Bradford, M. M. A rapid and sensitive method for the quantitation of microgram quantities of protein utilizing the principle of protein-dye binding. *Analytical biochemistry* **72**, 248-254 (1976).

38 De Vries, B., Van den Berg, W., Vitters, E. & Van de Putte, L. Quantitation of glycosaminoglycan metabolism in anatomically intact articular cartilage of the mouse patella: in vitro and in vivo studies with 35S-sulfate, 3H-glucosamine, and 3H-acetate. *Rheumatology international* **6**, 273-281 (1986).

39 Bronson, R. E., Bertolami, C. N. & Siebert, E. P. Modulation of fibroblast growth and glycosaminoglycan synthesis by interleukin-1. *Collagen and related research* **7**, 323-332 (1987).

Acknowledgements

This work was supported by the Région Lorraine research grant.

Author Contributions

M.O. and I.S. conceived and designed the experiments. I.S. and L.B. conducted the experiments. M.O., L.B. and I.S. analyzed the results. S.F.G., M.O., I.S. and L.B. contributed materials and analysis tools. M.O. and I.S. wrote the paper. All authors reviewed the manuscript.

Additional Information

Competing financial interests: The authors declare no competing financial interests.

Figure legends

Figure 1. Expression of FAM20B in HEK293 cells and digestion with PNGase F. HEK293 cells were transfected with pCMV-Fam20B tagged with Flag M2 and pCMV empty vector (control). **(a)** The expression was analyzed by Western blot. **(b)** The equal amount of proteins from control and Fam20B was digested with PGNase F and analyzed by western blot using anti-M2 Flag antibody.

Figure 2. Fam20B suppresses the synthesis of endogenous GAGs. HEK293 Cells were transfected with either Fam20B or empty plasmid (Control) and PG-GAG chains were radiolabelled using ^{35}S-sulphate incorporation method. The level of PG-GAG synthesis was analyzed following CPC precipitation of PG-GAGs by scintillation counting **(a)** and by SDS-PAGE **(b)**. The amount of ^{35}S-sulfate GAGs was normalized to DNA and relative to control. **(c)** The bar graph represents the quantification of GAG chains on the autoradiography of the SDS-PAGE. Data were presented as mean ± SD of three separate experiments. Statistical significance was evaluated using Student's t test (*, $P<0.05$).

Figure 3. Fam20B blocks the synthesis of CSPGs in CHO-K1 and HEK293 cells. CHO-K1 and HEK293 cells were co-transfected with pCMV-DCN-EGFP and either pCMV-Fam20B or empty pCMV (control) and **(a)** DCN-EGFP was immunopurified with the anti-GFP beads from culture medium of CHO-K1-transfected cells. **(b)** and **(c)** GAG-attached DCN-EGFP was specifically isolated by CPC precipitation method from CHO-K1 and HEK293 cell culture

medium, respectively. DCN-EGFP was analyzed by Western blot using anti-GFP antibodies. Data were presented as mean ± SD of three separate experiments.

Figure 4. Fam20B blocks the synthesis of HSPGs in CHO-K1 and HEK293 cells. CHO-K1 and HEK293 cells were co-transfected with SDC4$^{(\Delta CT)}$-EGFP and either pCMV-Fam20B or empty pCMV (control) and **(a)** SDC4$^{(\Delta CT)}$-EGFP was immunopurified with the anti-GFP beads from culture medium of CHO-K1-transfected cells. (**b**) and (**c**) GAG-attached SDC4$^{(\Delta CT)}$-EGFP was specifically isolated by CPC precipitation method from CHO-K1 and HEK293 cell culture medium, respectively. DCN-EGFP was analyzed by Western blot using anti-GFP antibodies. Data were presented as mean ± SD of three separate experiments.

Figure 5. Effect of Fam20B on the synthesis of endogenous decorin. Primary human skin fibroblasts and A549 cells were transfected with pCMV-Fam20B or empty pCMV (control) and decorin produced in the medium was analyzed following CPC precipitation by Western Blot using anti-decorin specific antibodies. **(a)** Western blot of decorin produced by primary skin fibroblast cells. **(b)** The bar graph represents the quantification of the Western blots. **(c)** Western blot of decorin produced by A549cell line. **(d)** The bar graph represents the quantification of the Western blots. Data were presented as mean ± SD of three separate experiments. Statistical significance was evaluated using Student's t test (*, $P<0.05$).

Figure 6. Effect of Fam20B on the synthesis of cell surface HSPGs. CHO-K1 cells were transfected with **(a)** empty pCMV (control) or **(b)** pCMV-Fam20B tagged with Flag M2 and expression of cell surface HSPGs was examined by immunofluorescence using anti-heparan sulphate antibody 10E4 (green). The expression of Fam20B was analyzed using anti-M2 flag antibody (red). Nuclei were stained (blue) using Hoechst/PBS solution.

Figure 7. The knockdown of Fam20B stimulates PG-GAG synthesis. (a) qRT-PCR analysis of the expression of Fam20B in HEK293 cells stably expressing an shRNA to Fam20B compared to cells expressing an shRNA control. **(b)** and **(c)** Analysis of PG-GAG synthesis level in HEK293 cells stably expressing shRNA to Fam20B and shRNA control by ^{35}S-sulphate incorporation method using scintillation counting and SDS-PAGE, respectively. **(d)** The bar graph represents a quantification of the radiography. **(e)** HEK293 cells stably expressing shRNA-Fam20B and shRNA-control were transfected with DCN-EGFP expression vector and synthesis of DCN-EGFP in the medium was analyzed by Western blot using anti-GFP specific antibodies. **(f)** The bar graph represents a quantification of the Western blot. **(g)** HEK293 cells stably expressing shRNA-Fam20B and shRNA-control were transfected with SDC4$^{(\Delta CT)}$-EGFP expression vector and synthesis of SDC4$^{(\Delta CT)}$-EGFP in the medium was analyzed by Western blot using anti-GFP specific antibodies. (**h**) The bar graph represents a quantification of the Western blot. Data were presented as mean ± SD of three separate experiments. Statistical significance was evaluated using Student's t test (*, $P<0.05$).

Figure 8. Effect of Fam20B on the synthesis of GAGs primed by the xyloside analog 4-Methylumbelliferyl-β-D-xylopyranoside. HEK293 and CHO-K1 cells were transfected with empty pCMV (control) or pCMV-Fam20B and incubated with the xyloside analog 4-Methylumbelliferyl-β-D-xylopyranoside and GAG primed chains were metabolically labelled by ^{35}S-sulfate incorporation as indicated in materials and method. **(a)** and **(b)** The level of GAG synthesis was analyzed following CPC precipitation of GAGs in the medium of HEK293 and CHO-K1 cells, respectively by SDS-PAGE. The amount of ^{35}S-sulfate GAGs was normalized to DNA and relative to control. **(c)** and **(d)** The bar graphs represent the quantification of ^{35}S-sullfate radiolabelled GAG chains on the autoradiography of the SDS-PAGE of A and B, respectively. Data were presented as mean ± SD of three separate experiments. Statistical significance was evaluated using Student's t test (*, $P<0.05$).

Figure 9. The aspartic acid residues Asp^{289} and Asp^{309} are essential for Fam20B function. The residues Asp^{289} and Asp^{309} were mutated with alanine and the mutants were expressed in HEK293 cells along with wild type Fam20B enzyme and empty vector as control. **(a)** Western blot analysis of the expression of wild-type, Fam20B^{D289A} and pCMV-Fam20B^{D309A} mutants using anti-M2 Flag antibody. β-actin was used as loading control. **(b)** Cells were co-transfected with DCN-EGFP along with Fam20B, Fam20B^{D289A}, pCMV-Fam20B^{D309A} or empty pCMV (control) and DCN-EGFP produced in the medium was analyzed by Western blot using anti-GFP antibodies. **(c)** Cells were co-transfected with SDC4$^{(\Delta CT)}$-EGF along with Fam20B, Fam20B^{D289A}, pCMV-Fam20B^{D309A} or empty pCMV empty (control) and SDC4$^{(\Delta CT)}$-EGF produced in the medium was analyzed by Western blot using anti-GFP antibodies. **(d)** PG-GAG chains produced in the medium

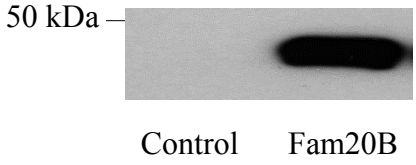
by HEK293 cells transfected with Fam20B, Fam20B^{D289A}, pCMV-Fam20B^{D309A} or empty vector (control) were metabolically labelled by ^{35}S-sulfate incorporation and isolated by CPC precipitation were separated by SDS-PAGE and revealed by autoradiography. **(e)** The bar graph represents the quantification of ^{35}S-sullfate radiolabelled GAG chains of the autoradiography. **(f)** A549 cells were transfected with Fam20B, Fam20B^{D289A}, pCMV-Fam20B^{D309A} or empty pCMV (control) and endogenous decorin secreted by the cells in the medium was analyzed by Western blot using anti-decorin specific antibodies. **(g)** The bar graph represents the quantification of the Western blot in F. Data were presented as mean ± SD of three separate experiments. Statistical significance was evaluated using Student's t test (*, P<0.05).

Figure 10. Fam20B supresses GAG chain synthesis following xylose addition on PG core protein. **(a)** CHO PgsB-618 cells were co-transfected with DCN-EGFP along with Fam20B or empty pCMV (control) and the expression of DCN-EGFP was analyzed in medium by Western blot using anti-EGFP antibodies. **(b)** The bar graph represents the quantification of the Western blot in A. **(c)** CHO PgsB-618 cells were co-transfected with SDC4$^{(\Delta CT)}$-EGFP along with Fam20B or empty pCMV (control) and the expression of SDC4$^{(\Delta CT)}$-EGFP was analyzed in medium by Western blot using anti-EGFP antibodies. **(d)** The bar graph represents the quantification of the Western blot in C. **(e)** CHO PgsB-618 cells were co-transfected with DCN-EGFP along with empty pCMV (control), pCMV-Fam20B, pCMV-β4GalT7 or pCMV-Fam20B and pCMV-β4GalT7, and DCN-EGFP produced in the medium was analyzed by Western blot using anti-decorin antibodies. Data were presented as mean ± SD of three separate experiments. Statistical significance was evaluated using Student's t test (*, P<0.05).

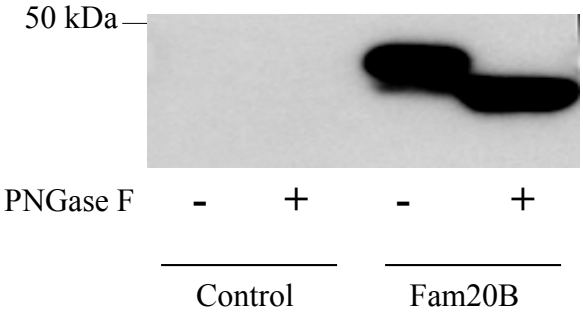
Figure 11. Fam20B reduces the proliferation and migration of cancer cell lines. (a) Glioblastoma cell line T98G and chondrosarcoma cell line SW1535 were plated in 96 well plates and transfected with pCMV-Fam20B or empty pCMV vector (control) and cell proliferation was measured by CyQUANT NF Cell Proliferation Assay Kit at 24 h and 48 h after transfection. (**b** and **d**) Migration of glioblastoma cell line T98G and chondrosarcoma cell line SW1553 transfected with Fam20B or pCMV (control) was assessed using scratch wound-healing assay as Materials and Methods section and cell migration was photographed at 0 and 24h after scratch by phase-contrast microscopy. **(c** and **e)** The bar graph depicting the number of cells that migrate in the scratch area after 6 h and 24 h. Data were presented as mean ± SD of three separate experiments with three replicates each. Statistical significance was evaluated using Student's t test (*, $P<0.05$).

Figure 1

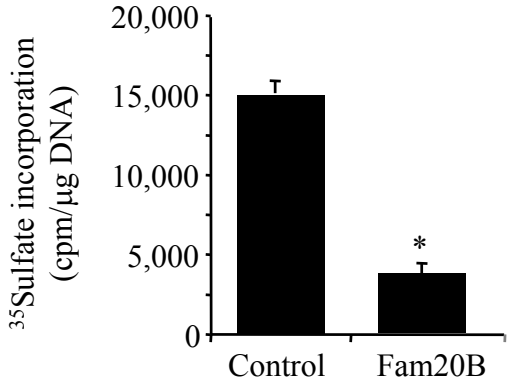
a



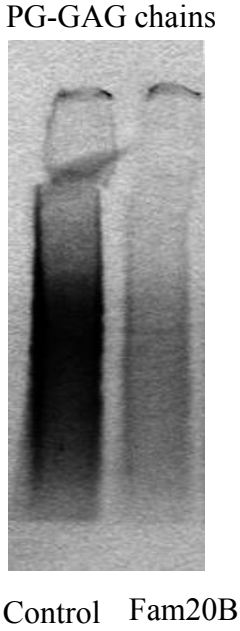
b



a


^{35}Sulfate incorporation
(cpm/μg DNA)
20,000
15,000
10,000
5,000
0
*
Control
Fam20B

b


PG-GAG chains
Control
Fam20B

c

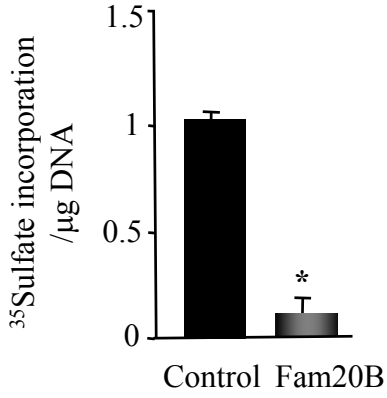
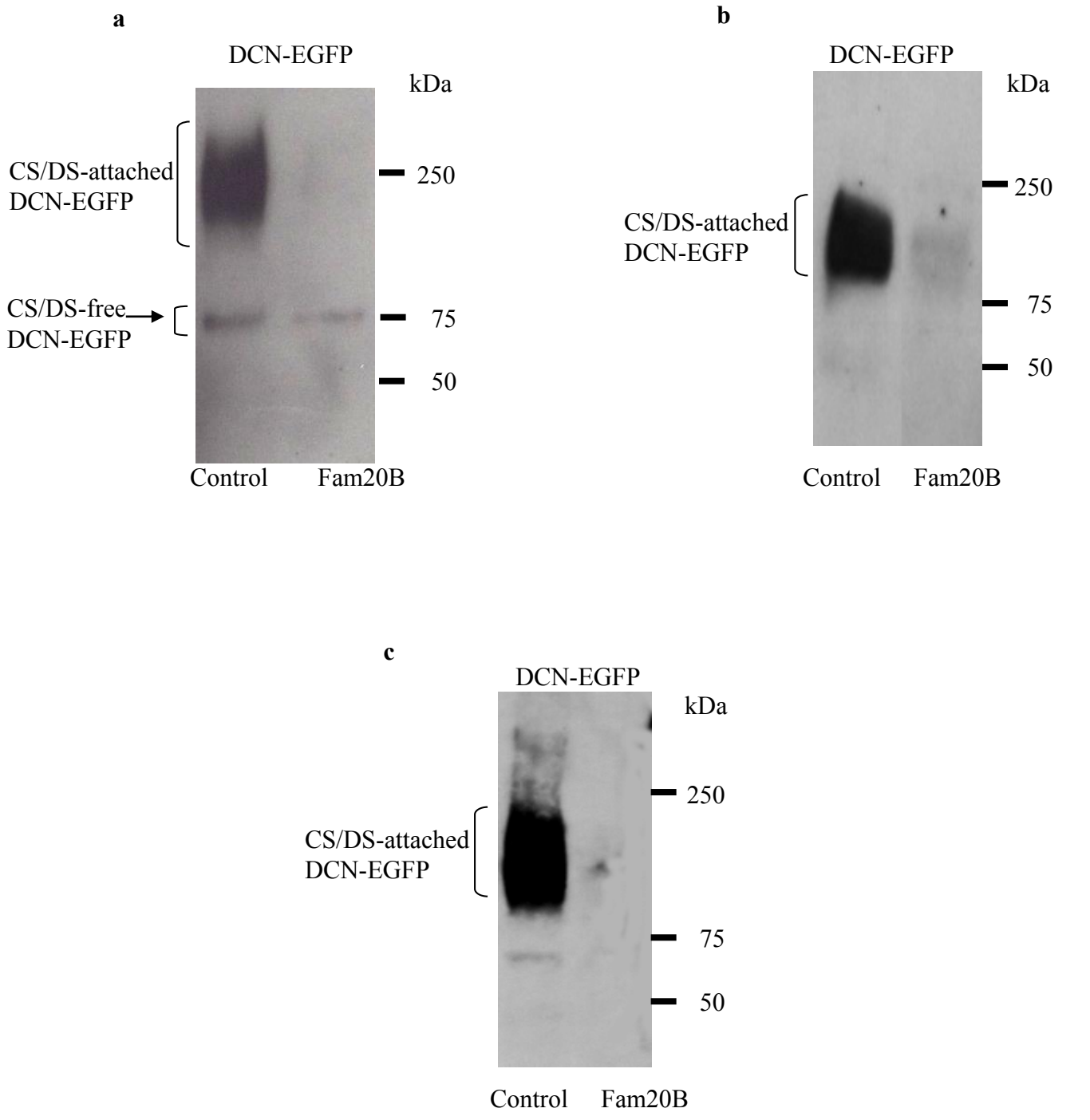
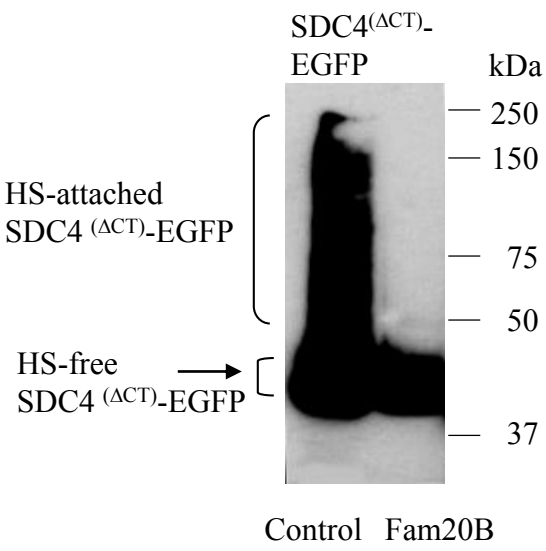

^{35}Sulfate incorporation
/μg DNA
1.5
1
0.5
0
*
Control
Fam20B

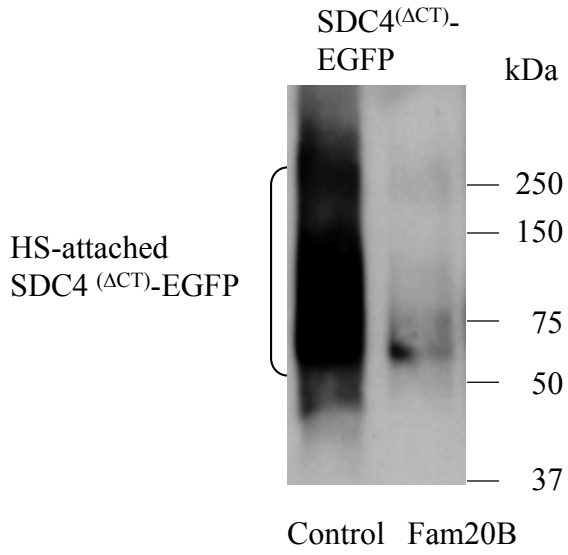
Figure 3


a
DCN-EGFP
kDa
CS/DS-attached
DCN-EGFP
CS/DS-free
DCN-EGFP
250
75
50
Control
Fam20B
b
DCN-EGFP
kDa
CS/DS-attached
DCN-EGFP
250
75
50
Control
Fam20B
c
DCN-EGFP
kDa
CS/DS-attached
DCN-EGFP
250
75
50
Control
Fam20B

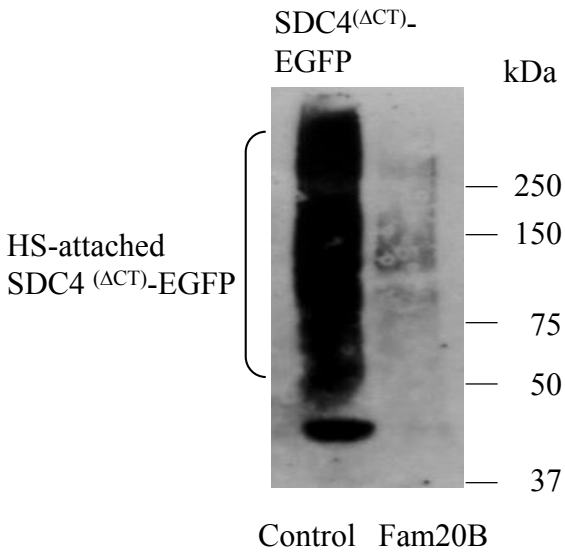
b


SDC4(ΔCT)-EGFP
kDa
250
150
75
50
37
HS-attached SDC4 (ΔCT)-EGFP
HS-free SDC4 (ΔCT)-EGFP
Control
Fam20B

c


SDC4(ΔCT)-EGFP
kDa
250
150
75
50
37
HS-attached SDC4 (ΔCT)-EGFP
Control
Fam20B

c


SDC4(ΔCT)-EGFP
kDa
250
150
75
50
37
HS-attached SDC4 (ΔCT)-EGFP
Control
Fam20B

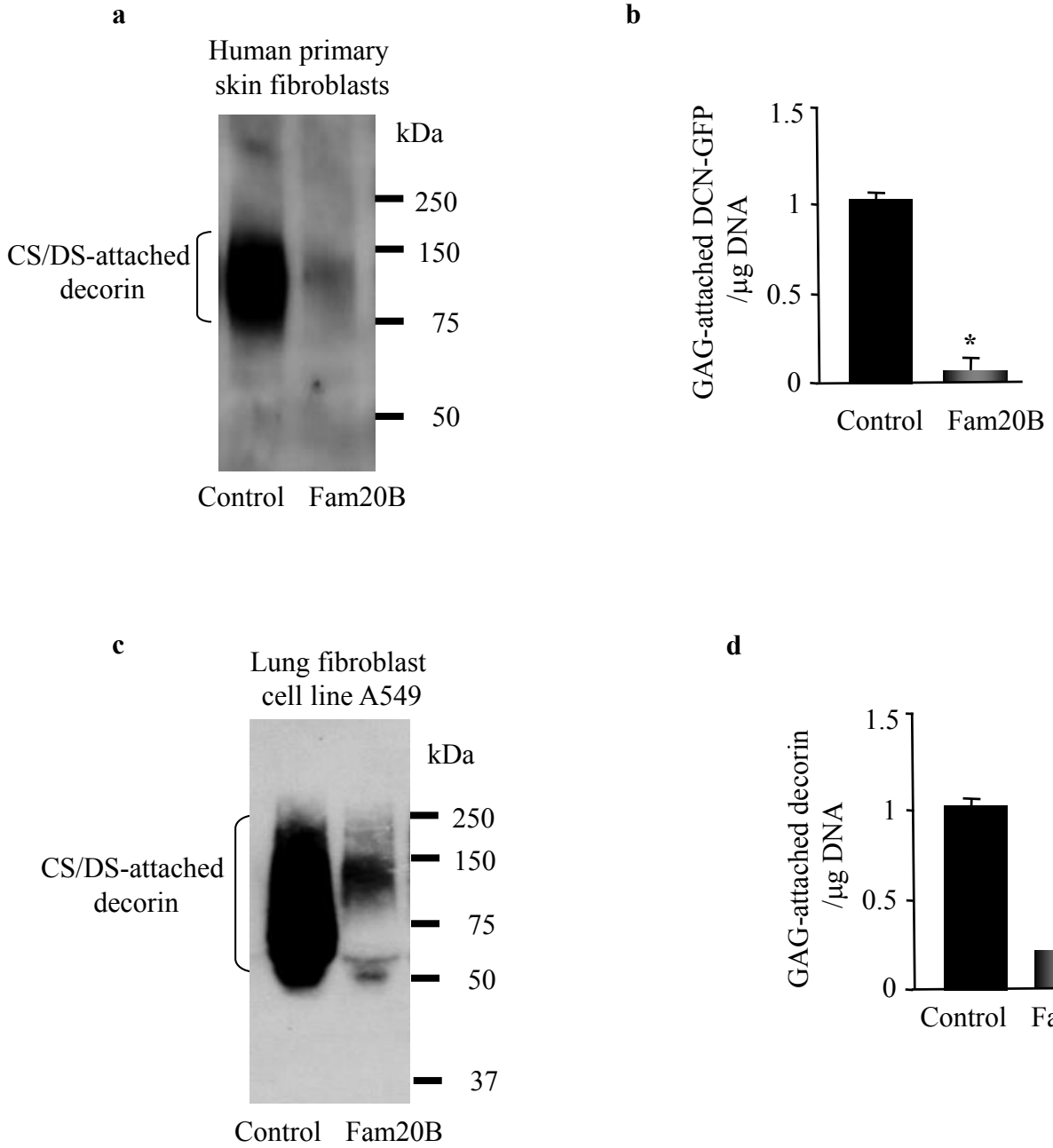
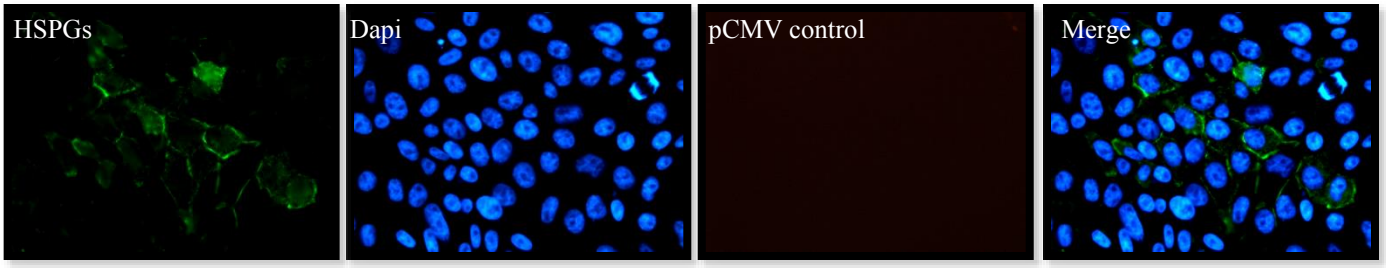
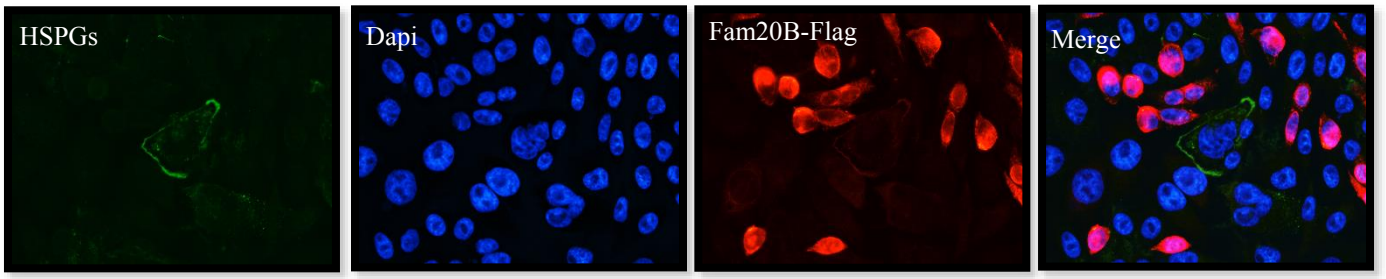

a
Human primary
skin fibroblasts
kDa
250
150
75
50
CS/DS-attached
decorin
Control
Fam20B
b
GAG-attached DCN-GFP
/μg DNA
1.5
1
0.5
0
*
Control
Fam20B
c
Lung fibroblast
cell line A549
kDa
250
150
75
50
37
CS/DS-attached
decorin
Control
Fam20B
d
GAG-attached decorin
/μg DNA
1.5
1
0.5
0
*
Control
Fam20B

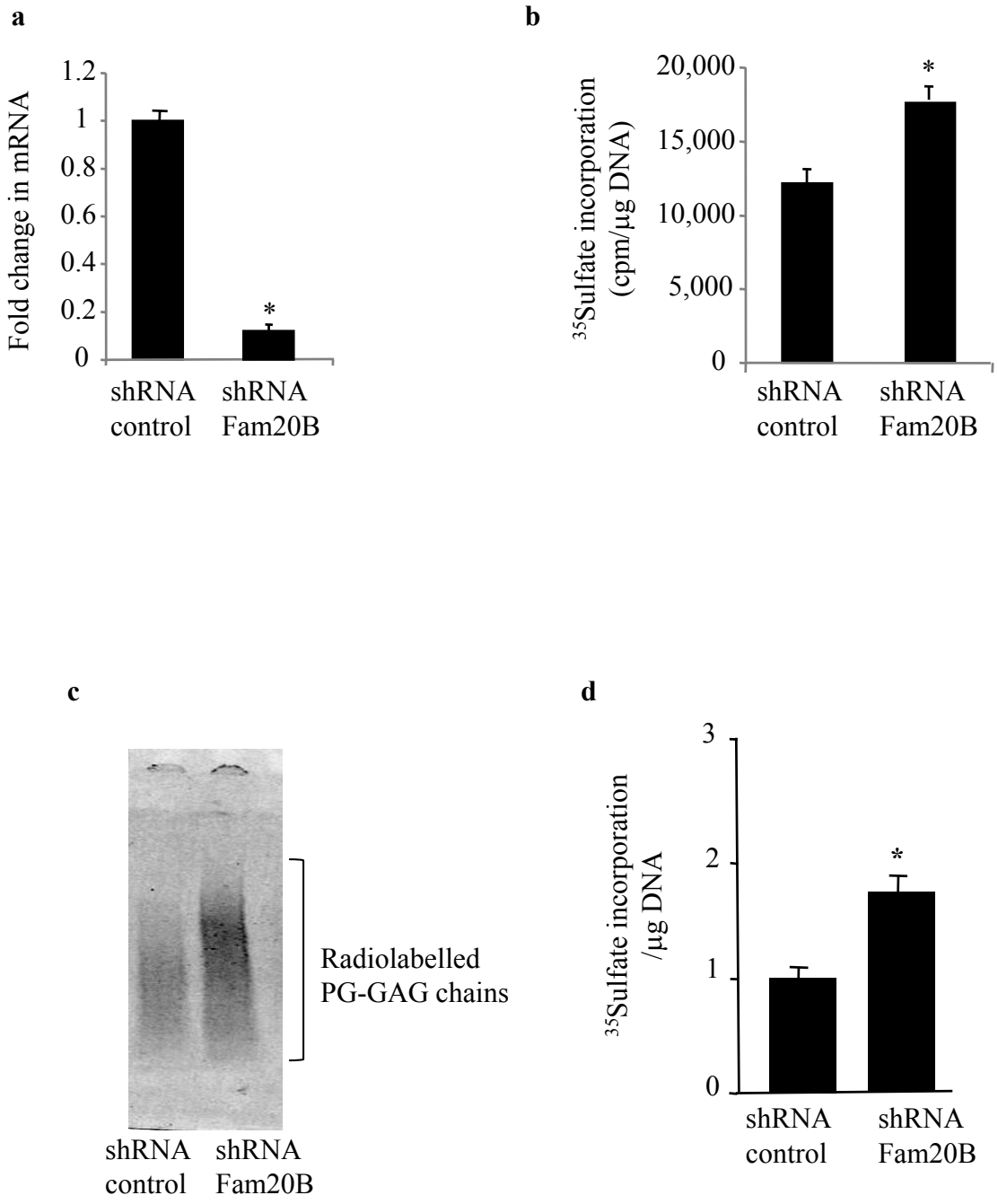
Figure 6

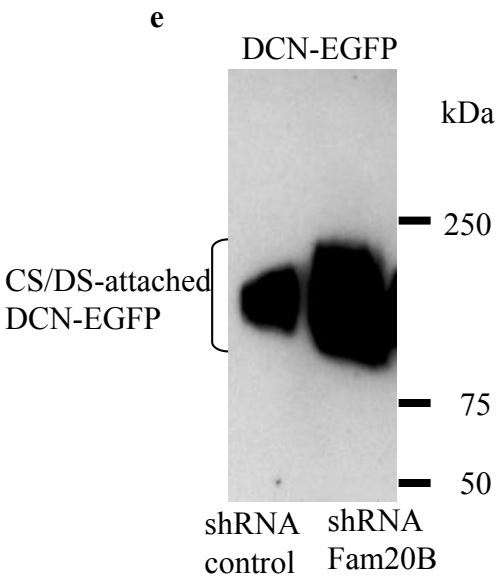
a

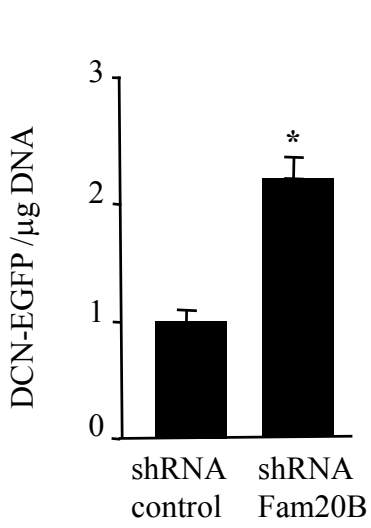


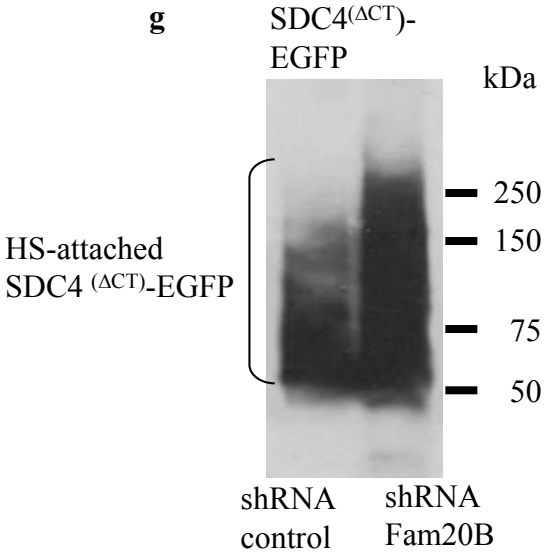
b

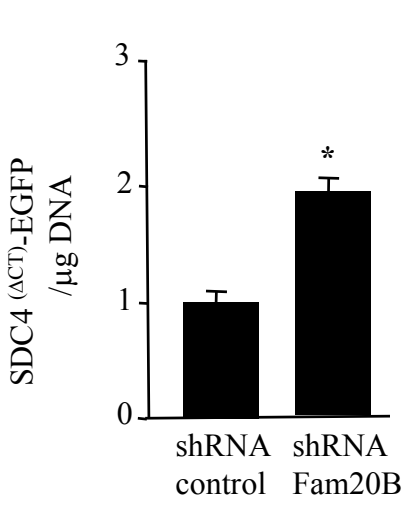


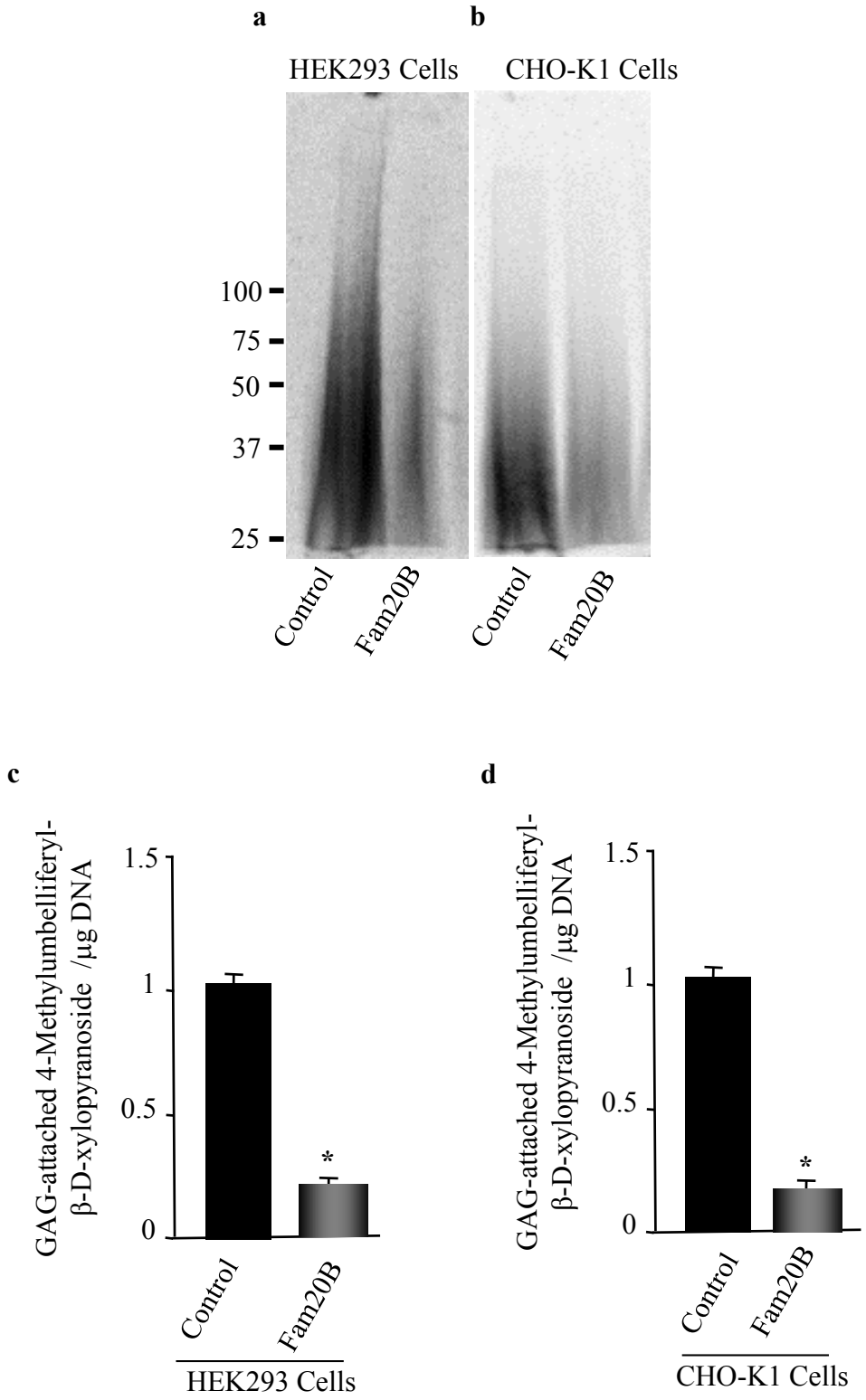

a
Fold change in mRNA
1.2
1
0.8
0.6
0.4
0.2
0
*
shRNA control
shRNA Fam20B
b
^{35}Sulfate incorporation (cpm/µg DNA)
20,000
15,000
10,000
5,000
0
*
shRNA control
shRNA Fam20B
c
Radiolabelled PG-GAG chains
shRNA control
shRNA Fam20B
d
^{35}Sulfate incorporation /µg DNA
3
2
1
0
*
shRNA control
shRNA Fam20B

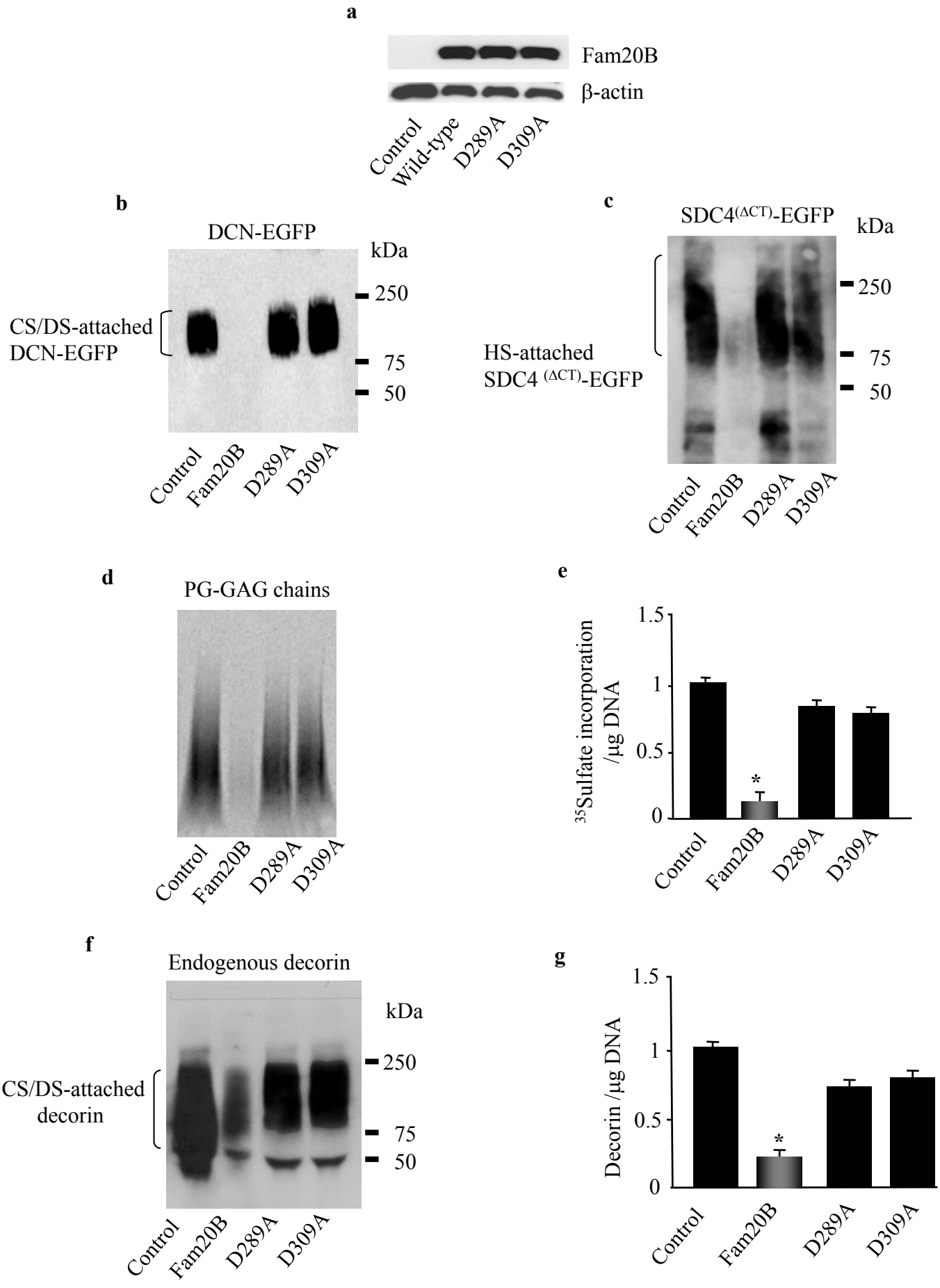

e
DCN-EGFP
kDa
250
75
50
CS/DS-attached
DCN-EGFP
shRNA
control
shRNA
Fam20B


f
DCN-EGFP /µg DNA
3
2
1
0
*
shRNA
control
shRNA
Fam20B


g
SDC4(ΔCT)-
EGFP
kDa
250
150
75
50
HS-attached
SDC4 (ΔCT)-EGFP
shRNA
control
shRNA
Fam20B


h
SDC4 (ΔCT)-EGFP
/µg DNA
3
2
1
0
*
shRNA
control
shRNA
Fam20B


a
b
HEK293 Cells
CHO-K1 Cells
100
75
50
37
25
Control
Fam20B
Control
Fam20B
c
d
GAG-attached 4-Methylumbelliferyl-β-D-xylopyranoside /μg DNA
1.5
1
0.5
0
*
Control
Fam20B
HEK293 Cells
CHO-K1 Cells


a
Fam20B
β-actin
Control
Wild-type
D289A
D309A
b
DCN-EGFP
kDa
250
75
50
CS/DS-attached
DCN-EGFP
Control
Fam20B
D289A
D309A
c
SDC4(ΔCT)-EGFP
kDa
250
75
50
HS-attached
SDC4 (ΔCT)-EGFP
Control
Fam20B
D289A
D309A
d
PG-GAG chains
Control
Fam20B
D289A
D309A
e
35Sulfate incorporation
/μg DNA
1.5
1
0.5
0
*
Control
Fam20B
D289A
D309A
f
Endogenous decorin
kDa
250
75
50
CS/DS-attached
decorin
Control
Fam20B
D289A
D309A
g
Decorin /μg DNA
1.5
1
0.5
0
*
Control
Fam20B
D289A
D309A

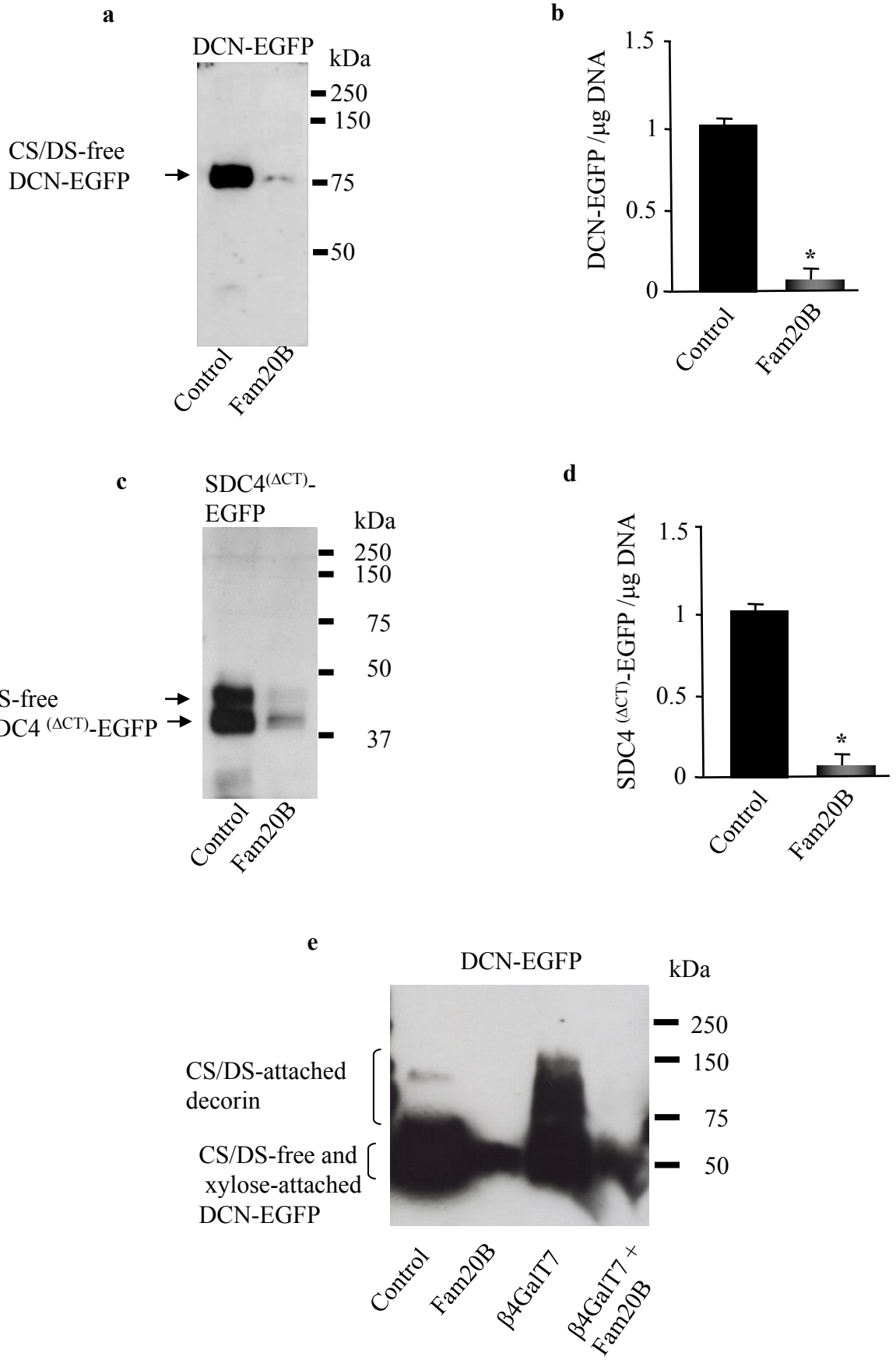
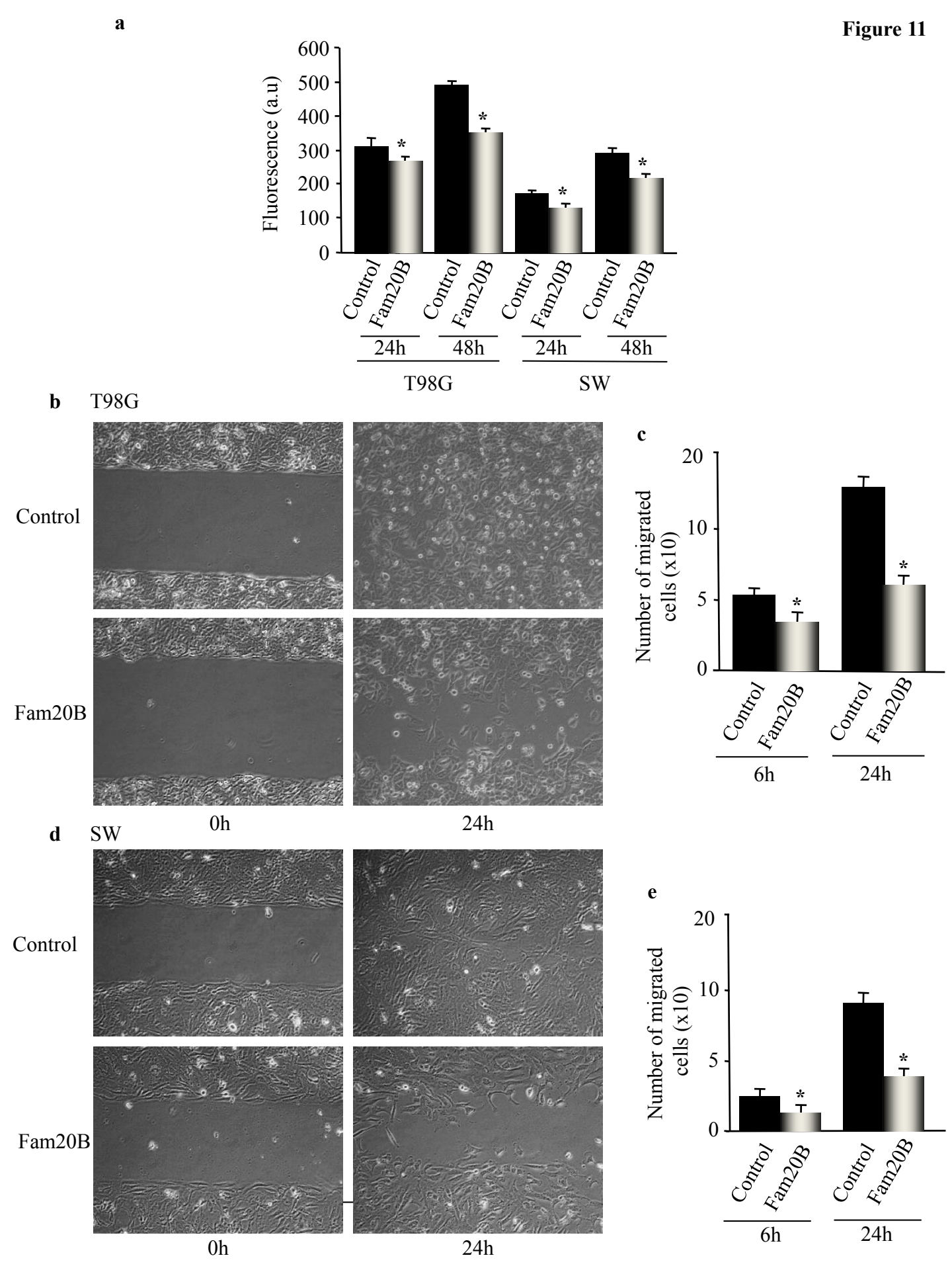

a
DCN-EGFP
kDa
250
150
75
50
CS/DS-free
DCN-EGFP
Control
Fam20B
b
DCN-EGFP /µg DNA
1.5
1
0.5
0
*
Control
Fam20B
c
SDC4(ΔCT)-
EGFP
kDa
250
150
75
50
37
HS-free
SDC4 (ΔCT)-EGFP
Control
Fam20B
d
SDC4 (ΔCT)-EGFP /µg DNA
1.5
1
0.5
0
*
Control
Fam20B
e
DCN-EGFP
kDa
250
150
75
50
CS/DS-attached
decorin
CS/DS-free and
xylose-attached
DCN-EGFP
Control
Fam20B
β4GalT7
β4GalT7 +
Fam20B

Figure 11


a
Fluorescence (a.u)
600
500
400
300
200
100
0
Control
Fam20B
Control
Fam20B
Control
Fam20B
Control
Fam20B
24h
48h
24h
48h
T98G
SW
b
T98G
Control
Fam20B
0h
24h
c
Number of migrated cells (x10)
20
10
5
0
Control
Fam20B
Control
Fam20B
6h
24h
d
SW
Control
Fam20B
0h
24h
e
Number of migrated cells (x10)
20
10
5
0
Control
Fam20B
Control
Fam20B
6h
24h

Publication No 3

PLOS | ONE

RESEARCH ARTICLE

Targeting of Proteoglycan Synthesis Pathway: A New Strategy to Counteract Excessive Matrix Proteoglycan Deposition and Transforming Growth Factor-β1-Induced Fibrotic Phenotype in Lung Fibroblasts

Irfan Shaukat[1], Lydia Barré[1], Narayanan Venkatesan[1], Dong Li[1], Jean-Claude Jaquinet[2], Sylvie Fournel-Gigleux[1], Mohamed Ouzzine[1]*

1 UMR 7365 CNRS-Université de Lorraine, Biopôle-Faculté de Médecine, CS 50184, 54505, Vandoeuvre-lès-Nancy, Cedex, France, **2** UMR 7311 CNRS-Institut de Chimie Organique et Analytique, Université d'Orléans-Pôle de Chimie, Rue de Chartres, 45067, Orléans, Cedex 02, France

* Mohamed.ouzzine@univ-lorraine.fr

CrossMark
click for updates

OPEN ACCESS

Citation: Shaukat I, Barré L, Venkatesan N, Li D, Jaquinet J-C, Fournel-Gigleux S, et al. (2016) Targeting of Proteoglycan Synthesis Pathway: A New Strategy to Counteract Excessive Matrix Proteoglycan Deposition and Transforming Growth Factor-β1-Induced Fibrotic Phenotype in Lung Fibroblasts. PLoS ONE 11(1): e0146499. doi:10.1371/journal.pone.0146499

Editor: Yong Zhou, University of Allabama at Birmingham, UNITED STATES

Received: September 11, 2015

Accepted: December 17, 2015

Published: January 11, 2016

Copyright: © 2016 Shaukat et al. This is an open access article distributed under the terms of the Creative Commons Attribution License, which permits unrestricted use, distribution, and reproduction in any medium, provided the original author and source are credited.

Data Availability Statement: All relevant data are within the paper.

Funding: Funding provided by Région Lorraine. The funder had no role in study design, data collection and analysis, decision to publish, or preparation of the manuscript.

Competing Interests: The authors have declared that no competing interests exist.

Abstract

Stimulation of proteoglycan (PG) synthesis and deposition plays an important role in the pathophysiology of fibrosis and is an early and dominant feature of pulmonary fibrosis. Transforming growth factor-β1 (TGF-β1) is a major cytokine associated with fibrosis that induces excessive synthesis of matrix proteins, particularly PGs. Owing to the importance of PGs in matrix assembly and in mediating cytokine and growth factor signaling, a strategy based on the inhibition of PG synthesis may prevent excessive matrix PG deposition and attenuates profibrotic effects of TGF-β1 in lung fibroblasts. Here, we showed that 4-MU4-deoxy-β-D-xylopyranoside, a competitive inhibitor of β4-galactosyltransferase7, inhibited PG synthesis and secretion in a dose-dependent manner by decreasing the level of both chondroitin/dermatan- and heparin-sulfate PG in primary lung fibroblasts. Importantly, 4-MU4-deoxy-xyloside was able to counteract TGF-β1-induced synthesis of PGs, activation of fibroblast proliferation and fibroblast-myofibroblast differentiation. Mechanistically, 4-MU4-deoxy-xyloside treatment inhibited TGF-β1-induced activation of canonical Smads2/3 signaling pathway in lung primary fibroblasts. The knockdown of β4-galactosyltransferase7 mimicked 4-MU4-deoxy-xyloside effects, indicating selective inhibition of β4-galactosyl-transferase7 by this compound. Collectively, this study reveals the anti-fibrotic activity of 4-MU4-deoxy-xyloside and indicates that inhibition of PG synthesis represents a novel strategy for the treatment of lung fibrosis.

Introduction

Pulmonary fibrosis is characterized by injury and loss of lung epithelial cells, abnormal accumulation of myofibroblasts, and excessive deposition of collagen and proteoglycans (PGs) in the extracellular matrix (ECM), resulting in a progressive loss of pulmonary function [1]. However, the pathological basis of fibrosis is not completely understood. Recent studies have shown that abnormal regulation of PGs plays an important role in the pathophysiology of fibrosis and is an early and dominant features of fibrosis [2]. Indeed, abnormal accumulation of PGs has been shown to occur in pulmonary fibrosis in both human and animal models [3, 4], and is a part of the exacerbated accumulation of ECM constituents during the fibrotic process. In addition, it has been reported that the synthesis of both the core protein and glycosaminoglycan (GAG) chain was altered during the development of fibrosis. A consistent finding in animal models of lung fibrosis is an increase in the synthesis of chondroitin-sulfate/dermatan-sulfate (CS/DS) GAGs associated with accumulation of versican, a large CS-containing PG that forms macromolecular aggregates with hyaluronic acid in the interstitial matrix, and of decorin, which plays a key role in regulating collagen fibril formation and the spatial arrangement of collagen fibers in the matrix [4]. Increased accumulation of versican and decorin has been also reported in patients with pulmonary fibrosis [5]. In parallel, increased accumulation of heparan-sulfate (HS) PGs such as syndecan 1 are also observed in bleomyin-induced lung fibrosis [6] and in human idiopathic pulmonary fibrosis (IPF) [7].

In contrast to the detailed profiling of PG core protein expression in the fibrotic lung, changes in GAG structure and composition have begun only recently to be explored in detail. GAG chains are responsible for many of the biological properties and functions of PGs such as matrix deposition, intracellular signaling, morphogenesis, cell proliferation and migration [8]. Therefore, alterations in the synthesis of GAGs may contribute to disease development in fibrosis. In line with this, our recent study identified increased GAG content during tissue repair in fibrosis [9].

It is widely accepted that TGF-β is the major cytokine associated with pulmonary fibrosis [10] and is able to induce the synthesis of collagens and PGs [11]. Indeed, we showed recently that TGF-β1 increased PG synthesis in rat lung fibrobalasts by inducing the expression of XT-I (xylosyltransferase I) and GlcAT-I (β1, 3-glucuronyltransferase I), which regulate the rate of the PG synthesis [9]. These enzymes in addition to β4Galactosyltransferase7 (β4GalT7) and β3Galactosyltransferase6 (β3GalT6) are responsible for the initiation of the synthesis of GAG chains by catalysing the formation of the linkage tetrasaccharide (GlcAβ1, 3Galβ1, 3Galβ1, 4Xylβ1-O-Ser) that attaches the GAG chain to the PG core protein. Therefore, inhibition of any of the enzymes involved in these early steps of GAG chains synthesis such as β4GalT7 may provide a new strategy to prevent excess PG synthesis and deposition in fibrosis. In addition, owing to the importance of GAG chains of PGs in mediating cytokine and growth factor signaling, this strategy may attenuates TGF-β signaling and the associated profibrotic effects. Interestingly, xyloside analogues such as 4-Methylumbelliferyl-β-D-xylopyranoside can function as GAG chain initiators without a core protein. They are processed by β4GalT7 which adds a galactose residue on the hydroxyl group at C4 position of xylose followed by addition of a second galactose residue by β3GalT6 and of a glucuronic acid moiety by GlcAT-I to complete the tetrasaccharide primer before subsequent polymerisation of the GAG chain by other enzymes of the GAG synthetic pathway [12]. Taking advantage from the properties of these xylose analogues, we synthesized a competitive inhibitor of β4GalT7, 4-Methylumbelliferyl 4-deoxy-β-D-xylopyranoside (referred hereafter as 4-MU4-deoxy-xyloside) an analogue of 4-Methylumbelliferyl-β-D-xylopyranoside (4-MU-xyloside) that lacks the hydroxyl acceptor group at the C4 position of the xylose residue, required for the attachment of galactose by

β4GalT7. Therefore, 4-MU4-deoxy-xyloside can bind to β4GalT7 but cannot be processed as in the case of 4-MU-xyloside. Here, we determined the ability of 4-MU4-deoxy-xyloside to reduce the synthesis and deposition of PGs in primary rat lung fibroblasts both in normal conditions and under TGF-β stimulation. We showed that 4-MU4-deoxy-xyloside inhibited PG synthesis and counteracted TGF-β1-induced PG synthesis in lung fibroblasts. We further demonstrated that 4-MU4-deoxy-xyloside antagonized TGF-β1 canonical signaling and reduced fibroblast proliferation. In addition, we bring evidence that 4-MU4-deoxy-xyloside prevented apparent fibroblast-to-myofibroblast trans-differentiation induced by TGF-β1, suggesting that inhibition of PG-GAG synthesis may provide a new therapeutic approach for IPF treatment.

Materials and Methods

Chemical and reagents

Cell culture medium (Dulbecco's modified Eagle's medium (DMEM)), Fetal Bovine Serum (FBS), Penicillin-Streptomycin, Glutamine, Phosphate Buffered Saline (PBS) were from Life Technology. Recombinant human TGF-β1 was from R&D Systems. Total and active TGF-β1 ELISA kit was from BioLegend. $Na_2[^{35}S]SO_4$ was from Perkin Elmer and 4-Methylumbelliferyl-β-D-xylopyranoside (4-MU-xyloside) from Sigma-Aldrich.

Synthesis of the 4-MU4-deoxy xyloside

4-Methylumbelliferyl 2, 3-di-O-benzoyl-β-D-xylopyranosid was prepared from 4-methylumbelliferyl β-D-xylopyranoside as previously reported [13] and 4-MU4-deoxy-xyloside was then prepared from the latter by radical deoxygenation followed by deprotection. The synthesized 4-MU4-deoxy-xyloside was able to inhibit β4GALT7 *in vitro* with an IC_{50} value of 1 mM [14].

Ethics Statement

Rats were acclimated for 1 week in the laboratory before use. Animals were housed in groups of three or four in solid-bottomed plastic cages with free access to tap water and food. Room temperature was set at 23 ± 1°C and animals were subjected to a 12 h light cycle (with light on from 06:00 to 18:00). All animal experiments were conducted according to the recommendations of European Directive 2010/63/UE and French legislation article R.214-88.

Cell culture and isolation

Primary rat lung fibroblasts were isolated as described before [15]. Briefly, rats were anesthetized by halothane then sacrificed by cervical dislocation to remove the lungs. The lungs were perfused by PBS in sterile conditions and minced into 2–3 mm pieces then digested in DMEM containing trypsin (2.5 mg/ml), collagenase (1 mg/ml), and DNase I (2 mg/ml) at 37°C with gentle stirring for 30 min. Lung cells were separated from undigested tissue and debris by centrifugation and washed twice with PBS. The cells were suspended in DMEM (4.5 mg/ml glucose) medium supplemented with 2 mM glutamin, 100 IU/ml penicillin, 100 μg/ml streptomycin and 10% FBS and grown in a culture plate at 37°C with humidified atmosphere in a 5% CO_2. After 24 h, the medium was replaced to remove the unattached cells. When the cells were confluent, they were trypsinized and amplified. The cells formed homogeneous monolayers morphologically consistent with fibroblast-like cells.

DNA transfection and luciferase assay

Lung fibroblasts ($5x10^6$ cells/ml in suspension) were co-transfected with 2 μg of the p $(CAGA)_{12}$-Lux reporter plasmid [16] and 100 ng of pRL-Tk plasmid encoding *Renilla*

luciferase, used as internal control, by nucleofection using Lonza Primary Fibroblasts Transfection Kit (Lonza) according to manufacturer's instructions. Cells were then seeded in 12-well plate at $1x10^5$ Cell/well. At 24 h post-transfection, cells were treated with 4-MU4-deoxy-xyloside and/or TGF-β1 (5 ng/ml) for 12 h in serum free medium as indicated in the figure legends. The luciferase activity was measured using a Dual Luciferase Reporter Assay System (Promega, Madison, WI, USA) and a Berthold luminometer (Bad Wildbad, Germany). $p(CAGA)_{12}$-Lux reporter luciferase activity was normalized to pRL-TK vector activity and was expressed relative to the basal activity of empty pGL3Basic vector.

SiRNA transfection

Lung fibroblasts were seeded in 6-well culture plate and grown for 24 h before transfection. Cells were transfected with the siRNA (25 nM) for β4GalT7 (GCCUGAACACUGUGAGGUA) (Sigma-aldrich) or siRNA control (Qiagen) using the DharmaFECT transfection reagent (Thermo Scientific, Waltham, MA) according to manufacturer's instructions. At 48 h post-transfection, cells were treated or not with TGF-β1 (5 ng/ml) for 3 h. The expression level of β4GalT7, αSMA, collagen I and TGF-β1 genes was analyzed by quantitative real-time PCR.

Quantitative real-time PCR

After treatment, total RNA was extracted from lung fibroblasts by the RNAeasey Kit (Qiagen), according to manufacturer's instructions. The cDNAs were synthesized from 500 ng of total RNA using iScript reverse transcription supermix (Bio-Rad). cDNAs were subjected to quantitative PCR using iTaq Universal SYBR Green Supermix. (Bio-Rad). The expression of β4GalT7, αSMA, collagen I and TGF-β1 was measured using specific primers (Qiagen). PCR cycling parameters were 30 s at 95°C; 40 cycles of 30 s at 95°C and 60 s at 60°C. Expression levels of target genes were normalized to ribosomal protein S29 RNA level.

Proteoglycan synthesis

Proteoglycan synthesis was measured by ^{35}S-sulfate incorporation as described by De Vries et al., [17]. Briefly, fibroblasts were grown in 6-well culture plate until 80% confluence then treated with either 4-MU4-deoxy-xyloside or 4-MU-xyloside in the absence or presence of TGF-β1 (5 ng/ml) for 24 h. At 6 h before the end of the treatment, cells were radiolabeled with 10 μCi/ml of ^{35}S-sulfate (Perkin Elmer, Courtabœuf, France). Culture medium was collected, digested with papain (1 mg/ml) and ^{35}S-labeled GAGs were precipitated by cetylpyridinium chloride (CPC), dissolved in solvable and mixed in scintillation fluid (Perkin Elmer, MA, USA). The radioactivity associated with GAGs was measured by liquid scintillation counting (Packard, Rungis, France).

To analyze endogenous PG-GAG chains or GAG chains primed with 4-MU-xyloside, cells were metabolically labelled with 10 μCi/ml of ^{35}S-sulfate (Perkin Elmer, Courtabœuf, France) for 24 h in the presence or not of 4-MU4-deoxy-xyloside. Culture medium was collected, digested with papain (1 mg/ml) and ^{35}S-labeled GAGs were precipitated by CPC. Isolated GAGs were analyzed by SDS-PAGE in 4–12% Nu-PAGE gel. After migration the gel was dried and exposed to autoradiography film. The radioactivity corresponding to GAGs was normalized with the amount of DNA of corresponding cells.

Cellular proliferation assay

The cell proliferation was measured by the CFSE incorporation as previously described [18]. Briefly, fibroblasts were trypsinized and washed twice with PBS then labelled with CFSE using

CellTrace™ CFSE Cell Proliferation Kit (Life technologies) according to manufacturer's instructions. Cells were then seeded onto a 12-well culture plate at $1x10^5$ cells/well and treated with 4-MU4-deoxy-xyloside and/or TGF-β1 (5 ng/ml) for 48 h. After treatment, the cells were analyzed on a Gallios FACS flow cytometer (Beckman coulter).

Cell viability assay

Fibroblast cells were seeded in a 96-well culture plate and incubated with 4-MU4-deoxy-xyloside in the presence or absence of TGF-β1 (5 ng/ml) for 24 h. Cells were then exposed to MTT for 3 h and lysed with the addition of 100 μl of DMSO. Subsequently, the cell viability was determined by measuring the absorbance at 550 nm using the microplate spectrophotometer Varioskan Flash Multimode reader (Fisher Scientific).

Western blotting

Fibroblasts were seeded in a 6-well culture plate and treated as indicated in the figure legends. The cells were then lysed in RIPA buffer and protein concentration was determined by Bradford method [19]. 30 μg of total protein was separated by SDS-PAGE and transferred onto the PVDF immobilon membrane (Millipore) then incubated overnight at 4°C with appropriate primary antibodies: anti-decorin (1:1000, R&D Systems), phospho-Smad2, phospho-Smad3 and Smad2/3 (1:1000, Cell Signaling Technology), αSMA (1: 5000, Sigma) and β-actin (1: 6000, Sigma-Aldrich) used as loading control. The protein bands were visualized by chemiluminescence using chemiluminescence luminol reagent (Bio-Rad). Densitometry analysis was performed using Image J software (version 1.46r, National Institute of health, Bethesda, MD, USA).

Immunofluorescence

Fibroblasts were grown on cover slips and treated or not with 4-MU4-deoxy-xyloside for 24 h. The cells were fixed in 4% paraformaldehyde then stained with the 10E4 monoclonal anti-HS antibodies (AMSBIO) and anti-mouse IgG coupled with Alexa Fluor 488 (Molecular Probes, Invitrogen). The nuclei were stained with Hoechst 33342 (Molecular Probes-Invitrogen). Representative micrographs were observed using inverted microscope Leica DMI3000 B (Leica Microsystems).

Quantification of active and total TGF-β1

Lung fibroblasts grown in 6-well culture plates were treated in serum free medium with 4-MU4-deoxy-xyloside and/or TGF-β1 (5 ng/ml) for 24 h. Then, cell culture supernatants were collected and both total and active TGF-β1 were quantified using LEGEND MAX™ Free Active TGF-β1 ELISA Kit according to manufacturer's instructions. Briefly, 50 μl of cell culture supernatants were transferred to the anti-TGF-β1 pre-coated 96-well plate in triplicate and incubated at room temperature for 2 h. Then, each well was washed and incubated with 100 μl TGF-β1 detection antibody solution for 1 h. Next, the wells were washed and incubated with 100 μl Avidin-HRP for 30 min. After washing, the plate was incubated with 100 μl of substrate solution for 10 min. Then, the reaction was stopped by addition of 100 μl of stop solution to each well and the absorbance was measured at 450 nm with the microplate spectrophotometer, Varioskan Flash Multimode reader (Fisher Scientific). The concentration of TGF-β1 was calculated using a standard curve. To assess the total amount of TGF-β1, acid activation was performed to release free active TGF-β1 before processing as indicated above.

Statistical analysis

The results are presented as mean ± SD of three independent experiments. Statistical differences between control and treated groups were evaluated using Student's test. A two-sided P-value <0.05 was considered statistically significant for all analyses.

Results

4-MU4-deoxy-xyloside inhibits PG synthesis in lung fibroblasts

With regard to the high level of PG synthesis and deposition in fibrosis, the development of strategies designed to tamper with PG production is clearly an attractive prospect for therapeutic application. Therefore, we investigated the ability of 4-MU4-deoxy-xyloside to inhibit PG synthesis in primary lung fibroblasts. We first analyzed the effect of 4-MU4-deoxy-xyloside on PG synthesis using ^{35}S-Sulfation incorporation to label total GAG chains of PGs. Lung primary fibroblast cells were grown in medium containing radioactive $Na_2{}^{35}SO_4$ in the absence (control) or presence of various concentrations of 4-MU4-deoxy-xyloside. The results clearly showed that the rate of PG synthesis decreased with increased concentration of 4-MU4-deoxy-xyloside (Fig 1A), indicating that 4-MU4-deoxy-xyloside inhibited PG synthesis in a dose-dependent manner in lung primary fibroblasts. Indeed, at concentrations of 4-MU4-deoxy-xyloside ranging from 500 μM to 1 mM, PG synthesis was inhibited by 50% to 80% (Fig 1A).

To confirm the inhibitory effect of 4-MU4-deoxy-xyloside on PG-GAG synthesis, we analyzed its effect on endogenous GAG chains and on the formation of GAG chains primed with 4-MU-xyloside. Indeed, 4-MU-xyloside is used as a substrate by the β4GalT7 enzyme and further processed by glycosyltransferases of GAG biosynthetic pathway leading to the formation and secretion in the medium of GAG chains. Primary lung fibroblasts were cultured in medium containing radioactive $Na_2{}^{35}SO_4$ in the absence (control) or presence of 4-MU4-deoxy-xyloside and 4-MU-xyloside. SDS-PAGE analysis of radiolabeled GAG chains clearly showed that 4-MU4-deoxy-xyloside decreased by about 50% the amount of endogenous GAG chains (Fig 1B and 1C). Similarly, 4-MU4-deoxy-xyloside reduced by about 48% the amount of GAG chains primed by 4-MU-xyloside (Fig 1B and 1C), indicating that it is able to inhibit synthesis of GAG chains.

4-MU4-deoxy-xyloside inhibits synthesis of both chondroitin- and heparan-sulfate PGs

Given that β4GalT7 catalyses a common step to the synthesis of both CS- and HS-PGs, we examined whether 4-MU4-deoxy-xyloside inhibits the synthesis of both PG types. We first analyzed the effect of 4-MU4-deoxy-xyloside on the synthesis of decorin, a CS/DS-attached PG secreted in large amount by human skin primary fibroblasts. To this end, skin primary fibroblast cells were grown in the absence (control) and presence of 4-MU4-deoxy-xyloside and GAG-attached PGs were isolated from culture medium by CPC precipitation method and analyzed by Western blot using anti-decorin specific antibodies. The results clearly showed that 4-MU4-deoxy-xyloside inhibited, in a dose dependent manner, the synthesis of decorin (Fig 2A). As shown in Fig 2B, 4-MU4-deoxy-xyloside reduced by about 60% and 70% the amount of decorin at 500 μM and 1 mM, respectively.

We next analyzed the effect of 4-MU4-deoxy-xyloside on the synthesis of HS-PGs by analysing the expression of cell surface HS-attached PGs by indirect immunofluorescence using 10E4 anti-HS monoclonal antibodies, which are commonly used to detect HS chains of PGs [20]. Prominent staining of the cell membrane was observed in non-treated fibroblasts cells, whereas only low signal could be detected in 4-MU4-deoxy-xyloside-treated cells (Fig 2C).

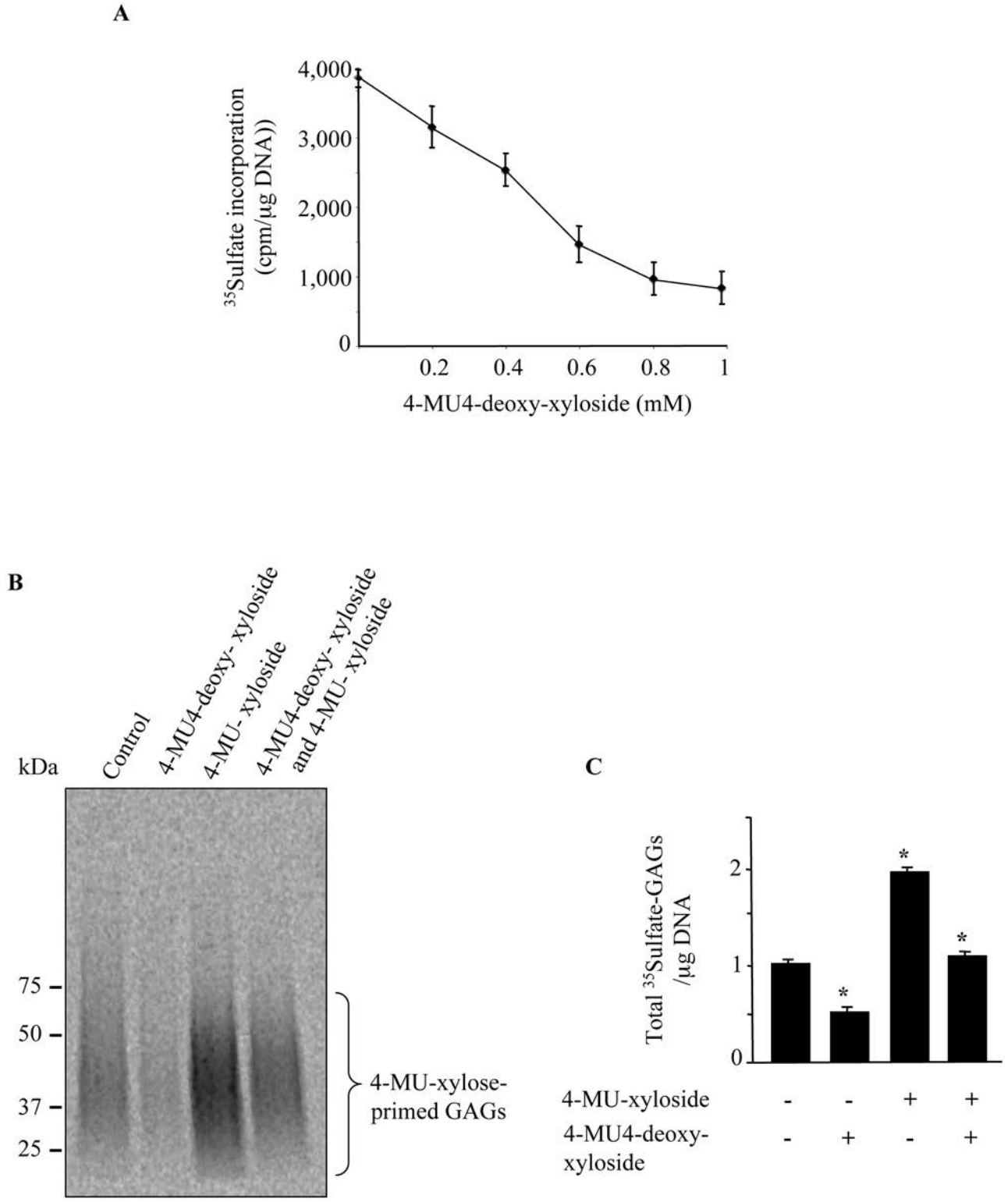


Fig 1. 4-MU4-deoxy-xyloside inhibits PG synthesis. (**A**) Primary rat lung fibroblasts were treated with various concentrations of 4-MU4-deoxy-xyloside for 24 h and the level of the PG synthesis was measured by ^{35}Sulfate incorporation for the last 6 h of the treatment. The control was treated with vehicle (DMSO). PG synthesis level was normalized to the amount of DNA. (**B**) Lung primary fibroblasts were incubated with or without 100 μM of 4-MU-xyloside in the presence and absence of 4-MU4-deoxy-xyloside (500 μM) and GAGs were metabolically labelled for 24 h with ^{35}Sulfate incorporation. Radiolabeled GAGs were isolated from the medium by CPC precipitation and analyzed by SDS-PAGE then visualized by autoradiography. Bar graph shows total ^{35}Sulfated GAGs normalized to DNA and relative to control (untreated). Data are expressed as mean ± SD of three separate experiments. *P<0.05 versus control.

doi:10.1371/journal.pone.0146499.g001

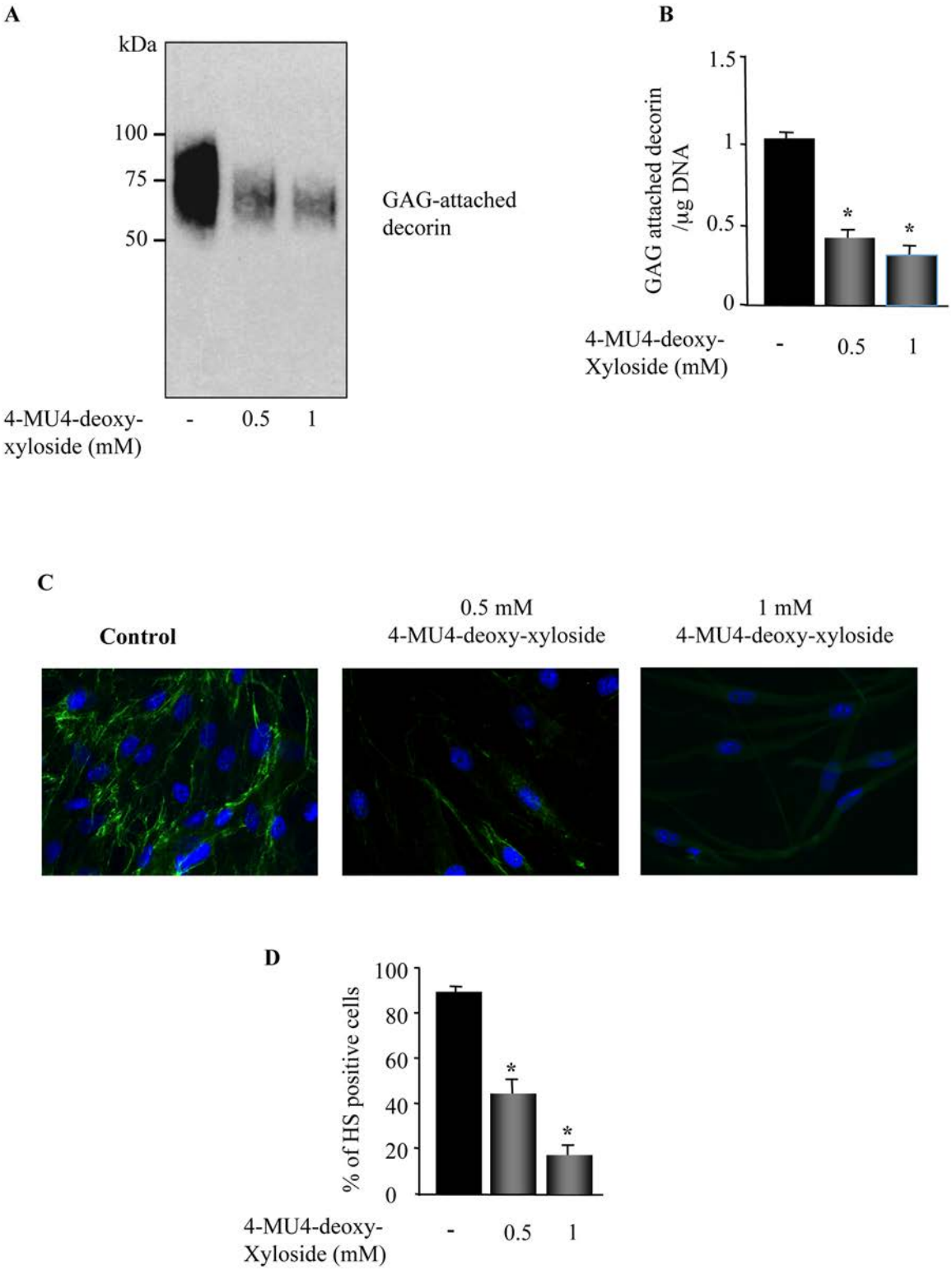


Fig 2. 4-MU4-deoxy-xyloside inhibits the synthesis of both chondroitin- and heparin- sulphate PGs. Fibroblasts were treated with 500 μM or 1 mM of 4-MU4-deoxy-xyloside or with DMSO (control) for 24 h and (**A**) CS/DS-attached decorin produced was precipitated from culture medium by CPC and analyzed by Western blot using anti-decorin antibody. The absence of decorin core protein is due the use of CPC which selectively precipitate CS/DS-attached decorin. **(B)** Bar graph shows the amount of GAG-attached decorin normalized to DNA and relative to control (DMSO). Data are expressed as mean ± SD of three separate experiments; *P<0.05 versus control. (**C**) Lung fibroblasts were analyzed for the expression of cell surface HS-attached PGs by

immunofluorescence using 10E4 monoclonal anti-HS antibodies. The Nuclei were stained by Hoechst dye. Representative micrographs were observed using inverted microscope Leica DMI3000 B (Leica Microsystems, Germany). The experiment was repeated twice. **(D)** The bar graph represented quantification of fluorescent intensity of heparin-sulphate in absence and presence of 4-MU4-deoxy-xyloside (500 μM or 1 mM). Data are expressed as mean ± SD of several images per condition; *P<0.05 versus control.

doi:10.1371/journal.pone.0146499.g002

Fluorescent intensity quantification indicated that 4-MU4-deoxy-xyloside-treated cells exhibited a decrease of about 58% and 85% at 500 μM and 1 mM, respectively compared to control (Fig 2D), indicating that 4-MU4-deoxy-xyloside strongly reduced the synthesis of HS-GAG chains of PGs. Altogether, these results demonstrated that targeting the β4GalT7 enzyme by 4-MU4-deoxy-xyloside is an efficient strategy to inhibit the synthesis of PGs in lung primary fibroblats.

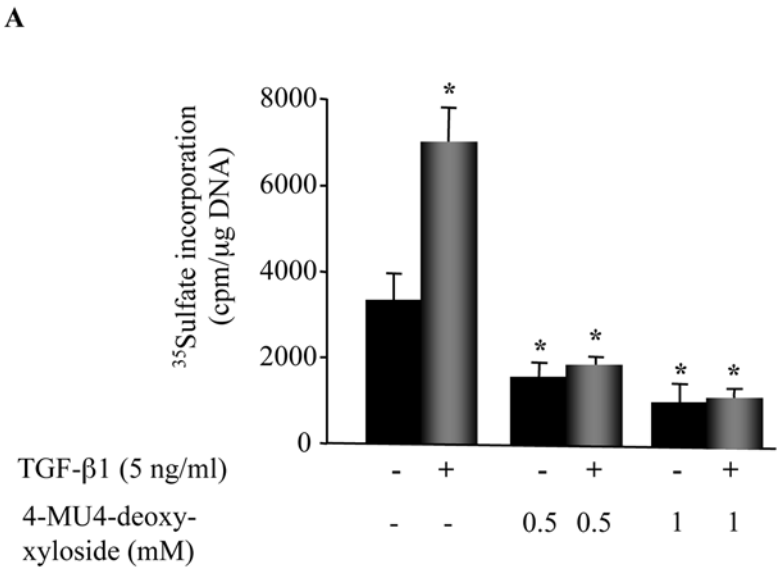
4-MU4-deoxy-xyloside inhibits TGF-β1-induced PG synthesis in primary lung fibroblasts

It has been shown that TGF-β1 is a major cytokine associated with fibrosis. TGF-β1 induces the synthesis of matrix proteins, particularly PGs leading to increased accumulation in the ECM, a process which is associated with fibrosis. Therefore, inhibiting TGF-β1-induced PG synthesis and deposition is of importance for the treatment of fibrosis. To determine whether 4-MU4-deoxy-xyloside is able to inhibit TGF-β1-induced increase of PG synthesis, lung fibroblasts were treated with TGF-β1 in the presence and absence of 4MU4-deoxy-xyloside for 24 h and PG synthesis was measured during the last 6 h of the treatment by ^{35}S-Sulfation incorporation method. The results showed that treatment with TGF-β1 stimulated by about 2-fold the synthesis of PGs, compared to non-treated cells whereas, 4-MU4-deoxy-xyloside inhibited PG synthesis by about 2.2-fold and 3.8-fold at 0.5mM and 1mM, respectively (Fig 3A). However, in the presence of 4MU4-deoxy-xyloside, treatment with TGF-β1 did not induce any significant increase in PG synthesis, a rather decrease in the synthesis was observed (Fig 3A).

To further analyse the effect of 4MU4-deoxy-xyloside on PG synthesis, GAG chains were metabolically radiolabelled by ^{35}S-Sulfation incorporation method for 24 h and newly synthesized radiolabeled PG-GAG chains were analyzed by SDS-PAGE. As shown in Fig 3B and 3C, 4-MU4-deoxy-xyloside significantly reduced the amount of endogenous GAG chains at both 0.5 mM and 1mM, compared to control (Fig 3B and 3C). Interestingly, while TGF-β1 induced a significant increase (75%) in the amount of GAG chains compared to control (Fig 3B and 3C), no significant changes in GAG chain content was produced by the cytokine in the presence of 4-MU4-deoxy-xyloside, a rather decrease was observed compared to control (Fig 3B and 3C). This clearly indicated that 4-MU4-deoxy-xyloside was able to counteract TGF-β1-induced increase in PG synthesis in lung primary fibroblasts.

4-MU4-deoxy-xyloside antagonizes TGF-β1-mediated Smad signaling

It is well known that PGs play a critical role in the regulation of many ligand-mediated signalisation [21], therefore we hypothesized that 4-MU4-deoxy-xyloside treatment may impair TGF-β1 signaling in fibroblasts. To evaluate the impact of 4-MU4-deoxy-xyloside on TGF-β1 signaling, we used a $(CAGA)_{12}$-Lux reporter which contains 12 copies of the Smad-binding site. As shown in Fig 4A, treatment of lung fibroblasts with TGF-β1 stimulated by about 10-fold the reporter activity, however this activation was strongly reduced in a dose dependent manner by 4-MU4-deoxy-xyloside (Fig 4A), indicating that 4-MU4-deoxy-xyloside antagonized the TGF-β1 signaling in primary lung fibroblasts. To further explore the intracellular



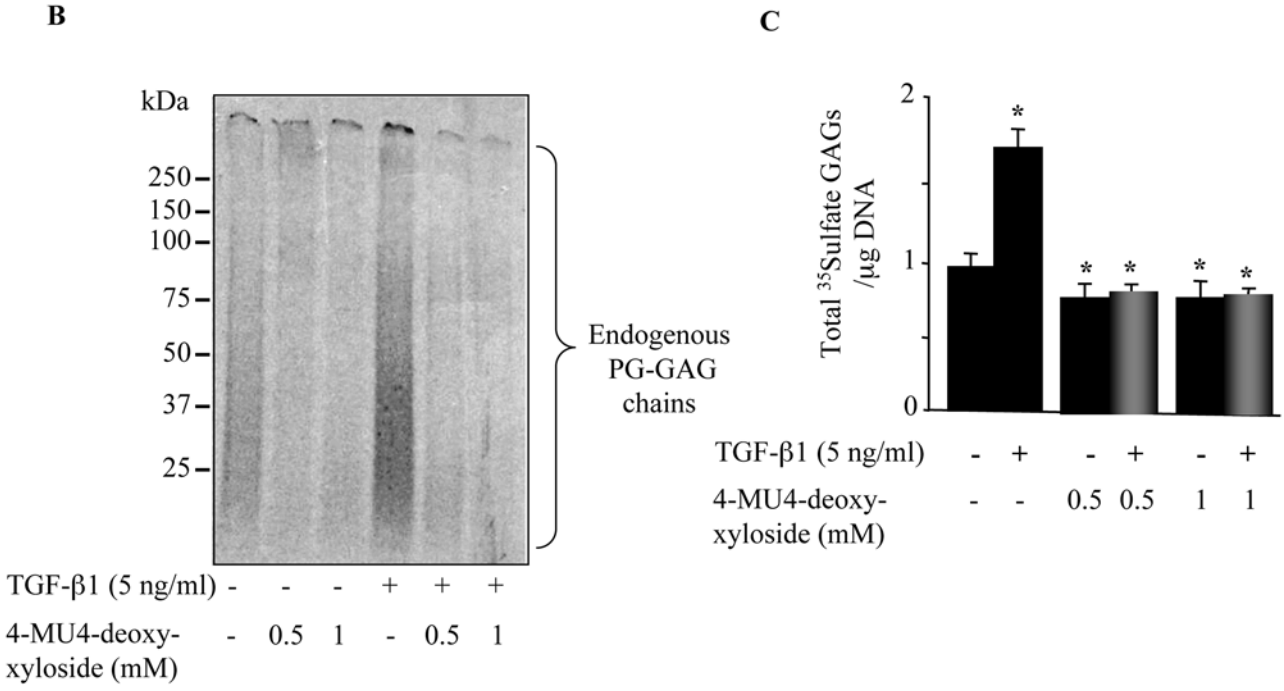


Fig 3. 4-MU4-deoxy-xyloside antagonized TGF-β1-induced PG synthesis in lung fibroblasts. Cells were treated with 500 μM or 1 mM of 4-MU4-deoxy-xyloside or DMSO (control) and/or TGF-β1 (5 ng/ml) for 24 h and (**A**) the level of PG synthesis was measured by the ^{35}Sulfate incorporation for the last 6 h of the treatment. The radioactivity associated with GAGs was evaluated by liquid scintillation counting after CPC precipitation and DNA normalization. Data are expressed as mean ± SD of three separate experiments; *P<0.05 versus control. (**B**) GAG chains were radiolabelled by ^{35}Sulfate incorporation and isolated by CPC method at 24 h after the treatment and analyzed by SDS-PAGE then visualized by autoradiography. Bar graph shows the amount of ^{35}Sulfate GAGs normalized to DNA and relative to control. Data are expressed as mean ± SD of three separate experiments; *P<0.05 versus control.

doi:10.1371/journal.pone.0146499.g003

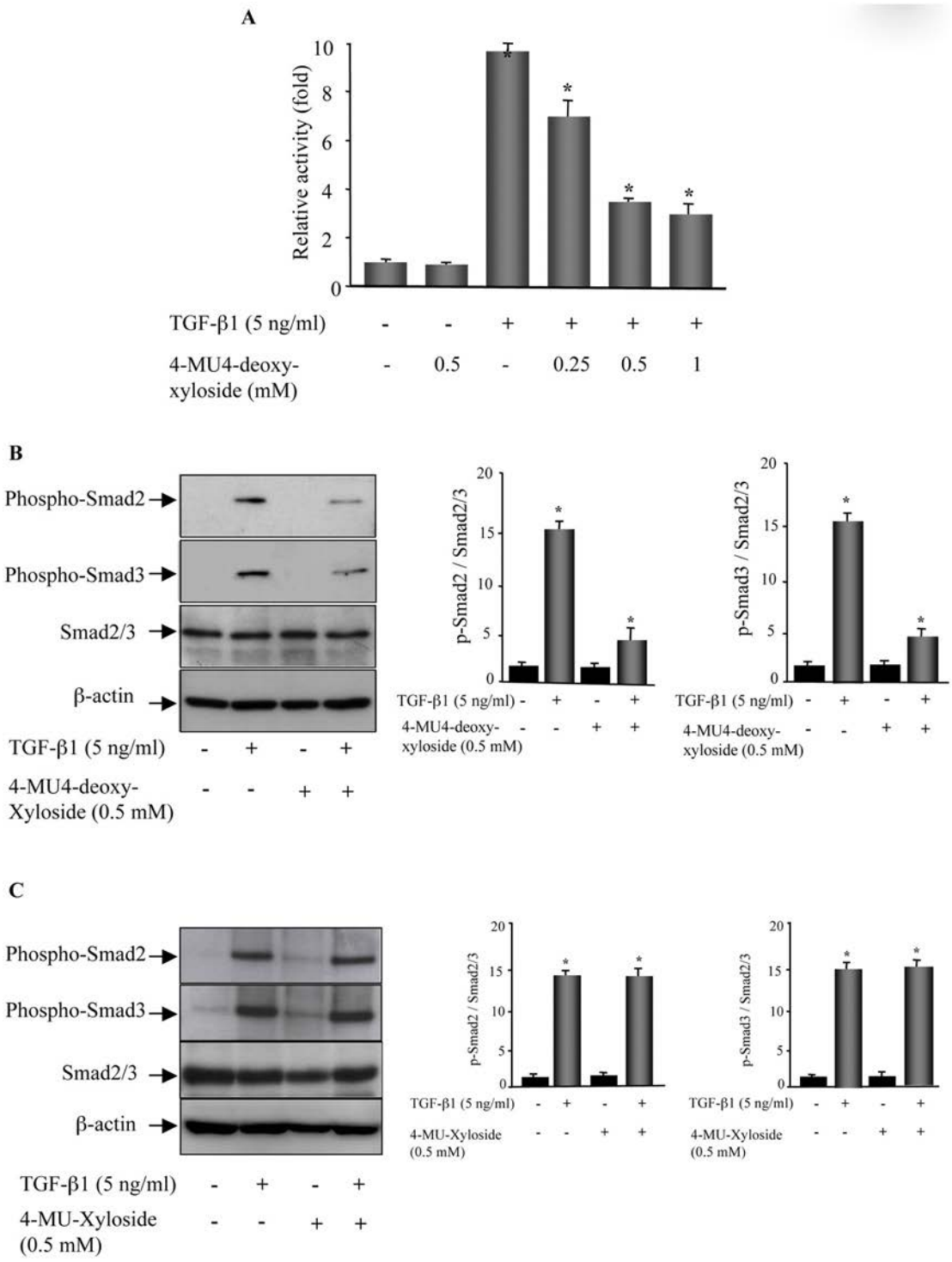


Fig 4. 4-MU4-deoxy-xyloside blocks TGF-β1 signaling. (**A**) Lung fibroblasts were co-transfected with $(CAGA)_{12}$-Lux reporter and pRL-TK (Renilla reporter) constructs and were incubated with DMSO (control) or with various concentrations of 4-MU4-deoxy-xyloside in the presence and absence TGF-β1 (5 ng/ml) for 24 h. The induction of the $(CAGA)_{12}$-Lux reporter was measured by luciferase assay. Luciferase activities were normalized to pRL-TK vector activity. Data are expressed as mean ± SD of three separate experiments; *P<0.05 versus control. **(B)** Cells were incubated with 500 μM of 4-MU4-deoxy-xyloside or **(C)** with 500 μM of 4-MU-xyloside for 24 h then stimulated or not with TGF-β1 (5 ng/ml) for 3 h and assayed by Western blot to assess the levels of phosphorylation of Smad2 and Smad3. Bar graphs show the expression of phospho-Smad2 and phospho-Smad3 relative to total Smad2/3 level normalized to β-actin and expressed relative to control lysates. Data are expressed as mean ± SD of three separate experiments; *P<0.05 versus control.

doi:10.1371/journal.pone.0146499.g004

signal transduction mechanism, we examined the effect of 4-MU4-deoxy-xyloside on the canonical Smad-dependent pathway. As shown in Fig 4B, 4-MU4-deoxy-xyloside significantly reduced TGF-β1-mediated phosphorylation of Smad2 and Smad3. However, this was not the case when 4-MU-xyloside was used (Fig 4C), indicating that 4-MU4-deoxy-xyloside, but not 4-MU-xyloside, repressed TGF-β1 canonical signaling pathway and suggested that soluble GAG chains primed by 4-MU-xyloside did not significantly affect TGF-β1 signaling.

4-MU4-deoxy-xyloside inhibits fibroblast proliferation

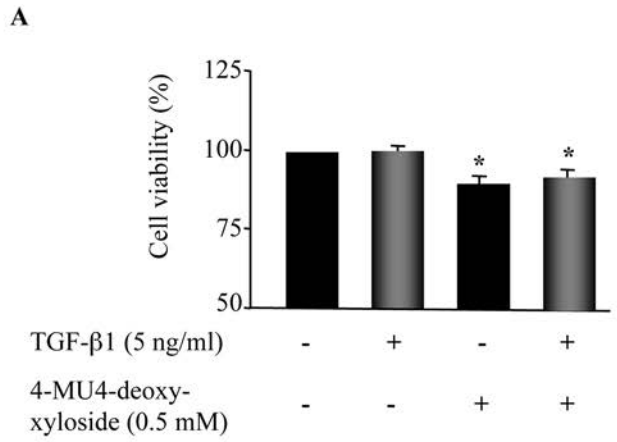
Because proliferation of fibroblasts/myofibroblasts and excessive production of matrix proteins are of major characteristics of pulmonary fibrosis, we then investigated the effect of 4-MU4-deoxy-xyloside on fibroblast proliferation. We first analyzed cell viability by MTT assay. As shown in Fig 5A, TGF-β1 stimulation did not impact the number of viable fibroblasts, whereas the cell viability was decreased by about 8% by 4-MU4-deoxy-xyloside treatment, compared to control. In the presence of TGF-β1, 4-MU4-deoxy-xyloside decreased cell viability by 3%, compared to TGF-β1-treated cells. These data indicated that 4-MU4-deoxy-xyloside is not cytotoxic. We next investigated the impact of 4-MU4-deoxy-xyloside on cell growth using CellTrace™ CFSE cell proliferation kit. TGF-β1 stimulation produced an increased of about 3% in cell proliferation, whereas treatment with 4-MU4-deoxy-xyloside induced a decrease of about 15% in fibroblast proliferation as indicated by delay in cell division measured by CFSE dye and flow cytometry (Fig 5B and 5C). In addition, 4-MU4-deoxy-xyloside was able to counteract the stimulatory effect of TGF-β1 on cell proliferation and maintain a significant decrease (14%) in cell proliferation even in the presence of TGF-β1 (Fig 5B and 5C).

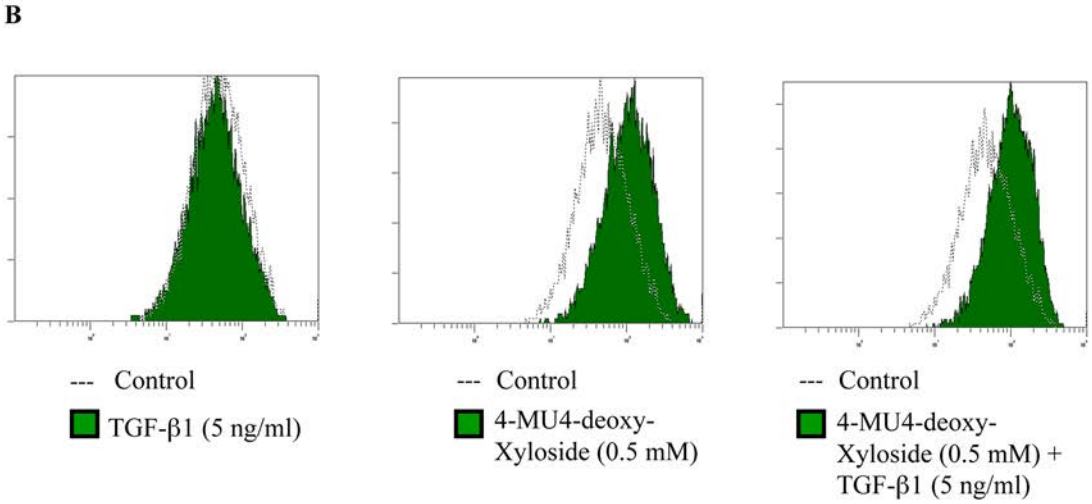
4-MU4-deoxy-xyloside reduces collagen synthesis in primary lung fibroblasts

Fibrosis is a process associated with overproduction of collagen type I, which together with PGs constitute the major contributor of the ECM deposition in the lung. We showed above that 4-MU4-deoxy-xyloside counteracts TGF-β1-induced increase in PG synthesis, we next examined the effect of 4-MU4-deoxy-xyloside on TGF-β1-induced production of fibrotic matrix collagen type I. Treatment of the cells with TGF-β1 increased by 4.7-fold the expression of collagen type I (Fig 6). Interestingly, in the presence of 4-MU4-deoxy-xyloside, TGF-β1-induced expression of collagen I was reduced by 70% (Fig 6), suggesting an anti-fibrotic role of 4-MU4-deoxy-xyloside in counteracting TGF-β1-induced ECM production.

4-MU4-deoxy-xyloside prevents fibrogenic activation of lung primary fibroblasts

In pulmonary fibrosis, TGF-β1 promotes transdifferentiation of quiescent fibroblasts into myofibroblasts which excessively produce ECM components [22, 23]. As 4-MU4-deoxy-xyloside was able to counteract TGF-β1 signaling, we therefore examined the effect of 4-MU4-deoxy-xyloside on TGF-β1-activation of fibroblasts by analysing the expression of α-smooth muscle actin (αSMA), a reliable marker of activation of fibroblasts. As shown in Fig 7A, qPCR analysis indicated a 3-fold induction in the expression of αSMA in TGF-β1-treated fibroblasts, compared to non-treated cells. However, in the presence of 4-MU4-deoxy-xyloside, TGF-β1 failed to induce the expression of αSMA. Similar results were obtained by Western blot (Fig 7B and 7C). This indicated that 4-MU4-deoxy-xyloside prevented fibroblast-to-myofibroblast trans-differentiation in response to TGF-β1.





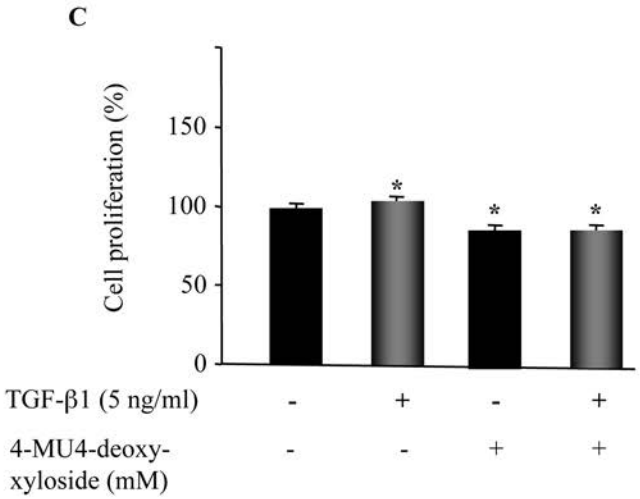


Fig 5. 4-MU4-deoxy-xyloside reduces cell viability and inhibits cell proliferation. Lung fibroblasts were treated with DMSO (Control) or with 500 μM of 4-MU4-deoxy-xyloside and/or TGF-β1 (5 ng/ml) for 24 h. **(A)** Cell viability was measured by MTT assay. The relative cell viability (%) was expressed as a percentage relative to control cells. **(B)** Cell proliferation was analyzed by CSFC labelling. **(C)** Bar graph shows cell proliferation expressed as percentage relative to control cells (DMSO). Data are expressed as mean ± SD of three separate experiments. *P<0.05 versus control.

doi:10.1371/journal.pone.0146499.g005

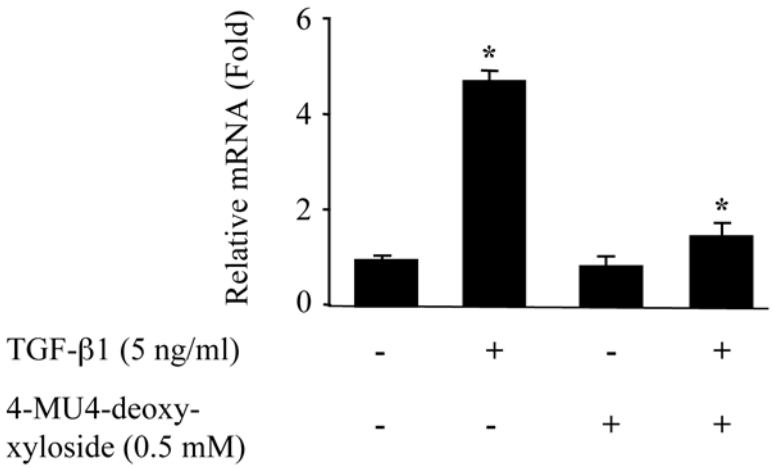


Fig 6. 4-MU4-deoxy-xyloside reduced TGF-β1-induced increased expression of collagen type 1. Lung fibroblasts were treated with 500 μM of 4-MU4-deoxy-xyloside and/or TGF-β1 (5 ng/ml) for 6 h and the expression of endogenous TGF-β1was analyzed by qPCR. The relative expression was normalized with ribosomal protein S29. Data are expressed as mean ± SD of three separate experiments, (*P<0.05).

doi:10.1371/journal.pone.0146499.g006

4-MU4-deoxy-xyloside inhibited the autocrine expression of TGF-β1 in primary lung fibroblasts

It is well known that TGF-β1 is expressed in an autocrine manner [24], therefore we examined whether 4-MU4-deoxy-xyloside could impair the endogenous TGF-β1 expression. Evaluation of TGF-β1 expression in response to external TGF-β1-stimulation showed an increase of about 3-fold, indicating that TGF-β1 is expressed in an autocrine manner in lung primary fibroblasts (Fig 8A). However, in the presence of 4-MU4-deoxy-xyloside, the induction of the expression of endogenous TGF-β1 transcripts by TGF-β1 was reduced by 30% (Fig 8A), indicating that 4-MU4-deoxy-xyloside was able to counteract to some extent the autocrine expression of TGF-β1 in lung primary fibroblasts.

We next measured active and total TGF-β1 levels in culture cell supernatant by ELISA. As shown in Fig 8B, the active and total TGF-β1 levels in culture supernatant of control cells were 28 ± 7 pg/ml and 287 ± 25 pg/ml, respectively, indicating that the total TGF-β1 level was about 10-fold higher than the active TGF-β1 level. Similar results were obtained when cells were treated with 4-MU4-deoxy-xyloside. Treatment with TGF-β1 increased by 1.5-fold and 7-fold the levels of total and active TGF-β1, respectively compared to control. Noteworthy, the total TGF-β1 level was only 2-fold higher than the active TGF-β1 level, indicating that stimulation of fibroblasts with TGF-β1 enhanced the secretion and activation of the cytokine. Interestingly, treatment with 4-MU4-deoxy-xyloside reduced TGF-β1-induced increased levels of total and active TGF-β1 by 20% and 30% (Fig 8B), respectively indicating that 4-MU4-deoxy-xyloside significantly reduced the activation and secretion of TGF-β1 in response to external TGF-β1 stimulation. Altogether, these results indicated that 4-MU4-deoxy-xyloside impairs TGF-β1-mediated activity in lung primary fibroblasts and pointed out the requirement for PG-GAGs for a profibrotic phenotype in lung fibroblast cells responding to TGF-β1.

Silencing of β4GalT7 impaired TGF-β1-induced effects in lung fibroblasts

To determine whether the effects produced by 4-MU4-deoxy-xyloside were specific to the inhibition of β4GalT7 enzyme activity, the expression of β4GalT7 was silenced by siRNA in lung

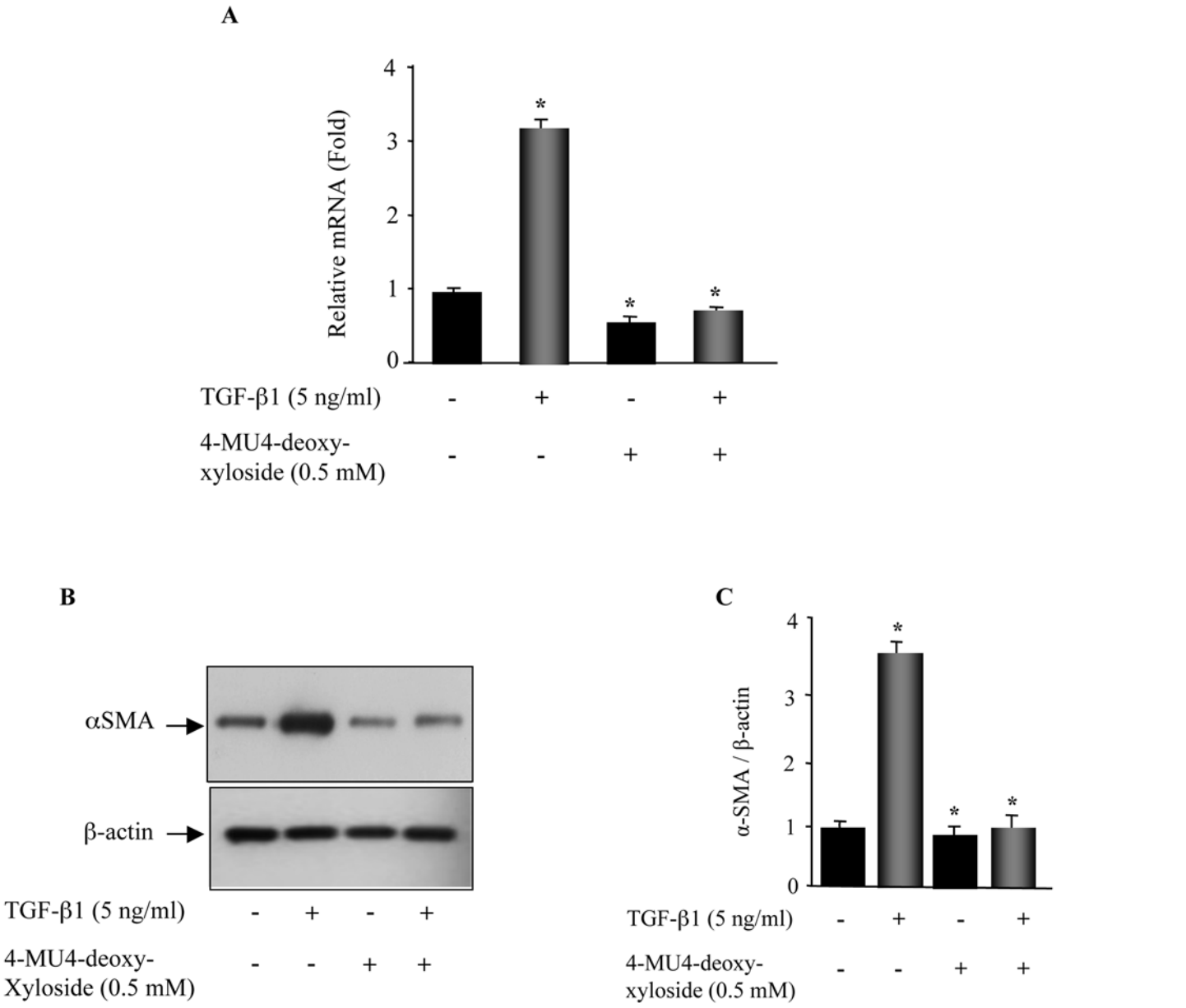


Fig 7. 4-MU4-deoxy-xyloside counteracts TGF-β1-induced fibroblast-to-myofibroblast trans-differentiation. Lung fibroblasts were treated with 500 μM of 4-MU4-deoxy-xyloside and/or TGF-β1 (5 ng/ml) for 24 h and the expression of αSMA was analyzed by qPCR (**A**) and by Western Blot (**B**). The relative expression was normalized with ribosomal protein S29. Data are expressed as mean ± SD of three separate experiments; *P<0.05 versus control. For Western blot, whole cell lysates were analysed αSMA content. β-actin was used as a loading control. **(C)** Bar graph shows the expression of αSMA relative to β-actin level and expressed relative to control lysate. Data are expressed as mean ± SD of three separate experiments; *P<0.05 versus control.

doi:10.1371/journal.pone.0146499.g007

fibroblasts and TGF-β1-induced effects were investigated. The knockdown of β4GalT7 decreased by about 75% the expression of β4GalT7, compared to control (Fig 9A) and reduced by 50% the level of PG synthesis (Fig 9B), indicating that silencing of β4GalT7 significantly impaired the synthesis of PGs. As observed for 4-MU4-deoxy-xyloside, silencing of β4GalT7 in lung fibroblasts counteracted TGF-β1-induced increase in PG synthesis. Indeed, TGF-β1 increased the level of PG synthesis by about 2-fold in control cells, whereas in β4GalT7

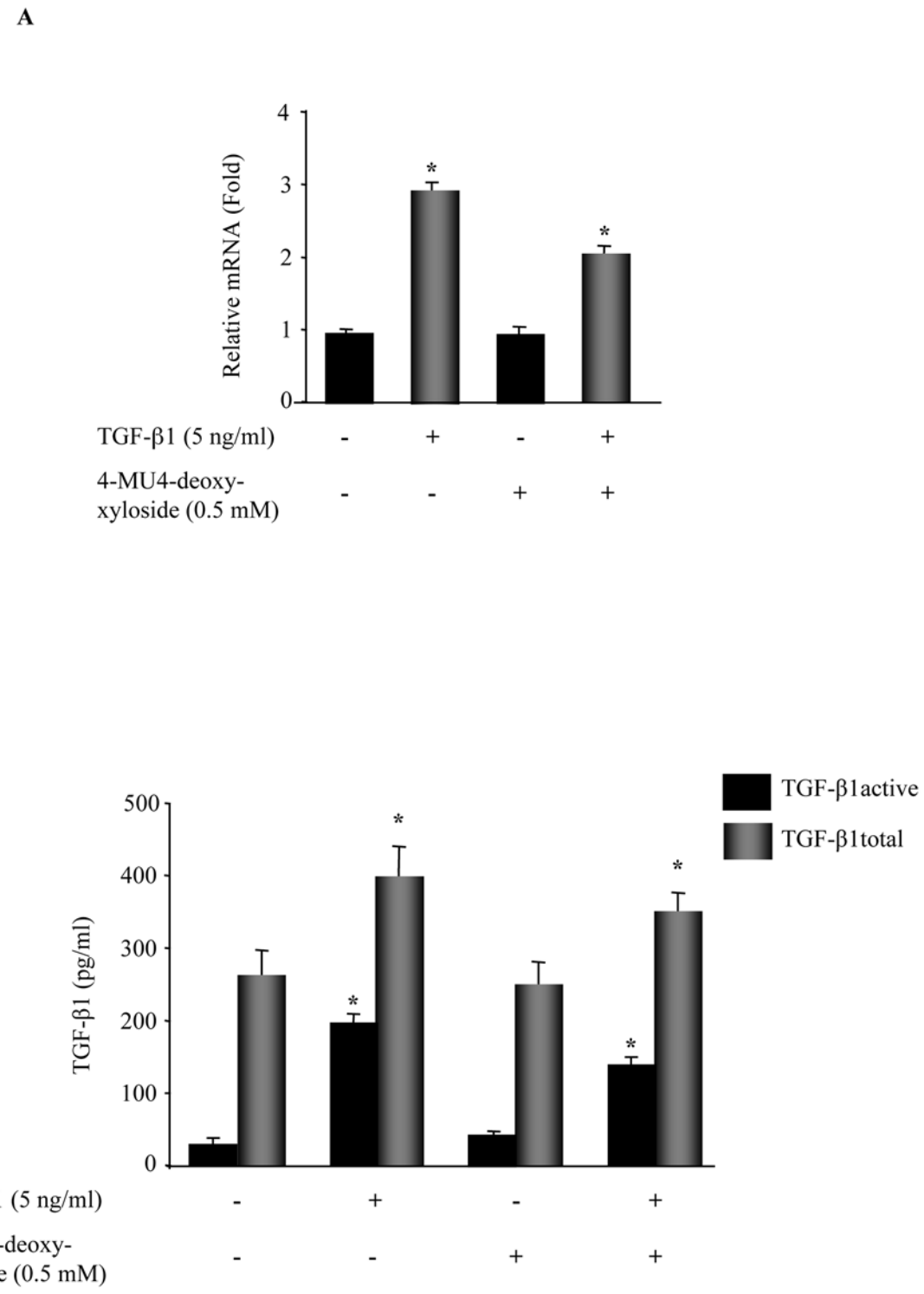


Fig 8. 4-MU4-deoxy-xyloside reduced TGF-β1-induced increased expression and actvation of endogenous TGF-β1. (A) Lung fibroblasts were treated with 500 μM of 4-MU4-deoxy-xyloside and/or TGF-β1 (5 ng/ml) for 6 h and the expression of endogenous TGF-β1was analyzed by qPCR. The relative expression was normalized with ribosomal protein S29. Data are expressed as mean ± SD of three separate experiments, (*P<0.05). **(B)** Fibroblasts were treated with 500 μM of 4-MU4-deoxy-xyloside and/or TGF-β1 (5 ng/ml) for 24 h and the total and active TGF-β1 levels were measured by ELISA in cell culture supernatants as described in Materials and methods section.

doi:10.1371/journal.pone.0146499.g008

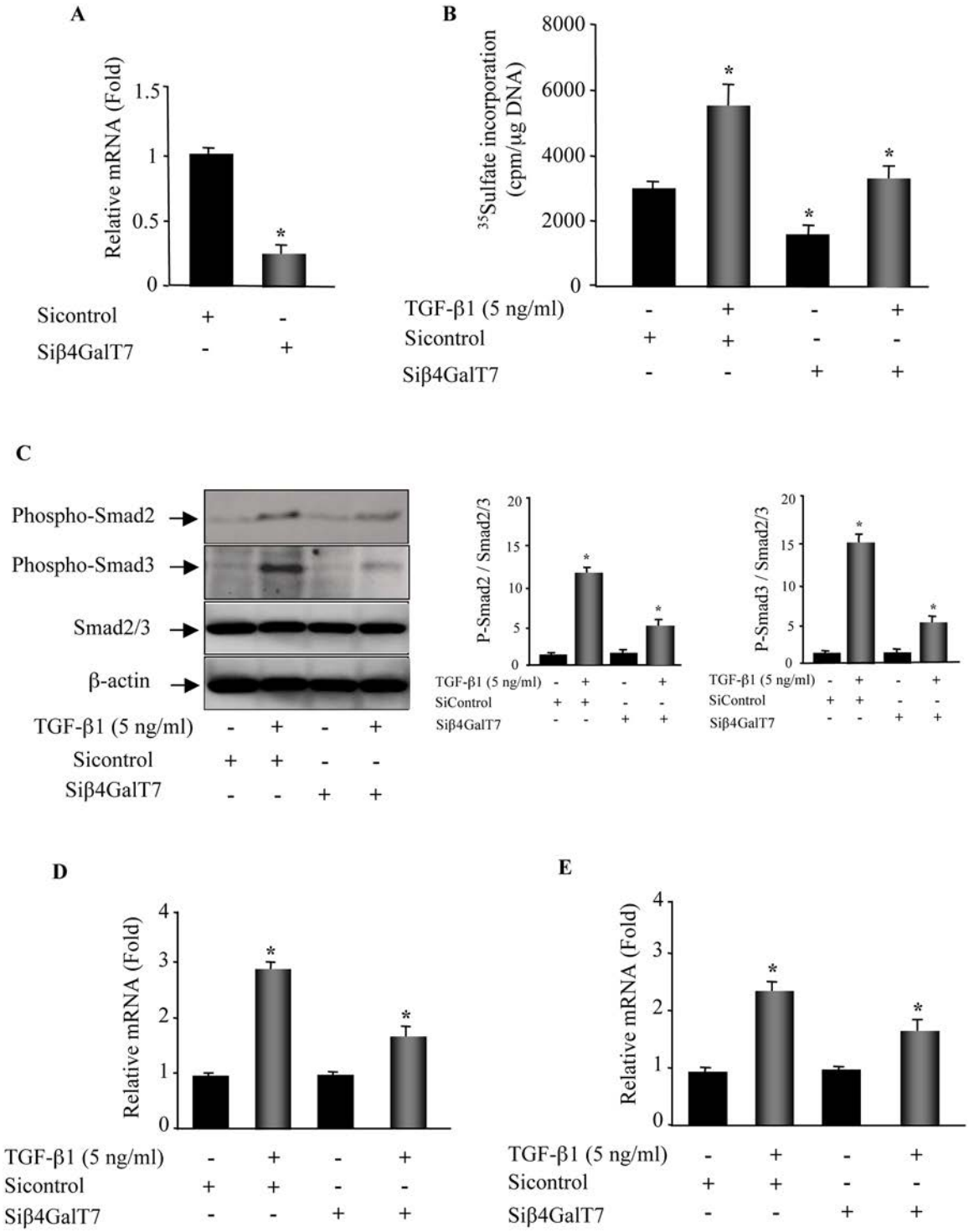


Fig 9. Silencing of β4GalT7 antagonized TGF-β1-induced expression of αSMA and TGFβ-1 and activation of Smad signaling pathway. (**A**) Lung fibroblasts were transfected with siRNA for β4GalT7 or siRNA control for 48 h and the expression of β4GalT7 was analysed by qPCR. (**B**) Cells transfected with Siβ4GalT7 or Sicontrol for 48 h were stimulated or not with TGF-β1 (5 ng/ml) for 24 h and the level of PG synthesis was measured by ^{35}Sulfate incorporation during the last 6h of TGF-β1 treatment. The radioactivity associated with GAGs was evaluated by liquid scintillation counting after CPC precipitation and normalized to DNA content. (**C**) Cells were transfected with Siβ4GalT7 or Sicontrol for 48 h then stimulated or not with TGF-β1 (5 ng/ml) for 3 h and assayed by Western blot to assess the levels of phosphorylation of Smad2 and Smad3. β-actin was used as a loading control. Bar graphs show the expression of phospho-Smad2 and phospho-Smad3 relative to total Smad2/3 level normalized to β-actin and expressed relative to control lysates. Data are expressed as mean ± SD of three separate experiments; *P<0.05 versus control. (**D**) and (**E**), the expression of αSMA and of endogenous TGF-β1 were

analysed by qPCR after 6 h of TGF-β1 treatment in fibroblasts transfected with Siβ4GalT7 and Sicontrol. The relative expression was normalized with ribosomal protein S29. Data are expressed as mean ± SD of three separate experiments; *P<0.05 versus control.

doi:10.1371/journal.pone.0146499.g009

knockdown cells the increase was only of about 14% (Fig 9B). Furthermore, investigation of the effect of β4GalT7 knockdown on TGF-β1 canonical signaling indicated that, as observed for 4-MU4-deoxy-xyloside, silencing of β4GalT7 antagonized TGF-β1-induced activation of Smad signaling pathway (Fig 9C). Moreover, similarly to 4-MU4-deoxy-xyloside, knockdown of β4GalT7 reduced TGF-β1-stimulated increase in the expression of αSMA from 3-fold to 1.5-fold (Fig 9D) and of endogenous TGF-β1 from 2.6-fold to 1.8-fold (Fig 9E), therefore antagonizing fibroblast-to-myofibroblast trans-differentiation and the autocrine expression of TGF-β1 induced by the cytokine. Altogether, these data showed that knockdown of β4GalT7 led to similar effects to those produced by 4-MU4-deoxy-xyloside in response to TGF-β1 stimulation in lung primary fibroblasts, indicating that the effects produced by 4-MU4-deoxy-xyloside were specific to the inhibition of β4GalT7 enzyme.

Discussion

Idiopathic pulmonary fibrosis is a progressive and fatal disease with no effective therapies. Lung transplantation is the only viable therapy for end stage organ failure [25, 26], therefore IPF represents a major unmet medical need for which novel therapeutic approaches are immediately required. Though inflammation has usually been considered as the major factor of lung fibrosis, emerging evidence [27] indicates that dysregulation of the ECM metabolism plays a critical role in pathogenesis of lung fibrosis, supporting studies on matrix production and deposition. One of the features of lung fibrosis is the accumulation of collagen and PGs in the ECM. The augmented levels of PGs in fibrosis is a part of the exacerbated accumulation of ECM constituents that is characteristic of the fibrotic process and as a cell response to increases in in the levels of profibrotic growth factors such as TGF-β. It is well known that PGs, owing to their ability to mediate the effects of several ligands, play a major role not only in ECM architecture but also in the regulation of several key cellular events such as proliferation and differentiation. Therefore, PG based therapies for IPF may be beneficial in clinical settings.

Earlier we have reported changes in glycosyltransferases as the underlying mechanism for abnormal PG biosynthetic activity in IPF, as well as the potential effect of TGF-β1 on PG-GAG biosynthetic machinery in pulmonary fibrosis [9]. Here we demonstrated for the first time that treatment of lung primary fibroblasts with 4-MU4-deoxy-xyloside, an inhibitor of β4GalT7, led to a strong decrease in PG synthesis. We demonstrated that 4-MU4-deoxy-xyloside inhibited the production and accumulation of both CS/DS-PGs and HS-PGs in primary fibroblasts. These observations indicated that 4-MU4-deoxy-xyloside could play an antifibrotic role in the formation of lung matrix by negatively regulating the synthesis of PGs.

TGF-β1 has been implicated as a key factor in the pathogenesis of fibrosis with stimulatory effects, among which are the increase of collagens, PGs, fibrotic growth factors [28]. Based on these reports, we investigated whether 4-MU4-deoxy-xyloside was able to prevent TGF-β1-induced increased PG synthesis in lung primary fibroblasts. Our results clearly showed that 4-MU4-deoxy-xyloside was able to counteract the increase in PG synthesis produced by the cytokine, indicating that 4-MU4-deoxy-xyloside is effective in preventing TGF-β1-induced production of PGs in lung primary fibroblasts.

Given that PGs are co-distributed with collagens in the ECM, and that small PGs such as decorin are critical for collagen deposition and integration into the ECM, inhibition of PG

synthesis by 4-MU4-deoxy-xyloside may influence the assembly of the ECM fibrils during lung fibrosis. Therefore, we examined whether 4-MU4-deoxy-xyloside affects the expression of other ECM proteins induced by TGF-β1 such as collagen type I, in addition to PG-GAGs. It was noted that fibroblasts cultured in the presence of 4-MU4-deoxy-xyloside alone produced no change in collagen I expression level. In contrast, 4-MU4-deoxy-xyloside inhibited the ability of TGF-β1 to increase collagen I transcripts. These findings indicate that collagen deposition into the ECM could be reduced in 4-MU4-deoxy-xyloside-treated fibroblasts. Previous studies have demonstrated that Smads act as crucial mediators for collagen regulation by TGF-β1 *in vitro*. It has been shown that transient overexpression of Smad3 in normal dermal fibroblasts mirrored the effect of TGF-β1 on collagen gene transcription [29], therefore inhibiting cellular Smad3 expression and/or phosphorylation would block type I collagen transcription by TGF-β1. Here we found that 4-MU4-deoxy-xyloside blocked the phosphorylation of Smad2/3, therefore a potential benefit of Smad2/3 inactivation by 4-MU4-deoxy-xyloside may favour inhibition of TGF-β1-induced collagen expression during fibrogenesis.

Increasing evidence points to the importance of fibroblast-to-myofibroblast trans-differentiation in fibrosis. Indeed, myofibroblasts express αSMA and regulate tissue regeneration, ECM production, cell-cell interaction and wound contraction [30]. TGF-β1 has been widely recognized as a key fibrogenic cytokine and has been demonstrated to activate fibroblasts differentiation into myofibroblasts *in vitro* and *in vivo* [31, 32] and to upregulate αSMA expression through the enhancement of Smad phosphorylation [33, 34]. Interestingly, we showed here that treatment of lung primary fibroblasts with 4-MU4-deoxy-xyloside prevented myofibroblast phenotype induced by TGF-β1 as evidenced by failure of TGF-β1 to induce the myofibroblast marker αSMA. These findings indicate that reduction of myofibroblast phenotype by 4-MU4-deoxy-xyloside might improve wound-healing and other features of tissue repair.

TGF-β1 is expressed in an autocrine manner [24] and understanding both active and total TGF-β1 levels would provide us with further insight into how TGF-β1 is involved in physiological and pathological conditions such as fibrosis. Our results demonstrated that the majority of TGF-β1 present in primary lung fibroblasts exists as a latent form with only a fraction being biologically active (10%). However, stimulation with TGF-β1 not only increased the secretion of TGF-β1, but also enhanced its activation as the active form represents up to 50% of the total levels of TGF-β1. Interestingly, treatment with 4-MU4-deoxy-xyloside reduced both secretion and activation of the cytokine, in response to external TGF-β1 stimulation.

To gain insight into the mechanism by which 4-MU4-deoxy-xyloside antagonized the effects of TGF-β1 in lung primary fibroblasts, we examined its effect on TGF-β signaling pathway. Once activated, TGF-β binds to TGFβ type II receptor leading to the recruitment of the TGFβ type I receptor which induces the phosphorylation of the downstream targets Smad2 and Smad3. TGF-β has another cell surface receptor, the HSPG β-glycan or TGF-β receptor III. This HSPG has two independent high-affinity binding domains for TGF-β [35], thus it can present TGF-β to the type II receptor to activate the canonical Smad signaling pathway [36]. It is well known that Smad signal transduction pathways are crucial in mediating TGF-β1 response in fibroblasts [37, 38]. Studies about fibroblasts derived from embryos null for either Smad3 or Smad2 revealed that TGF-β-regulated genes dependent on either Smad2 or Smad3 or both [39]. Investigation of the effect of 4-MU4-deoxy-xyloside on TGF-β1 phosphorylation of Smad2/3 and the expression of total Smad2/3 in lung primary fibroblasts showed that 4-MU4-deoxy-xyloside strongly attenuated the phosphorylation of Smad2 and Smad3 induced by TGF-β1. However, treatment with 4-MU-xyloside did not affected TGF-β1-induced Smad activation. Given that 4-MU-xyloside acts as a competitive acceptor with the endogenous core protein of PG for CS synthesis and primes soluble GAG chains of mainly CS-type, this suggests

that neither free CS-GAGs produced nor the competition with endogenous PG core proteins significantly alter TGF-β1 signaling.

To ascertain that the effects produced by 4-MU4-deoxy-xyloside in lung fibroblast cells were due to the specific inhibition of the β4GalT7, the expression of this enzyme was inhibited by siRNA in lung primary fibroblasts. The knockdown of β4GalT7 impaired TGF-β1-induced stimulation of PG synthesis, Smad signaling and, expression of αSMA and TGF-β1, thus leading to similar effects to those produced by 4-MU4-deoxy-xyloside and therefore, attributing the effects of 4-MU4-deoxy-xyloside to inhibition of the β4GalT7 enzyme.

The mechanism by which 4-MU4-deoxy-xyloside antagonized TGF-β1 signaling is unknown, however it has been shown that myoblasts require decorin for a full TGF-β cell response, by a mechanism that is dependent on the giant receptor lipoprotein receptor-related protein (LRP1) (74–75). We showed here that treatment of primary fibroblasts with 4-MU4-deoxy-xyloside led to strong decrease of PG synthesis in general and of decorin in particular. However, to determine whether this mechanism is relevant to lung fibroblasts needs further investigations. Noteworthy, TGF-β receptor type III or βglycan is an HS-PG that function as a TGF-β co-receptor by binding the TGF-β and presenting the ligand to the TGF-β type II receptor. Once bound to ligand, TGF-β type II receptor recruits and trans-phosphorylates the TGF-β type I receptor, activating its kinase function and leading to the phosphorylation of Smad2/3 [36]. Therefore, inhibition of HS-GAG chains synthesis may alter the function or the stability of this HSPG receptor and impairs TGF-β1 signaling.

To conclude, our present results demonstrate that 4-MU4-deoxy-xyloside affects fibroblast biosynthetic function and differentiation and reduced TGF-β1 auto-production which could affect in situ lung fibrotic repair. Collectively, our data suggest that 4-MU4-deoxy-xyloside holds therapeutic benefits as antifibrotic agent that may be valuable in pulmonary fibrosis.

Acknowledgments

The authors acknowledge Pr. Pierre Gillet for performing animal experiments and isolation of rat lung fibroblasts.

Author Contributions

Conceived and designed the experiments: MO IS. Performed the experiments: IS LB NV DL. Analyzed the data: MO NV. Contributed reagents/materials/analysis tools: JCJ SFG. Wrote the paper: MO IS.

References

1. Wynn TA. Integrating mechanisms of pulmonary fibrosis. The Journal of Experimental Medicine. 2011; 208(7):1339–50. doi: 10.1084/jem.20110551 PMID: 21727191
2. Gill S, Wight TN, Frevert CW. Proteoglycans: Key Regulators of Pulmonary Inflammation and the Innate Immune Response to Lung Infection. The Anatomical Record: Advances in Integrative Anatomy and Evolutionary Biology. 2010; 293(6):968–81. doi: 10.1002/ar.21094
3. Westergren-Thorsson G, Hernnäs J, Särnstrand B, Oldberg Å, Heinegård D, Malmström A. Altered expression of small proteoglycans, collagen, and transforming growth factor-beta 1 in developing bleomycin-induced pulmonary fibrosis in rats. Journal of Clinical Investigation. 1993; 92(2):632. PMID: 7688761
4. Venkatesan N, Ebihara T, Roughley P, Ludwig M. Alterations in Large and Small Proteoglycans in Bleomycin-Induced Pulmonary Fibrosis in Rats. American journal of respiratory and critical care medicine. 2000; 161(6):2066–73. doi: 10.1164/ajrccm.161.6.9909098 PMID: 10852789
5. Bensadoun ES, Burke AK, Hogg JC, Roberts CR. Proteoglycan deposition in pulmonary fibrosis. American journal of respiratory and critical care medicine. 1996; 154(6):1819–28. PMID: 8970376

6. Ebihara T, Venkatesan N, Tanaka R, Ludwig MS. Changes in Extracellular Matrix and Tissue Viscoelasticity in Bleomycin—induced Lung Fibrosis: Temporal Aspects. American journal of respiratory and critical care medicine. 2000; 162(4):1569–76. PMID: 11029378
7. Kliment C, Gochuico B, Kaminski N, Rosas I, Oury T. Contrasts between IPF and Mouse Models of Pulmonary Fibrosis. American journal of respiratory and critical care medicine. 2009; 179:A2716.
8. Sasisekharan R, Shriver Z, Venkataraman G, Narayanasami U. Roles of heparan-sulphate glycosaminoglycans in cancer. Nature Reviews Cancer. 2002; 2(7):521–8. PMID: 12094238
9. Venkatesan N, Tsuchiya K, Kolb M, Farkas L, Bourhim M, Ouzzine M, et al. Glycosyltransferases and Glycosaminoglycans in Bleomycin and Transforming Growth Factor-β1–Induced Pulmonary Fibrosis. American Journal of Respiratory Cell and Molecular Biology. 2014; 50(3):583–94. doi: 10.1165/rcmb.2012-0226OC PMID: 24127863
10. Lee CG, Cho SJ, Kang MJ, Chapoval SP, Lee PJ, Noble PW, et al. Early Growth Response Gene 1–mediated Apoptosis Is Essential for Transforming Growth Factor β1–induced Pulmonary Fibrosis. The Journal of Experimental Medicine. 2004; 200(3):377–89. doi: 10.1084/jem.20040104 PMID: 15289506
11. Kolb M, Margetts PJ, Sime PJ, Gauldie J. Proteoglycans decorin and biglycan differentially modulate TGF-β-mediated fibrotic responses in the lung. American Journal of Physiology-Lung Cellular and Molecular Physiology. 2001; 280(6):L1327–L34. PMID: 11350814
12. Kuberan B, Ethirajan M, Victor XV, Tran V, Nguyen K, Do A. "Click" Xylosides Initiate Glycosaminoglycan Biosynthesis in a Mammalian Cell Line. ChemBioChem. 2008; 9(2):198–200. PMID: 18085541
13. Eneyskaya EV, Ivanen DR, Shabalin KA, Kulminskaya AA, Backinowsky LV, Brumer Iii H, et al. Chemo-enzymatic synthesis of 4-methylumbelliferyl β-(1→ 4)-D-xylooligosides: new substrates for β-D-xylanase assays. Organic & Biomolecular Chemistry. 2005; 3(1):146–51.
14. Saliba M, Ramalanjaona N, Gulberti S, Bertin-Jung I, Thomas A, Dahbi S, et al. Probing the Acceptor Active Site Organization of the Human Recombinant β1, 4-Galactosyltransferase 7 and Design of Xyloside-based Inhibitors. Journal of Biological Chemistry. 2015; 290(12):7658–70. doi: 10.1074/jbc.M114.628123 PMID: 25568325
15. Venkatesan N, Roughley PJ, Ludwig MS. Proteoglycan expression in bleomycin lung fibroblasts: role of transforming growth factor-β1 and interferon-γ. American Journal of Physiology-Lung Cellular and Molecular Physiology. 2002; 283(4):L806–L14. PMID: 12225958
16. Dennler S, Itoh S, Vivien D, ten Dijke P, Huet S, Gauthier JM. Direct binding of Smad3 and Smad4 to critical TGF beta-inducible elements in the promoter of human plasminogen activator inhibitor-type 1 gene. The EMBO Journal. 1998; 17(11):3091–100. PMC1170648. PMID: 9606191
17. De Vries B, Van den Berg W, Vitters E, Van de Putte L. Quantitation of glycosaminoglycan metabolism in anatomically intact articular cartilage of the mouse patella: in vitro and in vivo studies with 35S-sulfate, 3H-glucosamine, and 3H-acetate. Rheumatology international. 1986; 6(6):273–81. PMID: 3809888
18. Quah BJC, Warren HS, Parish CR. Monitoring lymphocyte proliferation in vitro and in vivo with the intracellular fluorescent dye carboxyfluorescein diacetate succinimidyl ester. Nat Protocols. 2007; 2(9):2049–56. PMID: 17853860
19. Bradford MM. A rapid and sensitive method for the quantitation of microgram quantities of protein utilizing the principle of protein-dye binding. Analytical biochemistry. 1976; 72(1):248–54.
20. Leteux C, Chai W, Nagai K, Herbert CG, Lawson AM, Feizi T. 10E4 antigen of scrapie lesions contains an unusual nonsulfated heparan motif. Journal of Biological Chemistry. 2001; 276(16):12539–45. PMID: 11278655
21. Couchman JR. Transmembrane Signaling Proteoglycans. Annual Review of Cell and Developmental Biology. 2010; 26(1):89–114. doi: 10.1146/annurev-cellbio-100109-104126 PMID: 20565253.
22. Chambers RC, Leoni P, Kaminski N, Laurent GJ, Heller RA. Global expression profiling of fibroblast responses to transforming growth factor-β 1 reveals the induction of inhibitor of differentiation-1 and provides evidence of smooth muscle cell phenotypic switching. The American Journal of Pathology. 2003; 162(2):533–46. PMID: 12547711
23. Desmoulière A, Geinoz A, Gabbiani F, Gabbiani G. Transforming growth factor-beta 1 induces alpha-smooth muscle actin expression in granulation tissue myofibroblasts and in quiescent and growing cultured fibroblasts. The Journal of Cell Biology. 1993; 122(1):103–11. PMID: 8314838
24. Massagué J, Chen Y-G. Controlling TGF-β signaling. Genes & development. 2000; 14(6):627–44.
25. Mason DP, Brizzio ME, Alster JM, McNeill AM, Murthy SC, Budev MM, et al. Lung transplantation for idiopathic pulmonary fibrosis. The Annals of thoracic surgery. 2007; 84(4):1121–8. PMID: 17888957
26. George TJ, Arnaoutakis GJ, Shah AS. Lung transplant in idiopathic pulmonary fibrosis. Archives of Surgery. 2011; 146(10):1204–9. doi: 10.1001/archsurg.2011.239 PMID: 22006881

27. Keane MP, Strieter RM, Belperio JA. Mechanisms and mediators of pulmonary fibrosis. Critical Reviews™ in Immunology. 2005; 25(6):429–64.

28. Clarke D, Carruthers A, Mustelin T, Murray L. Matrix regulation of idiopathic pulmonary fibrosis: the role of enzymes. Fibrogenesis Tissue Repair. 2013; 6(1):1–9. doi: 10.1186/1755-1536-6-20

29. Ishida W, Mori Y, Lakos G, Sun L, Shan F, Bowes S, et al. Intracellular TGF-[beta] Receptor Blockade Abrogates Smad-Dependent Fibroblast Activation In Vitro and In Vivo. J Invest Dermatol. 2006; 126 (8):1733–44. PMID: 16741519

30. Kluwe J, Mencin A, Schwabe RF. Toll-like receptors, wound healing, and carcinogenesis. Journal of Molecular Medicine. 2009; 87(2):125–38. doi: 10.1007/s00109-008-0426-z PMID: 19089397

31. Hashimoto SHU, Gon Y, Takeshita I, Matsumoto KEN, Maruoka S, Horie T. Transforming growth factor-β1 induces phenotypic modulation of human lung fibroblasts to myofibroblast through a c-Jun-NH2-terminal kinase-dependent pathway. American journal of respiratory and critical care medicine. 2001; 163(1):152–7. PMID: 11208641

32. Sime PJ, Xing Z, Graham FL, Csaky KG, Gauldie J. Adenovector-mediated gene transfer of active transforming growth factor-beta1 induces prolonged severe fibrosis in rat lung. Journal of Clinical Investigation. 1997; 100(4):768. PMID: 9259574

33. Hu B, Wu Z, Phan SH. Smad3 mediates transforming growth factor-β–induced α-smooth muscle actin expression. American Journal of Respiratory Cell and Molecular Biology. 2003; 29(3):397–404. PMID: 12702545

34. Huang C, Shen S, Ma Q, Gill A, Pollock CA, Chen X-M. KCa3.1 mediates activation of fibroblasts in diabetic renal interstitial fibrosis. Nephrology Dialysis Transplantation. 2014; 29(2):313–24. doi: 10.1093/ndt/gft431

35. Esparza-López J, Montiel JL, Vilchis-Landeros MM, Okadome T, Miyazono K, López-Casillas F. Ligand Binding and Functional Properties of Betaglycan, a Co-receptor of the Transforming Growth Factor-β Superfamily. Specialized binding regions for transforming growth factor-beta and inhibin A. Specialized binding regions for transforming growth factor-β and inhibin A. Journal of Biological Chemistry. 2001; 276(18):14588–96. PMID: 11278442

36. López-Casillas F, Cheifetz S, Doody J, Andres JL, Lane WS, Massague J. Structure and expression of the membrane proteoglycan betaglycan, a component of the TGF-β receptor system. Cell. 1991; 67 (4):785–95. PMID: 1657406

37. Chen SJ, Yuan W, Lo S, Trojanowska M, Varga J. Interaction of Smad3 with a proximal smad-binding element of the human α2 (I) procollagen gene promoter required for transcriptional activation by TGF-β. J Cell Physiol. 2000; 183(3):381–92. PMID: 10797313

38. Verrecchia F, Chu M-L, Mauviel A. Identification of Novel TGF-β/Smad Gene Targets in Dermal Fibroblasts using a Combined cDNA Microarray/Promoter Transactivation Approach. Journal of Biological Chemistry. 2001; 276(20):17058–62. doi: 10.1074/jbc.M100754200 PMID: 11279127

39. Piek E, Ju WJ, Heyer J, Escalante-Alcalde D, Stewart CL, Weinstein M, et al. Functional Characterization of Transforming Growth Factor β Signaling in Smad2- and Smad3-deficient Fibroblasts. Journal of Biological Chemistry. 2001; 276(23):19945–53. doi: 10.1074/jbc.M102382200 PMID: 11262418

General discussion

General discussion

PGs are formed by the covalent attachment of the glycosaminoglycan (GAG) chains onto the core protein. Unlike DNA/RNA and proteins the synthesis of GAG chains is non-templet derived and they are synthesised by stepwise addition of sugar units by various enzymes. These sugar unites are also modified by sulphation at different positions and epimerization. Hence, PG-GAG are complex biomacromolecules present on the cell surface and ECM and they regulate various biological processes. Both PG core protein and GAG chains are required for various functions. However, it is now an established fact that GAG chains are responsible for most of the PGs functions (Couchman, 2010; Gesslbauer et al., 2013; Manon-Jensen et al., 2010). Both CSPGs and HSPGs are attached to the core protein with a common tetrasaccharide linker region formed by stepwise addition of individual sugar residues. The first step in the synthesis of common tetrasaccharide linker is the transfer of xylose from UDP-xylose to specific serine residues of core protein. This initial and rate limiting step is catalysed by xylosyltransferase (Götting et al., 2007; Wilson, 2004) and it has two isoforms, XT-I and XT-II encoded by *xylt-I* and *xylt-II* genes (Götting et al., 2007). XT-I is important in pathophysiology of osteoarthritis (Khair et al., 2013; Venkatesan et al., 2012; Venkatesan et al., 2009), whereas XT-II is mostly present in liver and XT-II KO mice develop polycystic liver diseases (Condac et al., 2007). XT is also secreted along with PGs into the extracellular matrix however the function of this secreted XT is still unknown. High level of XT-II was detected in the serum which is secreted from the platelets during blood coagulation process (Condac et al., 2009).

It has been previously shown that both XT-I and XT-II are able to initiate the GAG synthesis. We showed for the first time that GAG chains primed by XT-I displayed larger size compare to those primed by XT-II. PGs interaction with various ligands is mediated through GAG chains therefore the length of GAG chains might play a crucial role in this process.

The localization of XT-I and XT-II is still unclear, some groups suggest that XT is present in Golgi compartment, while other showed that xylosylation take place in the ER compartment (Schön et al., 2006b). We used specific antibodies to detect the localization of the XT isoforms by immunofluorescence and our results showed that XT-I is localized in the ER and completely co-localize with the ER marker calnexin, while XT-II is localized in the cis-Golgi and co-localize with the cis-Golgi marker GM130.

Targeting of XT-II to the ER using KDEL motif resulted in larger size GAGs indicating that the subcellular localization of XT enzyme dictates the size of the GAG chain. Interestingly, pulse and chase experiment showed that the GAG chains primed by XT-II were secreted earlier compare to the GAG chains primed by XT-I and by XT-II/KDEL. This confirms that the difference in GAG chains length is due to the difference in localization and sorting pathways of the GAG chains primed by XT-I and XT-II.

XT-I and XT-II mutations are reported in PXE (Schön et al., 2006d), diabetic neuropathy (Schön et al., 2006c), osteoarthritis (Schön et al., 2006a), abdominal arortic aneurysms (Götting et al., 2008b), diabetics (Götting et al., 2008a) and diabetic neuropathy (Bahr et al., 2006). The impact of these mutations on the GAG synthesis is unknown and only few contradictory reports on the A115S are available. In one report this mutant is associated with increased PG synthesis (Schön et al., 2006d) while in others it is associated with decreased PG biosynthesis (Ambrosius et al., 2009; Götting et al., 2008b) was reported. We showed that the XT-I mutants produce less GAG chains compare to wild-type enzyme and all are localized in the ER as wild-type XT-I. However, some mutants of the XT-II produce GAG chains similar like wild-type enzyme, whereas some mutants XT-II mutants did not initiate GAG synthesis. Further, the subcellular localization showed that R406C and P418L were retained in ER and did not show any enzyme activity. These mutants were not secreted into the ECM, while others mutants exhibit Golgi localization and were secreted into the ECM. Collectively, our results indicate that mutants of XT have altered GAG synthesis efficiency which might affect various cell functions.

The synthesis of CS- and HS-GAGs share a common tetrasaccharide primer, blocking of any step in the synthesis of this primer will obviously impact the synthesis of both CS and HS. We have demonstrated that phosphorylation of the xylose by Fam20B negatively regulates PG-GAG synthesis. Gain-of-function experiments showed that Fam20B strongly reduced PG-GAG chains synthesis, whereas loss-of-function increased the level of PG-GAG produced.

In agreement, a recent study in which overexpression of the xylose phosphatase (XYLP) that dephosphotylates xylose, increased PG synthesis for both CSPG and HSPG in Hela cells, whereas the knockdown of the phosphatase reduced the synthesis of both types of PGs (Koike et al., 2014). Our results also showed that Fam20B suppressed the synthesis of both

CS/DS-attached decorin and HS-attached syndecan-4 in CHO and HEK293 cells, whereas the knockdown of Fam20 led to an increase in the level of these PGs in the medium. This has been further confirmed using human skin and lung fibroblasts expressing high amount of endogenous decorin in the medium. We also showed that expression of Fam20B strongly attenuate the amount of cell surface HSPGs. Altogether, these data clearly demonstrate that Fam20B negatively regulates the synthesis of PGs of both types CS and HS. However, in contrast to this, it has been previously reported that stable expression of Fam20B in Hela cells enhanced PG-GAG synthesis (Koike et al., 2009). This raises the question whether Fam20B function in cell type specific manner. In this study we have used several cell lines as well as primary fibroblast cells and found that Fam20B blocks CSPG and HSPG synthesis in all the cells tested.

Previously, we have reported using synthetic xyloside analogs that β4GalT7 efficiently catalyzed the transfer of galactose residue onto the non-phosphorylated xyloside analogs, whereas the phosphorylated analog at 2-O position was not substrate, suggesting that the 2-O phosphorylation prevents the transfer of the galactose on xylose (Gulberti et al., 2005). Another group recently reported that most modifications of position 2 in xylose, rendered analogs less prone to galacosylation by β4GalT7 (Siegbahn et al., 2014). The same authors have shown previously that xylose analogs carrying modification on the 2-O position were not able to prime GAG synthesis in human cell lines (Siegbahn et al., 2011). These data indicate that the hydroxyl in position 2 might acts as a hydrogen bond acceptor. The crystal structure of β4GalT7 also revealed that the Tyr^{177}, Tyr^{179}, Trp^{207}, and Leu^{209} are important for the hydrophobic binding of the xylose and that the Asp^{211} forms a strong hydrogen bond with the OH present in the 4^{th} position of the acceptor xylose. Whereas, the Asp^{212} interacts via a hydrogen bond with the OH present at 2^{nd} position of the xylose (Tsutsui et al., 2013). Altogether, this indicates that phosphorylation of the xylose at 2-O position may alter this interaction or impair other essential interactions.

All the members of the Fam20 contain a conserved C-terminal domain including the catalytic domain DRHHYE and a DFG motif which is crucial for the metal ion binding. It has been shown that mutation of the aspartic acid residues present in the catalytic segment and in the

DFG motif of Fam20C abolished the enzyme activity (Tagliabracci et al., 2012). These aspartic acid residues are conserved in all members of the Fam20 family and correspond to Asp^{289} and Asp^{309} of the human Fam20B. Mutation of either of the two aspartic residues to alanine abolished the ability of Fam20B to block the synthesis of both CS- and HS-attached PGs, suggesting that mutation of Asp^{289} and Asp^{309} impaired Fam20B activity, consistent with the putative role of theses residues in catalysis and in the binding of the divalent cation Mn^{2+}, respectively. These results also confirm that Fam20B negatively regulates PG synthesis. It has been reported that EXTL2 transfer the GlcNAc residues on the tetrasaccharide when phosphorylated by Fam20B and this phosphorylated pentasaccharide could not be used for HS chain elongation and hence abolish GAG elongation (Koike et al., 2014). However, Katta et al., reported that overexpression of EXTL2 in HEK-293 cells did not affect the synthesis of PG-GAGs and showed that this is not due to lack of Fam20B in this cell line (Katta et al., 2015).

Our study strongly suggested that Fam20B acts immediately following the addition of xylose residue to block the synthesis of PG-GAG chains. This was supported by the facts that in CHO pgsB618 cells, deficient for β4GalT7, xyloside-modified decorin and syndecan 4 were produced in the medium, whereas in the presence of Fam20B their level was strongly reduced, suggesting that following Fam20B modification they are degraded inside the cells. We showed that this process was dependent on an active Fam20B enzyme. In addition, given that pgsB618 cells add only a xylose residue on PG core proteins these results indicate that addition of only xylose on the core protein is sufficient for Fam20B activity and strongly suggest that Fam20B acts immediately following the addition of xylose residue to block the synthesis of PG-GAG chains.

The importance of PGs and their GAG chains in cell proliferation and migration is well established (Mythreye and Blobe, 2009) and numerous PGs have been implicated in tumor growth and metastasis (Afratis et al., 2012). We have showed that expression of Fam20B reduced cell proliferation and migration in chondrosarcoma cells. This indicates that Fam20B-dependent inhibition of PG-GAG synthesis could contribute to the cell proliferation and migration defects in Fam20B-transfected chondrosarcoma cells.

Pulmonary fibrosis is characterized by extensive deposition of PGs, collagen fibers and myofibroblast proliferation. Until now, no effective therapies have been discovered, lung transplantation is the only viable therapy for end stage organ failure (George et al., 2011; Mason et al., 2007). TGF-β1 is the major cytokine mediates fibrosis. It is well known that PGs interact with several ligands through their GAG chains. Therefore, PG based therapies might be beneficial in clinical settings.

We have studied the effect of 4-MU4-deoxy-xyloside on TGF-β1-induced fibrosis in lung primary fibroblasts. We showed for the first time that treatment of lung primary fibroblasts with 4-MU4-deoxy-xyloside, a competent inhibitor of β4GalT7, led to a strong decrease in PG synthesis. We demonstrated that 4-MU4-deoxy-xyloside inhibited the production and accumulation of both CS/DS-PGs and HS-PGs in primary fibroblasts. Therefore, we hypothesized that reduction of the PGs synthesis by 4-MU4-deoxy-xyloside could play an antifibrotic role.

Our results showed that 4-MU4-deoxy-xyloside counteract TGF-β1-induced PG synthesis in lung primary fibroblasts. Treatment with 4-MU4-deoxy-xyloside also reduce collagen accumulation and deposition in the ECM, TGF-β1 activates fibroblasts differentiation into myofibroblasts *in vitro* and *in vivo* (Hashimoto et al., 2001; Sime et al., 1997) and upregulates αSMA expression through the enhancement of Smad phosphorylation (Hu et al., 2003; Huang et al., 2014). Interestingly, we showed that treatment of lung primary fibroblasts with 4-MU4-deoxy-xyloside prevented myofibroblast trans-differentiation induced by TGF-β1 by reducing the expression of the α-SMA.

Activated TGF-β binds to TGFβ type II receptor leading to the recruitment of the TGFβ type I receptor, which induces the phosphorylation of the downstream targets Smad2 and Smad3 (canonical pathway). TGF-β receptor III, the HSPG β-glycan, has two independent high-affinity binding domains for TGF-β (Esparza-López et al., 2001) and it can present TGF-β to the type II receptor to activate the canonical Smad signalling pathway (López-Casillas et al., 1991) which are crucial for TGF-β1 mediating response in fibroblasts (Chen et al., 2000; Verrecchia et al., 2001). Therefore, to understand the mechanism by which 4-MU4-deoxy-xyloside antagonized the effects of TGF-β1 in lung primary fibroblasts, we examined its effect TGF-β1 canonical signaling pathway. Investigation of the effect of 4-MU4-deoxy-xyloside on TGF-β1 induce phosphorylation

of Smad2/3 in lung primary fibroblasts showed that 4-MU4-deoxy-xyloside strongly attenuated the phosphorylation of Smad2 and Smad3 by TGF-β1, therefore indicating that inhibition of PG synthesis impaired TGF-β/Smad signaling pathway.

To determine that the effects produced by 4-MU4-deoxy-xyloside in lung fibroblast were due to specific inhibition of the β4GalT7, the expression of this enzyme was inhibited by siRNA in lung primary fibroblasts. Knockdown of β4GalT7 impaired TGF-β1-induced stimulation of PG synthesis, activation of Smad signaling pathway and increased expression of αSMA and TGF-β1, thus leading to similar effects to those produced by 4-MU4-deoxy-xyloside. Therefore, attributing the effects of 4-MU4-deoxy-xyloside to inhibition of the β4GalT7 enzyme. Collectively, our data suggest that targeting PGs biosynthesis pathways might act as novel therapeutics to treat pulmonary fibrosis.

Conclusions and perspectives

Conclusions and perspectives

Based on this work we could draw these conclusions, both XT-I and XT-II produce CSPGs and HSPGs, however, we showed that GAG chains primed by XT-I are longer compare to those initiated by XT-II. Moreover we showed that XT-II is more efficient compare to XT-I. It was controversial that whether xylosylation occur in the ER or Golgi, we have showed for the first time that XT-I is present in the ER, whereas XT-II is localized in the cis-Golgi. GAG chains primed by XT-II were secreted earlier compare to those initiated by XT-I, revealing that the GAG chains exhibit different sorting pathways.

The XT-I mutants studied produce less PG-GAGs compare to wild-type XT-I and localized in the ER. However, XT-II mutants R406C and P418L were retained in the ER and could not initiate GAG synthesis. Altogether, ours results showed that genetic mutations of XT-I and XT-II impaired PG synthesis and hence alter ECM composition/structure or/and cellular function.

The family of sequence similarity 20 (Fam20) comprises three members (Fam20-A, -B, -C). Fam20A and Fam20C phosphorylate majority of proteins and plays a crucial role in bone and teeth mineralization. However, Fam20B phosphorylate the xylose at 2-O position present in linker region of GAGs. We showed that gain-of-function of Fam20B negatively regulates the synthesis of CSPGs and HSPGs in various cell lines. Our results indicate that overexpression of Fam20B reduced cell migration and proliferation. Our results suggested that phosphorylation of the xylose occurs before the attachment of the galactose residue. We also showed that conserved aspartic acid residues (D298 and D309) are essential for the activity of Fam20B and that mutation of these residues abolish its catalytic activity.

Fibrosis is characterized by excessive deposition of PGs and collagen in the ECM and transdifferentiation of fibroblasts to myofibroblasts. Extensive accumulation of PGs play an important role in the pathogenesis of the pulmonary fibrosis, hence, inhibition of PGs synthesis might attenuates profibrotic effects of TGF-β1 in lung fibroblasts. We showed that 4-MU4-deoxy-xyloside inhibited CS- and HSPGs synthesis in a dose-dependent manner in primary lung fibroblasts. Importantly, 4-MU4-deoxy-xyloside was able to counteract TGF-β1-induced fibroblast-myofibroblast differentiation and TGF-β1 conical signaling (Figure 40).

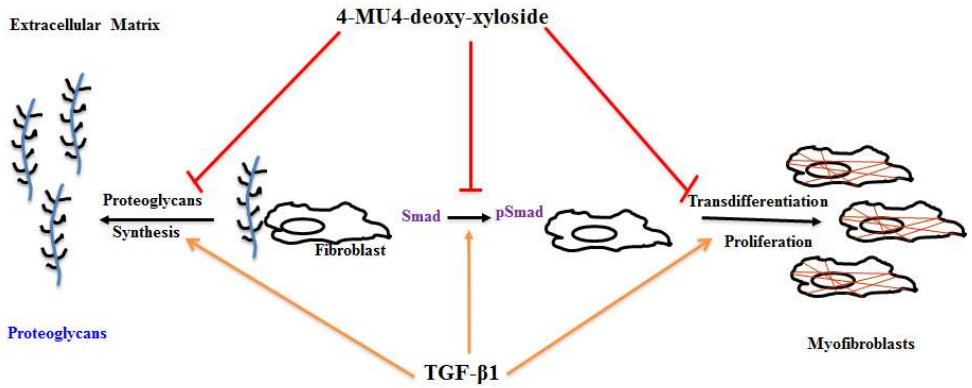


Figure 40:- Effects of 4-MU4-deoxy-xyloside on TGF-β1 induced fibrotic markers in primary lung fibroblast. Treatment with TGF-β1 enhanced PGs biosynthesis and transdifferentiation of fibroblast to myofibroblast through activation of canonical signaling pathway. However co-treatment with 4-MU4-deoxy-xyloside counteract these fibrotic phenotype.

As a prospective of this work we purposed that XT-I KO mice might be valuable to determine the physiological role of this enzyme. XT-I KO mice have not been reported yet, however XT-II KO mice are viable and develop polycystic liver and kidney disease. It will be interesting to solve the 3D ystal structure of XT to get better understanding of amino acid residues that interact with acceptor core protein and donor UDP-xylose. XT-I and XT-II primed GAG chains might have different sulphation pattern, hence it might be valuable to study the sulphation pattern of the GAG chains. We also believe that study of the secretion pathways of CS- and HSPGs primed by cell expressing XT-I or XT-II using live cell imaging techniques will be of great interest for the understanding of differences observed in GAG chain initiation by XT-I and XT-II.

Fam20B KO mice died at embryonic stage, however the underlining mechanism is not studied. Therefore, it is interesting to develop the in vivo model to explore physiological role of Fam20B. Until now, no genetic variants are reported for Fam20B. Hence, the family study might be an advantage to discover novel mutation in patients with PG-associated pathologies.

We showed that 4-MU4-deoxy-xyloside inhibits TGF-β1-induced PG production and fibrotic markers in primary lung fibroblast. It would be an advantage to test the effect of 4-MU4-deoxy-

xyloside in vivo in bleomycin-induced pulmonary fibrosis in mice or rat. It might be beneficial to test the effect of 4-MU4-deoxy-xyloside on skin, cardiac and liver fibrosis.

Bibliography

Bibliography

Aebi, M., 2013. N-linked protein glycosylation in the ER. Biochimica et Biophysica Acta (BBA) - Molecular Cell Research 1833, 2430-2437.

Afratis, N., Gialeli, C., Nikitovic, D., Tsegenidis, T., Karousou, E., Theocharis, A.D., Pavão, M.S., Tzanakakis, G.N., Karamanos, N.K., 2012. Glycosaminoglycans: key players in cancer cell biology and treatment. FEBS Journal 279, 1177-1197.

Almeida, R., Levery, S.B., Mandel, U., Kresse, H., Schwientek, T., Bennett, E.P., Clausen, H., 1999. Cloning and Expression of a Proteoglycan UDP-Galactose: β-Xylose β1, 4-Galactosyltransferase IA SEVENTH MEMBER OF THE HUMAN β4-GALACTOSYLTRANSFERASE GENE FAMILY. Journal of Biological Chemistry 274, 26165-26171.

Ambrosius, M., Kleesiek, K., Götting, C., 2009. The xylosyltransferase I gene polymorphism c.343G>T (p.A115S) is associated with decreased serum glycosaminoglycan levels. Clinical Biochemistry 42, 1-4.

Amenta, A.R., Creely, H.E., Mercado, M.L.T., Hagiwara, H., McKechnie, B.A., Lechner, B.E., Rossi, S.G., Wang, Q., Owens, R.T., Marrero, E., 2012. Biglycan is an extracellular MuSK binding protein important for synapse stability. The Journal of neuroscience 32, 2324-2334.

Bahr, C., Schön, S., Kuhn, J., Groop, P., Parkkonen, M., Wessman, M., Kleesiek, K., Götting, C., 2006a. Novel sequence variants in the human xylosyltransferase I gene and their role in diabetic nephropathy. Diabetic Medicine 23, 681-684.

Bahr, C., Schön, S., Kuhn, J., Groop, P.H., Parkkonen, M., Wessman, M., Kleesiek, K., Götting, C., 2006b. Novel sequence variants in the human xylosyltransferase I gene and their role in diabetic nephropathy. Diabetic Medicine 23, 681-684.

Baker, J.R., Rodén, L., Stoolmiller, A.C., 1972. Biosynthesis of chondroitin sulfate proteoglycan xylosyl transfer to Smith-degraded cartilage proteoglycan and other exogenous acceptors. Journal of Biological Chemistry 247, 3838-3847.

Barbouri, D., Afratis, N., Gialeli, C., Vynios, D.H., Theocharis, A.D., Karamanos, N., 2014. Syndecans as modulators and potential pharmacological targets in cancer progression. Frontiers in Oncology 4.

Berendsen, A.D., Fisher, L.W., Kilts, T.M., Owens, R.T., Robey, P.G., Gutkind, J.S., Young, M.F., 2011. Modulation of canonical Wnt signaling by the extracellular matrix component biglycan. Proceedings of the National Academy of Sciences 108, 17022-17027.

Bi, X.-L., Yang, W., 2013. Biological functions of decorin in cancer. Chinese journal of cancer 32, 266.

Bishop, J.R., Schuksz, M., Esko, J.D., 2007. Heparan sulphate proteoglycans fine-tune mammalian physiology. Nature 446, 1030-1037.

Bolton, K., Segal, D., McMillan, J., Jowett, J., Heilbronn, L., Abberton, K., Zimmet, P., Chisholm, D., Collier, G., Walder, K., 2008. Decorin is a secreted protein associated with obesity and type 2 diabetes. Int. J. Obesity 32, 1113-1121.

Bradford, M.M., 1976. A rapid and sensitive method for the quantitation of microgram quantities of protein utilizing the principle of protein-dye binding. Analytical biochemistry 72, 248-254.
Breton, C., Bettler, E., Joziasse, D.H., Geremia, R.A., Imberty, A., 1998. Sequence-Function Relationships of Prokaryotic and Eukaryotic Galactosyltransferases. Journal of Biochemistry 123, 1000-1009.

Brinkmann, T., Weilke, C., Kleesiek, K., 1997. Recognition of acceptor proteins by UDP-D-xylose proteoglycan core protein β-D-xylosyltransferase. Journal of Biological Chemistry 272, 11171-11175.

Bui, C., Huber, C., Tuysuz, B., Alanay, Y., Bole-Feysot, C., Leroy, J.G., Mortier, G., Nitschke, P., Munnich, A., Cormier-Daire, V., 2014. XYLT1 mutations in Desbuquois dysplasia type 2. The American Journal of Human Genetics 94, 405-414.

Bui, C., Talhaoui, I., Chabel, M., Mulliert, G., Coughtrie, M.W., Ouzzine, M., Fournel-Gigleux, S., 2010. Molecular characterization of β1, 4-galactosyltransferase 7 genetic mutations linked to the progeroid form of Ehlers–Danlos syndrome (EDS). FEBS Letters 584, 3962-3968.

Buraschi, S., Neill, T., Goyal, A., Poluzzi, C., Smythies, J., Owens, R.T., Schaefer, L., Torres, A., Iozzo, R.V., 2013. Decorin causes autophagy in endothelial cells via Peg3. Proceedings of the National Academy of Sciences 110, E2582-E2591.

Busse-Wicher, M., Wicher, K.B., Kusche-Gullberg, M., 2014. The extostosin family: Proteins with many functions. Matrix Biology 35, 25-33.

Byers, P.H., Murray, M.L., 2013. Ehlers–Danlos syndrome: A showcase of conditions that lead to understanding matrix biology. Matrix Biology.

Campbell, P., Jacobsson, I., Benzing-Purdie, L., Rodén, L., Fessler, J.H., 1984. Silk—A new substrate for UDP-d-xylose: Proteoglycan core protein β-d-xylosyltransferase. Analytical biochemistry 137, 505-516.

Campbell, S.C., Krueger, R.C., Schwartz, N.B., 1990. Deglycosylation of chondroitin sulfate proteoglycan and derived peptides. Biochemistry 29, 907-914.

Campos-Xavier, A.B., Martinet, D., Bateman, J., Belluoccio, D., Rowley, L., Tan, T.Y., Baxová, A., Gustavson, K.-H., Borochowitz, Z.U., Innes, A.M., Unger, S., Beckmann, J.S., Mittaz, L.,

Ballhausen, D., Superti-Furga, A., Savarirayan, R., Bonafé, L., 2009. Mutations in the Heparan-Sulfate Proteoglycan Glypican 6 (GPC6) Impair Endochondral Ossification and Cause Recessive Omodysplasia. The American Journal of Human Genetics 84, 760-770.

Cartault, F., Munier, P., Jacquemont, M.-L., Vellayoudom, J., Doray, B., Payet, C., Randrianaivo, H., Laville, J.-M., Munnich, A., Cormier-Daire, V., 2015. Expanding the clinical spectrum of B4GALT7 deficiency: homozygous p. R270C mutation with founder effect causes Larsen of Reunion Island syndrome. Europ. J. Hum. Genet. 23, 49-53.

Casanova, J.C., Kuhn, J., Kleesiek, K., Götting, C., 2008. Heterologous expression and biochemical characterization of soluble human xylosyltransferase II. Biochemical and Biophysical Research Communications 365, 678-684.

Chen, S., Birk, D.E., 2013. The regulatory roles of small leucine-rich proteoglycans in extracellular assembly. FEBS Journal.

Cho, S.H., Seymen, F., Lee, K.E., Lee, S.K., Kweon, Y.S., Kim, K.J., Jung, S.E., Song, S.J., Yildirim, M., Bayram, M., 2012. Novel FAM20A mutations in hypoplastic amelogenesis imperfecta. Human mutation 33, 91-94.

Choi, Y., Chung, H., Jung, H., Couchman, J.R., Oh, E.-S., 2011. Syndecans as cell surface receptors: unique structure equates with functional diversity. Matrix Biology 30, 93-99.

Condac, E., Dale, G.L., Bender-Neal, D., Ferencz, B., Towner, R., Hinsdale, M.E., 2009. Xylosyltransferase II is a significant contributor of circulating xylosyltransferase levels and platelets constitute an important source of xylosyltransferase in serum. Glycobiology 19, 829-833.
Condac, E., Silasi-Mansat, R., Kosanke, S., Schoeb, T., Towner, R., Lupu, F., Cummings, R.D., Hinsdale, M.E., 2007. Polycystic disease caused by deficiency in xylosyltransferase 2, an initiating enzyme of glycosaminoglycan biosynthesis. Proceedings of the National Academy of Sciences of the United States of America 104, 9416-9421.

Couchman, J.R., 2010. Transmembrane Signaling Proteoglycans. Annual Review of Cell and Developmental Biology 26, 89-114.

Cowman, M.K., Lee, H.-G., Schwertfeger, K.L., McCarthy, J.B., Turley, E.A., 2015. The Content and Size of Hyaluronan in Biological Fluids and Tissues. Frontiers in Immunology 6.

Cozza, G., Tagliabracci, V.S., Dixon, J.E., Pinna, L.A., 2015. “Genuine” Casein Kinase (Fam20C): The Mother of the Phosphosecretome. Kinomics: Approaches and Applications.

Cuellar, K., Chuong, H., Hubbell, S.M., Hinsdale, M.E., 2007. Biosynthesis of chondroitin and heparan sulfate in chinese hamster ovary cells depends on xylosyltransferase II. Journal of Biological Chemistry 282, 5195-5200.

D'Angelo, M., Greene, R.M., 1991. Transforming growth factor-β modulation of glycosaminoglycan production by mesenchymal cells of the developing murine secondary palate. Developmental Biology 145, 374-378.

David, G., Bai, X.M., Van Der Schueren, B., Cassiman, J.-J., Van Den Berghe, H., 1992. Developmental changes in heparan sulfate expression: in situ detection with mAbs. The Journal of Cell Biology 119, 961-975.

De Vries, B., Van den Berg, W., Vitters, E., Van de Putte, L., 1986. Quantitation of glycosaminoglycan metabolism in anatomically intact articular cartilage of the mouse patella: in vitro and in vivo studies with 35S-sulfate, 3H-glucosamine, and 3H-acetate. Rheumatology international 6, 273-281.

Dick, G., Akslen-Hoel, L.K., Grøndahl, F., Kjos, I., Prydz, K., 2012. Proteoglycan Synthesis and Golgi Organization in Polarized Epithelial Cells. J. Histochem. Cytochem. 60, 926-935.
Domowicz, M.S., Sanders, T.A., Ragsdale, C.W., Schwartz, N.B., 2008. Aggrecan is expressed by embryonic brain glia and regulates astrocyte development. Developmental Biology 315, 114-124.

Duncan, G., McCormick, C., Tufaro, F., 2001. The link between heparan sulfate and hereditary bone disease: finding a function for the EXT family of putative tumor suppressor proteins. Journal of Clinical Investigation 108, 511-516.

Dyck, S.M., Karimi-Abdolrezaee, S., 2015. Chondroitin sulfate proteoglycans: Key modulators in the developing and pathologic central nervous system. Experimental Neurology 269, 169-187.
Eames, B.F., Singer, A., Smith, G.A., Wood, Z.A., Yan, Y.-L., He, X., Polizzi, S.J., Catchen, J.M., Rodriguez-Mari, A., Linbo, T., Raible, D.W., Postlethwait, J.H., 2010. UDP xylose synthase 1 is required for morphogenesis and histogenesis of the craniofacial skeleton. Developmental Biology 341, 400-415.

Eames, B.F., Yan, Y.-L., Swartz, M.E., Levic, D.S., Knapik, E.W., Postlethwait, J.H., Kimmel, C.B., 2011. Mutations in *fam20b* and *xylt1* Reveal That Cartilage Matrix Controls Timing of Endochondral Ossification by Inhibiting Chondrocyte Maturation. PLoS Genet 7, e1002246.
Edwards, I.J., 2012. Proteoglycans in prostate cancer. Nat Rev Urol 9, 196-206.

Elderbroom, J.L., Huang, J.J., Gatza, C.E., Chen, J., How, T., Starr, M., Nixon, A.B., Blobe, G.C., 2014. Ectodomain shedding of TβRIII is required for TβRIII-mediated suppression of TGF-β signaling and breast cancer migration and invasion. Molecular biology of the cell 25, 2320-2332.
Esko, J.D., Selleck, S.B., 2002. Order Out of Chaos: Assembly of Ligand Binding Sites in Heparan Sulfate 1. Annual Review of Biochemistry 71, 435-471.

Faiyaz-Ul-Haque, M., Zaidi, S., Al-Mureikhi, M., Kennedy, S., Al-Thani, G., Tsui, L., Teebi, A., 2011. A novel missense mutation in the galactosyltransferase-I (B4GALT7) gene in a family exhibiting facioskeletal anomalies and Ehlers-Danlos syndrome resembling the progeroid type. QNRS Repository 2011, 2759.

Faiyaz-Ul-Haque, M., Zaidi, S.H.E., Al-Ali, M., Al-Mureikhi, M.S., Kennedy, S., Al-Thani, G., Tsui, L.C., Teebi, A.S., 2004. A novel missense mutation in the galactosyltransferase-I (B4GALT7) gene in a family exhibiting facioskeletal anomalies and Ehlers–Danlos syndrome resembling the progeroid type. American Journal of Medical Genetics Part A 128, 39-45.

Fico, A., Maina, F., Dono, R., 2011. Fine-tuning of cell signaling by glypicans. Cell. Mol. Life Sci. 68, 923-929.

Filmus, J., Capurro, M., 2014. The role of glypicans in Hedgehog signaling. Matrix Biology 35, 248-252.

Filmus, J., Capurro, M., Rast, J., 2008. Glypicans. Genome biology 9, 224.

Ford-Perriss, M., Turner, K., Guimond, S., Apedaile, A., Haubeck, H.-D., Turnbull, J., Murphy, M., 2003. Localisation of specific heparan sulfate proteoglycans during the proliferative phase of brain development. Dev. Dyn. 227, 170-184.

Fukunaga, Y., Sobue, M., Suzuki, N., Kushida, H., Suzuki, S., Suzuki, S., 1975. Synthesis of a fluorogenic mucopolysaccharide by chondrocytes in cell culture with 4-methylumbelliferyl β-d-xyloside. Biochimica et Biophysica Acta (BBA) - General Subjects 381, 443-447.

Galligani, L., Hopwood, J., Schwartz, N.B., Dorfman, A., 1975. Stimulation of synthesis of free chondroitin sulfate chains by beta-D-xylosides in cultured cells. Journal of Biological Chemistry 250, 5400-5406.

Gandhi, N.S., Mancera, R.L., 2008. The Structure of Glycosaminoglycans and their Interactions with Proteins. Chemical Biology & Drug Design 72, 455-482.

Garud, D.R., Tran, V.M., Victor, X.V., Koketsu, M., Kuberan, B., 2008. Inhibition of Heparan Sulfate and Chondroitin Sulfate Proteoglycan Biosynthesis. Journal of Biological Chemistry 283, 28881-28887.

Gesslbauer, B., Theuer, M., Schweiger, D., Adage, T., Kungl, A.J., 2013. New targets for glycosaminoglycans and glycosaminoglycans as novel targets. Expert Review of Proteomics 10, 77-95.

Gharbaran, R., 2015. Advances in the molecular functions of syndecan-1 (SDC1/CD138) in the pathogenesis of malignancies. Critical reviews in oncology/hematology 94, 1-17.

Giráldez, A.J., Copley, R.R., Cohen, S.M., 2002. HSPG modification by the secreted enzyme Notum shapes the Wingless morphogen gradient. Developmental cell 2, 667-676.

Götte, M., Kresse, H., 2005. Defective Glycosaminoglycan Substitution of Decorin in a Patient With Progeroid Syndrome Is a Direct Consequence of Two Point Mutations in the Galactosyltransferase I (ß4galT-7) Gene. Biochemical genetics 43, 65-77.

Götte, M., Spillmann, D., Yip, G.W., Versteeg, E., Echtermeyer, F.G., van Kuppevelt, T.H., Kiesel, L., 2008. Changes in heparan sulfate are associated with delayed wound repair, altered cell migration, adhesion and contractility in the galactosyltransferase I (ß4GalT-7) deficient form of Ehlers–Danlos syndrome. Human Molecular Genetics 17, 996-1009.

Götting, C., Hendig, D., Adam, A., Schön, S., Schulz, V., Szliska, C., Kuhn, J., Kleesiek, K., 2005. Elevated xylosyltransferase I activities in pseudoxanthoma elasticum (PXE) patients as a marker of stimulated proteoglycan biosynthesis. Journal of Molecular Medicine 83, 984-992.

Götting, C., Kuhn, J., Brinkmann, T., Kleesiek, K., 1998. Xylosylation of alternatively spliced isoforms of Alzheimer APP by xylosyltransferase. J. Protein Chem. 17, 295-302.

Götting, C., Kuhn, J., Kleesiek, K., 2007. Human xylosyltransferases in health and disease. Cell. Mol. Life Sci. 64, 1498-1517.

Götting, C., Kuhn, J., Kleesiek, K., 2008a. Serum Xylosyltransferase Activity in Diabetic Patients as a Possible Marker of Reduced Proteoglycan Biosynthesis. Diabetes Care 31, 2018-2019.

Götting, C., Kuhn, J., Zahn, R., Brinkmann, T., Kleesiek, K., 2000a. Molecular cloning and expression of human UDP-D-xylose: proteoglycan core protein β-D-xylosyltransferase and its first isoform XT-II. Journal of molecular biology 304, 517-528.

Götting, C., Kuhn, J., Zahn, R., Brinkmann, T., Kleesiek, K., 2000b. Molecular Cloning and Expression of Human UDP-d-Xylose:Proteoglycan Core Protein β-d-Xylosyltransferase and its First Isoform XT-II. Journal of molecular biology 304, 517-528.

Götting, C., Müller, S., Schöttler, M., Schön, S., Prante, C., Brinkmann, T., Kuhn, J., Kleesiek, K., 2004. Analysis of the DXD Motifs in Human Xylosyltransferase I Required for Enzyme Activity. Journal of Biological Chemistry 279, 42566-42573.

Götting, C., Prante, C., Schillinger, M., Exner, M., Domanovits, H., Raith, M., Kuhn, J., Kleesiek, K., 2008b. Xylosyltransferase I variants and their impact on abdominal aortic aneurysms. Clinica Chimica Acta 391, 41-45.

Götting, C., Sollberg, S., Kuhn, J., Weilke, C., Huerkamp, C., Brinkmann, T., Krieg, T., Kleesiek, K., 1999. Serum xylosyltransferase: a new biochemical marker of the sclerotic process in systemic sclerosis. Journal of investigative dermatology 112, 919-924.

Grebner, E.E., Hall, C.W., Neufeld, E.F., 1966a. Glycosylation of serine residues by a uridine diphosphate-xylose: Protein xylosyltransferase from mouse mastocytoma. Archives of Biochemistry and Biophysics 116, 391-398.

Grebner, E.E., Hall, C.W., Neufeld, E.F., 1966b. Incorporation of D-xylose-C 14 into glycoprotein by particles from hen oviduct. Biochemical and Biophysical Research Communications 22, 672-677.

Gregory, J.D., Laurent, T.C., Rodén, L., 1964. Enzymatic degradation of chondromucoprotein. Journal of Biological Chemistry 239, 3312-3320.

Grimpe, B., 2011. Deoxyribozymes: new therapeutics to treat central nervous system disorders. Frontiers in molecular neuroscience 4.

Grimpe, B., Pressman, Y., Bunge, M.B., Silver, J., 2005. The role of proteoglycans in Schwann cell/astrocyte interactions and in regeneration failure at PNS/CNS interfaces. Molecular and Cellular Neuroscience 28, 18-29.

Grimpe, B., Silver, J., 2004. A novel DNA enzyme reduces glycosaminoglycan chains in the glial scar and allows microtransplanted dorsal root ganglia axons to regenerate beyond lesions in the spinal cord. The Journal of neuroscience 24, 1393-1397.

Gulberti, S., Lattard, V., Fondeur, M., Jacquinet, J.C., Mulliert, G., Netter, P., Magdalou, J., Ouzzine, M., Fournel-Gigleux, S., 2005a. Modifications of the glycosaminoglycan-linkage region of proteoglycans: phosphorylation and sulfation determine the activity of the human beta1,4-galactosyltransferase 7 and beta1,3-glucuronosyltransferase I. TheScientificWorldJournal [electronic resource]. 5, 510-514.

Gulberti, S., Lattard, V., Fondeur, M., Jacquinet, J.C., Mulliert, G., Netter, P., Magdalou, J., Ouzzine, M., Fournel-Gigleux, S., 2005b. Phosphorylation and sulfation of oligosaccharide substrates critically influence the activity of human β1,4-galactosyltransferase 7 (GalT-I) and β1,3-glucuronosyltransferase I (GlcAT-I) involved in the biosynthesis of the glycosaminoglycan-protein linkage region of proteoglycans. Journal of Biological Chemistry 280, 1417-1425.

Hacker, U., Nybakken, K., Perrimon, N., 2005. Heparan sulphate proteoglycans: the sweet side of development. Nat Rev Mol Cell Biol 6, 530-541.

Hashemian, S., Marschinke, F., af Bjerkén, S., Strömberg, I., 2014. Degradation of proteoglycans affects astrocytes and neurite formation in organotypic tissue cultures. Brain Res. 1564, 22-32.
Helting, T., Rodén, L., 1968. Studies on the biosynthesis of the chondroitin sulfate-protein linkage region. Biochemical and Biophysical Research Communications 31, 786-791.

Hendig, D., Tarnow, L., Kuhn, J., Kleesiek, K., Götting, C., 2008. Identification of a xylosyltransferase II gene haplotype marker for diabetic nephropathy in type 1 diabetes. Clinica Chimica Acta 398, 90-94.

Hoffmann, H.-P., Schwartz, N.B., Rodén, L., Prockop, D.J., 1984. Location of xylosyltransferase in the cisternae of the rough endoplasmic reticulum of embryonic cartilage cells. Connective Tissue Research 12, 151-163.

Holmes, E.H., Yen, T.-Y., Thomas, S., Joshi, R., Nguyen, A., Long, T., Gallet, F., Maftah, A., Julien, R., Macher, B.A., 2000. Human α1, 3/4 Fucosyltransferases CHARACTERIZATION OF HIGHLY CONSERVED CYSTEINE RESIDUES ANDN-LINKED GLYCOSYLATION SITES. Journal of Biological Chemistry 275, 24237-24245.

Horwitz, A.L., Dorfman, A., 1968. SUBCELLUAR SITES FOR SYNTHESIS OF CHONDROMUCOPROTEIN OF CARTILAGE. The Journal of Cell Biology 38, 358-368.

Huber, S., Winterhalter, K.H., Vaughan, L., 1988. Isolation and sequence analysis of the glycosaminoglycan attachment site of type IX collagen. Journal of Biological Chemistry 263, 752-756.

Iozzo, R.V., 2005. Basement membrane proteoglycans: from cellar to ceiling. Nat Rev Mol Cell Biol 6, 646-656.

Iozzo, R.V., Schaefer, L., 2015. Proteoglycan form and function: A comprehensive nomenclature of proteoglycans. Matrix Biology.

Ishikawa, H.O., Takeuchi, H., Haltiwanger, R.S., Irvine, K.D., 2008. Four-jointed is a Golgi kinase that phosphorylates a subset of cadherin domains. Science 321, 401-404.

Izumikawa, T., Sato, B., Mikami, T., Tamura, J.-i., Igarashi, M., Kitagawa, H., 2015. GlcUAβ1-3Galβ1-3Galβ1-4Xyl(2-O-phosphate) is the preferred substrate for chondroitin N-acetylgalactosaminyltransferase-1. Journal of Biological Chemistry.

Järveläinen, H., Sainio, A., Wight, T.N., 2015. Pivotal role for decorin in angiogenesis. Matrix Biology 43, 15-26.

Jaureguiberry, G., Parry, D., Quentric, M., Himmerkus, N., Koike, T., Poulter, J., Klootwijk, E., Robinette, S., Howie, A., Patel, V., 2013. Nephrocalcinosis (Enamel Renal Syndrome) Caused by Autosomal Recessive FAM20A Mutations. Nephron Physiology 122, 1-6.

Jin, C.L., Oh, J.-H., Han, M., Shin, M.K., Yao, C., Park, C.-H., Jin, Z.H., Chung, J.H., 2015. UV irradiation-induced production of monoglycosylated biglycan through downregulation of xylosyltransferase 1 in cultured human dermal fibroblasts. Journal of Dermatological Science 79, 20-29.

Johnsson, R., Mani, K., Ellervik, U., 2007. Synthesis and biology of bis-xylosylated dihydroxynaphthalenes. Bioorganic & Medicinal Chemistry 15, 2868-2877.

Kantaputra, P.N., Kaewgahya, M., Khemaleelakul, U., Dejkhamron, P., Sutthimethakorn, S., Thongboonkerd, V., Iamaroon, A., 2014. Enamel-renal-gingival syndrome and FAM20A mutations. American Journal of Medical Genetics Part A 164, 1-9.

Katta, K., Imran, T., Busse-Wicher, M., Grønning, M., Czajkowski, S., Kusche-Gullberg, M., 2015. Reduced expression of EXTL2, a member of the EXT family of glycosyltransferases, in human embryonic kidney 293 cells results in longer heparan sulfate chains. Journal of Biological Chemistry 282, 32802-32810.

Kearns, A.E., Vertel, B.M., Schwartz, N.B., 1993. Topography of glycosylation and UDP-xylose production. Journal of Biological Chemistry 268, 11097-11104.

Khair, M., Bourhim, M., Barré, L., Li, D., Netter, P., Magdalou, J., Fournel-Gigleux, S., Ouzzine, M., 2012. Regulation of Xylosyltransferase I gene expression by interleukin 1β in human primary chondrocyte cells: mechanism and impact on proteoglycan synthesis. Journal of Biological Chemistry.

Khair, M., Bourhim, M., Barré, L., Li, D., Netter, P., Magdalou, J., Fournel-Gigleux, S., Ouzzine, M., 2013. Regulation of Xylosyltransferase I Gene Expression by Interleukin 1β in Human Primary Chondrocyte Cells MECHANISM AND IMPACT ON PROTEOGLYCAN SYNTHESIS. Journal of Biological Chemistry 288, 1774-1784.

Kischel, P., Waltregny, D., Dumont, B., Turtoi, A., Greffe, Y., Kirsch, S., De Pauw, E., Castronovo, V., 2010. Versican overexpression in human breast cancer lesions: known and new isoforms for stromal tumor targeting. Int. J. Cancer 126, 640-650.

Koike, T., Izumikawa, T., Sato, B., Kitagawa, H., 2014. Identification of Phosphatase That Dephosphorylates Xylose in the Glycosaminoglycan-Protein Linkage Region of Proteoglycans. Journal of Biological Chemistry 289, 6695-6708.

Koike, T., Izumikawa, T., Tamura, J.I., Kitagawa, H., 2009. FAM20B is a kinase that phosphorylates xylose in the glycosaminoglycan–protein linkage region. Biochemical Journal 421, 157-162.

Kolset, S.O., Pejler, G., 2011. Serglycin: a structural and functional chameleon with wide impact on immune cells. The Journal of Immunology 187, 4927-4933.

Koslowski, R., Pfeil, U., Fehrenbach, H., Kasper, M., Skutelsky, E., Wenzel, K., 2001. Changes in xylosyltransferase activity and in proteoglycan deposition in bleomycin-induced lung injury in rat. European Respiratory Journal 18, 347-356.

Koziel, L., Kunath, M., Kelly, O.G., Vortkamp, A., 2004. Ext1-dependent heparan sulfate regulates the range of Ihh signaling during endochondral ossification. Developmental cell 6, 801-813.

Kuhn, J., Götting, C., Beahm, B.J., Bertozzi, C.R., Faust, I., Kuzaj, P., Knabbe, C., Hendig, D., 2015. Xylosyltransferase II is the predominant isoenzyme which is responsible for the steady-state level of xylosyltransferase activity in human serum. Biochemical and Biophysical Research Communications 459, 469-474.

Kuhn, J., Götting, C., Schnölzer, M., Kempf, T., Brinkmann, T., Kleesiek, K., 2001. First isolation of human UDP-D-xylose: proteoglycan core protein β-D-xylosyltransferase secreted from cultured JAR choriocarcinoma cells. Journal of Biological Chemistry 276, 4940-4947.

Kuhn, J., Gressner, O.A., Götting, C., Gressner, A.M., Kleesiek, K., 2009. Increased serum xylosyltransferase activity in patients with liver fibrosis. Clinica Chimica Acta 409, 123-126.

Kuhn, J., Müller, S., Schnölzer, M., Kempf, T., Schön, S., Brinkmann, T., Schöttler, M., Götting, C., Kleesiek, K., 2003. High-level expression and purification of human xylosyltransferase I in High Five insect cells as biochemically active form. Biochemical and Biophysical Research Communications 312, 537-544.

Kusano, Y., Yoshitomi, Y., Munesue, S., Okayama, M., Oguri, K., 2004. Cooperation of syndecan-2 and syndecan-4 among cell surface heparan sulfate proteoglycans in the actin cytoskeletal organization of Lewis lung carcinoma cells. Journal of Biochemistry 135, 129-137.

Labropoulou, V.T., Skandalis, S.S., Ravazoula, P., Perimenis, P., Karamanos, N.K., Kalofonos, H.P., Theocharis, A.D., 2013. Expression of syndecan-4 and correlation with metastatic potential in testicular germ cell tumours. BioMed research international 2013.

Lau, L.W., Keough, M.B., Haylock-Jacobs, S., Cua, R., Döring, A., Sloka, S., Stirling, D.P., Rivest, S., Yong, V.W., 2012. Chondroitin sulfate proteoglycans in demyelinated lesions impair remyelination. Ann. Neurol. 72, 419-432.

Laville, J., Lakermance, P., Limouzy, F., 1994. Larsen's syndrome: review of the literature and analysis of thirty-eight cases. Journal of Pediatric Orthopaedics 14, 63-73.

Lee, H., Kim, Y., Choi, Y., Choi, S., Hong, E., Oh, E.-S., 2011. Syndecan-2 cytoplasmic domain regulates colon cancer cell migration via interaction with syntenin-1. Biochemical and Biophysical Research Communications 409, 148-153.

Leonova, E.I., Galzitskaya, O.V., 2013. Structure and functions of syndecans in vertebrates. Biochemistry Moscow 78, 1071-1085.

Leonova, E.I., Galzitskaya, O.V., 2015. Cell communication using intrinsically disordered proteins: what can syndecans say? J. Biomol. Struct. Dyn. 33, 1037-1050.

Leteux, C., Chai, W., Nagai, K., Herbert, C.G., Lawson, A.M., Feizi, T., 2001. 10E4 antigen of scrapie lesions contains an unusual nonsulfated heparan motif. Journal of Biological Chemistry 276, 12539-12545.

Li, L., Ly, M., Linhardt, R.J., 2012. Proteoglycan sequence. Molecular BioSystems 8, 1613-1625.
Li, M., Shuman, C., Fei, Y.L., Cutiongco, E., Bender, H.A., Stevens, C., Wilkins-Haug, L., Day-Salvatore, D., Yong, S.L., Geraghty, M.T., Squire, J., Weksberg, R., 2001. GPC3 mutation analysis in a spectrum of patients with overgrowth expands the phenotype of Simpson-Golabi-Behmel syndrome. American Journal of Medical Genetics 102, 161-168.

Li, Y., Liu, Y., Xia, W., Lei, D., Voorhees, J.J., Fisher, G.J., 2013. Age-dependent alterations of decorin glycosaminoglycans in human skin. Sci. Rep. 3.

Liang, S., Xu, J., Cao, W., Li, H., Hu, C., 2013. Human decorin regulates proliferation and migration of human lung cancer A549 cells. Chin Med J (Engl) 126, 4736-4741.
Lohmander, L.S., Shinomura, T., Hascall, V.C., Kimura, J.H., 1989. Xylosyl tra
nsfer to the core protein precursor of the rat chondrosarcoma proteoglycan. Journal of Biological Chemistry 264, 18775-18780.

López-Casillas, F., Cheifetz, S., Doody, J., Andres, J.L., Lane, W.S., Massague, J., 1991. Structure and expression of the membrane proteoglycan betaglycan, a component of the TGF-β receptor system. Cell 67, 785-795.

Lugemwa, F.N., Esko, J., 1991. Estradiol beta-D-xyloside, an efficient primer for heparan sulfate biosynthesis. Journal of Biological Chemistry 266, 6674-6677.

Mani, K., Belting, M., Ellervik, U., Falk, N., Svensson, G., Sandgren, S., Cheng, F., Fransson, L.-Å., 2004a. Tumor attenuation by 2(6-hydroxynaphthyl)-β-d-xylopyranoside requires priming of heparan sulfate and nuclear targeting of the products. Glycobiology 14, 387-397.

Mani, K., Cheng, F., Sandgren, S., Van Den Born, J., Havsmark, B., Ding, K., Fransson, L.-Å., 2004b. The heparan sulfate–specific epitope 10E4 is NO-sensitive and partly inaccessible in glypican-1. Glycobiology 14, 599-607.

Mani, K., Havsmark, B., Persson, S., Kaneda, Y., Yamamoto, H., Sakurai, K., Ashikari, S., Habuchi, H., Suzuki, S., Kimata, K., 1998. Heparan/chondroitin/dermatan sulfate primer 2-(6-hydroxynaphthyl)-O-β-d-xylopyranoside preferentially inhibits growth of transformed cells. Cancer Res. 58, 1099-1104.

Mann, D.M., Yamaguchi, Y., Bourdon, M.A., Ruoslahti, E., 1990. Analysis of glycosaminoglycan substitution in decorin by site-directed mutagenesis. Journal of Biological Chemistry 265, 5317-5323.

Manon-Jensen, T., Itoh, Y., Couchman, J.R., 2010. Proteoglycans in health and disease: The multiple roles of syndecan shedding. FEBS Journal 277, 3876-3889.

Manon-Jensen, T., Multhaupt, H.A.B., Couchman, J.R., 2013. Mapping of matrix metalloproteinase cleavage sites on syndecan-1 and syndecan-4 ectodomains. FEBS Journal 280, 2320-2331.

Matsuo, I., Kimura-Yoshida, C., 2013. Extracellular modulation of Fibroblast Growth Factor signaling through heparan sulfate proteoglycans in mammalian development. Curr. Opin. Genet. Dev. 23, 399-407.

McCormick, C., Duncan, G., Goutsos, K.T., Tufaro, F., 2000. The putative tumor suppressors EXT1 and EXT2 form a stable complex that accumulates in the Golgi apparatus and catalyzes the synthesis of heparan sulfate. Proceedings of the National Academy of Sciences 97, 668-673.
Mikami, T., Kitagawa, H., 2013. Biosynthesis and function of chondroitin sulfate. Biochimica et Biophysica Acta (BBA) - General Subjects 1830, 4719-4733.

Mis, E.K., Liem Jr, K.F., Kong, Y., Schwartz, N.B., Domowicz, M., Weatherbee, S.D., 2014. Forward genetics defines Xylt1 as a key, conserved regulator of early chondrocyte maturation and skeletal length. Developmental Biology 385, 67-82.

Mizumoto, S., Ikegawa, S., Sugahara, K., 2013. Human Genetic Disorders Caused by Mutations in Genes Encoding Biosynthetic Enzymes for Sulfated Glycosaminoglycans. Journal of Biological Chemistry 288, 10953-10961.

Mizumoto, S., Yamada, S., Sugahara, K., 2015. Molecular interactions between chondroitin–dermatan sulfate and growth factors/receptors/matrix proteins. Current Opinion in Structural Biology 34, 35-42.

Moses, J., Oldberg, Å., Cheng, F., Fransson, L.-Å., 1997. Biosynthesis of the Proteoglycan Decorin Transient 2-Phosphorylation of Xylose during Formation of the Trisaccharide Linkage Region. Eur. J. Biochem. 248, 521-526.

Muir, H., 1958. The nature of the link between protein and carbohydrate of a chondroitin sulphate complex from hyaline cartilage. Biochemical Journal 69, 195.

Müller, B., Prante, C., Kleesiek, K., Götting, C., 2009. Identification and characterization of the human xylosyltransferase I gene promoter region. Journal of Biological Chemistry 284, 30775-30782.

Müller, B., Prante, C., Knabbe, C., Kleesiek, K., Götting, C., 2013. First identification and functional analysis of the human xylosyltransferase II promoter. Glycoconjugate journal 30, 237-245.

Muller, S., Schottler, M., Schon, S., Gotting, C., Disse, J., Prante, C., Brinkmann, T., Kuhn, J., Kleesiek, K., 2006. Human xylosyltransferase I and N-terminal truncated forms: functional characterization of the core enzyme. Biochemical Journal 394, 163-171.

Muller, S., Schottler, M., Schon, S., GOTTING, C., PRANTE, C., BRINKMANN, T., KUHN, J., Kleesiek, K., 2005. Human xylosyltransferase I: functional and biochemical characterization of cysteine residues required for enzymic activity. Biochemical Journal 386, 227-236.

Munns, Craig F., Fahiminiya, S., Poudel, N., Munteanu, Maria C., Majewski, J., Sillence, David O., Metcalf, Jordan P., Biggin, A., Glorieux, F., Fassier, F., Rauch, F., Hinsdale, Myron E., 2015. Homozygosity for Frameshift Mutations in XYLT2 Result in a Spondylo-Ocular Syndrome with Bone Fragility, Cataracts, and Hearing Defects. The American Journal of Human Genetics 96, 971-978.

Mythreye, K., Blobe, G.C., 2009a. Proteoglycan signaling co-receptors: roles in cell adhesion, migration and invasion. Cell. Signal. 21, 1548-1558.

Mythreye, K., Blobe, G.C., 2009b. The type III TGF-β receptor regulates epithelial and cancer cell migration through β-arrestin2-mediated activation of Cdc42. Proceedings of the National Academy of Sciences 106, 8221-8226.

Nadanaka, S., Kitagawa, H., 2014. EXTL2 controls liver regeneration and aortic calcification through xylose kinase-dependent regulation of glycosaminoglycan biosynthesis. Matrix Biology 35, 18-24.

Nadanaka, S., Zhou, S., Kagiyama, S., Shoji, N., Sugahara, K., Sugihara, K., Asano, M., Kitagawa, H., 2013. EXTL2, a Member of the EXT Family of Tumor Suppressors, Controls Glycosaminoglycan Biosynthesis in a Xylose Kinase-dependent Manner. Journal of Biological Chemistry 288, 9321-9333.

Nalbant, D., Youn, H., Nalbant, S.I., Sharma, S., Cobos, E., Beale, E.G., Du, Y., Williams, S.C., 2005. FAM20: an evolutionarily conserved family of secreted proteins expressed in hematopoietic cells. BMC genomics 6, 11.

Nastase, M.V., Young, M.F., Schaefer, L., 2012. Biglycan A Multivalent Proteoglycan Providing Structure and Signals. Journal of Histochemistry & Cytochemistry 60, 963-975.
Neill, T., Schaefer, L., Iozzo, R.V., 2012. Decorin: a guardian from the matrix. The American Journal of Pathology 181, 380-387.

Neill, T., Schaefer, L., Iozzo, R.V., 2014. Instructive roles of extracellular matrix on autophagy. The American Journal of Pathology 184, 2146-2153.

Neill, T., Torres, A., Buraschi, S., Iozzo, R.V., 2013. Decorin has an appetite for endothelial cell autophagy. Autophagy 9, 1626-1628.

Nguyen, T.K., Tran, V.M., Sorna, V., Eriksson, I., Kojima, A., Koketsu, M., Loganathan, D., Kjellén, L., Dorsky, R.I., Chien, C.-B., 2013. Dimerized glycosaminoglycan chains increase FGF signaling during zebrafish development. ACS chemical biology 8, 939-948.

Nigro, J., Dilley, R.J., Little, P.J., 2002. Differential effects of gemfibrozil on migration, proliferation and proteoglycan production in human vascular smooth muscle cells. Atherosclerosis 162, 119-129.
Nilsson, U., Jacobsson, M., Johnsson, R., Mani, K., Ellervik, U., 2009. Antiproliferative effects of peracetylated naphthoxylosides. Bioorg. Med. Chem. Lett. 19, 1763-1766.

Nishikawa, H., Ueno, A., Nishikawa, S., Kido, J.-i., Ohishi, M., Inoue, H., Nagata, T., 2000. Sulfated glycosaminoglycan synthesis and its regulation by transforming growth factor-β in rat clonal dental pulp cells. Journal of endodontics 26, 169-171.

Nuwayhid, N., Glaser, J.H., Johnson, J.C., Conrad, H.E., Hauser, S.C., Hirschberg, C.B., 1986. Xylosylation and glucuronosylation reactions in rat liver Golgi apparatus and endoplasmic reticulum. Journal of Biological Chemistry 261, 12936-12941.

O'Sullivan, J., Bitu, Carolina C., Daly, Sarah B., Urquhart, Jill E., Barron, Martin J., Bhaskar, Sanjeev S., Martelli-Júnior, H., dos Santos Neto, Pedro E., Mansilla, Maria A., Murray, Jeffrey C., Coletta, Ricardo D., Black, Graeme C.M., Dixon, Michael J., 2011. Whole-Exome Sequencing Identifies FAM20A Mutations as a Cause of Amelogenesis Imperfecta and Gingival Hyperplasia Syndrome. The American Journal of Human Genetics 88, 616-620.

Okajima, T., Fukumoto, S., Furukawa, K., Urano, T., Furukawa, K., 1999. Molecular Basis for the Progeroid Variant of Ehlers-Danlos Syndrome identification and characterization of two mutations in galactosyltransferase I gene. Journal of Biological Chemistry 274, 28841-28844.

Okayama, M., Kimata, K., Suzuki, S., 1973. The Influence of α-Nitrophenyl β-D-Xyloside on the Synthesis of Proteochondroitin Sulfate by Slices of Embryonic Chick Cartilage. The Journal of Biochemistry 74, 1069-1073.

Ouzzine, M., Barré, L., Netter, P., Magdalou, J., Fournel-Gigleux, S., 2006. Role of the carboxyl terminal stop transfer sequence of UGT1A6 membrane protein in ER targeting and translocation of upstream lumenal domain. FEBS Letters 580, 1953-1958.

Perrimon, N., Bernfield, M., 2000. Specificities of heparan sulphate proteoglycans in developmental processes. Nature 404, 725-728.

Pfeil, U., Wenzel, K.-W., 2000. Purification and some properties of UDP-xylosyltransferase of rat ear cartilage. Glycobiology 10, 803-807.

Poli, A., Wang, J., Domingues, O., Planagumà, J., Yan, T., Rygh, C.B., Skaftnesmo, K.O., Thorsen, F., McCormack, E., Hentges, F., 2013. Targeting glioblastoma with NK cells and mAb against NG2/CSPG4 prolongs animal survival. Oncotarget 4, 1527.

Pönighaus, C., Ambrosius, M., Casanova, J.C., Prante, C., Kuhn, J., Esko, J.D., Kleesiek, K., Götting, C., 2007. Human xylosyltransferase II is involved in the biosynthesis of the uniform

tetrasaccharide linkage region in chondroitin sulfate and heparan sulfate proteoglycans. Journal of Biological Chemistry 282, 5201-5206.
Pönighaus, C., Speirs, H.J.L., Morris, B.J., Kuhn, J., Kleesiek, K., Götting, C., 2009. Xylosyltransferase gene variants and their role in essential hypertension. American Journal of Hypertension 22, 432-436.

Prante, C., Milting, H., Kassner, A., Farr, M., Ambrosius, M., Schön, S., Seidler, D.G., El Banayosy, A., Körfer, R., Kuhn, J., 2007. Transforming growth factor β1-regulated xylosyltransferase I activity in human cardiac fibroblasts and its impact for myocardial remodeling. Journal of Biological Chemistry 282, 26441-26449.

Price, M.A., Colvin Wanshura, L.E., Yang, J., Carlson, J., Xiang, B., Li, G., Ferrone, S., Dudek, A.Z., Turley, E.A., McCarthy, J.B., 2011. CSPG4, a potential therapeutic target, facilitates malignant progression of melanoma. Pigment cell & melanoma research 24, 1148-1157.

Prydz, K., Dalen, K.T., 2000. Synthesis and sorting of proteoglycans. Journal of Cell Science 113, 193-205.

Pujol, J.-P., Chadjichristos, C., Legendre, F., Baugé, C., Beauchef, G., Andriamanalijaona, R., Galéra, P., Boumediene, K., 2008. Interleukin-1 and Transforming Growth Factor-ß 1 as Crucial Factors in Osteoarthritic Cartilage Metabolism. Connective Tissue Research 49, 293-297.

Ramakrishnan, B., Qasba, P.K., 2010. Crystal structure of the catalytic domain of Drosophila β1, 4-galactosyltransferase-7. Journal of Biological Chemistry 285, 15619-15626.

Raman, K., Ninomiya, M., Nguyen, T.K.N., Tsuzuki, Y., Koketsu, M., Kuberan, B., 2011. Novel glycosaminoglycan biosynthetic inhibitors affect tumor-associated angiogenesis. Biochemical and Biophysical Research Communications 404, 86-89.

Ritelli, M., Chiarelli, N., Zoppi, N., Dordoni, C., Quinzani, S., Traversa, M., Venturini, M., Calzavara-Pinton, P., Colombi, M., 2015. Insights in the etiopathology of galactosyltransferase II (GalT-II) deficiency from transcriptome-wide expression profiling of skin fibroblasts of two sisters with compound heterozygosity for two novel B3GALT6 mutations. Molecular Genetics and Metabolism Reports 2, 1-15.

Roberts, J., Kahle, M.P., Bix, G.J., 2012. Perlecan and the Blood-Brain Barrier: Beneficial Proteolysis? Frontiers in Pharmacology 3.

Roch, C., Kuhn, J., Kleesiek, K., Götting, C., 2010. Differences in gene expression of human xylosyltransferases and determination of acceptor specificities for various proteoglycans. Biochemical and Biophysical Research Communications 391, 685-691.

Roughley, P.J., Mort, J.S., 2014. The role of aggrecan in normal and osteoarthritic cartilage. Journal of Experimental Orthopaedics 1, 8.

Saliba, M., Ramalanjaona, N., Gulberti, S., Bertin-Jung, I., Thomas, A., Dahbi, S., Lopin-Bon, C., Jacquinet, J.-C., Breton, C., Ouzzine, M., Fournel-Gigleux, S., 2015. Probing the acceptor active site organization of the human recombinant β1,4-galactosyltransferase 7 and design of xyloside-based inhibitors. Journal of Biological Chemistry.

Sarraj, M.A., Escalona, R.M., Western, P., Findlay, J.K., Stenvers, K.L., 2013. Effects of TGFbeta2 on Wild-Type and Tgfbr3 Knockout Mouse Fetal Testis. Biol. Reprod. 88, 66, 61-13.
Sarrazin, S., Lamanna, W.C., Esko, J.D., 2011. Heparan Sulfate Proteoglycans. Cold Spring Harbor Perspectives in Biology 3, a004952.

Savery, M.D., Jiang, J.X., Park, P.W., Damiano, E.R., 2013. The endothelial glycocalyx in syndecan-1 deficient mice. Microvascular Research 87, 83-91.

Schaefer, L., Babelova, A., Kiss, E., Hausser, H.-J., Baliova, M., Krzyzankova, M., Marsche, G., Young, M.F., Mihalik, D., Götte, M., 2005. The matrix component biglycan is proinflammatory and signals through Toll-like receptors 4 and 2 in macrophages. Journal of Clinical Investigation 115, 2223.

Schön, S., Huep, G., Prante, C., Müller, S., Christ, R., Hagena, F.W., Kuhn, J., Kleesiek, K., Götting, C., 2006a. Mutational and functional analyses of xylosyltransferases and their implication in osteoarthritis. Osteoarthritis and Cartilage 14, 442-448.

Schön, S., Prante, C., Bahr, C., Kuhn, J., Kleesiek, K., Götting, C., 2006b. Cloning and Recombinant Expression of Active Full-length Xylosyltransferase I (XT-I) and Characterization of Subcellular Localization of XT-I and XT-II. Journal of Biological Chemistry 281, 14224-14231.
Schön, S., Prante, C., Bahr, C., Tarnow, L., Kuhn, J., Kleesiek, K., Götting, C., 2006c. The xylosyltransferase I gene polymorphism c.343G>t (p.A125S) is a risk factor for diabetic nephropathy in type 1 diabetes. Diabetes Care 29, 2295-2299.

Schön, S., Prante, C., Müller, S., Schöttler, M., Tarnow, L., Kuhn, J., Kleesiek, K., Götting, C., 2005. Impact of polymorphisms in the genes encoding xylosyltransferase I and a homologue in type 1 diabetic patients with and without nephropathy. Kidney International 68, 1483-1490.
Schön, S., Schulz, V., Prante, C., Hendig, D., Szliska, C., Kuhn, J., Kleesiek, K., Götting, C., 2006d. Polymorphisms in the xylosyltransferase genes cause higher serum XT-I activity in patients with pseudoxanthoma elasticum (PXE) and are involved in a severe disease course. Journal of Medical Genetics 43, 745-749.

Schreml, J., Durmaz, B., Cogulu, O., Keupp, K., Beleggia, F., Pohl, E., Milz, E., Coker, M., Ucar, S.K., Nürnberg, G., 2013. The missing “link”: an autosomal recessive short stature syndrome caused by a hypofunctional XYLT1 mutation. Human genetics, 1-11.

Schreml, J., Durmaz, B., Cogulu, O., Keupp, K., Beleggia, F., Pohl, E., Milz, E., Coker, M., Ucar, S.K., Nürnberg, G., 2014. The missing “link”: an autosomal recessive short stature syndrome caused by a hypofunctional XYLT1 mutation. Human genetics 133, 29-39.

Schwartz, N.B., Domowicz, M., 2002. Chondrodysplasias due to proteoglycan defects. Glycobiology 12, 57R-68R.
Schwartz, N.B., Dorfman, A., 1975. Purification of rat chondrosarcoma xylosyltransferase. Archives of Biochemistry and Biophysics 171, 136-144.

Schwartz, N.B., Rodén, L., 1974. Biosynthesis of chondroitin sulfate. Purification of UDP-d-xylose:core protein β-d-xylosyltransferase by affinity chromatography. Carbohydrate Research 37, 167-180.

Seidler, D., Faiyaz-Ul-Haque, M., Hansen, U., Yip, G., Zaidi, S.E., Teebi, A., Kiesel, L., Götte, M., 2006a. Defective glycosylation of decorin and biglycan, altered collagen structure, and abnormal phenotype of the skin fibroblasts of an Ehlers–Danlos syndrome patient carrying the novel Arg270Cys substitution in galactosyltransferase I (β4GalT-7). Journal of Molecular Medicine 84, 583-594.

Seidler, D.G., 2012. The galactosaminoglycan-containing decorin and its impact on diseases. Current Opinion in Structural Biology 22, 578-582.

Seidler, D.G., Faiyaz-Ul-Haque, M., Hansen, U., Yip, G.W., Zaidi, S.H., Teebi, A.S., Kiesel, L., Götte, M., 2006b. Defective glycosylation of decorin and biglycan, altered collagen structure, and abnormal phenotype of the skin fibroblasts of an Ehlers–Danlos syndrome patient carrying the novel Arg270Cys substitution in galactosyltransferase I (β4GalT-7). Journal of Molecular Medicine 84, 583-594.

Shi, X., Liang, W., Yang, W., Xia, R., Song, Y., 2014. Decorin is responsible for progression of non-small-cell lung cancer by promoting cell proliferation and metastasis. Tumor Biology, 1-10.
Shriver, Z., Liu, D., Sasisekharan, R., 2002. Emerging views of heparan sulfate glycosaminoglycan structure/activity relationships modulating dynamic biological functions. Trends in cardiovascular medicine 12, 71-77.

Siegbahn, A., Aili, U., Ochocinska, A., Olofsson, M., Rönnols, J., Mani, K., Widmalm, G., Ellervik, U., 2011. Synthesis, conformation and biology of naphthoxylosides. Bioorganic & Medicinal Chemistry 19, 4114-4126.

Siegbahn, A., Manner, S., Persson, A., Tykesson, E., Holmqvist, K., Ochocinska, A., Rönnols, J., Sundin, A., Mani, K., Westergren-Thorsson, G., 2014a. Rules for priming and inhibition of glycosaminoglycan biosynthesis; probing the β4GalT7 active site. Chemical Science 5, 3501-3508.

Siegbahn, A., Manner, S., Persson, A., Tykesson, E., Holmqvist, K., Ochocinska, A., Ronnols, J., Sundin, A., Mani, K., Westergren-Thorsson, G., Widmalm, G., Ellervik, U., 2014b. Rules for priming and inhibition of glycosaminoglycan biosynthesis; probing the [small beta]4GalT7 active site. Chemical Science 5, 3501-3508.

Simpson, M.A., Scheuerle, A., Hurst, J., Patton, M.A., Stewart, H., Crosby, A.H., 2009. Mutations in FAM20C also identified in non-lethal osteosclerotic bone dysplasia. Clinical Genetics 75, 271-276.

Sreelatha, A., Kinch, L.N., Tagliabracci, V.S., 2015. The secretory pathway kinases. Biochimica et Biophysica Acta (BBA)-Proteins and Proteomics.

Stoolmiller, A.C., Horwitz, A.L., Dorfman, A., 1972. Biosynthesis of the Chondroitin Sulfate Proteoglycan PURIFICATION AND PROPERTIES OF XYLOSYLTRANSFERASE. Journal of Biological Chemistry 247, 3525-3532.

Susarla, B.T.S., Laing, E.D., Yu, P., Katagiri, Y., Geller, H.M., Symes, A.J., 2011. Smad proteins differentially regulate transforming growth factor-β-mediated induction of chondroitin sulfate proteoglycans. J. Neurochem. 119, 868-878.

Swarup, V.P., Mencio, C.P., Hlady, V., Kuberan, B., 2013. Sugar glues for broken neurons. Biomolecular concepts 4, 233-257.

Szatmári, T., Dobra, K., 2013. The role of syndecan-1 in cellular signaling and its effects on heparan sulfate biosynthesis in mesenchymal tumors. Frontiers in Oncology 3.

Tagliabracci, V.S., Engel, J.L., Wen, J., Wiley, S.E., Worby, C.A., Kinch, L.N., Xiao, J., Grishin, N.V., Dixon, J.E., 2012a. Secreted Kinase Phosphorylates Extracellular Proteins That Regulate Biomineralization. Science 336, 1150-1153.

Tagliabracci, V.S., Pinna, L.A., Dixon, J.E., 2012. Secreted protein kinases. Trends in biochemical sciences.

Tagliabracci, V.S., Wiley, S.E., Guo, X., Kinch, L.N., Durrant, E., Wen, J., Xiao, J., Cui, J., Nguyen, K.B., Engel, J.L., 2015. A single kinase generates the majority of the secreted phosphoproteome. Cell 161, 1619-1632.

Tagliabracci, V.S., Xiao, J., Dixon, J.E., 2013b. Phosphorylation of substrates destined for secretion by the Fam20 kinases. Biochemical Society Transactions 41, 1061-1065.

Tone, Y., Pedersen, L.C., Yamamoto, T., Izumikawa, T., Kitagawa, H., Nishihara, J., Tamura, J.-i., Negishi, M., Sugahara, K., 2008. 2-O-Phosphorylation of Xylose and 6-O-Sulfation of Galactose in the Protein Linkage Region of Glycosaminoglycans Influence the Glucuronyltransferase-I Activity Involved in the Linkage Region Synthesis. Journal of Biological Chemistry 283, 16801-16807.

Tran, V.M., Nguyen, T.K.N., Sorna, V., Loganathan, D., Kuberan, B., 2013. Synthesis and Assessment of Glycosaminoglycan Priming Activity of Cluster-xylosides for Potential Use as Proteoglycan Mimetics. ACS chemical biology 8, 949-957.

Troeberg, L., Nagase, H., 2012. Proteases involved in cartilage matrix degradation in osteoarthritis. Biochimica et Biophysica Acta (BBA) - Proteins and Proteomics 1824, 133-145.
Tsuda, M., Kamimura, K., Nakato, H., Archer, M., Staatz, W., Fox, B., Humphrey, M., Olson, S., Futch, T., Kaluza, V., 1999. The cell-surface proteoglycan Dally regulates Wingless signalling in Drosophila. Nature 400, 276-280.

Tsutsui, Y., Ramakrishnan, B., Qasba, P.K., 2013. Crystal Structures of β-1,4-Galactosyltransferase 7 Enzyme Reveal Conformational Changes and Substrate Binding. Journal of Biological Chemistry 288, 31963-31970.

Tsuzuki, Y., Nguyen, T.K.N., Garud, D.R., Kuberan, B., Koketsu, M., 2010. 4-Deoxy-4-fluoro-xyloside derivatives as inhibitors of glycosaminoglycan biosynthesis. Bioorg. Med. Chem. Lett. 20, 7269-7273.

van Horssen, J., Wesseling, P., van den Heuvel, L.P., de Waal, R.M., Verbeek, M.M., 2003. Heparan sulphate proteoglycans in Alzheimer's disease and amyloid-related disorders. The Lancet Neurology 2, 482-492.

Venero Galanternik, M., Kramer, Kenneth L., Piotrowski, T., 2015. Heparan Sulfate Proteoglycans Regulate Fgf Signaling and Cell Polarity during Collective Cell Migration. Cell Reports 10, 414-428.

Venkatesan, N., Barré, L., Bourhim, M., Magdalou, J., Mainard, D., Netter, P., Fournel-Gigleux, S., Ouzzine, M., 2012. Xylosyltransferase-I Regulates Glycosaminoglycan Synthesis during the Pathogenic Process of Human Osteoarthritis. PLoS ONE 7, e34020.

Venkatesan, N., Barré, L., Magdalou, J., Mainard, D., Netter, P., Fournel-Gigleux, S., Ouzzine, M., 2009. Modulation of xylosyltransferase I expression provides a mechanism regulating glycosaminoglycan chain synthesis during cartilage destruction and repair. The FASEB Journal 23, 813-822.

Venkatesan, N., Tsuchiya, K., Kolb, M., Farkas, L., Bourhim, M., Ouzzine, M., Ludwig, M.S., 2014. Glycosyltransferases and Glycosaminoglycans in Bleomycin and Transforming Growth Factor-β1–Induced Pulmonary Fibrosis. American Journal of Respiratory Cell and Molecular Biology 50, 583-594.

Vernier, R.L., Steffes, M.W., Sisson-Ross, S., Mauer, S.M., 1992. Heparan sulfate proteoglycan in the glomerular basement membrane in type 1 diabetes mellitus. Kidney Int 41, 1070-1080.

Vertel, B.M., Walters, L.M., Flay, N., Kearns, A.E., Schwartz, N.B., 1993. Xylosylation is an endoplasmic reticulum to Golgi event. Journal of Biological Chemistry 268, 11105-11112.

Victor, X.V., Nguyen, T.K.N., Ethirajan, M., Tran, V.M., Nguyen, K.V., Kuberan, B., 2009. Investigating the Elusive Mechanism of Glycosaminoglycan Biosynthesis. Journal of Biological Chemistry 284, 25842-25853.

Vogel, P., Hansen, G., Read, R., Vance, R., Thiel, M., Liu, J., Wronski, T., Smith, D., Jeter-Jones, S., Brommage, R., 2012. Amelogenesis imperfecta and other biomineralization defects in Fam20a and Fam20c null mice. Veterinary Pathology Online 49, 998-1017.

Vogl-Willis, C.A., Edwards, I.J., 2004. High-glucose-induced structural changes in the heparan sulfate proteoglycan, perlecan, of cultured human aortic endothelial cells. Biochimica et Biophysica Acta (BBA) - General Subjects 1672, 36-45.

Voglmeir, J., Voglauer, R., Wilson, I.B., 2007. XT-II, the second isoform of human peptide-O-xylosyltransferase, displays enzymatic activity. Journal of Biological Chemistry 282, 5984-5990.
Wang, H., Sun, W., Ma, J., Pan, Y., Wang, L., Zhang, W.-B., 2015. Biglycan mediates suture expansion osteogenesis via potentiation of Wnt/β-catenin signaling. J. Biomech. 48, 432-440.

Wang, J., Svendsen, A., Kmiecik, J., Immervoll, H., Skaftnesmo, K.O., Planagumà, J., Reed, R.K., Bjerkvig, R., Miletic, H., Enger, P.Ø., 2011. Targeting the NG2/CSPG4 proteoglycan retards tumour growth and angiogenesis in preclinical models of GBM and melanoma. PLoS ONE 6, e23062.

Wang, Y., Wong, S.S., Fukuda, M.N., Zu, H., Liu, Z., Tang, Q., Appert, H.E., 1994. Identification of functional cysteine residues in human galactosyltransferase. Biochemical and Biophysical Research Communications 204, 701-709.

Wegrowski, Y., Maquart, F.-X., 2004. Involvement of stromal proteoglycans in tumour progression. Critical reviews in oncology/hematology 49, 259-268.

Wen, J., Xiao, J., Rahdar, M., Choudhury, B.P., Cui, J., Taylor, G.S., Esko, J.D., Dixon, J.E., 2014. Xylose phosphorylation functions as a molecular switch to regulate proteoglycan biosynthesis. Proceedings of the National Academy of Sciences 111, 15723-15728.

Whitelock, J.M., Melrose, J., Iozzo, R.V., 2008. Diverse Cell Signaling Events Modulated by Perlecan†. Biochemistry 47, 11174-11183.

Wiggins, C.A.R., Munro, S., 1998. Activity of the yeast MNN1 α-1,3-mannosyltransferase requires a motif conserved in many other families of glycosyltransferases. Proceedings of the National Academy of Sciences 95, 7945-7950.

Wight, T.N., Kang, I., Merrilees, M.J., 2014. Versican and the control of inflammation. Matrix Biology 35, 152-161.

Wilson, I., 2004a. The never-ending story of peptide O-xylosyltransferase. CMLS, Cell. Mol. Life Sci. 61, 794-809.

Wilson, I.B.H., 2004b. The never-ending story of peptide O-xylosyltransferase. CMLS, Cell. Mol. Life Sci. 61, 794-809.

Wrighton, K.H., 2015. Cell signalling: One kinase targets many secreted proteins. Nature Reviews Molecular Cell Biology 16, 452-453.

Wu, I., Wu, D.C., Huang, C.C., Lin, H.S., Chen, Y.K., Tsai, H.J., Lu, C.Y., Chou, S.H., Chou, Y.P., Li, L.H., 2010. Plasma decorin predicts the presence of esophageal squamous cell carcinoma. Int. J. Cancer 127, 2138-2146.

Wu, Y., Xing, X., Xu, S., Ma, H., Cao, L., Wang, S., Luo, Y., 2013. Novel and recurrent mutations in the EXT1 and EXT2 genes in Chinese kindreds with multiple osteochondromas. Journal of Orthopaedic Research.

Xiao, J., Tagliabracci, V.S., Wen, J., Kim, S.-A., Dixon, J.E., 2013. Crystal structure of the Golgi casein kinase. Proceedings of the National Academy of Sciences 110, 10574 - 10579.

Yan, J., Stringer, S.E., Hamilton, A., Charlton-Menys, V., Götting, C., Müller, B., Aeschlimann, D., Alexander, M.Y., 2011. Decorin GAG Synthesis and TGF-β Signaling Mediate Ox-LDL–Induced Mineralization of Human Vascular Smooth Muscle Cells. Arteriosclerosis, Thrombosis, and Vascular Biology 31, 608-615.

You, W.-K., Yotsumoto, F., Sakimura, K., Adams, R., Stallcup, W., 2014. NG2 proteoglycan promotes tumor vascularization via integrin-dependent effects on pericyte function. Angiogenesis 17, 61-76.

Zittermann, S.I., Capurro, M.I., Shi, W., Filmus, J., 2010. Soluble glypican 3 inhibits the growth of hepatocellular carcinoma in vitro and in vivo. Int. J. Cancer 126, 1291-1301.

Résumé En Français

Résumé En Français

Introduction

Les protéoglycanes (PGs) sont composés d'une protéine core et d'une ou plusieurs chaînes de glycosaminoglycanes (GAGs) liées de manière covalente sur certains résidus sérines de la protéine core. Les PGs sont parmi les composants majoritaires de la matrice extracellulaire et sont également présents à la surface des cellules. Ils jouent un rôle essentiel dans divers processus biologiques tels que la différentiation, l'adhésion et la migration cellulaires. Les PGs interagissent avec différentes cytokines et facteurs de croissance et avec des ligands protéiques variés et sont capables de médier leur effet intracellulaire (Couchman, 2010; Iozzo and Schaefer, 2015; Prydz and Dalen, 2000).

Les PGs sont classés en quatre familles selon leur localisation cellulaire et subcellulaire. La première famille est celle des PGs intracellulaires qui contient un seul membre, la serglycine. Celle-ci est stockée dans des granules intracellulaires et elle est relarguée suite à l'action de certains stimuli spécifiques [Kolset and Pejler, 2011]. La deuxième famille comprend les PGs de surface cellulaire et comprend les syndécanes (1, 2, 3 et 4), le CSPG4/NG2, le bétaglycan et le phosphacan qui sont attachés aux membranes cellulaires par des domaines transmembranaires et les glypicans (1 à 6) attachés à la surface cellulaire via des ancres glycosyl-phosphatidyl-inositol (GPI). La troisième famille regroupe les PGs péricellulaires et de la membrane basale. Ils sont attachés à la membrane cellulaire via des intégrines et sont également présents au niveau des membranes basales. Cette famille inclut le perlécan, l'agrine, les collagènes XVIII et XV. La quatrième classe est celle des PGs extracellulaires et est subdivisée entre hyalectans, qui comprend l'agrécane, le versicane, le neurocane et le brévicane, et non hyalectans comprenant les SLRPs (décorine et biglycan notamment) et non SLRPs (testicans) (Iozzo and Schaefer, 2015). En fonction des chaînes de GAGs attachées à la protéine core, les PGs sont classés en PGs à héparane-sulfate (HSPGs), PGs à dermatane-sulfate (DSPGs), PGs à chondroïtine-sulfate (CSPGs) et PGs à kératane-sulfate (KSPGs).

Les PGs sont impliqués dans la régulation de différentes voies de signalisation telles que les voies de Wnt, du Fibroblast Growth Factor (FGF), de Hedgehog (Hh) et de la bone morphogenetic protein (BMP). Les HSPGs sont importants pour l'homéostasie des tissus et jouent un rôle crucial

dans la survie, la division, la migration et la différentiation cellulaire ainsi que dans le développement de cancers. L'interaction des HSPGs avec différents récepteurs est principalement médiée par les chaînes de GAGs (Sarrazin et al., 2011). La dégradation des HSPGs transmembranaires par des métalloprotéinases de la matrice (MMPs) influence les différentes voies de signalisation car les chaînes de GAGs ne sont alors plus disponibles pour assurer les interactions entre les récepteurs et leur ligands (Giráldez et al., 2002; Manon-Jensen et al., 2010; Manon-Jensen et al., 2013).

Les CS/DSPGs jouent également un rôle crucial dans différents processus biologiques tels que le développement du cerveau et les cancers. De même que les HSPGs de surface, ils interagissent avec des facteurs de croissance, des récepteurs de la surface cellulaire et des protéines matricielles (Mizumoto et al., 2015). La décorine et le biglycan agissent comme des inhibiteurs endogènes de pan-récepteurs à tyrosine kinase (RTK). La décorine interagit avec différents récepteurs et influence leur signalisation en aval et médie l'autophagie dans les cellules endothéliales vasculaires, ainsi elle agit comme un protecteur de la matrice. L'agrécane est majoritairement présent au sein du cartilage et forme des agrégats denses qui attirent l'eau et maintient l'assemblage des fibres de collagènes. Il est également responsable de la capacité de résistance aux forces de compression du cartilage et se comporte comme un lubrifiant au niveau de l'articulation (Roughley and Mort, 2014). L'expression de l'agrécane est influencée par différentes cytokines. Le vérsicane joue un rôle crucial dans l'inflammation, facilite la migration des leucocytes et interagit avec différents récepteurs (Wight et al., 2014). Dans les tissus mous tels que le poumon, c'est l'élastine qui est majoritairement présente et résiste à l'accumulation/adhésion des monocytes pour former une architecture tissulaire stable. Mais lors de l'inflammation, l'expression du vérsicane est augmentée et cause une adhésion des monocytes qui va déstabiliser la structure du tissu (Wight et al., 2014).

Les HS et CS/DS sont synthétisées à partir de la même amorce tétrasaccharidique et sont formées par l'addition séquentielle de résidus sucrés. La première étape dans la formation de l'amorce tétrasaccharidique est la xylosylation de sérines spécifiques sur la protéine core par la xylosyltransférase (XT) qui présente 2 isoformes (XT-I et XT-II), les deux étant capables d'initier la synthèse des GAGs. Après la xylosylation, deux résidus galactose sont ajoutés par la GalT-I

(β1,4-galactosyltransferase I, β4GalT7) et la GalT-II (β1,3-galactosyltransferase II, β3GalT6). Le quatrième résidu, un acide glucuronique, est transféré par la GlcAT-I (β1,3-glucuronyltransferase I,). L'addition du cinquième résidu conditionne la synthèse de HS ou de CS (Götting et al., 2007). La xylosylation de la protéine core par la XT est considérée comme l'étape limitante de biosynthèse des PGs. Les deux isoformes de la XT présentent une topologie transmembranaire avec des domaines cytoplasmiques et transmembranaires courts alors que le domaine extracellulaire renferme le domaine catalytique et la région stem.

Les XTs ont été purifiées à partir de différents tissus (épiphyse embryonnaire de poulet, chondrosarcome de rat, cartilage embryonnaire de rat, cartilage embryonnaire de poulet, cartilage d'oreille de rat) et de différentes lignées cellulaires (JAR choriocarcinome et High Five lignée cellulaire).

La localisation subcellulaire des XTs reste controversée, certaines études indiquent qu'elles sont localisées dans le RE alors que d'autres études suggèrent une localisation au niveau du Golgi (Wilson, 2004). Nuwayhid et al., et Lohmander et al., ont montré que la xylosylation a lieu au niveau du Golgi dans le foie et dans les chondrocytes et chondrosarcomes de rat (Lohmander et al., 1989; Nuwayhid et al., 1986). Hoffmann et al., (1984) ont également suggérés que la xylosylation a lieu dans le RER. Par la suite, Vertel et al., (1993) ont utilisé la microscopie électronique pour visualiser le processus de xylosylation et ont montré que la XT responsable est localisée dans le RE. Le même groupe a suggèré qu'après la xylosylation dans le RE l'élongation des chaînes de GAGs continue dans le Golgi (Kearns et al., 1993). Plus tard, une étude de Schön et al., (2006) a rapporté que les deux isoformes XT-I et XT-II sont localisées au niveau du Golgi.

Il a été montré que la XT-I est sécrétée, avec les PGs nouvellement synthétisés, dans le milieu extracellulaire et peut ainsi être utilisée comme biomarqueur des conditions pathologiques associées aux perturbations de la synthèse PGs (Götting et al., 2007). Cependant, une autre étude a montré que la XT-II est l'isoforme majoritairement présente dans le sérum et dérive des plaquettes (Condac et al., 2009). L'augmentation de l'activité xylosyltransférase a été observée chez des patients soufrant de pathologies telles que la sclérose systémique (SSc), la fibrose cutanée, hépatique et pulmonaire, la pseudoxanthome élastique (PXE), la cardiomyopathie dilatée, l'arthrose et l'arthrite rhumatoïde. Une diminution de l'activité xylosyltransférase est également

décrite dans différents processus pathogéniques tels que le vieillissement du cartilage, l'infertilité masculine et l'arthrose traitée par les AINS (Götting et al., 2007). Des polymorphismes de la XT-I et de la XT-II ont été associées à différentes pathologies telles que le diabète de type I, la néphropathie diabétique, la PXE et l'arthrose (Götting et al., 2007). Les mutations de la XT-I et de la XT-II ont été rapportées dans différentes pathologies associées aux PGs et les auteurs suggèrent qu'elles pourraient constituées un facteur de risque en cas de maladie.

Récemment, une mutation génétique de la XT-I a été découverte chez des patients présentant un syndrome de petite taille caractérisé par des traits du visage distincts et une déficience intellectuelle modérée (Schreml et al., 2014). Les mutations de la XT-I ont été également identifiées chez des patients atteints de dysplasie de Desbuquois de type 2 présentant un nanisme important et une déficience intellectuelle (Bui et al., 2014). Récemment, il a été montré qu'une mutation au niveau du gène de la XT-I chez la souris induit un nanisme associé à une diminution de la signalisation Ihh. (Mis et al., 2014). Dans le cas de la XT-II, les souris invalidées pour le gène de la XT-II développent des kystes hépatiques. En outre, le foie des souris XT-II/KO présente une taille et un poids qui sont plus élevés que chez les souris sauvages (Condac et al., 2007). Les souris déficientes en XT-II développent également des complications rénales et présentent une déficience de la production en décorine et en versicane.

D'autre part, il a été montré que le résidu xylose peut être modifié par phosphorylation en position 2-O et que cette modification est présente à la fois dans les HSPG et les CSPG, alors que la sulfatation du galactose se produit en position 4 et 6. Cette modification a lieu uniquement dans le cas de la synthèse des CS et pourrait être impliquée dans la synthèse sélective des CS/DS (Prydz et Dalen, 2000). La phosphorylation du résidu xylose est catalysée par la kinase Fam20B, appartenant à la famille de Similarité de séquence 20 qui comprend trois membres (Fam20A, Fam20B, Fam20C) (Koike et al, 2009; Nalbant et al, 2005). Fam20A et Fam20C sont principalement exprimées dans les tissus biominéralisés. Les mutations de Fam20A sont associées à des désordres dentaires, alors que les mutations de Fam20C causent le syndrome de Raine qui est caractérisé par une dysplasie osseuse ostéosclérotique létale. La structure 3D de la kinase Fam20C de *C. Elegans* a été récemment résolue et montre un repliement de type protéine kinase comprenant cinq ponts disulfures et deux résidus asparagine pour la *N*-glycosylation. Fam20C

contient un motif DHG qui interagit avec des ions métalliques Mn^{2+} nécessaires à l'activité enzymatique et le motif DRHHYE comprenant l'acide aspartique catalytique. Ces résidus sont conservés dans toute la famille Fam20 (Xiao et al., 2013).

Il a été précédemment montré au sein de notre équipe que la GalT-I (β4GalT7) transfère de manière efficace le galactose sur le xylose non modifié, par contre ce transfert est totalement inhibé quand le xylose est phosphorylé en position 2-O (Gulberti et al., 2005). Ceci suggère que le phosphate bloquerait l'élongation des chaînes de GAGs et que seuls les xyloses non modifiés permettront la formation des chaînes matures. Ainsi, la phosphorylation régulerait la synthèse des chaînes de GAGs des PGs. Récemment, il a été montré que la phosphorylation du xylose par la Fam20B augmente la synthèse des GAGs, alors que son inhibition diminue la synthèse. Les même auteurs ont montré que la GalT-II (β3GalT6) présente une plus forte activité envers le disaccharide Gal-Xyl(P)-Ben) phosphorylé, alors qu'il est incapable de transférer le galactose sur le disaccharide Gal-Xyl-Ben non phosphorylé (Wen et al., 2014). Le même groupe a rapporté que le trisaccharide phosphorylé est un meilleur accepteur pour la GlcAT-I comparé à la forme non-phosphorylée et que l'addition de l'acide glucuronique par la GlcAT-I aboutit à la déphosphorylation rapide du xylose par l'action de la phosphatase 2-phosphoxylose (XYLP) et par la suite à l'élongation de la chaîne de GAGs (Tone et al., 2008). Dans le cas où le tétrasaccharide n'est pas déphosphorylé la EXTL2 transfère le GlcNAc sur le tétrasaccharide phosphorylé et met fin à la synthèse de la chaîne de GAG. Ainsi, la phosphorylation du xylose régulerait la biosynthèse des PGs à HS. Cependant, d'autres travaux ont montré que les souris invalidées pour le gène de la EXTL2 produisent plus de GAGs comparées aux souris sauvages (Nadanaka et al., 2013).

La synthèse des chaînes de GAGs peut être modulée par des xylosides exogènes. Ces xylosides synthétiques possèdent une aglycone hydrophobe permettant leur pénétration dans la cellule. Ces analogues de xylosides ont la capacité d'initier la synthèse des GAGs in vivo (Fukunaga et al, 1975;. Helting et Roden 1968; . Johnsson et al, 2007;. Victor et al, 2009). Récemment, des xylosides inhibiteurs de la synthèse de GAGs ont été développés dans lesquels le groupe OH accepteur en position C4 pour la fixation du galactose est remplacé par un groupement fluoro (Garud et al, 2008;. Raman et al, 2011;. Tsuzuki et al., 2010). Ces xylosides inhibiteurs sont importants pour l'inhibition sélective et réversible de la synthèse des GAGs.

Matériels et méthodes

Les différentes lignées cellulaires (PgsA-745, PgsB-618, CHO-KI, HEK-293, SW-1354, HepG2) sont obtenues auprès de l'ATCC. Les fibroblastes pulmonaires primaires de rat ont été isolés par digéction à la trypsine (2,5 mg/ml), collagénase (1 mg/ml) et DNase I (2 mg/ml) comme décrit précédemment (Venkatesan et al., 2002). Les cellules sont cultivées dans du milieu DMEM ou DMEM-F12 supplémenté avec 2 mM de glutamine, 100 UI/ml de pénicilline, 100 µg/ml de streptomycine et 10% de sérum bovin fœtal inactivé à la chaleur (SVF).

Les ADNc de la XT-I, la XT-II, la Fam20B, la décorine et le syndécane-4 humains ont été clonés par PCR à partir d'une banque d'ADNc de placenta humain QUICK-Clone ™ ADNc en utilisant l'Advantage GC2 Polymerase Kit (Clontech). Le produit de PCR a été extrait du gel et ligué dans le vecteur pCR2.1-TOPO (Invitrogen). La région codante de chaque gène est excisée et liguée dans le vecteur d'expression. Les vecteurs d'expression utilisés sont pCMV, pcDNA, pEGFP. Le plasmide shRNA est construit et cloné dans le vecteur pGeneClip en utilisant le GeneClip U1 Hairpin Cloning Systems (Promega). Les différentes mutations ont été conçues par PCR en utilisant le kit de mutagenèse dirigée QuikChange site-directed mutagenesis kit (Agilent). Le produit de PCR a été digéré par l'enzyme de restriction Dpnl pour éliminer les brins parentaux non mutés et cloné dans les cellules compétentes XL10-Gold.

La transfection des cellules eucaryotes est réalisée à l'aide de l'ExGen500. Les cellules sont cultivées dans des plaques 6 puits à une confluence de 80% et transfectées avec 1 µg de plasmide en présence de 10 µl d'ExGen500 (Euromedex). La XT-I, la XT-II et leurs mutants sont transfectés de façon stable dans les cellules CHO-PgsA-745. Le shRNA-Fam20B est également transfecté de manière stable dans les cellules HEK-293. Dans le cas de la transfection stable, les cellules sont co-transfectées avec 1 µg de plasmide d'intérêt et 200 ng de pSVneo codant pour le gène de résistance à la néomycine. Les clones exprimant le gène de façon stable sont isolés en utilisant un milieu sélectif contenant de la généticine (G418) à 1 mg/ml. L'expression de la protéine recombinante est analysée par immunoblot en utilisant des anticorps spécifiques. Dans le cas de la transfection transitoire de la décorine et du syndécane, les cellules sont cultivées jusqu'à 80% de

confluence et transfectées avec 1 µg de plasmide et le milieu de culture est récolté après 48h de transfection. Pour la transfection des cultures primaires de fibroblastes de poumon de rat, le kit de transfection Lonza Primary Fibroblasts Transfection Kit (Lonza) a été utilisé conformément aux instructions du fabricant. Les fibroblastes ont été co-transfectées avec des concentrations croissantes avec le plasmide $(CAGA)_{12}$-Lux rapporteur inductible par le TGFβ (Dennler et al., 1998) et 100 ng de pRL-TK codant pour la luciférase Renilla utilisée comme contrôle interne.

Pour le traitement des fibroblastes primaires de poumon de rat, les cellules sont cultivées jusqu'à 80% de confluence dans une plaque 6 puits et traitées ou non avec du 4-MU4-désoxy-xyloside en présence et en absence du TGF-β1 (5 ng/ml).

Pour isoler la protéine d'intérêt, les cellules sont lysées dans du tampon RIPA contenant un cocktail d'inhibiteurs de protéases et la concentration protéique est déterminée par la méthode de Bradford (Bradford, 1976). Pour l'analyse de la N-glycosylation, 20 µg de protéines ont été digérés avec la PNGase F (New England Biolabs) et analysés par Western blot. Les protéines du milieu ont été précipitées, soit par le TCA (pour l'analyse des protéines) ou par le CPC (pour l'analyse des GAGs) et le culot a été dissout dans 30 µl de tampon de Laemmli et dénaturé à 95°C pendant 5 minutes avant d'être analysé sur le gel. Les PGs en fusion avec l'EGFP sont immunopurifiés par des billes magnétiques couplées à un anticorps anti-GFP (Miltenyi Biotech, µMACS) et analysés par Western Blot.

Pour le Western Blot, des quantités équivalentes d'échantillons protéiques ont été préparées, dénaturées avec un tampon Laemmli et chargé sur des gels gradients NuPAGE Bis-Tris 4-12% ou des gels 10%. Les protéines ont été séparées par électrophorèse et transférées sur une membrane de PVDF. Les membranes ont été bloquées dans 5% (p/v) de lait écrémé en poudre et hybridées avec des anticorps primaires appropriés pendant la nuit à 4 °C. Le lendemain, après lavage dans du TBST, les membranes sont hybridées avec l'anticorps secondaire conjugué à la peroxydase et incubées pendant 1 heure à température ambiante. Après lavage, les membranes ont été incubées dans du réactif de chimioluminescence, enveloppées dans du film plastique et exposées sur un film autoradiographique.

La synthèse des PGs est mesurée par incorporation de ^{35}S-sulfate comme décrit par De Vries et al (1986). Les cellules ont été cultivées jusqu'à 80% de confluence dans une plaque 6 puits et transfectées ou traitées et radiomarquées avec 10 µCi/ml de ^{35}S-sulfate (Perkin Elmer) pendant 6h ou 24h. Le milieu de culture a été récolté, digéré par la papaïne (1mg/ml) et des aliquots de GAGs marqués par le ^{35}S ont été précipités par le CPC et dissouts dans du liquide de scintillation (Ultima Gold, Perkin Elmer). La radioactivité a été mesurée en utilisant un compteur à scintillation liquide. Pour l'analyse des GAGs par SDS-PAGE, les GAGs sont précipités par le CPC et sont séparés par migration sur des gels gradients NuPAGE Bis-Tris 4-12%. Après migration, le gel est séché et exposé à un film d'autoradiographie.

La prolifération cellulaire a été mesurée par le colorant fluorescent CFSE. Les cellules ont été marquées avec le kit de prolifération cellulaire CFSE CellTraceTM Kit (Life technologies) et analysées par cytomètrie en flux (Beckman Coulter). La viabilité des cellules a été analysée par le test au MTT. Le dosage de la luciférase est effectué avec le kit Dual Luciferase (Promega) pour estimer à la fois l'activité du rapporteur (CAGA)12-Lux et la Renilla Luciferase. Les cellules sont lysées et l'activité luciférase est mesurée en utilisant un luminomètre Berthold.

Pour l'immunofluorescence, les cellules ont été cultivées sur des lamelles en verre dans des plaques 24 puits et transfectées ou traitées. Par la suite, les cellules ont été rincées avec du PBS et fixées avec 4% de paraformaldéhyde. Les cellules sont perméabilisées avec 0,1% de Triton-X100 et bloquées avec 0,2% de gélatine et hybridées avec l'anticorps primaire pendant 20 minutes. Après plusieurs lavages, les cellules sont hybridées avec l'anticorps secondaire et les noyaux sont colorés avec du colorant de Hoechst. Enfin, les lamelles sont montées sur lames dans du Moviol.

Buts et objectifs

Les principaux objectifs de cette étude sont :

1) Déterminer le rôle de la XT-I et de la XT-II dans la synthèse des PGs et l'impact de leur variations génétiques sur la localisation subcellulaire et la synthèse des GAGs.

2) Etudier le rôle de la kinase Fam20B dans la synthèse des PGs.

3) Déterminer l'impact de l'inhibition de la synthèse des GAGs par un xylosides synthétique sur les effets fibrotiques du TGFβ1.

Résultats et discussion

La majorité des enzymes impliquées dans la synthèse des GAGs sont présentes dans l'appareil de Golgi, cependant la localisation des XTs est encore controversée, en particulier celle de la XT-I. Nous avons étudié la localisation subcellulaire de la XT-I et la XT-II et avons montré que les deux isoformes présentent des localisations différentes. En effet, la XT-I est co-localisée avec le marqueur du RE, la calnexine et la XT-II est co-localisée avec un marqueur du cis-Golgi, la GM130.

En utilisant la décorine et le syndécane 4 comme protéines rapporteurs des PGs à CS et HS, respectivement, nous avons montré que la XT-I et la XT-II sont capables d'initier la synthèse des deux types de PGs. Cependant, l'efficacité d'initiation de la synthèse par la XT-I semble être réduite par rapport à celle de la XT-II. De façon intéressante, nous avons montré que les chaînes de GAGs amorcées par la XT-I sont de tailles plus longues, comparées à celles initiées par la XT-II. Ce fait est important car la longueur des chaînes de GAG pourrait jouer un rôle primordial dans les interactions ligand-GAG et par conséquent dans la signalisation médiée par les PGs et dans les interactions avec des composants cellulaires et au sein de la MEC.

Afin de confirmer que la XT-I produit des chaînes plus longues que la XT-II, nous avons surexprimé la XT-I dans les cellules exprimant de manière stable la XT-II. De manière intéressante, l'expression de XT-I augmente la taille des chaînes de GAGs de manière dose-dépendante. En outre, nous avons observé que l'inhibition de la sulfatation par le chlorate de sodium augmente la taille des chaînes de GAGs dans les cellules exprimant la XT-I, alors qu'il est sans effet sur les chaînes initiées par la XT-II. Nous avons ensuite montré que la XT-II est clivée par la γ-sécrétase et sécrétée dans le milieu extracellulaire, contrairement à la XT-I, suggérant que la forme circulante de l'activité XT dans le sérum proviendrait de la XT-II.

Afin de déterminer si la différence entre les chaînes initiées par la XT-I et la XT-II est due à la différence de localisation des deux enzymes, nous avons conçu une XT-II avec le motif KDEL permettant sa rétention dans le RE. De façon intéressante, les chaînes de GAGs initiées par la XT-II/KDEL sont plus longues, comparées à celles amorcées par la XT-II. Ceci suggère que la différence dans les chaînes de GAG initiées par la XT-I et la XT-II serait liée à leurs localisations subcellulaires respectives. De façon intéressante, l'analyse par "Pulse-chasse" de la maturation et la sécrétion des PGs a permis de montrer que les PGs initiés par la XT-I sont sécrétés dans le milieu extracellulaire avec un retard important par rapport à ceux initiés par la XT-II, suggérant des processus de maturation et/ou des voies de sécrtions différentes.

Plusieurs études ont montré l'existence d'un polymorphisme au niveau du gène *XYLT1* de la XT-I et du gène *XYLT2* de la XT-II, toutefois l'impact de ces mutations sur la synthèse des PGs n'a pas encore été étudié. Par conséquent, nous avons analysé l'effet des mutants de la XT-I (A115S, R406W, T665M, R481W et R598C) et de la XT-II (D56N, P115L, P305L, R406C et P418L) sur la synthèse des PGs. Nous avons montré que les mutants de la XT-I sont localisés dans le RE et sont capables d'initier la synthèse des PGs mais à des taux moins importants que l'enzyme sauvage. Dans le cas de la XT-II, les mutants P115L et P305L sont localisés dans le Golgi et initient la synthèse des GAGs avec une efficacité similaire à l'enzyme sauvage. Alors que, les mutants R406C et P418L sont incapables d'initier la synthèse de GAGs et sont localisés dans le RE, suggérant un repliement incorrect de ces mutants conduisant à leur rétention dans le RE.

La kinase Fam20B est responsable de la 2-O-phosphorylation du xylose du tétrasaccharide de liaison des chaînes de GAGs. Contrairement aux premières études sur Fam20B qui montrent que cette kinase induit la synthèse des PGs, nous avons montré par l'analyse des PGs endogènes et par l'expression de la décorine (CS/DSPG) et du syndecane 4 (HSPG) dans différentes lignées cellulaires (CHO, HEK-293, SW et HepG2) que Fam20B bloque la synthèse des chaînes de GAGs, HS et CS. Nous avons ensuite étudié l'effet de l'inhibition par shRNA de l'expression de Fam20B sur la synthèse des PGs et avons montré que l'inhibition de Fam20B induit la synthèse des CS- et HS-PG. L'effet de l'inhibition de Fam20B sur la synthèse des GAGs endogènes a été également analysé par incorporation de ^{35}S-sulfate. Enfin, nous avons montré que l'action de Fam20B a lieu

juste après l'addition du xylose et que cette modification empêche la production des PGs conduisant probablement à leur dégradation ntracellulaire. Des études structure/fonction de Fam20B ont été également menées et ont montré l'importance des résidus acides aspartiques, D289 et D309 dans la fonction de Fam20B. Enfin, nous avons montré que l'expression de Fam20 réduit fortement la prolifération et la migration cellulaires, deux processus dépendants des GAGs.

Il a été montré que la synthèse des PGs et de leurs chaînes de GAGs est fortement augmentée dans certaines pathologies fibrotiques sous l'effet du TGFβ. Par conséquent, l'inhibition sélective de la synthèse des chaînes de GAGs pourrait constituer une stratégie intéressante contre ces pathologies. Nous avons synthétisé un xyloside dépourvu du groupe hydroxyle en position C4, le 4-MU-4-désoxy-xyloside, et avons montré qu'il est capable d'inhiber la synthèse des GAGs de manière dose-dépendante dans les fibroblastes primaires en culture. Nous avons ensuite montré que le 4-désoxy-4MU-xyloside inhibe la synthèse des PGs induite par le TGF-β1 dans les fibroblastes primaires de poumon.

Afin de déterminer les mécanismes moléculaires impliqués, nous avons évalué l'impact du 4-MU4-désoxy-xyloside sur la signalisation du TGF-β1 dans les fibroblastes primaires. Nous avons montré en utilisant un gène rapporteur de l'induction de la voie de signalisation Smad, le (ACGA)12-Lux, que le TGF-β1 induit de façon significative le gène rapporteur dans les fibroblastes. Cependant, cette induction est fortement diminuée par le traitement des cellules avec le 4-MU4-désoxy-xyloside. Ensuite, nous avons analysé l'effet de la 4-MU4-désoxy-xyloside sur la signalisation du TGF-β1 dans les fibroblastes primaires et avons montré que le 4-MU4-désoxy-xyloside inhibe l'activation de la voie canonique Smad-dépendante en réduisant considérablement la phosphorylation par le TGF-β1 de Smad2 et Smad3. Nous avons ensuite montré que le 4-MU4-désoxy-xyloside inhibe la prolifération des fibroblastes et empêche la trans-différenciation des fibroblastes en myofibroblastes par le TGF-β1.

Conclusions et perspectives

Nous avons montré dans un premier temps que la XT-I est localisée dans le RE alors que la XT-II est localisée dans le Golgi et que les chaînes de GAG initiées par les deux isoformes sont différentes. Tous les mutants XT-I étudiés sont localisés dans le RE, mais la synthèse de GAG est moins importante comparée à l'enzyme sauvage. La XT-II et ses mutants sont sécrétés dans la MEC. Cependant, deux mutants de la XT-II sont localisés dans le RE et sont inactifs et ne sont pas sécrétés. Les souris XT-II/KO sont viables et présentent une polykystose principalement dans le foie et dans une moindre mesure dans les reins. Cependant, les souris XT-I/KO n'ont pas encore été décrites. Par contre, des mutations de la XT-I ont été décrites et certaines sont associées à un nanisme important chez l'homme, témoignant une implication dans le développement ostéoarticulaire.

Nous avons montré que Fam20B inhibe la synthèse des GAGs et par conséquent, régule de manière négative la synthèse des PGs. L'analyse de l'effet de Fam20B sur la prolifération et la migration cellulaire des chondrosarcomes, tumeurs du cartilage, montre que ces deux processus sont fortement perturbés après expression de Fam20B, confirmant ainsi le rôle des GAGs dans ces processus cellulaires. Les souris invalidées pour le gène *FAM20B* meurent à un stade embryonnaire précoce. Ainsi, il serait intéressant d'étudier l'inhibition ou la surexpession de Fam20B dans d'autres modèles comme le xénope afin d'explorer son rôle dans le développement.

Le 4-MU4-désoxy-xyloside inhibe la synthèse des GAGs induite par le TGF-β1 réduisant ainsi l'accumulation des PGs au niveau de la matrice et de ce fait pourrait contrecarrer la synthèse et le dépôt excessif de ces composants de la matrice au cours des fibroses pulmonaires et cutanées. Il serait donc intéressant de tester cet inhibiteur *in vivo* dans des modèles de fibrose chez l'animal.

Bibliographie

Bradford, M.M. 1976. A rapid and sensitive method for the quantitation of microgram quantities of protein utilizing the principle of protein-dye binding. *Analytical biochemistry* 72:248-254.

Bui, C., C. Huber, B. Tuysuz, Y. Alanay, C. Bole-Feysot, J.G. Leroy, G. Mortier, P. Nitschke, A. Munnich, and V. Cormier-Daire. 2014. XYLT1 mutations in Desbuquois dysplasia type 2. *The American Journal of Human Genetics* 94:405-414.

Condac, E., G.L. Dale, D. Bender-Neal, B. Ferencz, R. Towner, and M.E. Hinsdale. 2009. Xylosyltransferase II is a significant contributor of circulating xylosyltransferase levels and platelets constitute an important source of xylosyltransferase in serum. *Glycobiology* 19:829-833.

Condac, E., R. Silasi-Mansat, S. Kosanke, T. Schoeb, R. Towner, F. Lupu, R.D. Cummings, and M.E. Hinsdale. 2007. Polycystic disease caused by deficiency in xylosyltransferase 2, an initiating enzyme of glycosaminoglycan biosynthesis. *Proceedings of the National Academy of Sciences of the United States of America* 104:9416-9421.

Couchman, J.R. 2010. Transmembrane Signaling Proteoglycans. *Annual Review of Cell and Developmental Biology* 26:89-114.

De Vries, B., W. Van den Berg, E. Vitters, and L. Van de Putte. 1986. Quantitation of glycosaminoglycan metabolism in anatomically intact articular cartilage of the mouse patella: in vitro and in vivo studies with 35S-sulfate, 3H-glucosamine, and 3H-acetate. *Rheumatology international* 6:273-281.

Dennler, S., S. Itoh, D. Vivien, P. ten Dijke, S. Huet, and J.M. Gauthier. 1998. Direct binding of Smad3 and Smad4 to critical TGF beta-inducible elements in the promoter of human plasminogen activator inhibitor-type 1 gene. *The EMBO Journal* 17:3091-3100.

Fukunaga, Y., M. Sobue, N. Suzuki, H. Kushida, S. Suzuki, and S. Suzuki. 1975. Synthesis of a fluorogenic mucopolysaccharide by chondrocytes in cell culture with 4-methylumbelliferyl β-d-xyloside. *Biochimica et Biophysica Acta (BBA) - General Subjects* 381:443-447.

Garud, D.R., V.M. Tran, X.V. Victor, M. Koketsu, and B. Kuberan. 2008. Inhibition of Heparan Sulfate and Chondroitin Sulfate Proteoglycan Biosynthesis. *Journal of Biological Chemistry* 283:28881-28887.

Giráldez, A.J., R.R. Copley, and S.M. Cohen. 2002. HSPG modification by the secreted enzyme Notum shapes the Wingless morphogen gradient. *Developmental cell* 2:667-676.

Götting, C., J. Kuhn, and K. Kleesiek. 2007. Human xylosyltransferases in health and disease. *Cell. Mol. Life Sci.* 64:1498-1517.

Gulberti, S., V. Lattard, M. Fondeur, J.C. Jacquinet, G. Mulliert, P. Netter, J. Magdalou, M. Ouzzine, and S. Fournel-Gigleux. 2005. Phosphorylation and sulfation of oligosaccharide substrates critically influence the activity of human β1,4-galactosyltransferase 7 (GalT-I) and β1,3-glucuronosyltransferase I (GlcAT-I) involved in the biosynthesis of the glycosaminoglycan-protein linkage region of proteoglycans. *Journal of Biological Chemistry* 280:1417-1425.

Helting, T., and L. Rodén. 1968. Studies on the biosynthesis of the chondroitin sulfate-protein linkage region. *Biochemical and Biophysical Research Communications* 31:786-791.

Hoffmann, H.-P., N.B. Schwartz, L. Rodén, and D.J. Prockop. 1984. Location of xylosyltransferase in the cisternae of the rough endoplasmic reticulum of embryonic cartilage cells. *Connective Tissue Research* 12:151-163.

Iozzo, R.V., and L. Schaefer. 2015. Proteoglycan form and function: A comprehensive nomenclature of proteoglycans. *Matrix Biology*

Johnsson, R., K. Mani, and U. Ellervik. 2007. Synthesis and biology of bis-xylosylated dihydroxynaphthalenes. *Bioorganic & Medicinal Chemistry* 15:2868-2877.

Kearns, A.E., B.M. Vertel, and N.B. Schwartz. 1993. Topography of glycosylation and UDP-xylose production. *Journal of Biological Chemistry* 268:11097-11104.

Koike, T., T. Izumikawa, J.I. Tamura, and H. Kitagawa. 2009. FAM20B is a kinase that phosphorylates xylose in the glycosaminoglycan–protein linkage region. *Biochemical Journal* 421:157-162.

Kolset, S.O., Pejler, G., 2011. Serglycin: a structural and functional chameleon with wide impact on immune cells. The Journal of Immunology 187, 4927-4933.

Lohmander, L.S., T. Shinomura, V.C. Hascall, and J.H. Kimura. 1989. Xylosyl transfer to the core protein precursor of the rat chondrosarcoma proteoglycan. *Journal of Biological Chemistry* 264:18775-18780.

Manon-Jensen, T., Y. Itoh, and J.R. Couchman. 2010. Proteoglycans in health and disease: The multiple roles of syndecan shedding. *FEBS Journal* 277:3876-3889.

Manon-Jensen, T., H.A.B. Multhaupt, and J.R. Couchman. 2013. Mapping of matrix metalloproteinase cleavage sites on syndecan-1 and syndecan-4 ectodomains. *FEBS Journal* 280:2320-2331.

Mis, E.K., K.F. Liem Jr, Y. Kong, N.B. Schwartz, M. Domowicz, and S.D. Weatherbee. 2014. Forward genetics defines Xylt1 as a key, conserved regulator of early chondrocyte maturation and skeletal length. *Developmental Biology* 385:67-82.

Mizumoto, S., S. Yamada, and K. Sugahara. 2015. Molecular interactions between chondroitin–dermatan sulfate and growth factors/receptors/matrix proteins. *Current Opinion in Structural Biology* 34:35-42.

Nadanaka, S., S. Zhou, S. Kagiyama, N. Shoji, K. Sugahara, K. Sugihara, M. Asano, and H. Kitagawa. 2013. EXTL2, a Member of the EXT Family of Tumor Suppressors, Controls Glycosaminoglycan Biosynthesis in a Xylose Kinase-dependent Manner. *Journal of Biological Chemistry* 288:9321-9333.

Nalbant, D., H. Youn, S.I. Nalbant, S. Sharma, E. Cobos, E.G. Beale, Y. Du, and S.C. Williams. 2005. FAM20: an evolutionarily conserved family of secreted proteins expressed in hematopoietic cells. *BMC genomics* 6:11.

Nuwayhid, N., J.H. Glaser, J.C. Johnson, H.E. Conrad, S.C. Hauser, and C.B. Hirschberg. 1986. Xylosylation and glucuronosylation reactions in rat liver Golgi apparatus and endoplasmic reticulum. *Journal of Biological Chemistry* 261:12936-12941.

Prydz, K., and K.T. Dalen. 2000. Synthesis and sorting of proteoglycans. *Journal of Cell Science* 113:193-205.

Raman, K., M. Ninomiya, T.K.N. Nguyen, Y. Tsuzuki, M. Koketsu, and B. Kuberan. 2011. Novel glycosaminoglycan biosynthetic inhibitors affect tumor-associated angiogenesis. *Biochemical and Biophysical Research Communications* 404:86-89.

Roughley, P.J., and J.S. Mort. 2014. The role of aggrecan in normal and osteoarthritic cartilage. *Journal of Experimental Orthopaedics* 1:8.

Sarrazin, S., W.C. Lamanna, and J.D. Esko. 2011. Heparan Sulfate Proteoglycans. *Cold Spring Harbor Perspectives in Biology* 3:a004952.

Schön, S., C. Prante, C. Bahr, J. Kuhn, K. Kleesiek, and C. Götting. 2006. Cloning and Recombinant Expression of Active Full-length Xylosyltransferase I (XT-I) and Characterization of Subcellular Localization of XT-I and XT-II. *Journal of Biological Chemistry* 281:14224-14231.

Schreml, J., B. Durmaz, O. Cogulu, K. Keupp, F. Beleggia, E. Pohl, E. Milz, M. Coker, S.K. Ucar, and G. Nürnberg. 2014. The missing "link": an autosomal recessive short stature syndrome caused by a hypofunctional XYLT1 mutation. *Human genetics* 133:29-39.

Tone, Y., L.C. Pedersen, T. Yamamoto, T. Izumikawa, H. Kitagawa, J. Nishihara, J.-i. Tamura, M. Negishi, and K. Sugahara. 2008. 2-O-Phosphorylation of Xylose and 6-O-Sulfation of Galactose in the Protein Linkage Region of Glycosaminoglycans Influence the Glucuronyltransferase-I Activity Involved in the Linkage Region Synthesis. *Journal of Biological Chemistry* 283:16801-16807.

Tsuzuki, Y., T.K.N. Nguyen, D.R. Garud, B. Kuberan, and M. Koketsu. 2010. 4-Deoxy-4-fluoro-xyloside derivatives as inhibitors of glycosaminoglycan biosynthesis. *Bioorg. Med. Chem. Lett.* 20:7269-7273.

Venkatesan, N., Roughley, P.J., Ludwig, M.S., 2002. Proteoglycan expression in bleomycin lung fibroblasts: role of transforming growth factor-β1 and interferon-γ. American Journal of Physiology-Lung Cellular and Molecular Physiology 283, L806-L814.

Vertel, B.M., L.M. Walters, N. Flay, A.E. Kearns, and N.B. Schwartz. 1993. Xylosylation is an endoplasmic reticulum to Golgi event. *Journal of Biological Chemistry* 268:11105-11112.

Victor, X.V., T.K.N. Nguyen, M. Ethirajan, V.M. Tran, K.V. Nguyen, and B. Kuberan. 2009. Investigating the Elusive Mechanism of Glycosaminoglycan Biosynthesis. *Journal of Biological Chemistry* 284:25842-25853.

Wen, J., J. Xiao, M. Rahdar, B.P. Choudhury, J. Cui, G.S. Taylor, J.D. Esko, and J.E. Dixon. 2014. Xylose phosphorylation functions as a molecular switch to regulate proteoglycan biosynthesis. *Proceedings of the National Academy of Sciences* 111:15723-15728.

Wight, T.N., I. Kang, and M.J. Merrilees. 2014. Versican and the control of inflammation. *Matrix Biology* 35:152-161.

Wilson, I. 2004. The never-ending story of peptide O-xylosyltransferase. *CMLS, Cell. Mol. Life Sci.* 61:794-809.

Xiao, J., V.S. Tagliabracci, J. Wen, S.-A. Kim, and J.E. Dixon. 2013. Crystal structure of the Golgi casein kinase. *Proceedings of the National Academy of Sciences*

Résumé

Les protéoglycans (PGs) à héparane- (HS) et chondroïtine-sulfate (CS) jouent un rôle essentiel dans la régulation de nombreux processus biologiques tels que la différenciation cellulaire, la signalisation, la prolifération et la morphogenèse. En effet, les PGs via leurs chaînes de glycosaminoglycanes (GAGs) agissent comme des récepteurs pour des facteurs de croissance, des enzymes et des protéines d'adhésion cellulaire, modulant ainsi leur biodisponibilité, la formation de gradient et leur activité. La synthèse des chaînes de CS et d'HS est initiée par le transfert d'un résidu xylose sur des sérines de la protéine "core" des PGs par les xylosyltransferases (XT), XT-I et XT-II. Ces enzymes catalysent une étape limitante régulant la biosynthèse des GAGs. En plus de la régulation par les XT, la synthèse des GAGs peut être régulée par la phosphorylation du xylose en position 2-O par la kinase Fam20B.

Il a été montré que la XT-I et la XT-II sont capables de restaurer la synthèse des PGs dans les cellules déficientes en activité xylosyltransférase, suggérant ainsi qu'elles sont fonctionnellement redondantes. Cependant, les rôles spécifiques de la XT-I et de la XT-II et l'impact de leurs mutations génétiques sur la synthèse des CS et des HS ne sont pas connus. Au cours de cette thèse, nous avons montré que la XT-I initie la synthèse des PGs avec des chaînes de CS et d'HS de tailles plus longues que celle initiée par la XT-II et avons démontré que cela est lié à leurs localisations subcellulaires respectives. En outre, nous avons montré d'une part que les mutations génétiques de la XT-I réduisent fortement la capacité de l'enzyme à initier la synthèse des GAGs et d'autre part que deux mutations de la XT-II conduisent à la mislocalisation de l'enzyme et l'abrogation de sa capacité à initier la synthèse des chaînes de CS et d'HS. En outre, nous avons démontré en utilisant différentes lignées cellulaires et des mutants inactifs que la kinase Fam20B régule négativement le processus de synthèse des chaînes de GAGs et par conséquent que la phosphorylation du résidu xylose par Fam20B entraîne un blocage dans la polymérisation des chaînes de GAGs.

Mots clés : Xylosyltransférases, protéoglycans, glycosaminoglycanes, chondroïtine, héparane, Fam20B

Abstract

Heparan- (HS) and chondroitin-sulfate (CS) proteoglycans (PGs) are essential regulators of many biological processes including cell differentiation, signalization, proliferation and morphogenesis. Indeed, PGs act through their glycosaminoglycan (GAG) chains as receptors for growth factors, enzymes and cell adhesion proteins, thereby modulating their bioavailability, gradient formation and biological activity. The assembly of HS and CS GAG chains is initiated by the transfer of xylose to serine residues of PG core protein by the xylosyltransferases (XT) enzymes, XT-I and XT-II. These enzymes catalyze a rate-limiting step in the biosynthesis pathway and therefore considered as a regulating factors in the GAG biosynthesis process. Beside the regulation by XT enzymes, GAG chain synthesis may also be regulated by phosphorylation of the xylose residue at 2-O position by the kinase Fam20B.

It has been shown that XT-I and XT-II are able to restore GAG-attached PG synthesis in xylosyltransferase-deficient cells, suggesting that they are functionally redundant. However, nothing is known of the specific roles of XT-I and XT-II if any and of the impact of XT-I and XT-II mutations on the synthesis of CS- and HS-PG. Here, we showed that XT-I initiates PGs with large size CS- and HS-GAG chains compared to XT-II and demonstrated that this was linked to their subcellular localisation. In addition, we have addressed the question of whether genetic mutations of XT-I and XT-II associated with various diseases impact CS- and HS-PG synthesis and found that mutations in XT-I strongly reduced the capacity of the enzyme to initiate the synthesis of both CS and HS GAG chains. However, two mutations in XT-II abrogated the capacity of the enzyme to initiate CS and HS GAGs and led to the mislocalisation of the enzyme. Furthermore, we demonstrated using variouse cell lines and dead mutants that Fam20B negatively regulates GAG synthesis process and that phosphorylation of xylose residue by this kinase resulted in a blokage of the polymerisation procees of the GAG chain.

Key words: Xylosyltransferases, proteoglycans, glycosaminoglycans, chondroïtin, heparan, Fam20B